New Folder Name STACKS NOTEBOOKS

FILE: T920030

BATCH
START

STACKS BOOK1

STAPLE
OR
DIVIDER

Oct 17, 1992

Tests for measuring resonances of support structure

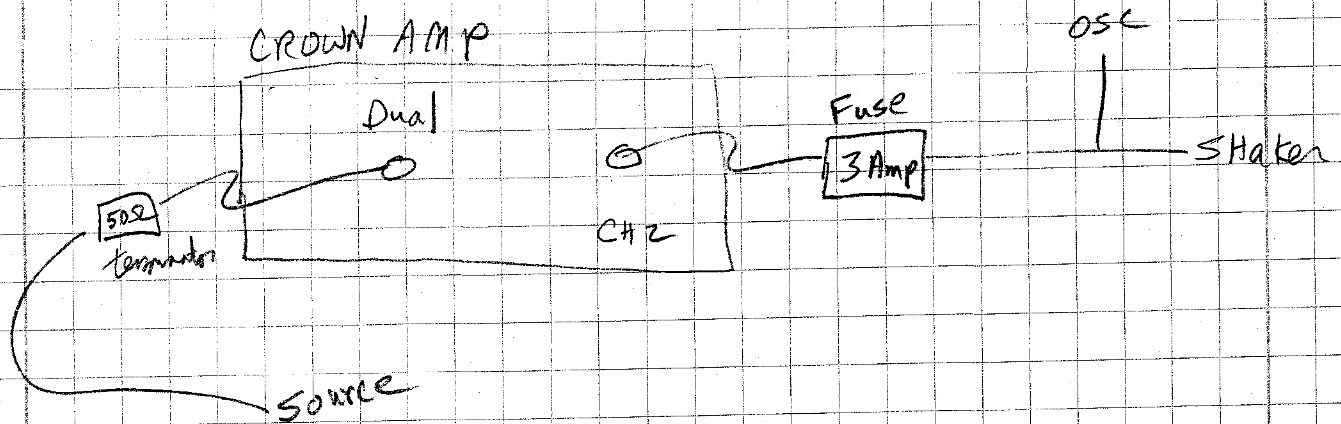

① Had to use channel 2 + dual since had grounding problems when looked at channel 1

② Used 50Ω terminator so that 60 Hertz wouldn't drive shaker when source was off

(terminator lowers source voltage by a factor of 2 since FFT has a 50Ω internal impedance

- source level initially set at 50 mV_{rms} (full gain)
- this gave output to shaker of $5 V_{peak-p} \Rightarrow \frac{2.5}{\sqrt{2}}$ rms
- if assume 1 Ω resistance of shaker ~ $\frac{2.5}{\sqrt{2}}$ amps allowing shaker

- changed source level to 100 mV_{rms} (full gain)
- voltage to shaker is 14.5 V_{pk} = $\frac{7.25A}{\sqrt{2}}$ $R_{SH} = 1$

  3 Amp fuse did not break $= 5.6 A_{rms}$

  Believe $R_{SH} \sim 2$ $\Rightarrow$ $\boxed{I_{SA} = 2.8\ A_{rms}}$

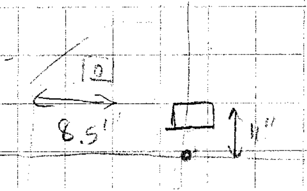

16:00

Drive current -to- cable x-fer function

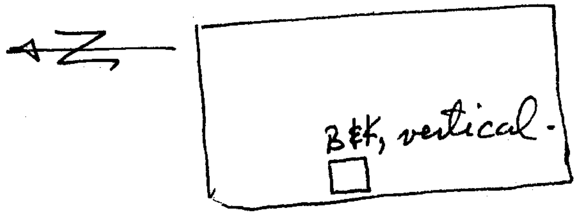

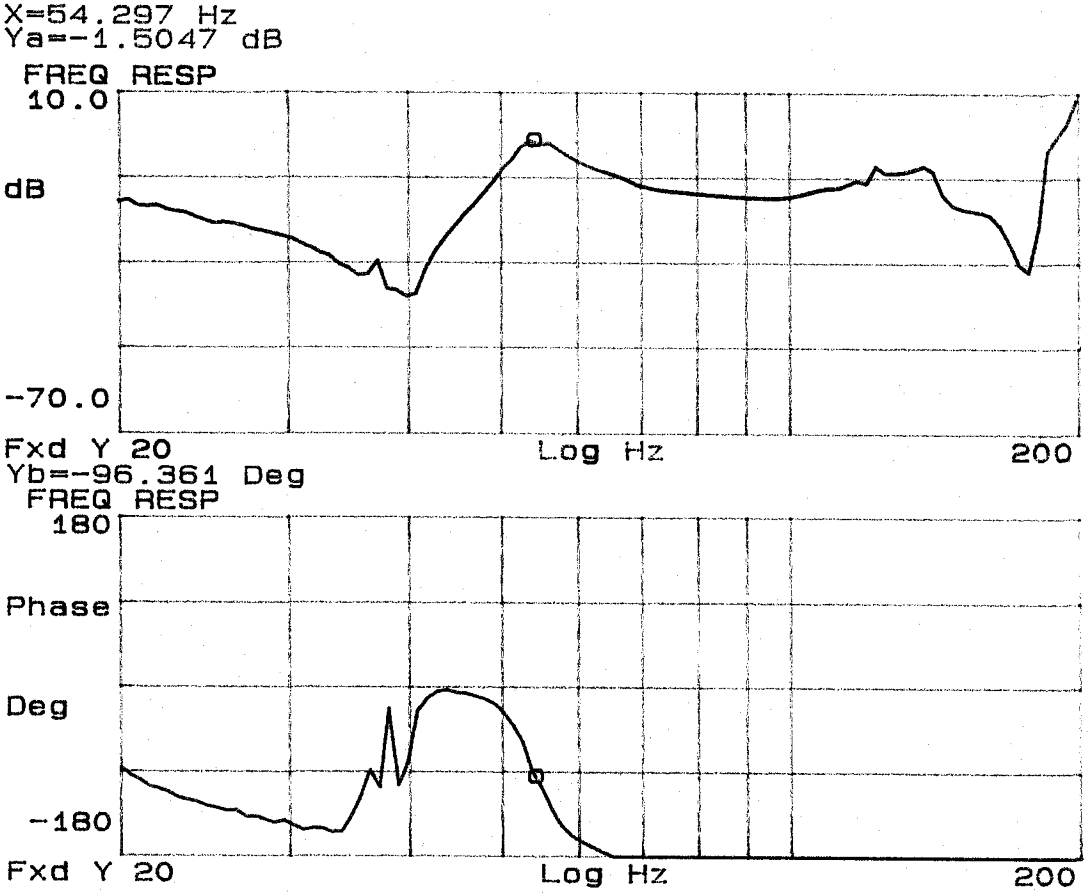

Oct 7, 1992
.00 PM

ansfer Fctn from shaker table to Top of
pport plate (unloaded) : Vertical to Vertical

Disk: Lisa-STACK TEST
File: Sup

Source Level = 100 mV$_{rms}$
Amp Gain (Crown) = 8
Avg = 5
Integ time = 500msec - 2 sec
Resln = 160 pt/dec

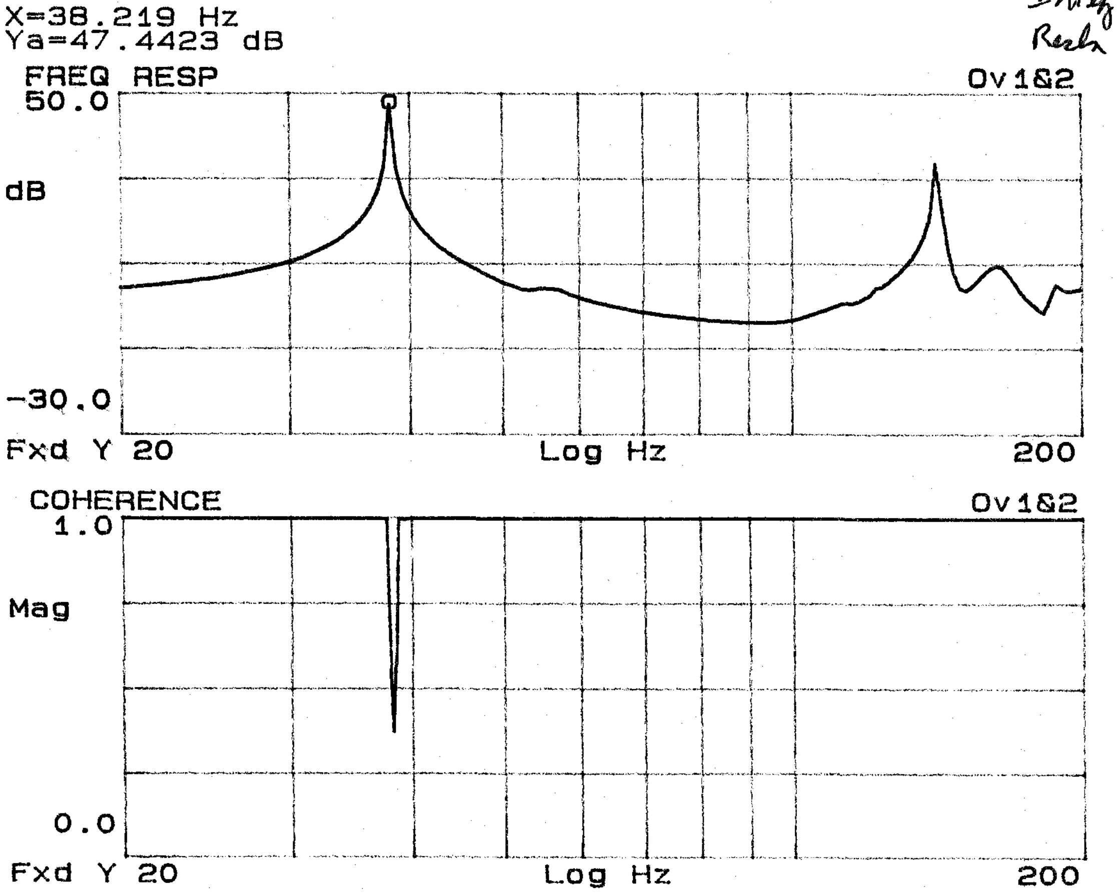

- Shaker was shaking vertically
- 1 accelerometer on top plate
- 1 accelerometer on shaker table
- Believe peaks above 100 Hz are acoustic coupling

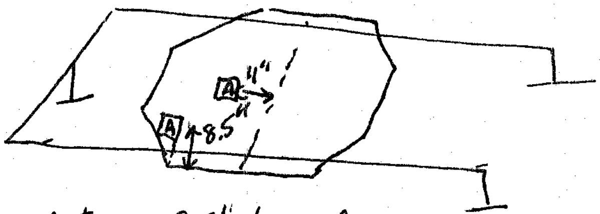

Accel on top plate was 8.5" from edge
Accel on shaker table was 11" from center

Oct 7, 1992
6:15 PM

ransfer Fctn from shaker table to top of
upport plate (unloaded): Vertical to Vertical

Pick° Lisa - Stack Setup
File: Sup 1

Source Level = 100 mV rms
Amp Gain (Crown) = 8
Avg = 5
Integ time = 500 msec - 2 sec
Resln = 160 pt/dec

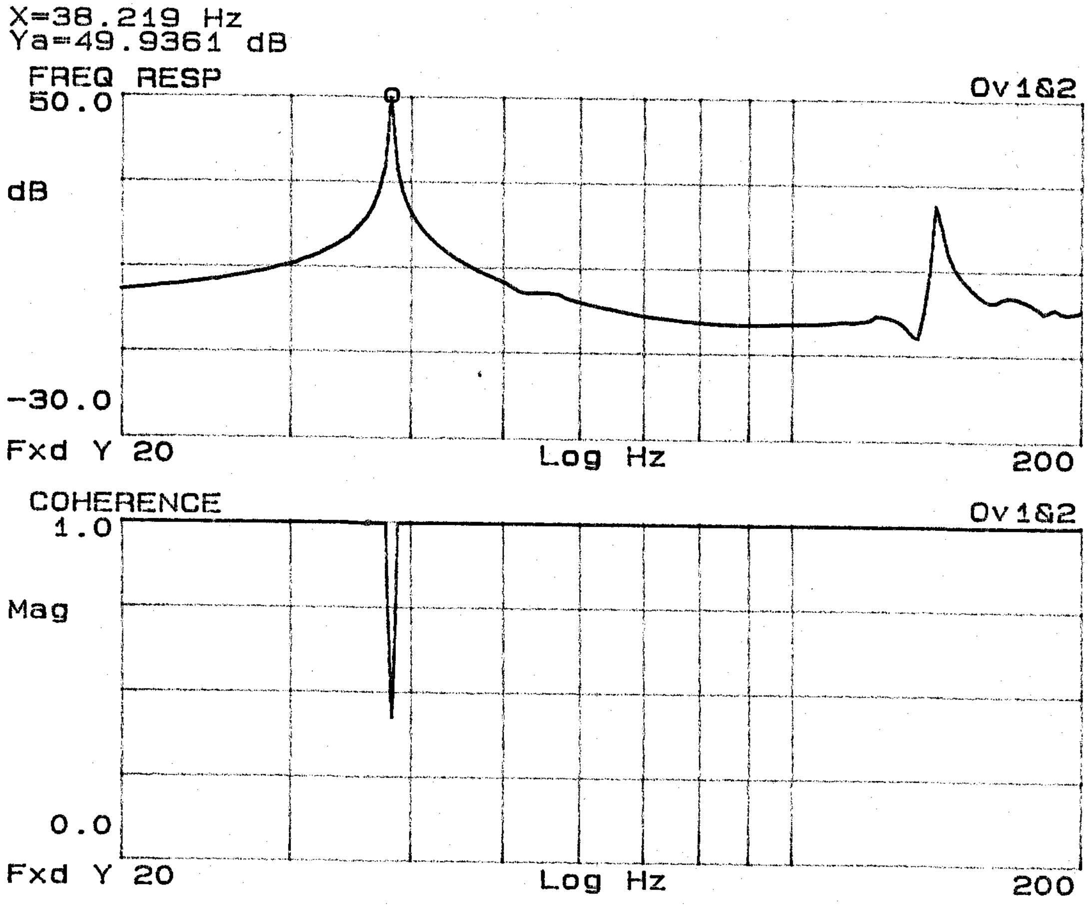

- shaker shaking vertically
- 1 accelerometer on center of top plate
- 1 accelerometer on shaker table (11" from center)
- Plot is same as Sup

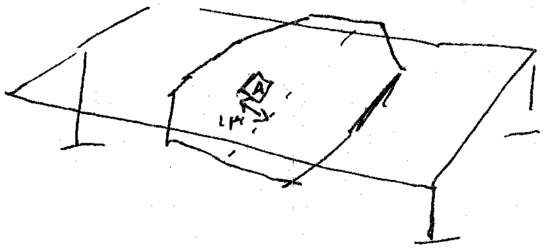

10:20AM.

Powerspectrum

Accelerometer 886910 on Newport table at 18.5", 3.5"

Source - ground noise

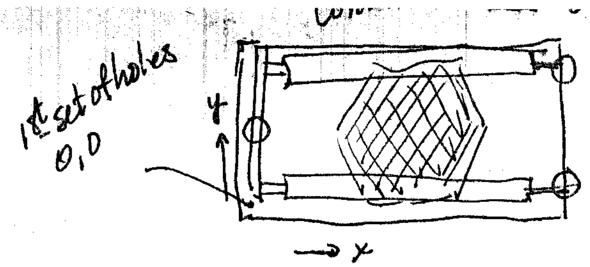

file - 55T

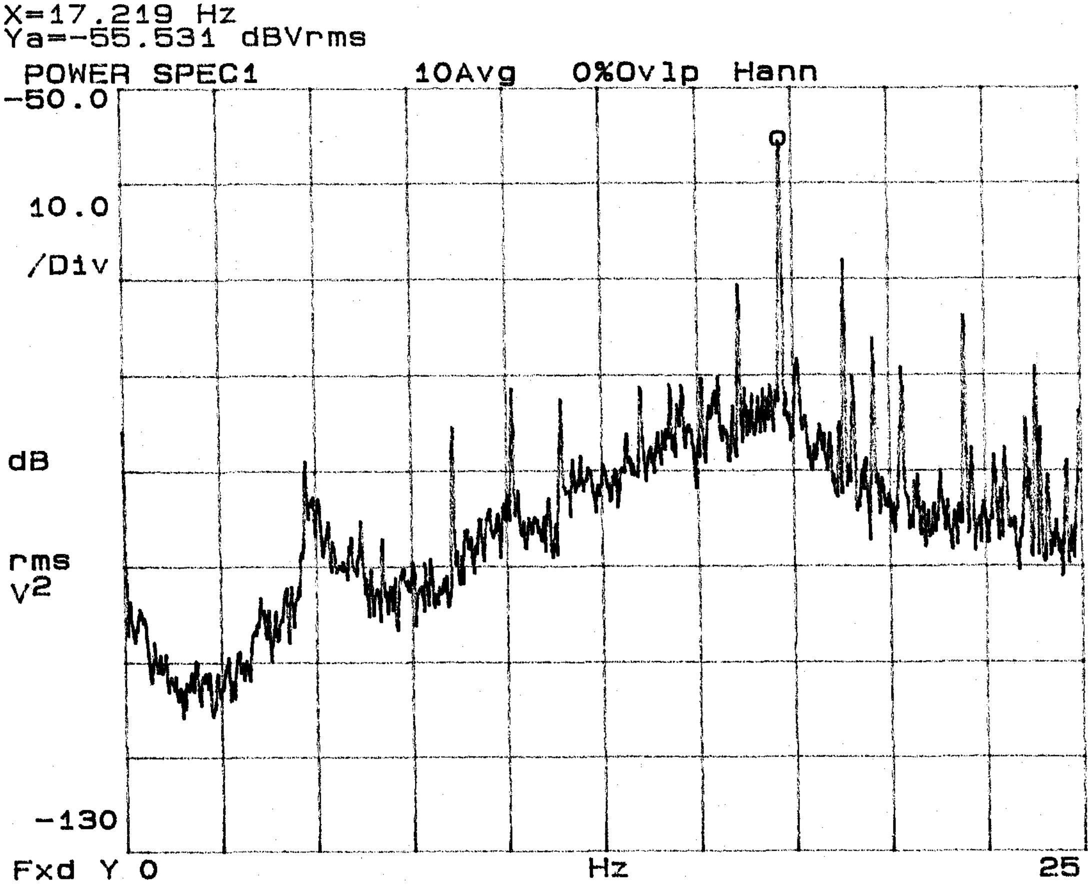

resonance of Newport table and lower support structure on viton springs ≈ 17 hz

10/12/92.

10:53AM.

file SST 1

Same as previous meas.
except. 0-100hz.
and average = 25

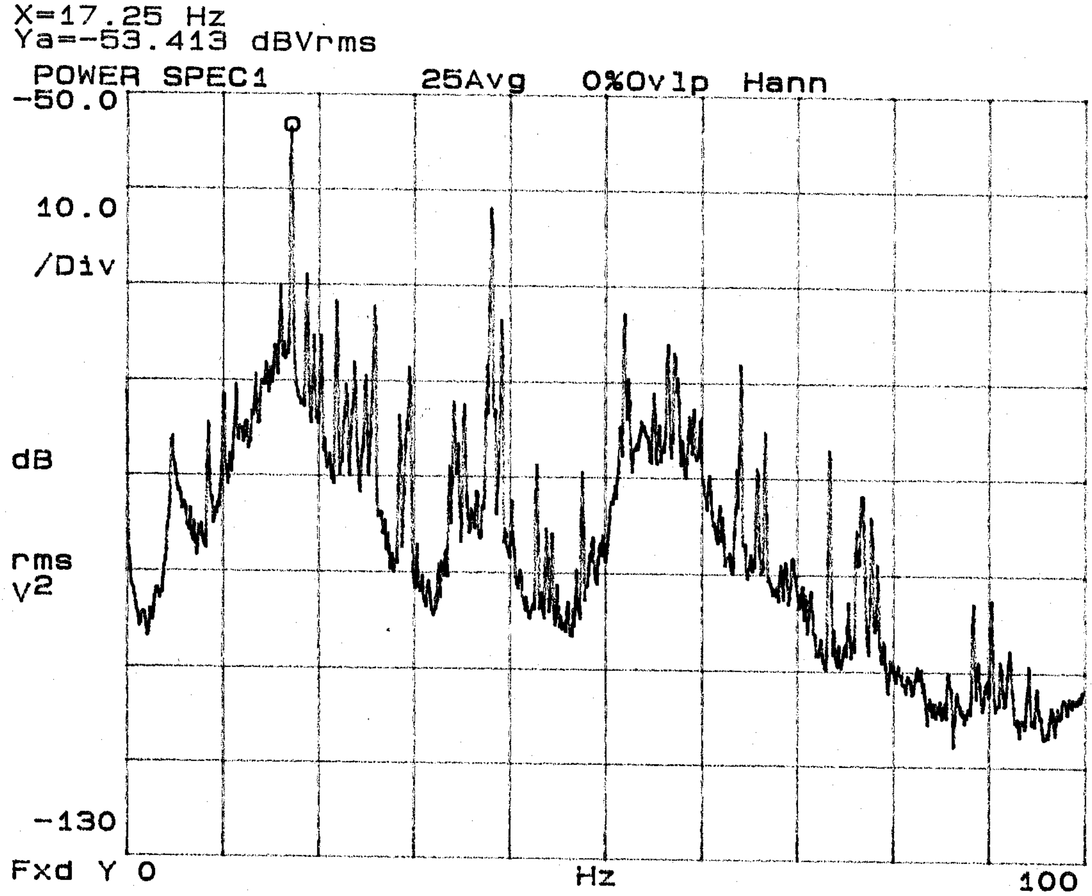

SST2

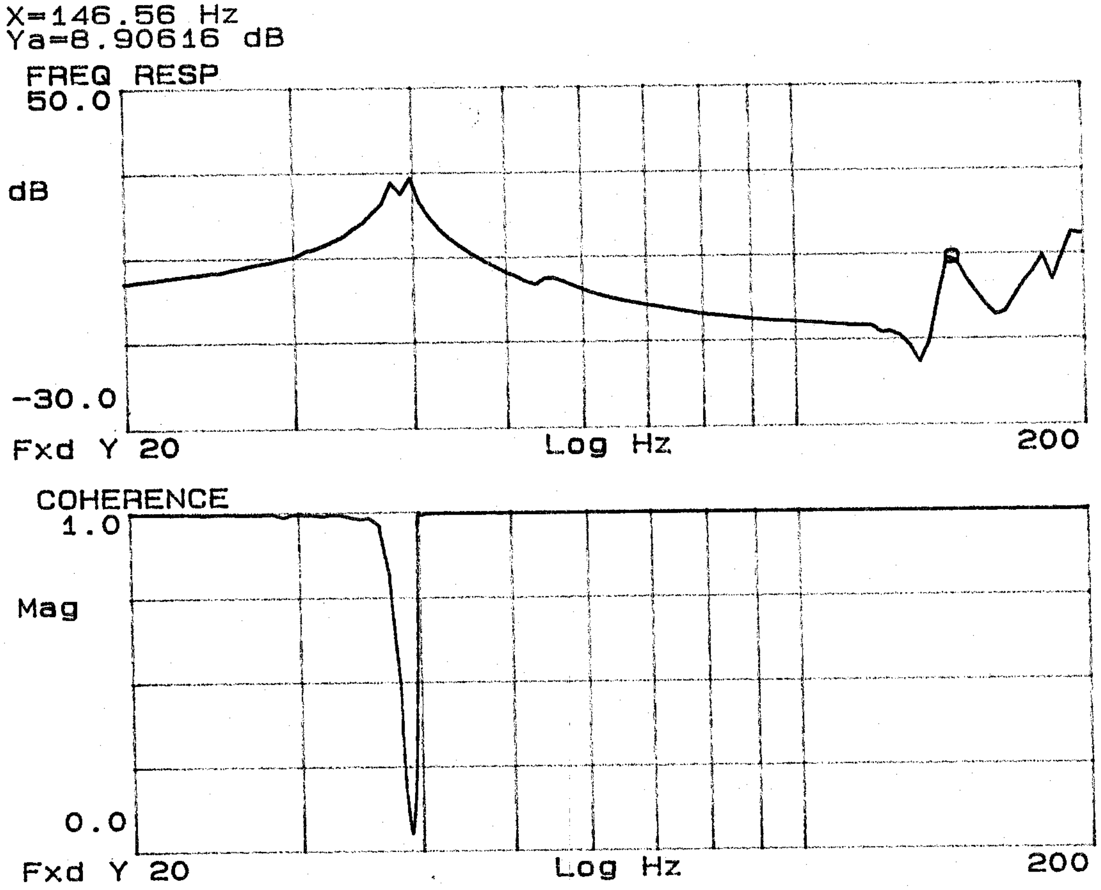

10/12/92.
11:30 AM.

vertical transfer function

#886909 in center of stack bottom plate

#886910 at cross beam support plate.

FFT source level 58 mV RMS

CROWN Amp at max. gain

Scope shows ~ 7 volts peak to peak.

10/12/92.

1:51 pm.

vertical transfer function on Newport table
with Acc. 1 at base of cross bar and
Acc 2 at corner of
cross bar (on crossbar)

file SST3

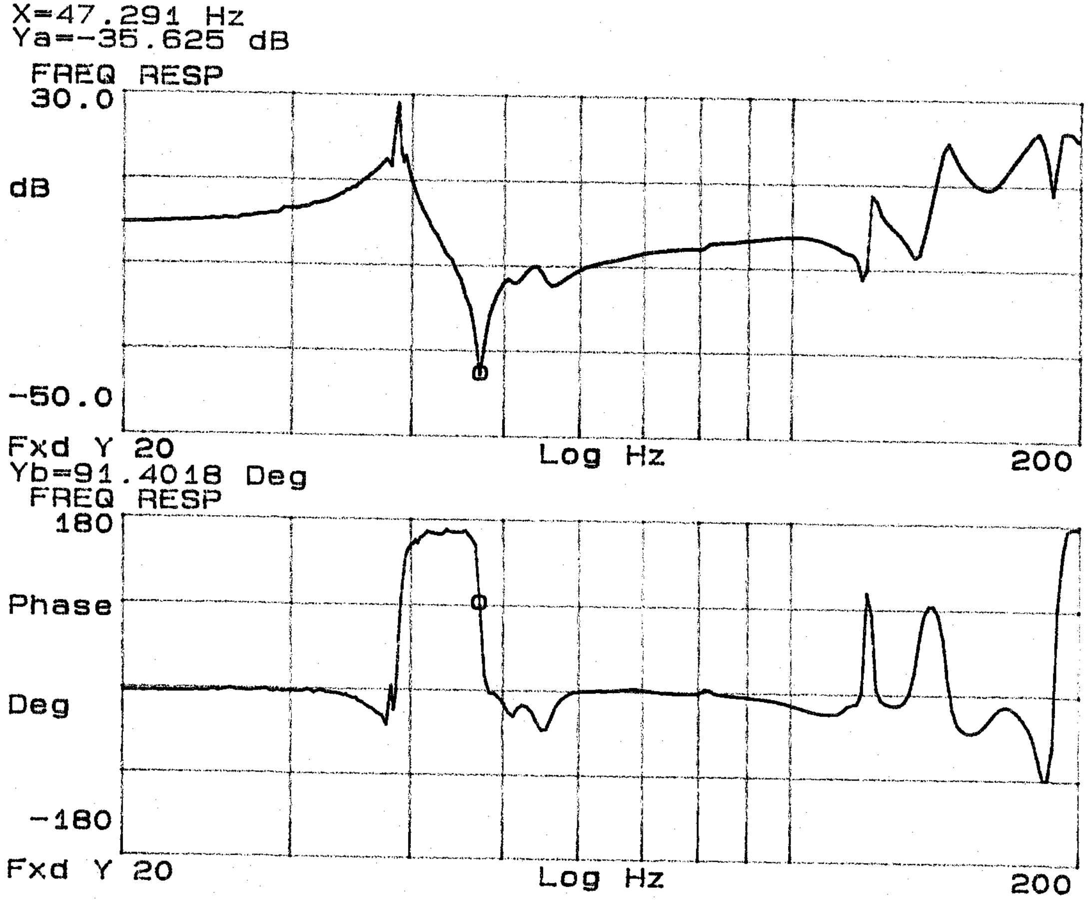

now rotate shaker to horizontal orientation

mount Acc 2 in Center of stack bottom plate
Acc 1 on base plate for cross bar support

both Accs oriented horizontally E-W as is shaker

2:20 PM

File SST4

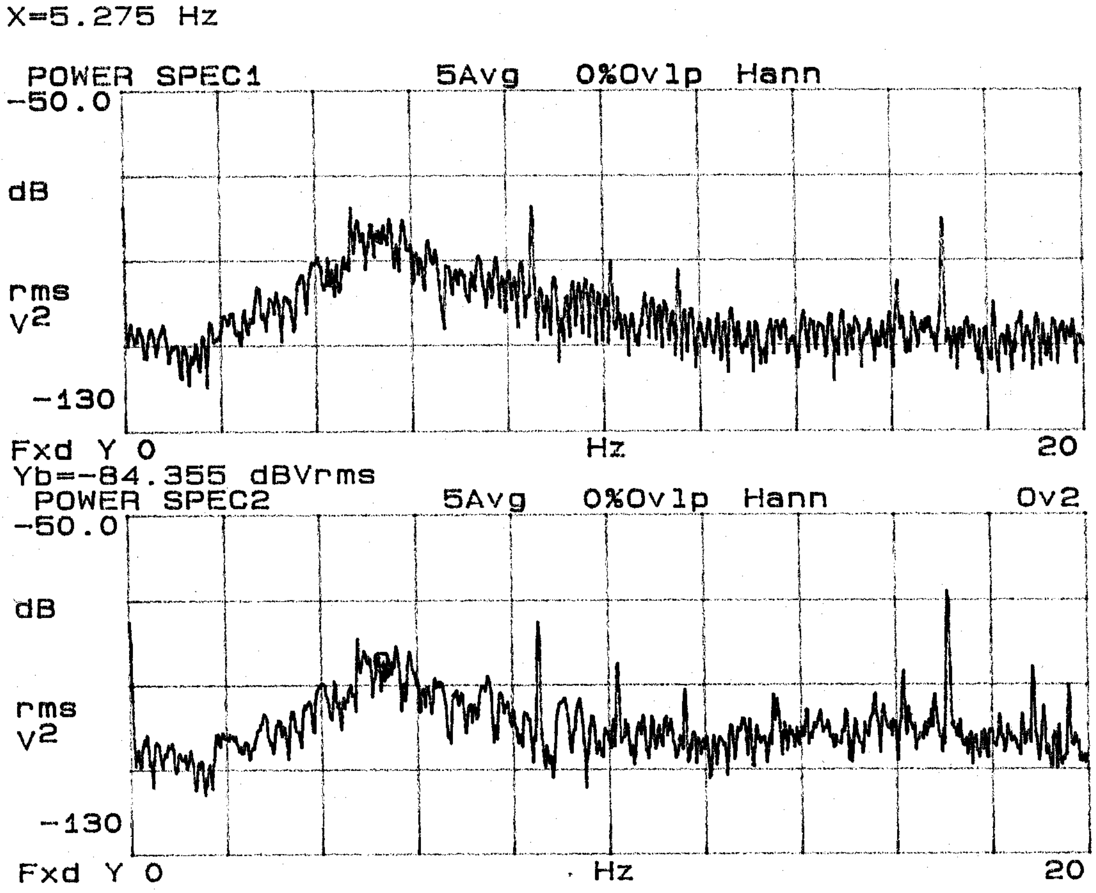

- ground noise excited ~~transfer function (Horizontal to Horizontal)~~ Power Spectrum
- Bottom accelerometer is taped on support plate in horizontal position

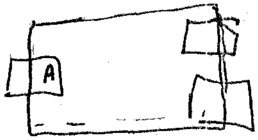

- ~~Top accelerometer on center of plate~~
- 5 averages

shows that horizontal resonance of plate + SS on rubber springs is ~ 5.275 Hz

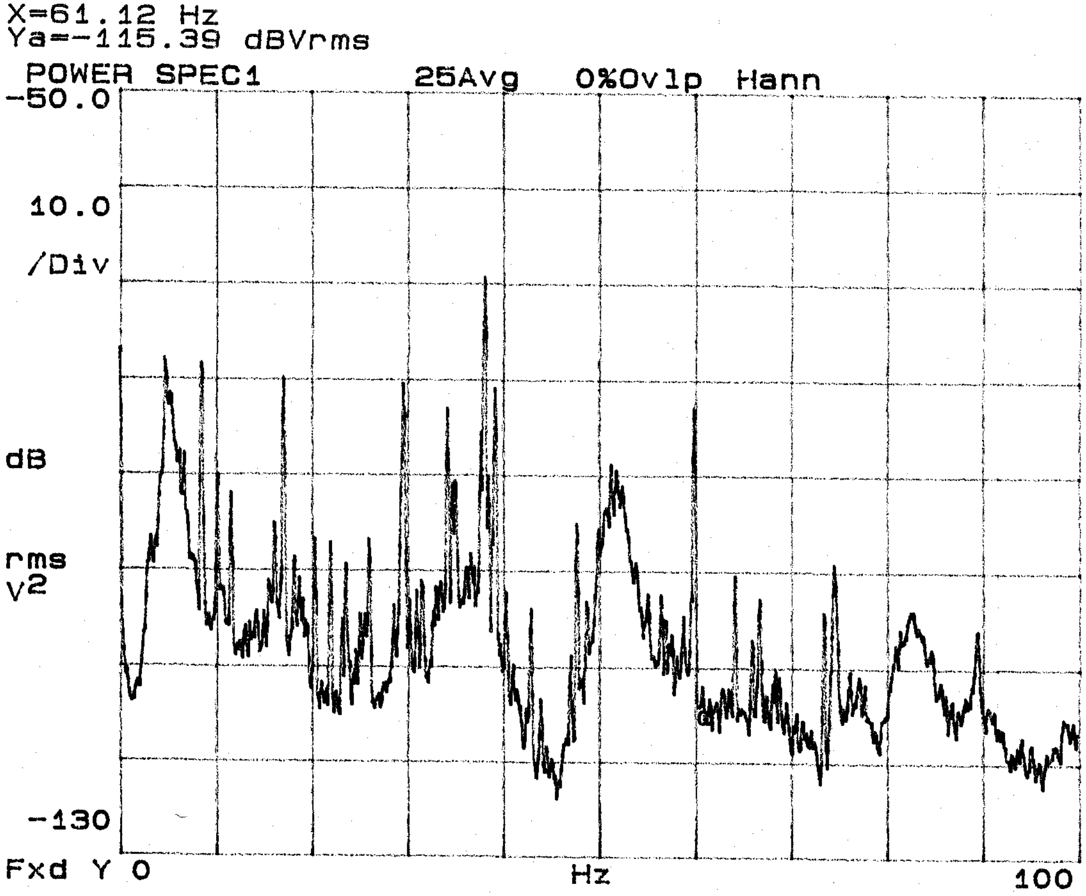

file SST5
horizontal - ground excited
power spectrum Acc 1
in pos. A on prev. plot.

Oct. 12, 1992
3:00 PM
File: SST6

- horizontal to horizontal transfer fctn with shaker excitation

ve=5
ytime = 500 msec
0 pt/dec
nce level = 50 mV rms
ll gain on crown

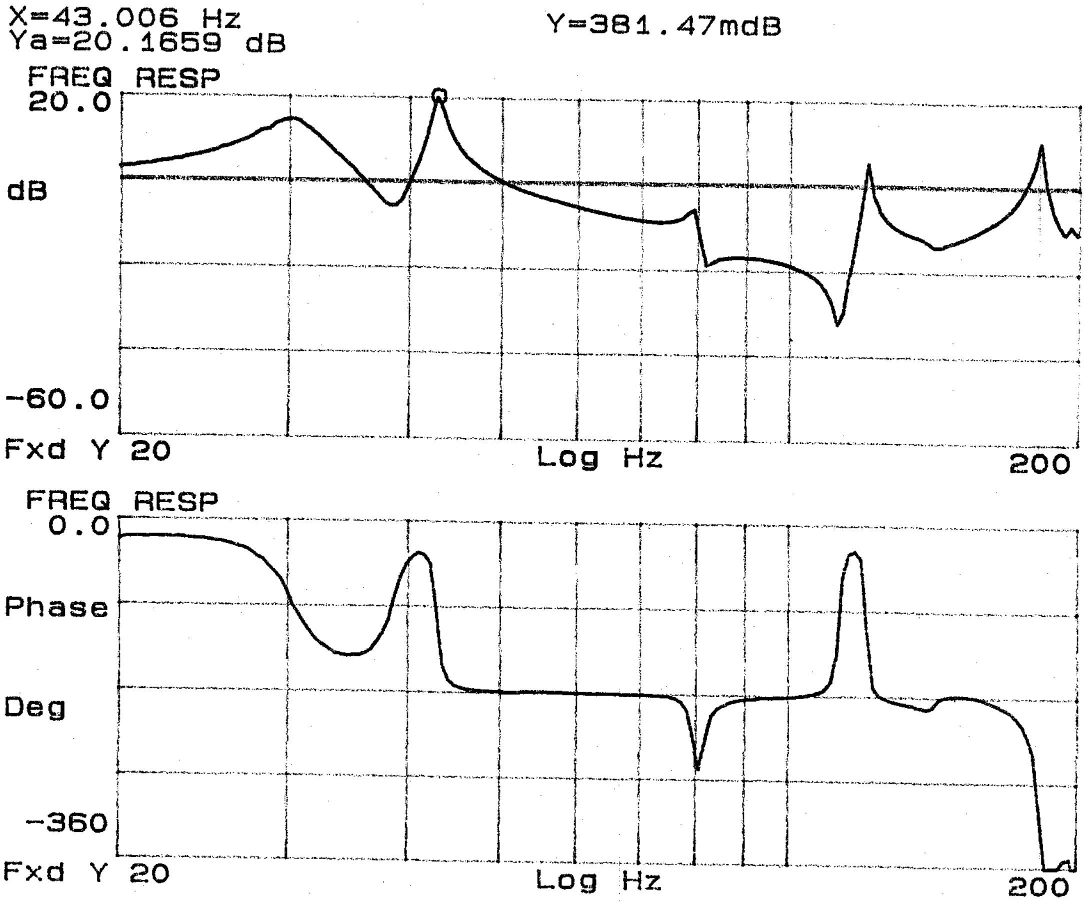

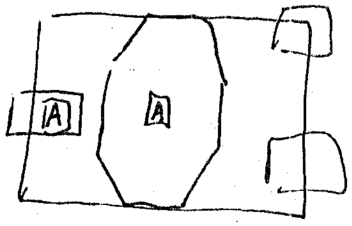

- Top accelerometer on center of plate
- Bottom accelerometer taped on position [A] on support plate bolted to optical table

Shaker drive is: oriented in transverse direction

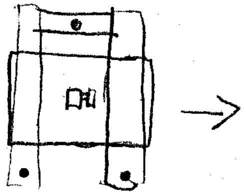

Oct 12, 1992
3:45 PM

- Transfer Function from horizontal to horizontal motion
- Same as SST6 but bottom accelerometer was placed close to Shaker

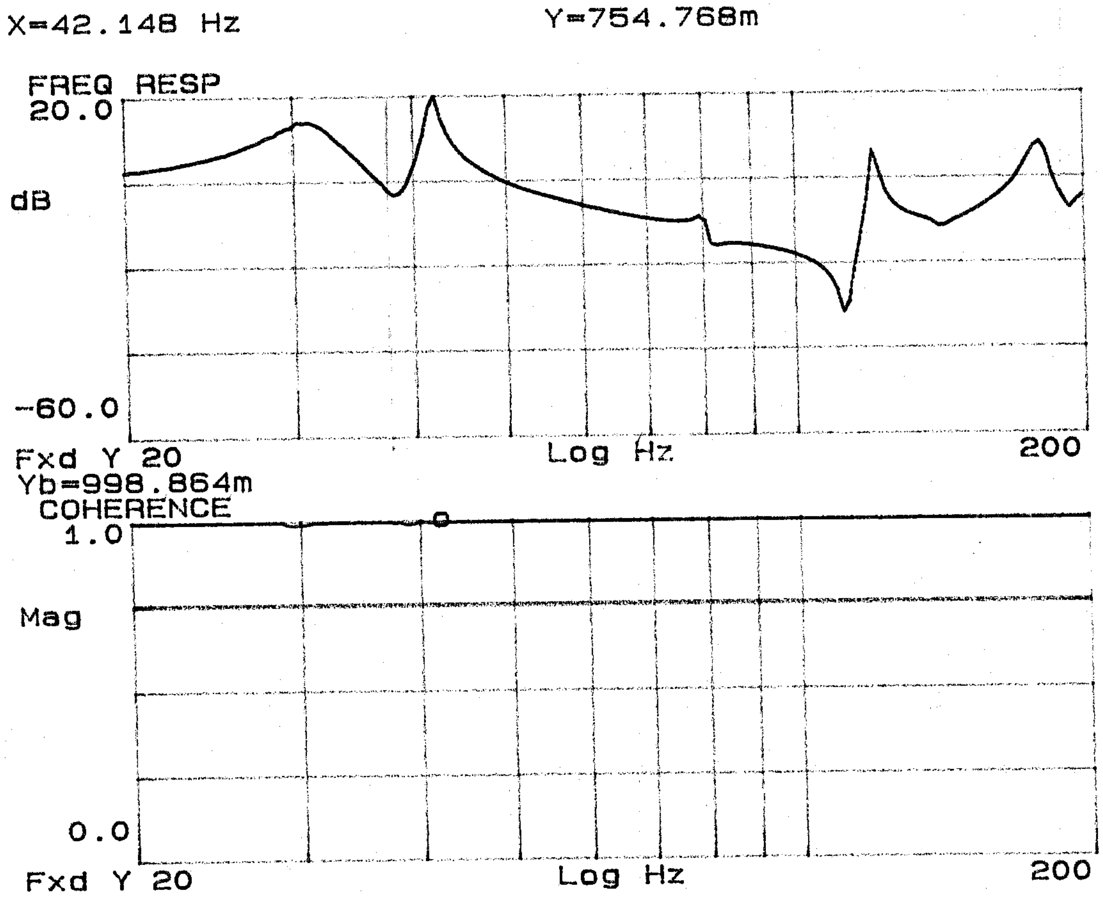

File:SST7

File SST8

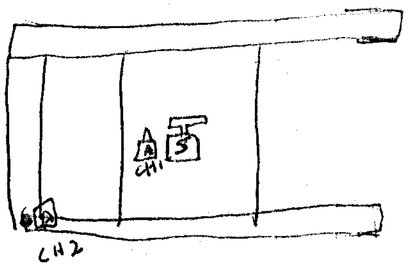

Oct 12, 1992
4:00 PM

- Horizontal drive in transverse direction (same as SST7)
- Vertical to vertical transfer fctn
- Top accelerometer at corner of support structure
- Bottom accelerometer plate by leg

SST9

SST10

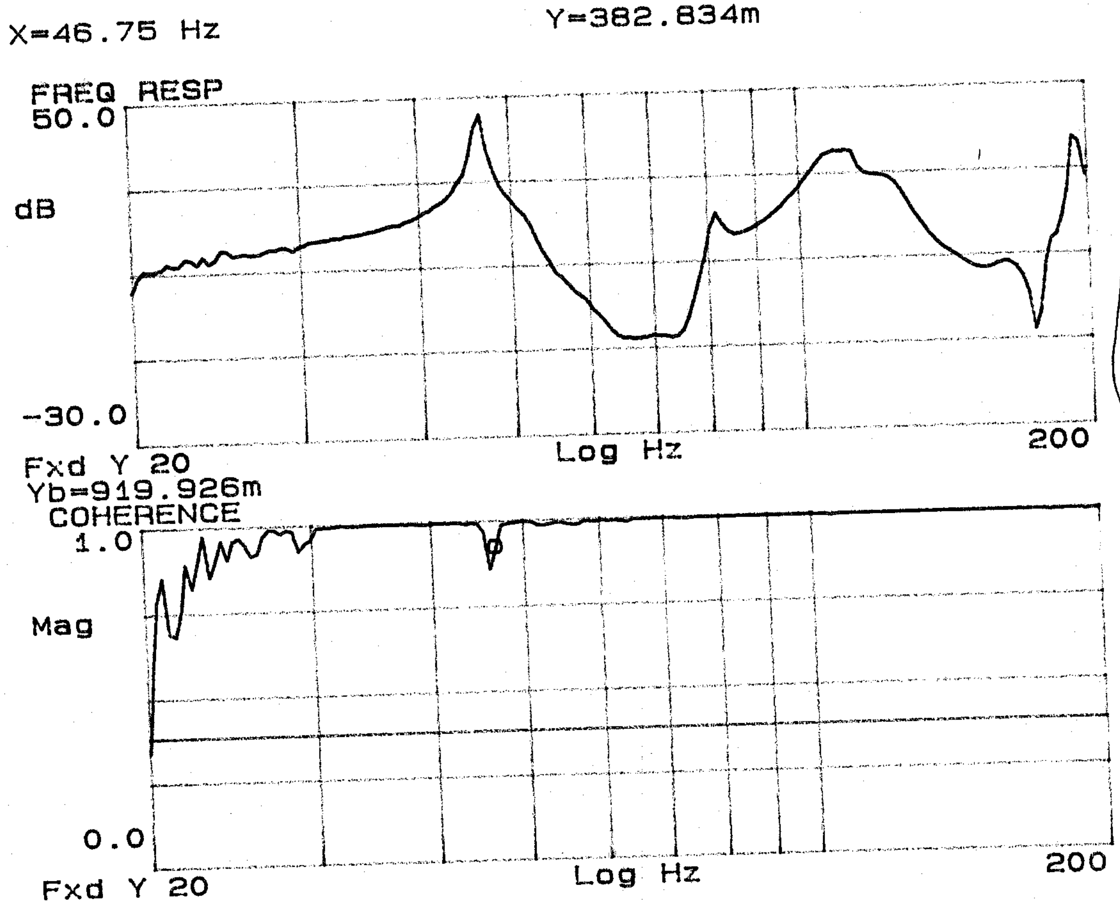

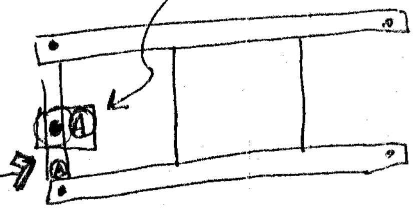

[illegible]
4:45 PM

- Horizontal Drive
- Transfer function from Horizontal to Horizontal

X=46.75 Hz
Ya=-13.098 dB

Y=-54.497mdB

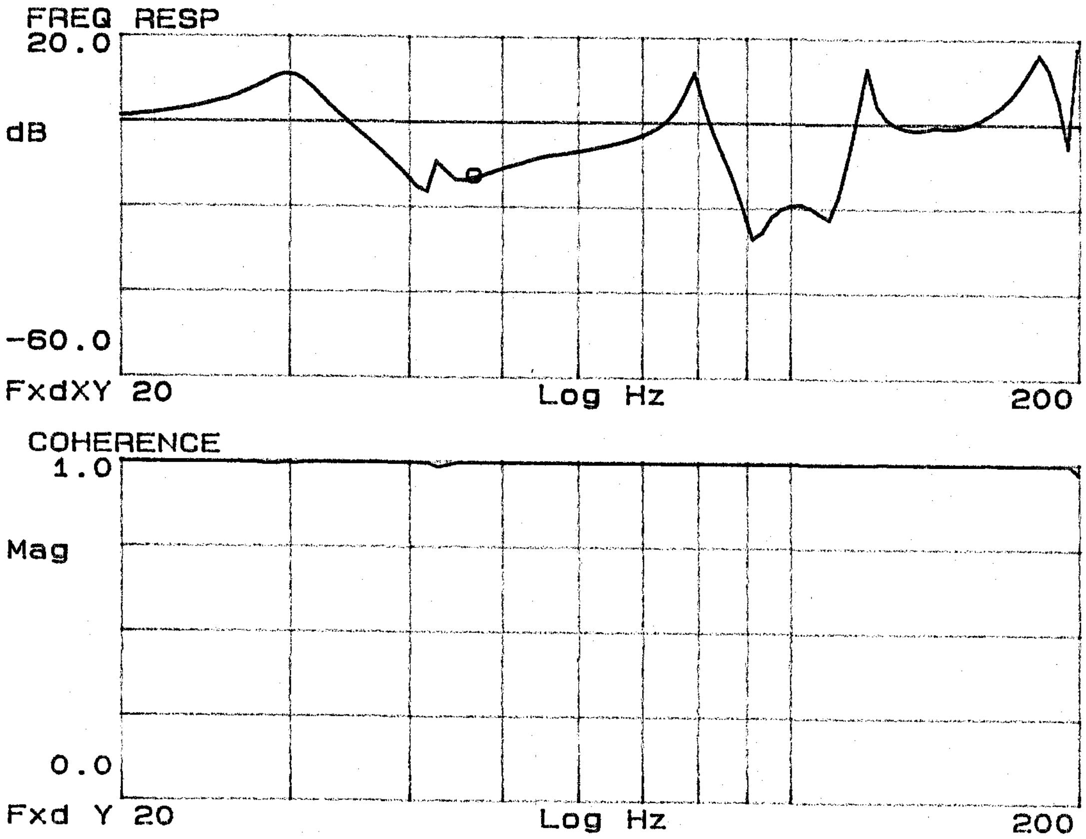

SST11

SST12

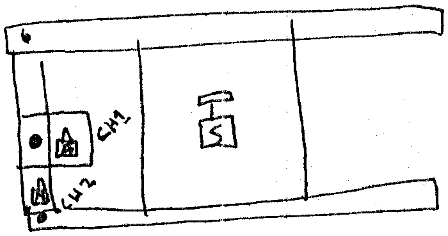

Oct 12, 1992

Power Spectrum of Floor in Horizontal Direction

SST13

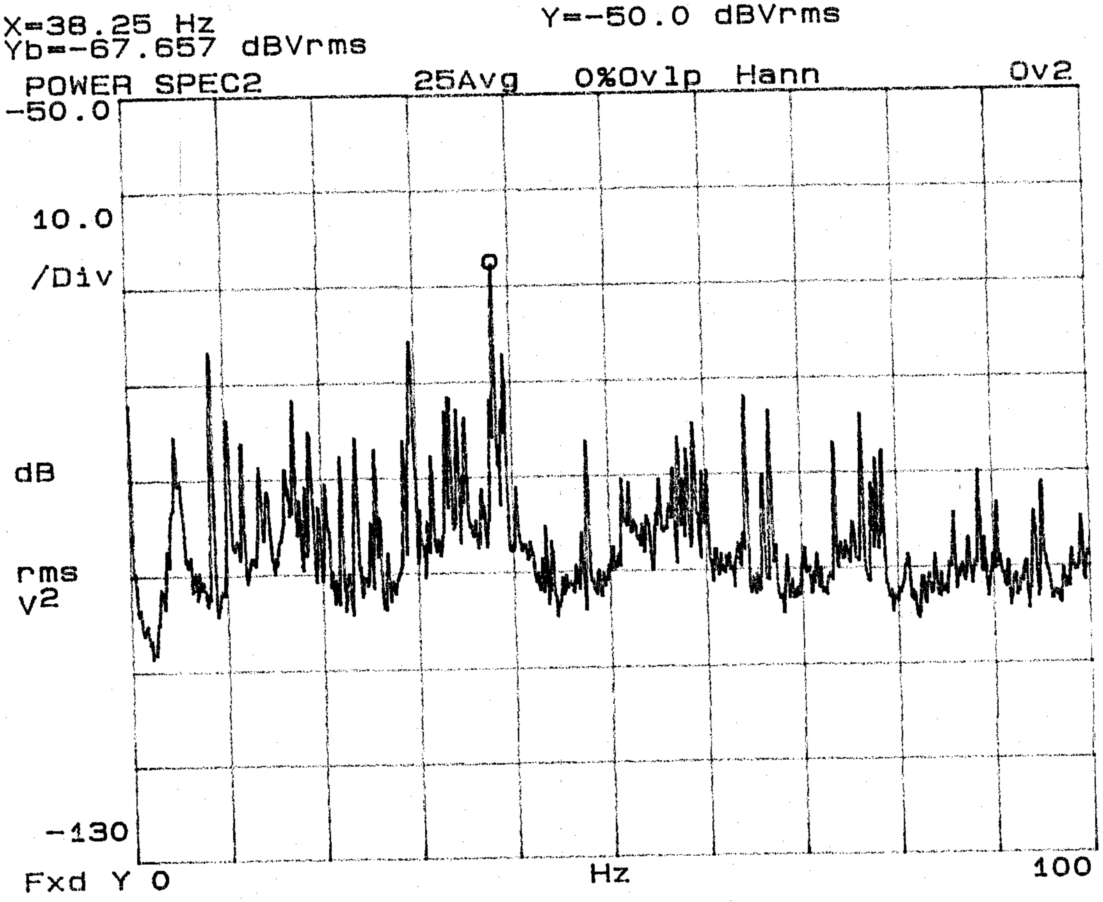

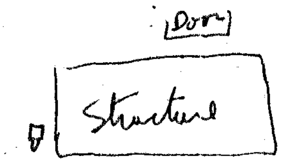

Oct 12, 1992

Power Spectrum of Floor in Vertical direction

door

structure

SST14

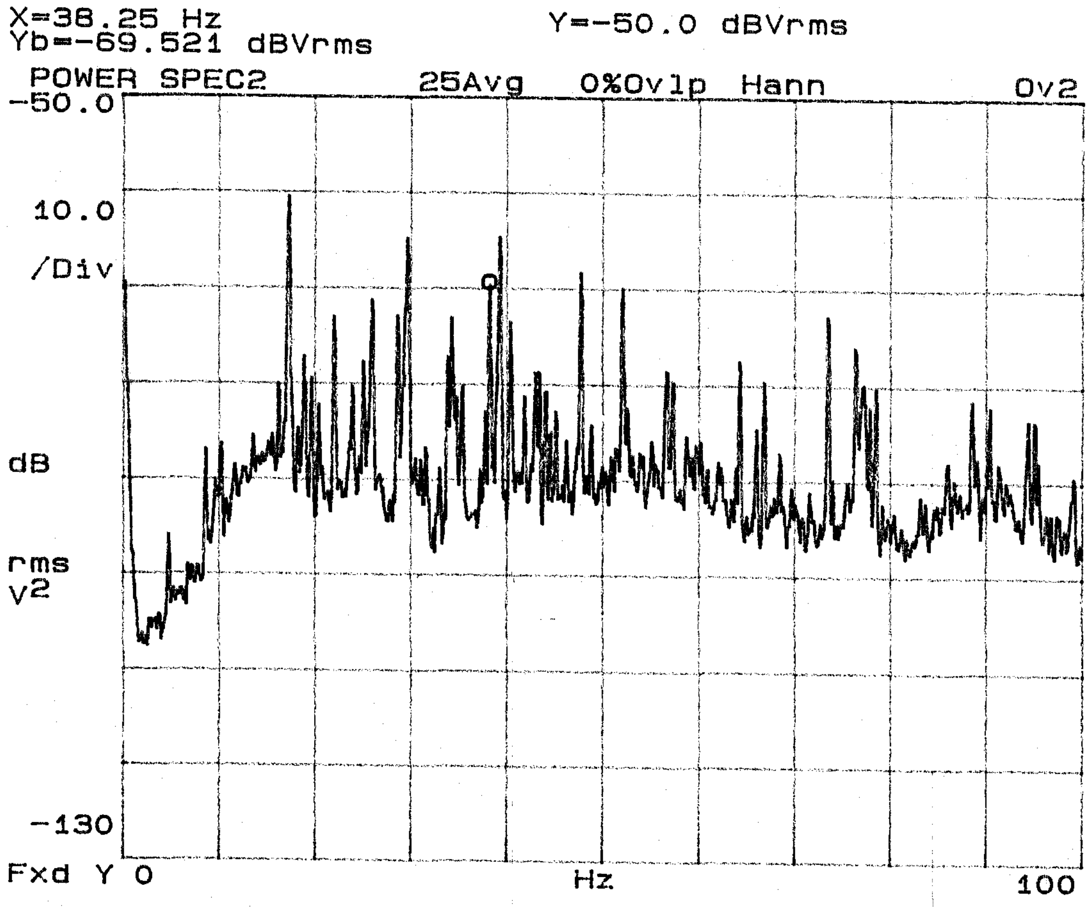

Transfer fctn from
floor to table (optics)
in vertical direction
using ground noise
excitation

SST15

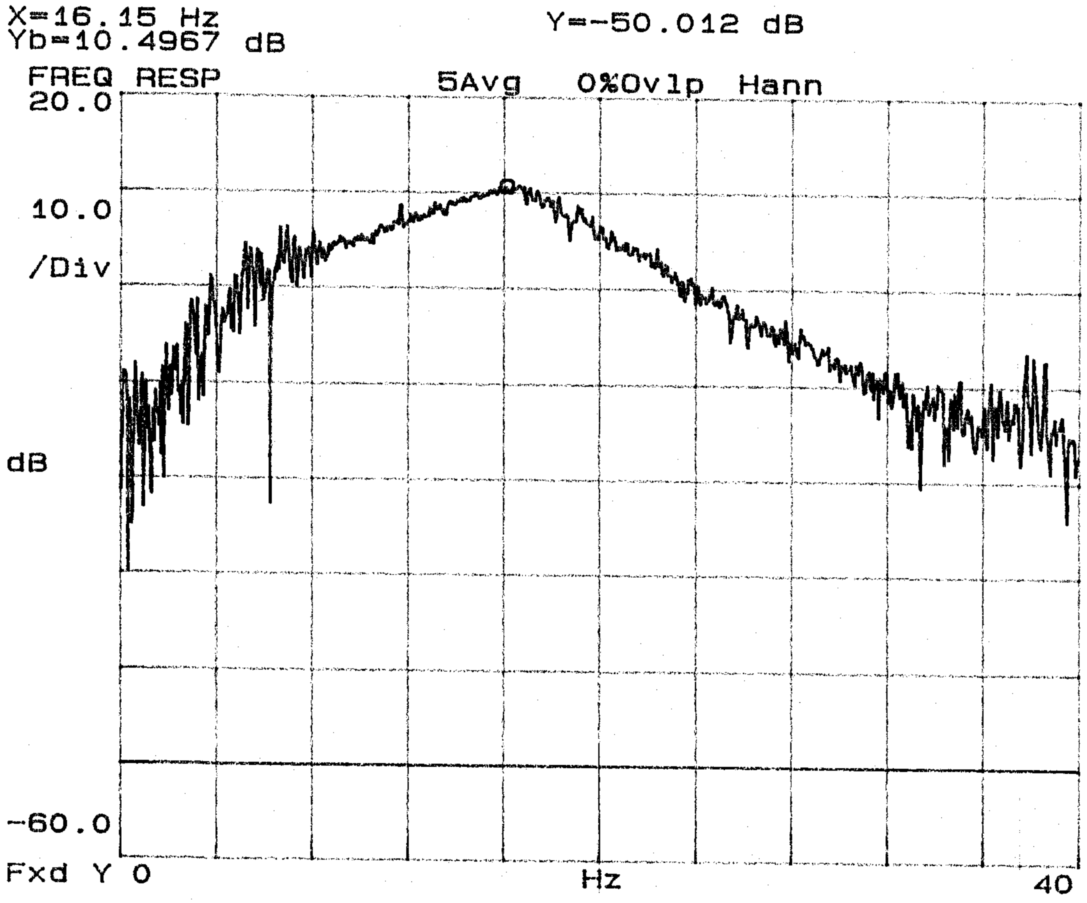

Power spectrum of accel on support

'' '' '' '' '' optics table SST16

10:30 AM

Driven by shaker

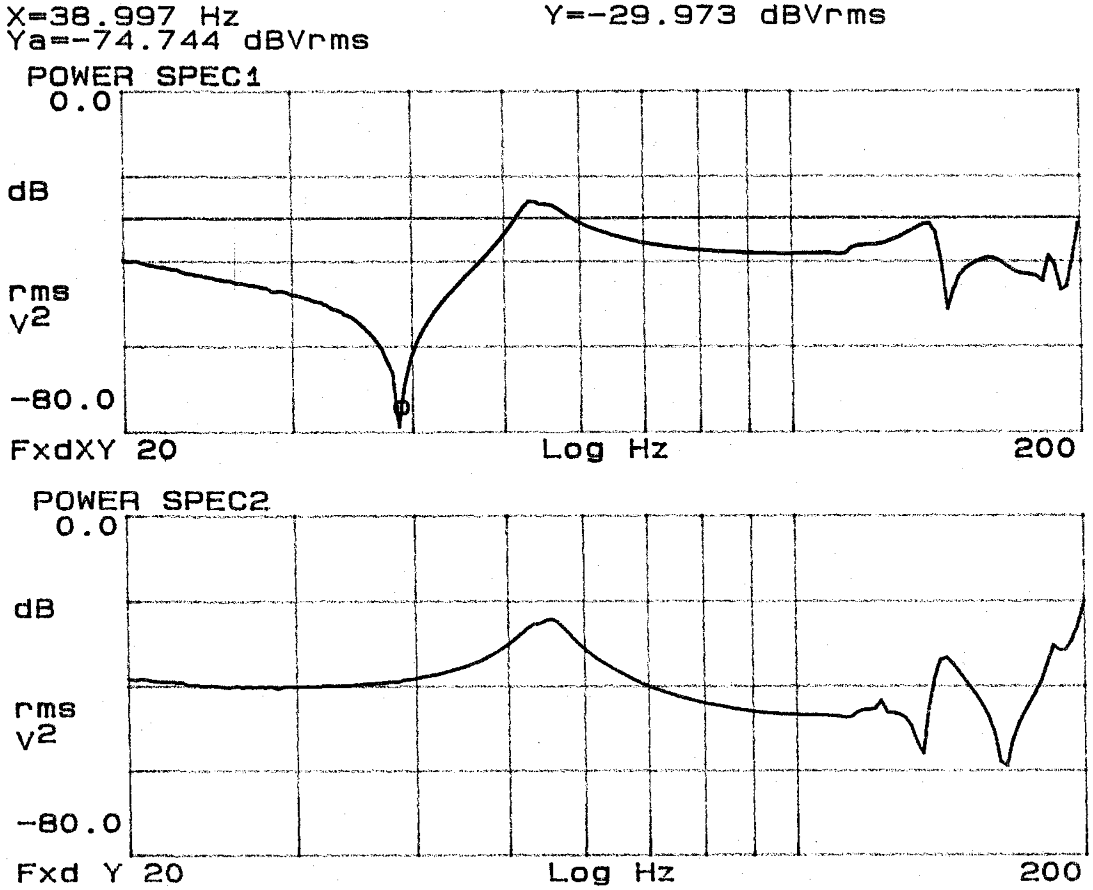

SST16

SST17

Oct 13, 1992
11:30

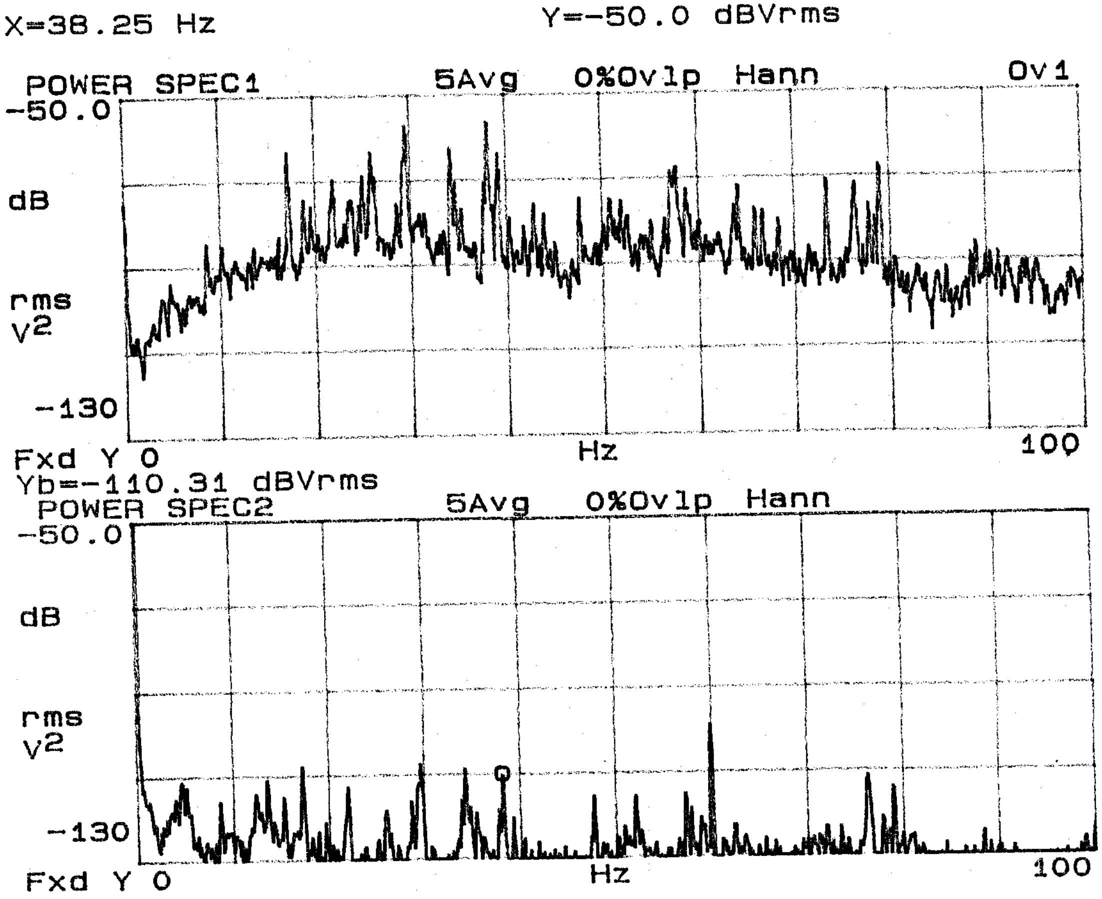

SST18

Power Spectrum of accelerometer at another floor location.

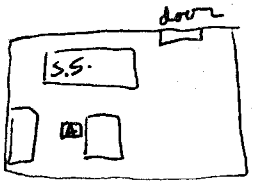

SST19

Power Spectrum of speaker in instrument rack

Oct 15, 1992
11:45 AM

TF

JF1

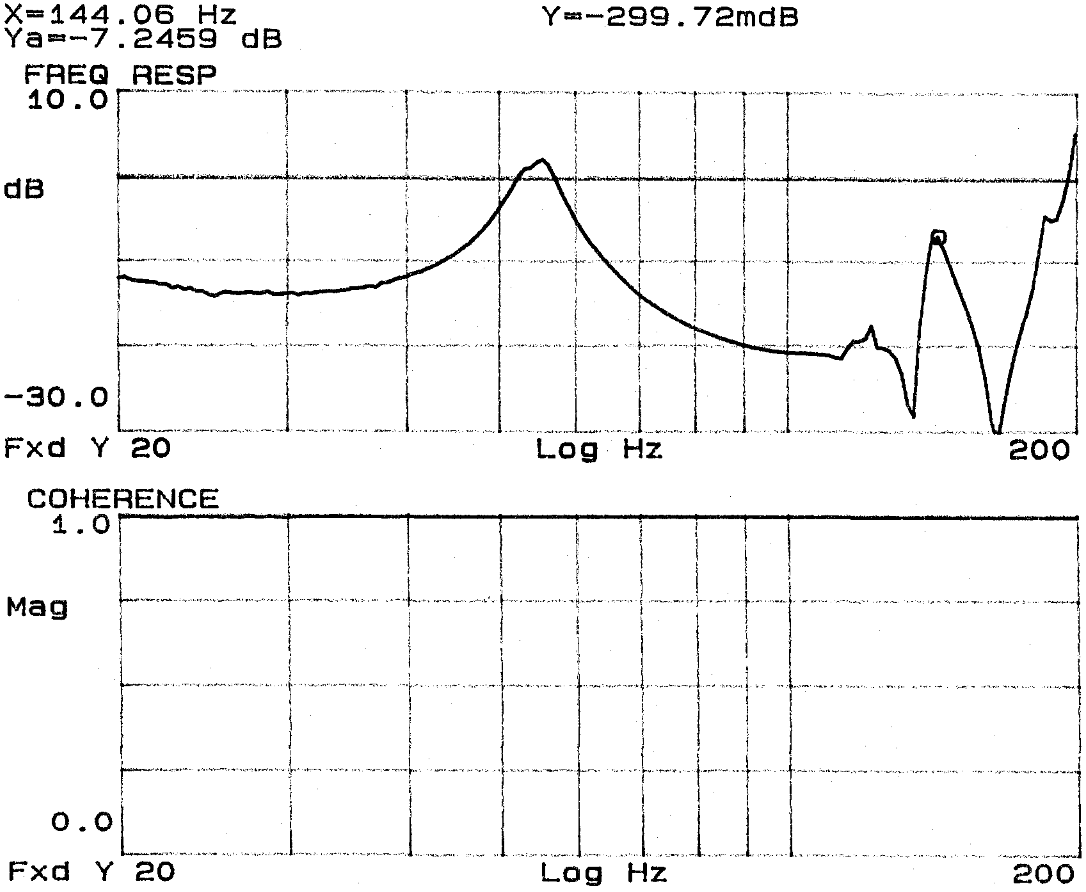

Transfer fctn from Shaker source voltage to voltage of accelerometer on center of support structure in vertical direction

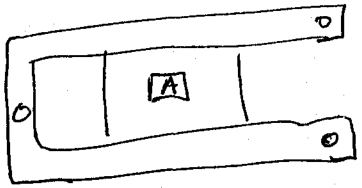

- Transfer Fctn from Vertical shaker voltage to vertical motion on cross-bar

Oct 15, 1992
3.45 PM

TF 2

TF 3

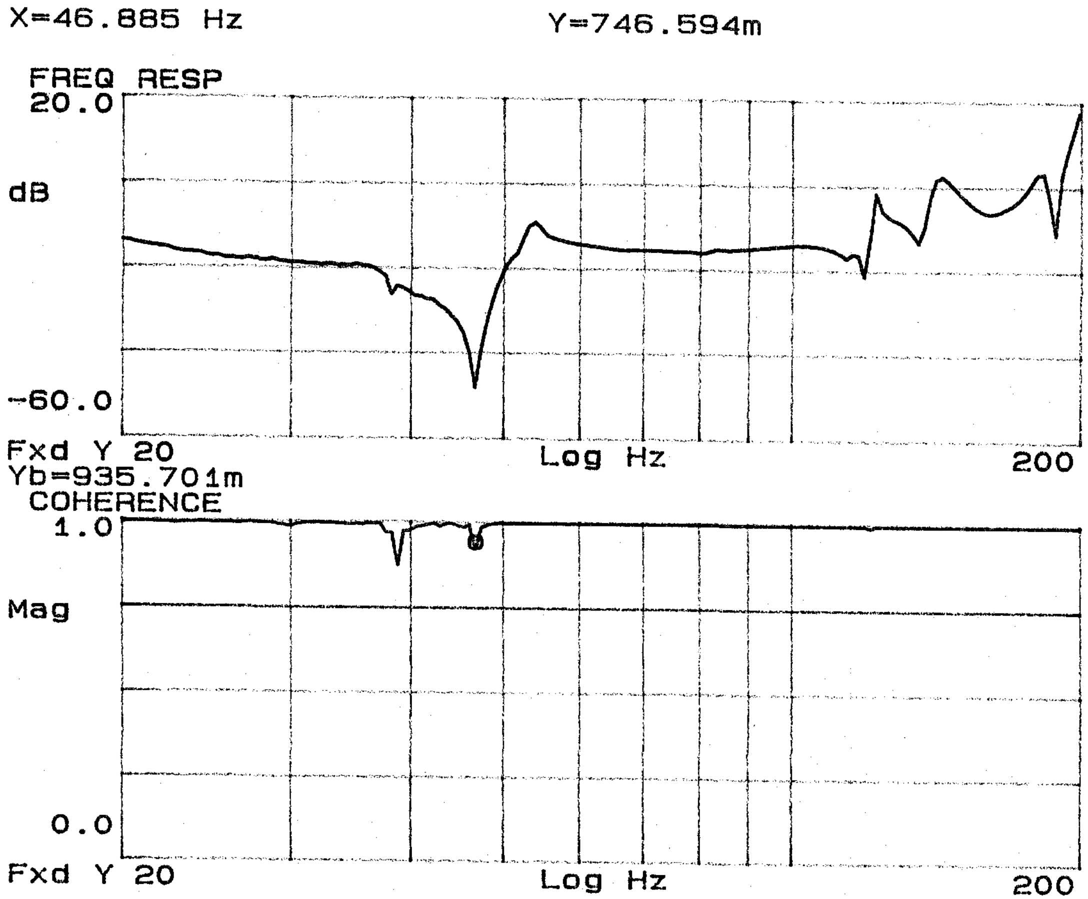

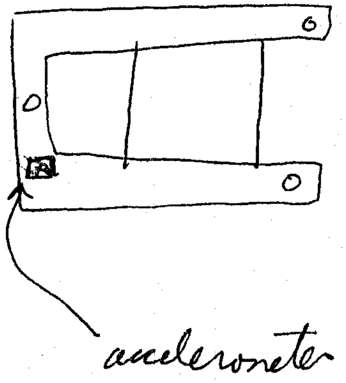

Oct.14,199

Vertical Transfer ftns from source voltage to 3 support points — All 3 were identical

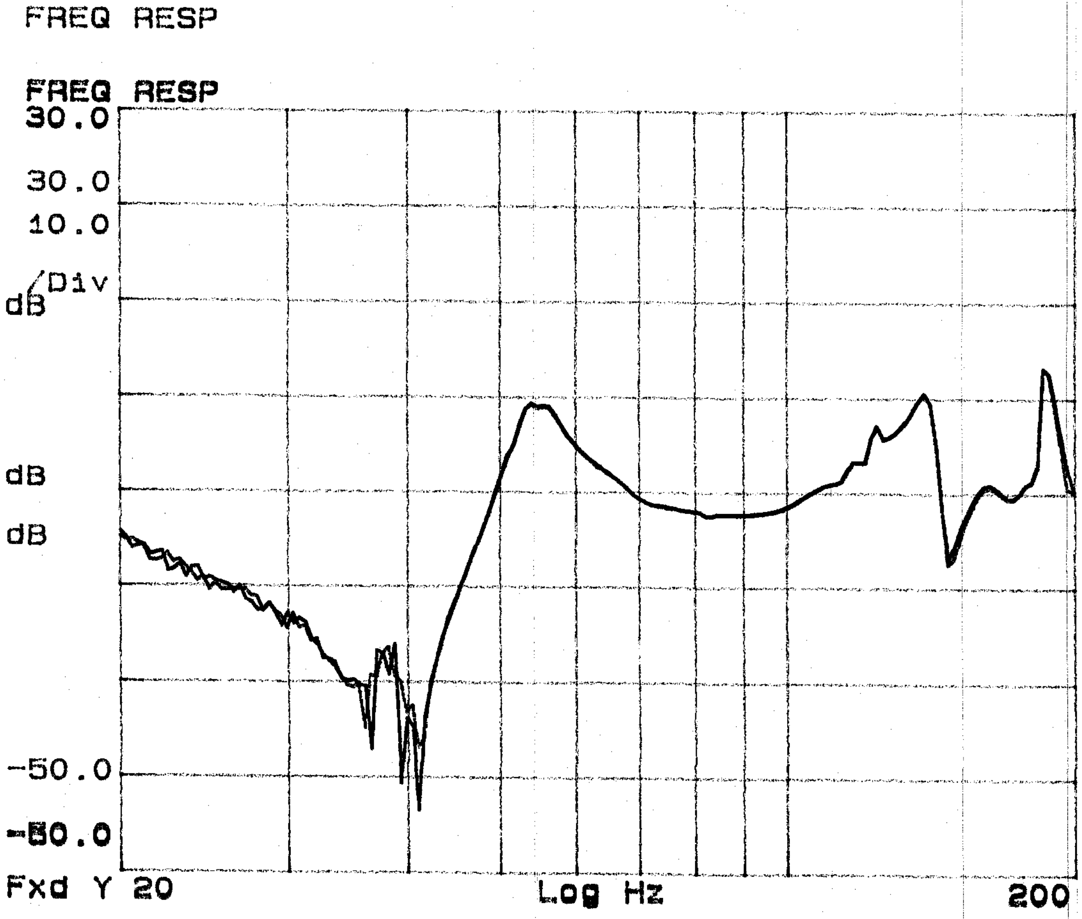

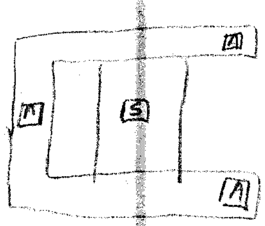

Oct. 19, 1992
1:55 PM

Vertical transfer fcn to
Source voltage to accelerometer
next to shaker

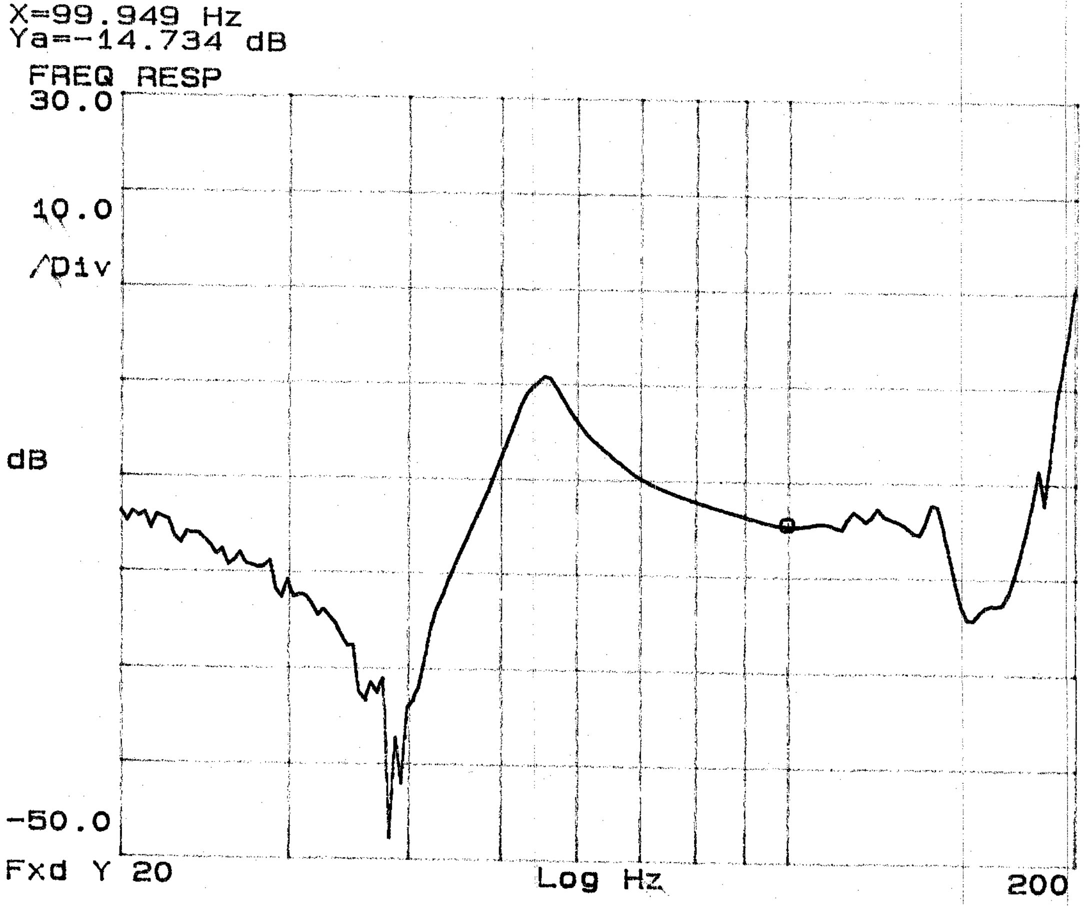

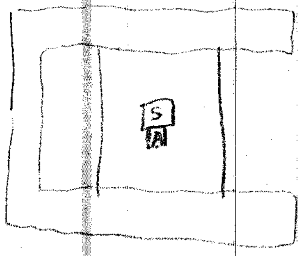

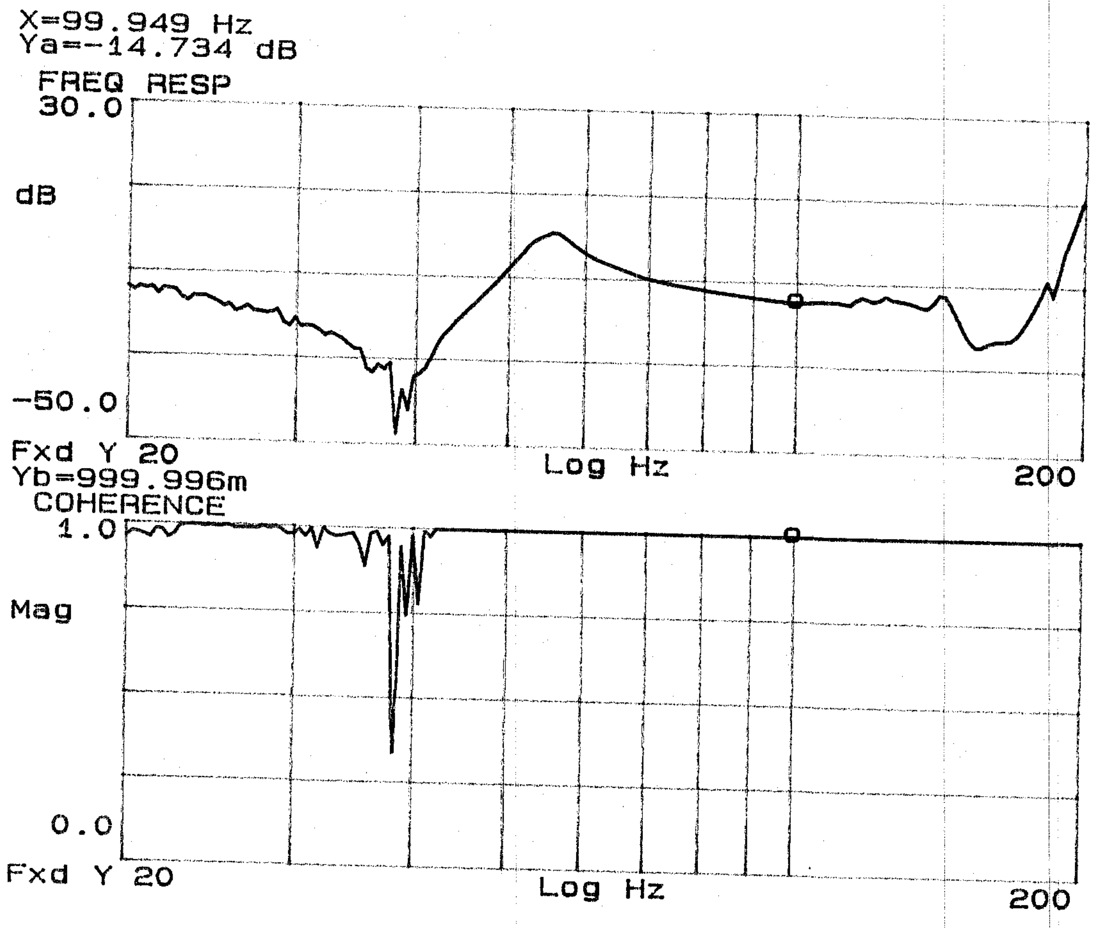
X=99.949 Hz
Ya=-14.734 dB
FREQ RESP
30.0
dB
-50.0
Fxd Y 20
Log Hz
200
Yb=999.996m
COHERENCE
1.0
Mag
0.0
Fxd Y 20
Log Hz
200

Oct, 19, 1992
2:05 PM

Vertical transfer fctn
from source voltage
to accelerometer voltage

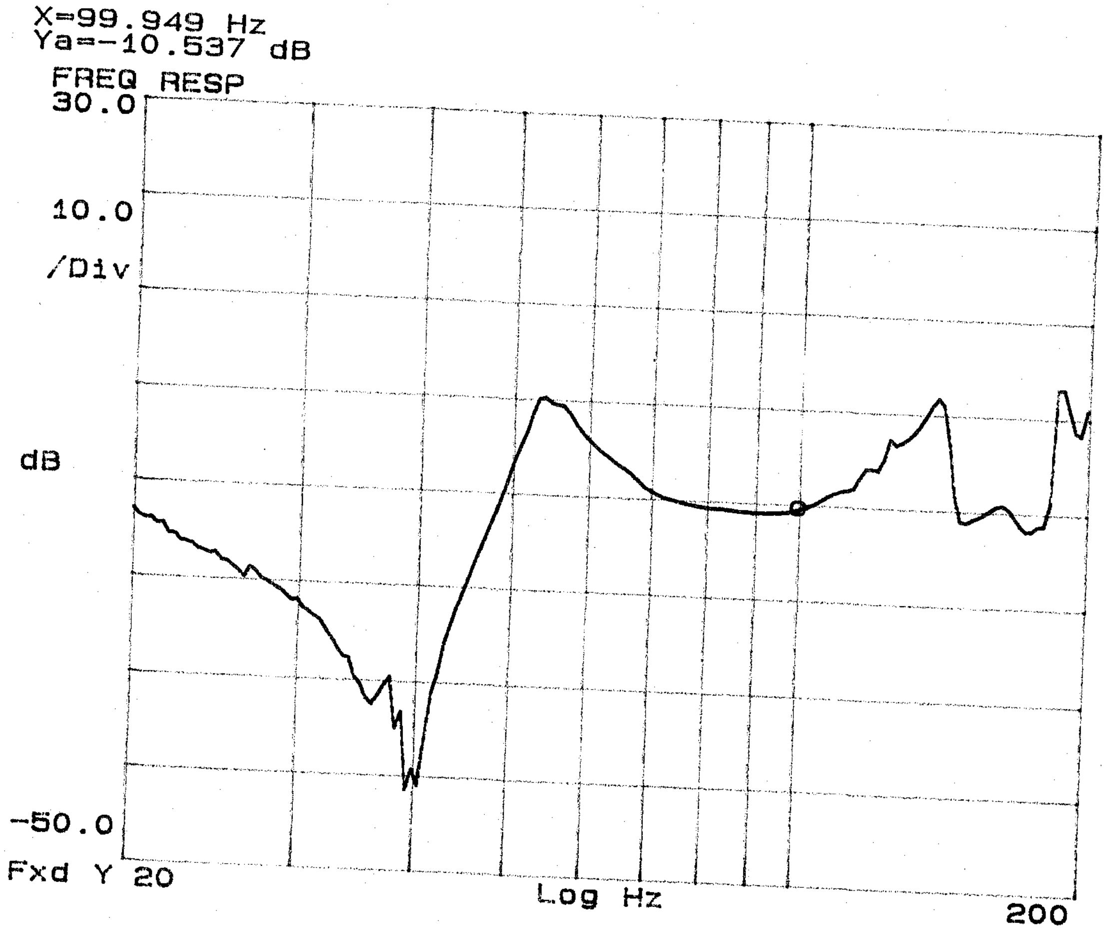

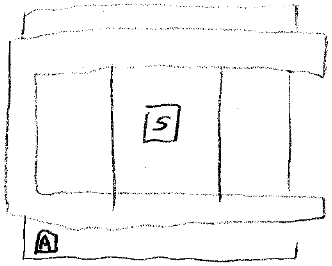

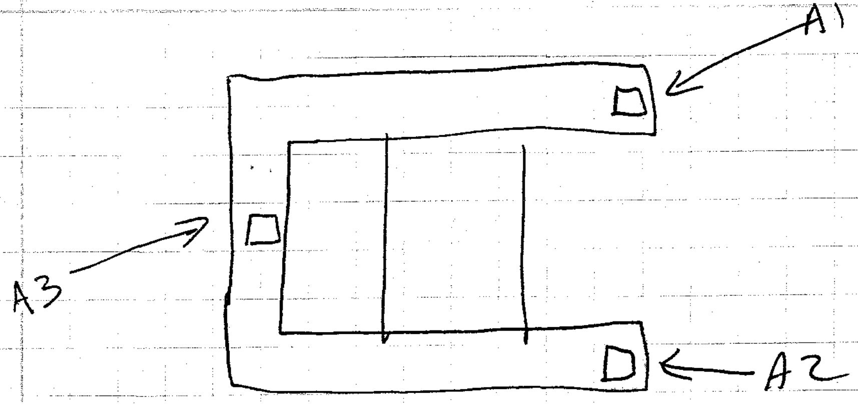

Did transfer functions from source shaker voltage to each of the three plates that the support structure are mounted on (in vertical position) - they were all identical over a 200 Hz span

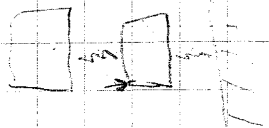

1:30 PM

Transfer function in vertical direction from floor to optics table (ground noise excited)

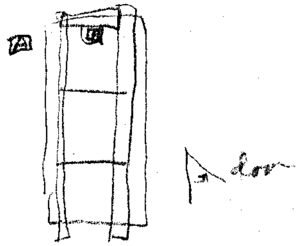

Accelerometer at base of optics table and at base of drift compensation under cross bar

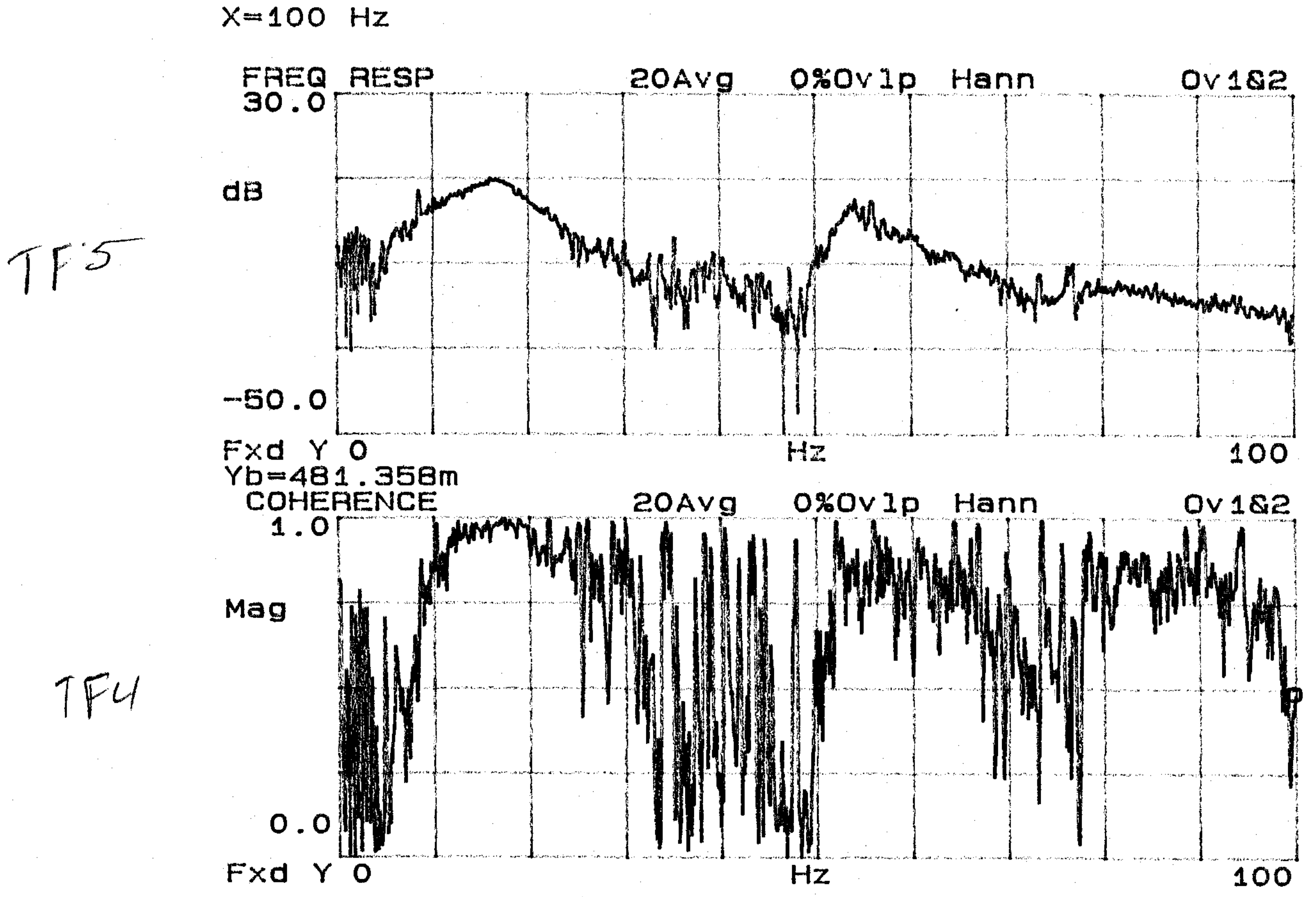

October 19, 1992
1:45 PM

Transfer function in vertical direction from floor to top of base plate

TF6

TF7

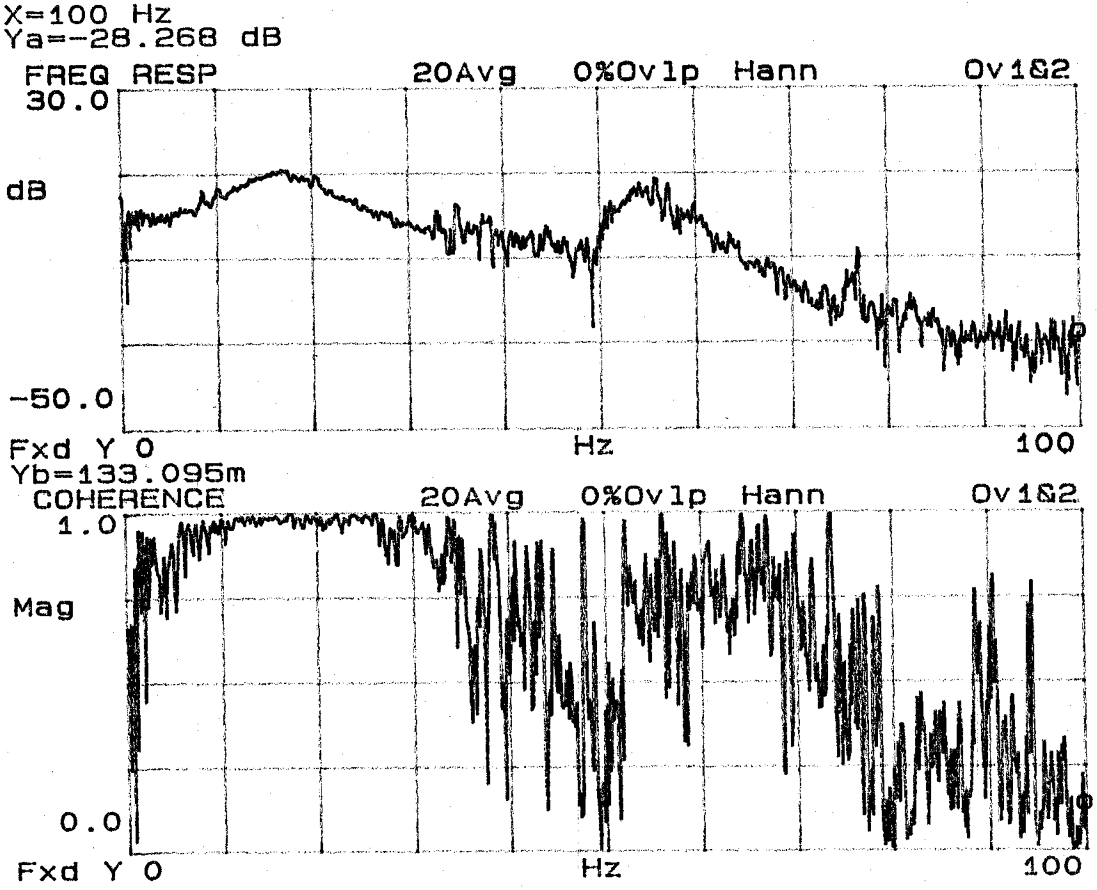

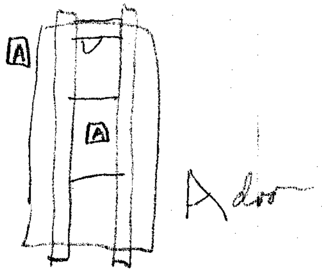

Accelerometer at base of optics table and in center of base base plate

10/14/92
4:30 Pm

— Vertical to horiz. transfer fctr.

TF8

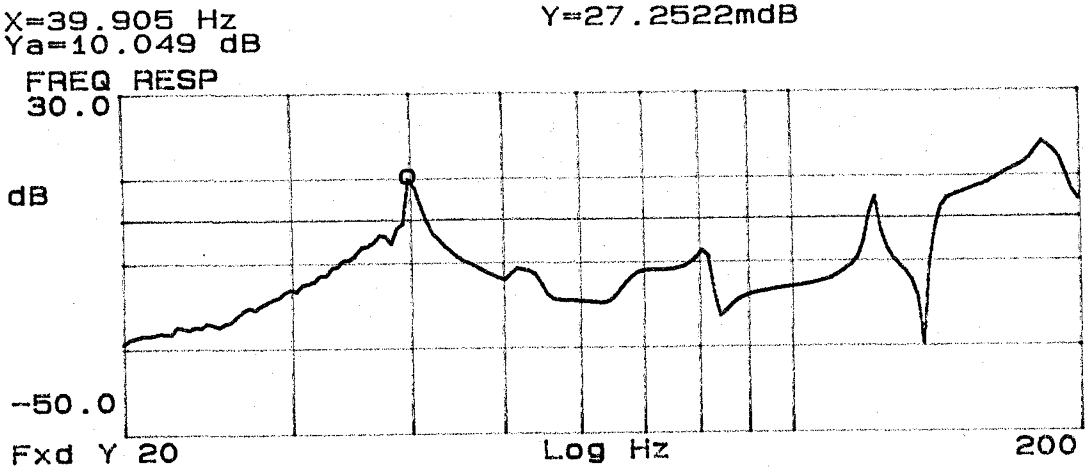

- Shaker is shaking vertically
- accelerometer on optics table at North diff compensator
- accelerometer on N-W side of support structure

TF9

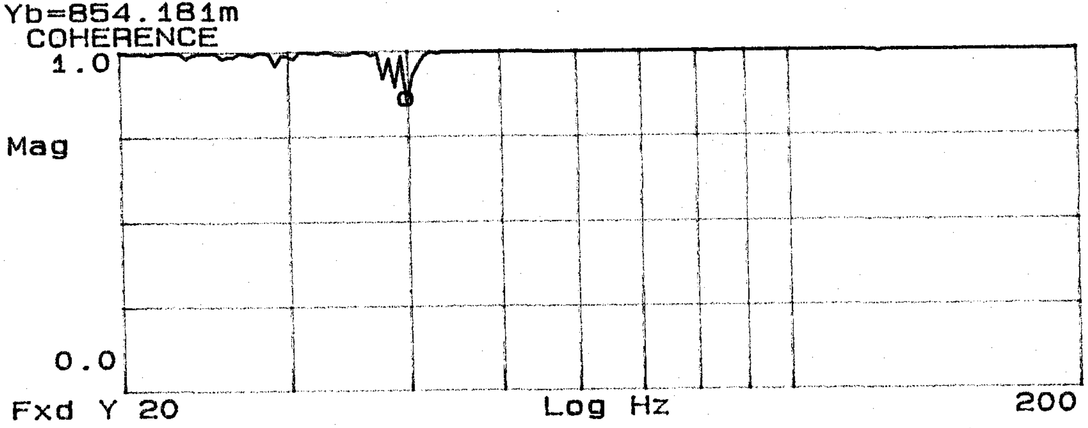

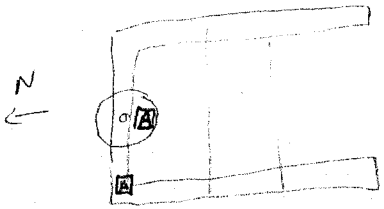

Ave=2
Integ time=500msec
Source level=100mVrms
Gain setting=max

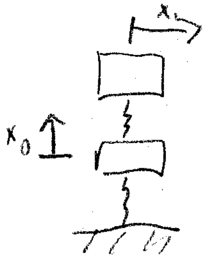

10/14/92
5:00 PM

- Vertical to horiz transfer fctn.

TF10

TF11

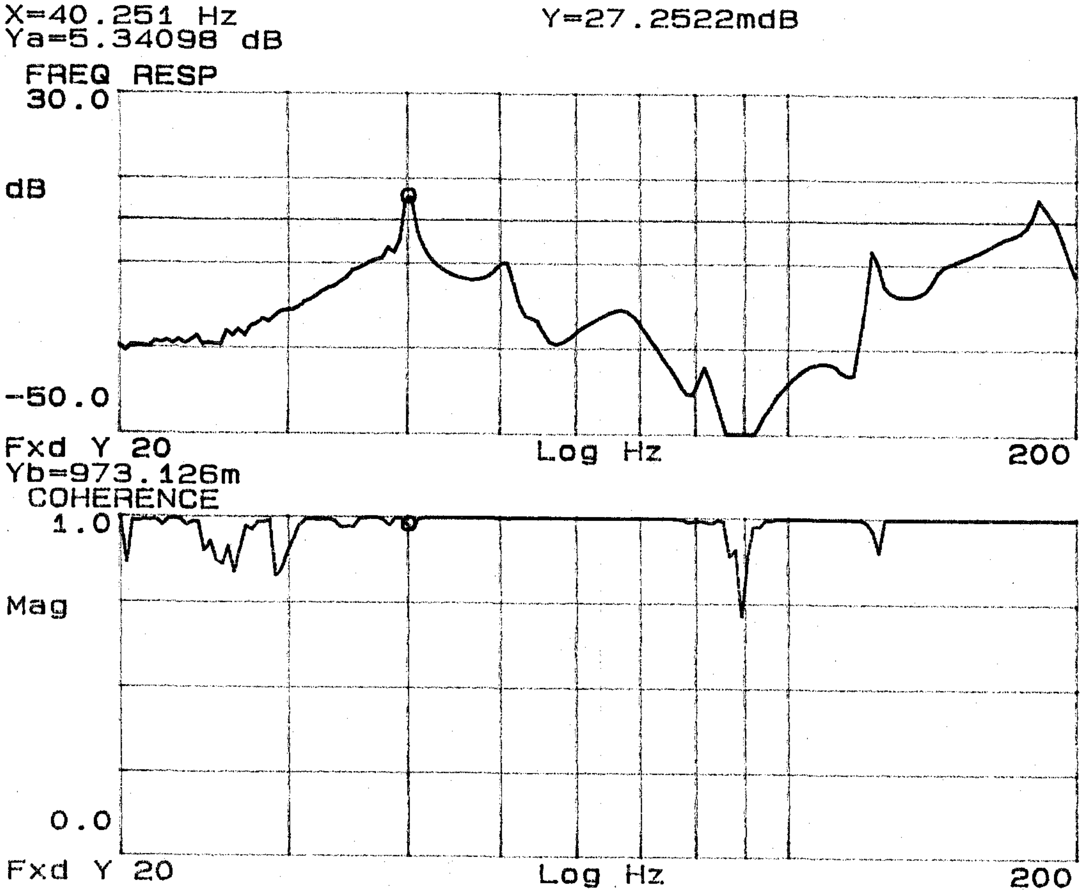

- shaker is shaking vertically
- accelerometer on optics table at North drift compensator
- accelerometer on center of support structure

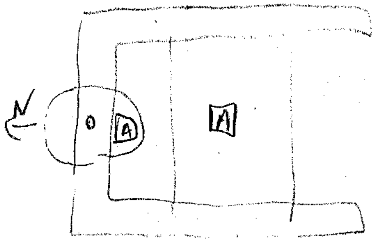

Ave: 2
Integ time: 500 msec
Source level: 100mV rms
Gain setting: max

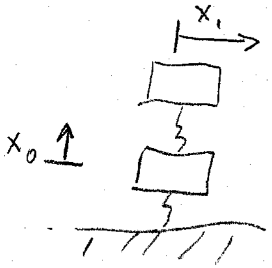

10/19/92
5:15 PM

- V to V transfer fctn
- V shaking
- accel on NW corner of SS (Top)
- accel on North drift compensator on optics table (Bottom)

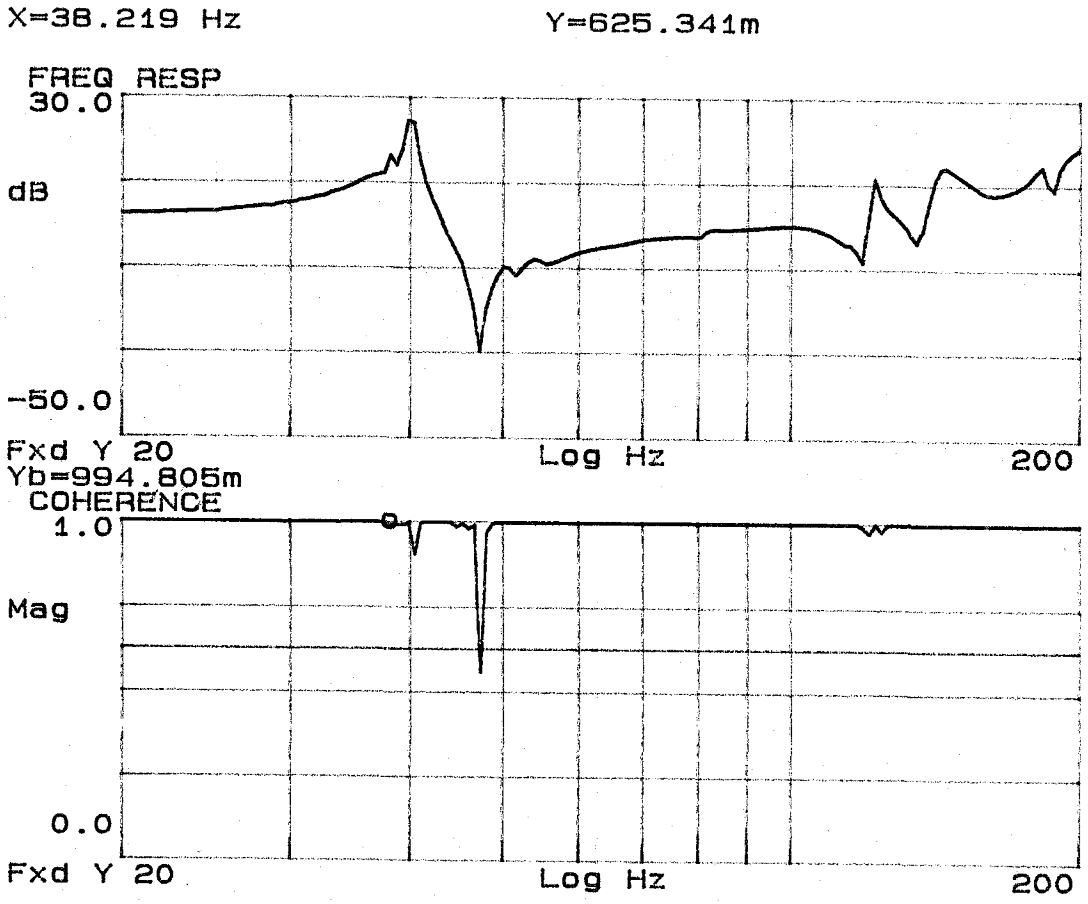

TF12

TF13

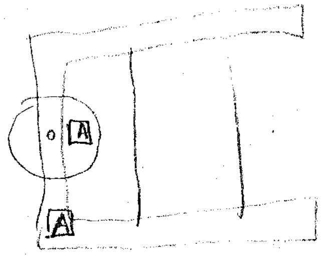

- Same as SST3.
- Note resonance has shifted

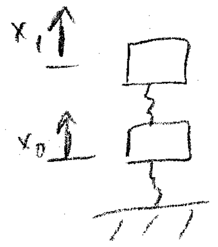

10/19/92
5:35 PM

- Y to V transfer fctn
with V shaking

- accel on center of SS (top)
- accel on North drift
compensator on optics table
(Bottom

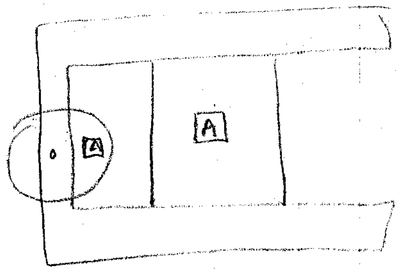

TF14

TF15

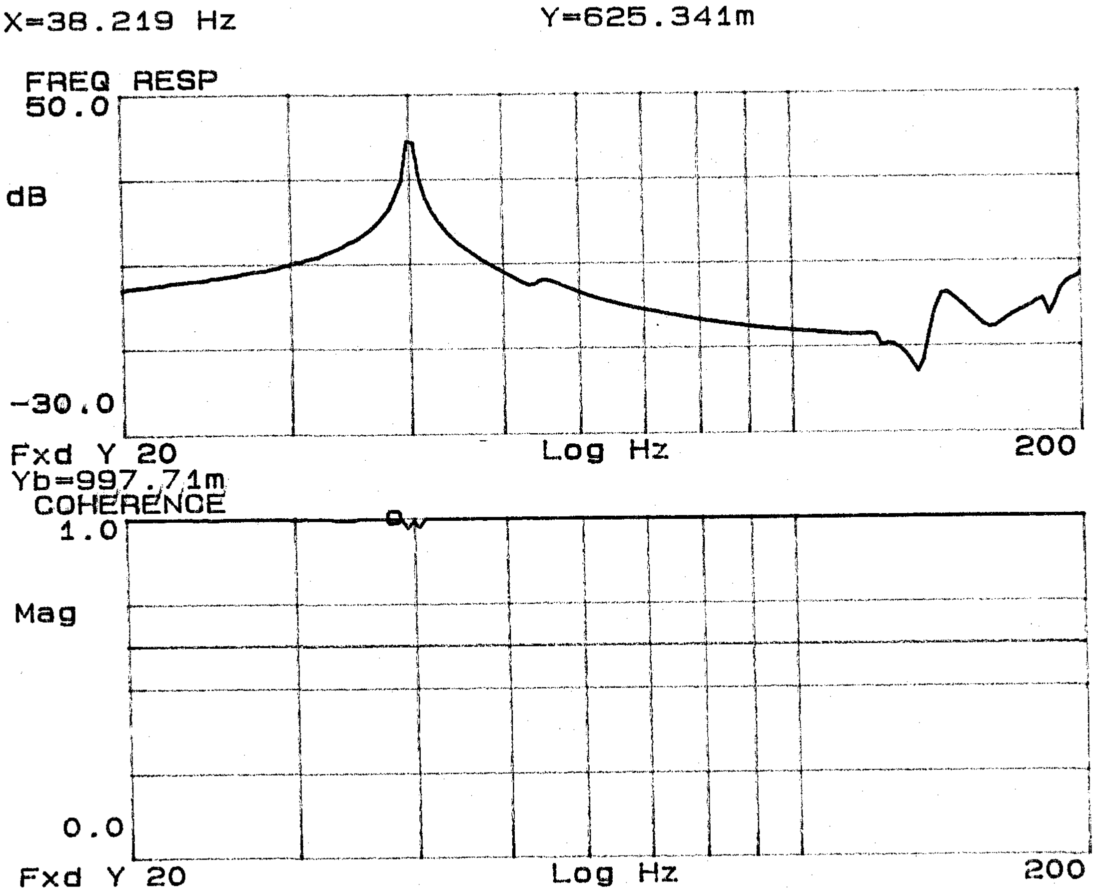

- Same as SS12
- Note resonances shifted

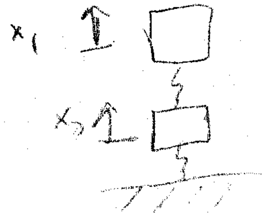

Oct. 20, 1992
9:00 AM

Transfer Fctn from Source voltage to accelerometer at base of North drift compensation

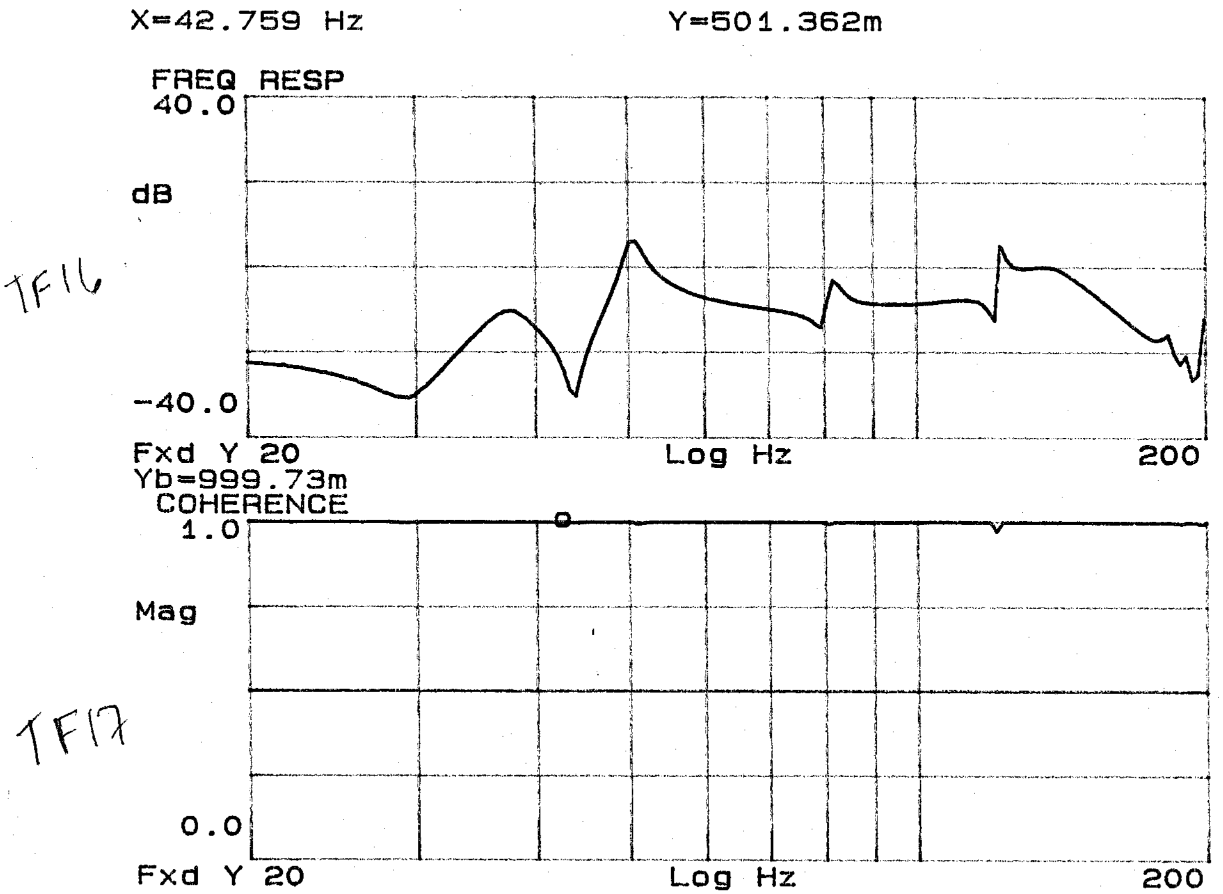

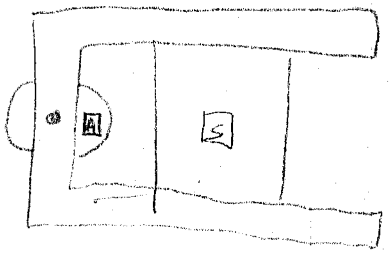

Source = 100mVrms

Oct. 20, 1992
9:50 PM

H-TF from source voltage to accelerometer at base of Southwest drift compensation

TF18

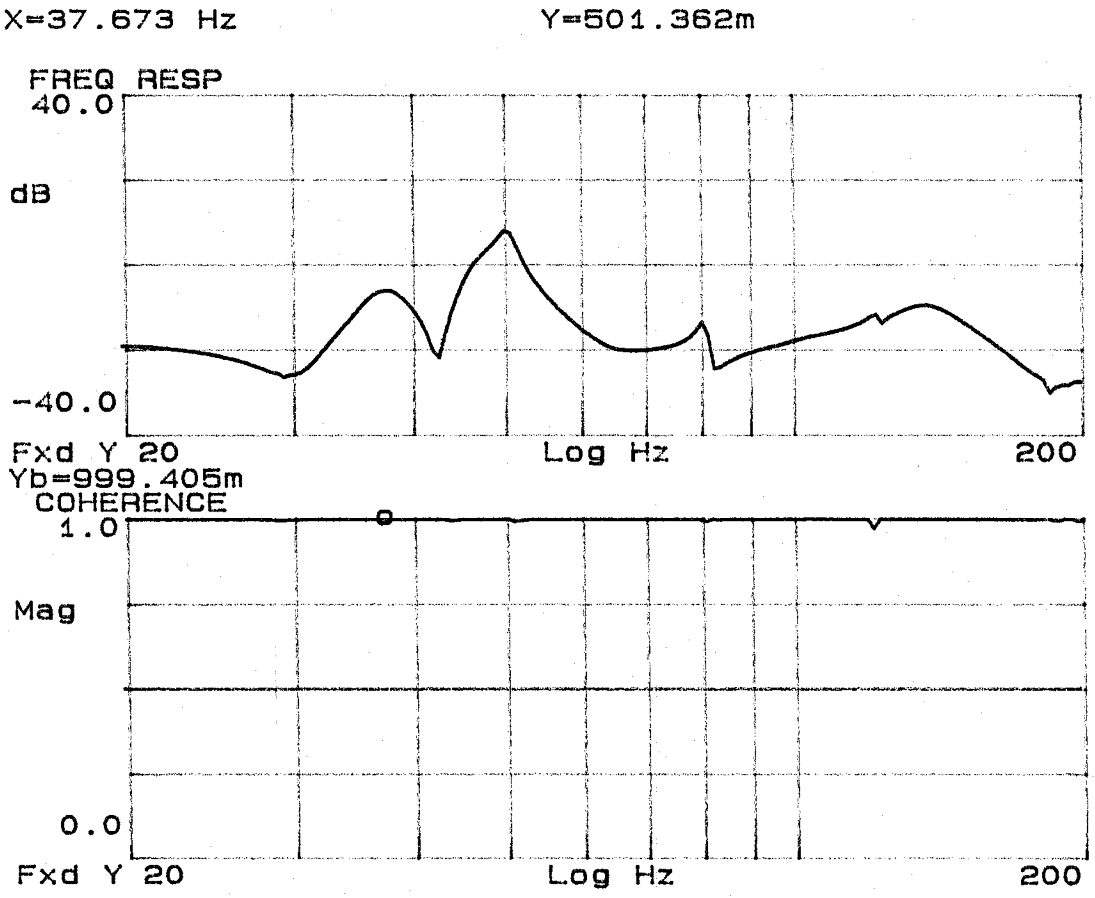

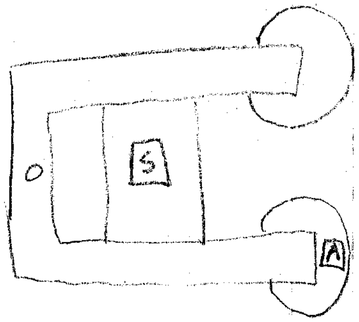

Source=100mVrms

Oct 20, 1992
12:00 PM

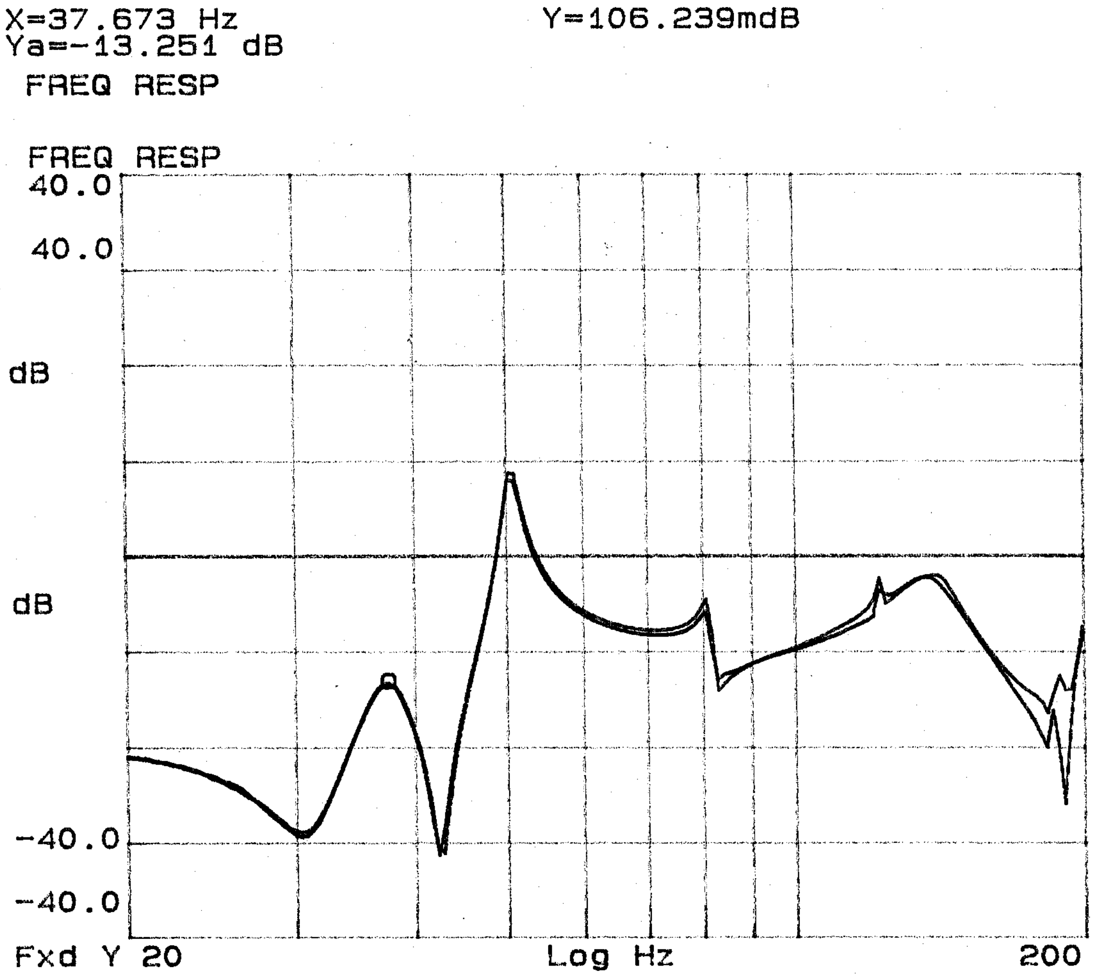

- Transfer fctns from source voltage to horizontal accelerometer position
- Shaker in horizontal orientation
- Source = 100 mVrms
  gain = full

blue : TF20

black : TF21

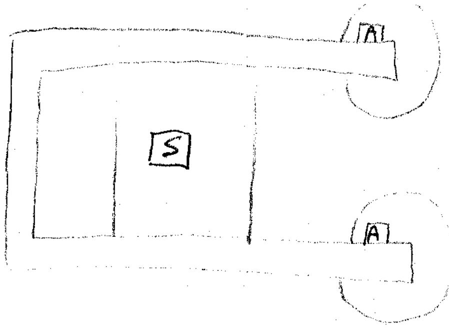

TF20 is from shaker to drift compensation on SE side (accel on drift compensation support plate)

TF 21 is from shaker to drift compensation on SW side (accel on drift compensation support plate)

Shows that table is acting as a rigid body in the horizontal direction

[illegible]

1:00 PM

- TF from Source voltage to horiz accel.
- shaker in horiz position
- Source level 100mV rms gain = full

thin: TF21

thick: TF16

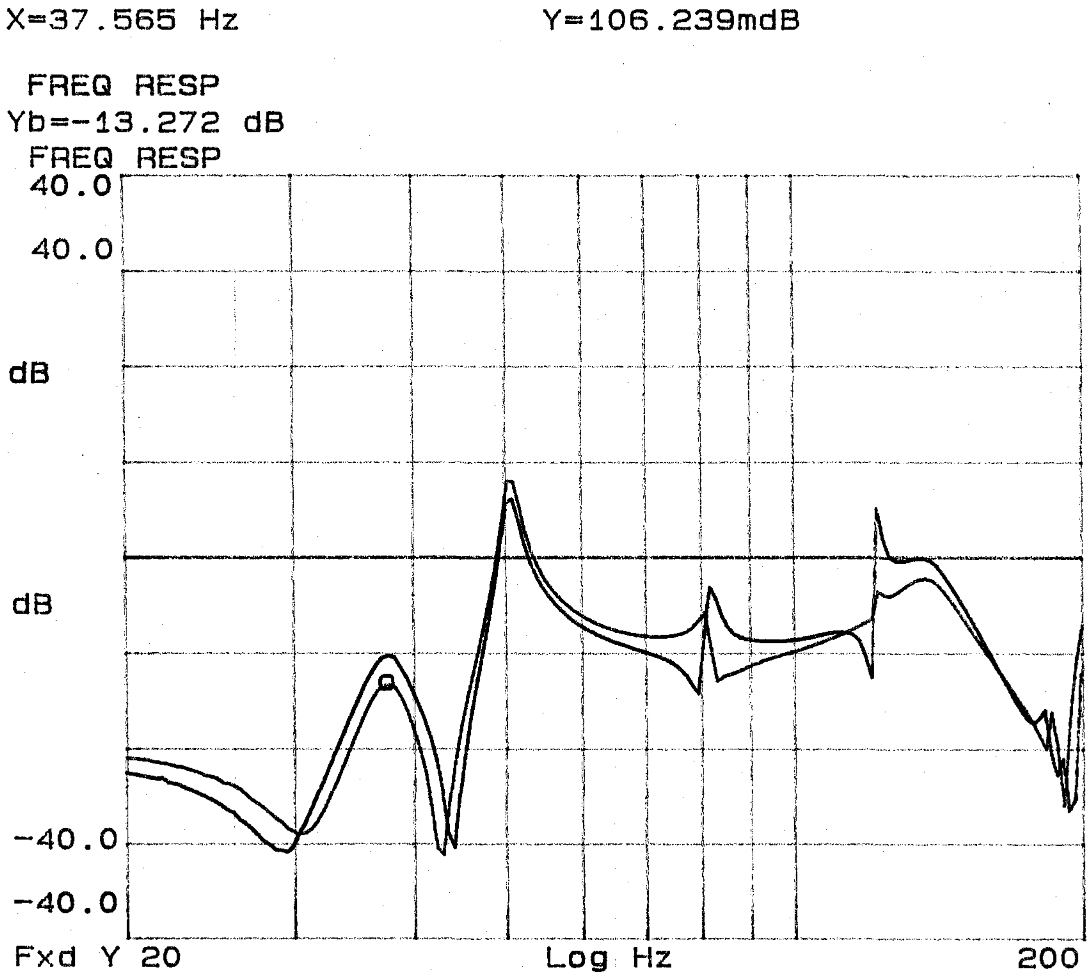

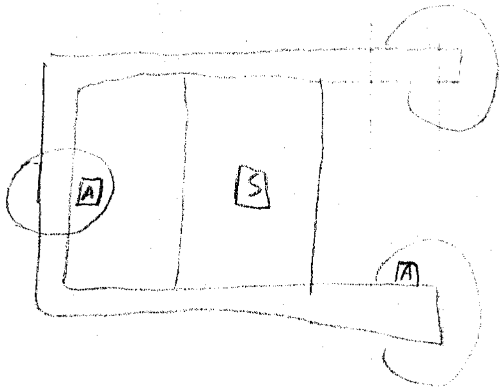

TF16 is from shaker to drift compensation on North side
TF21 is from shaker to drift compensation on SW side

3:00 PM

- TF from source voltage to horizontal accel.
- shaker in horiz position
- source level: 100mVrms
gain = full

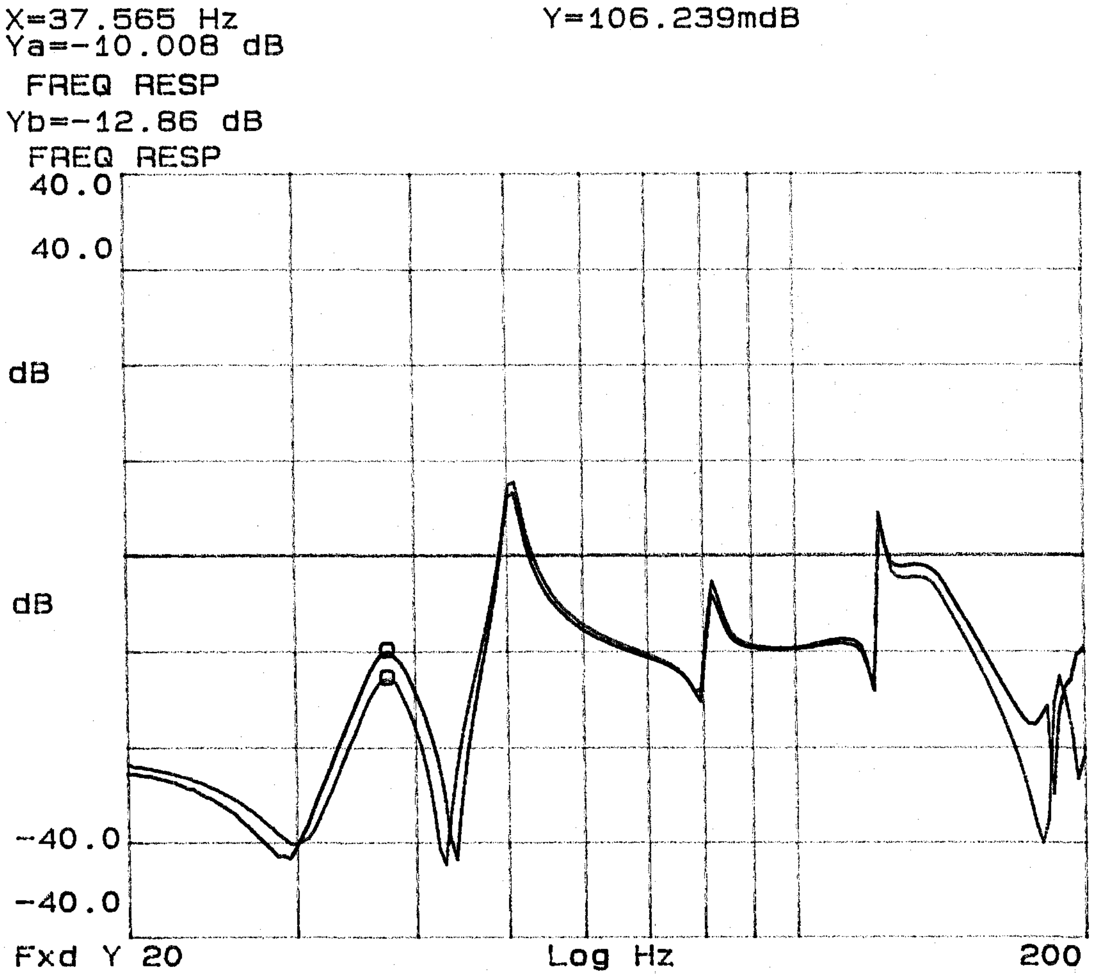

Blue: TF16

Black: TF22

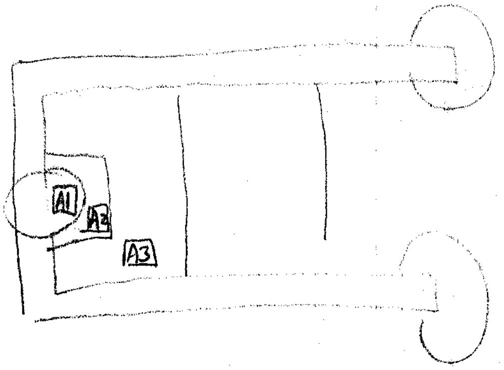

TF22 is transfer fcn from source voltage to A2 (same as source to A3)
TF16 is transfer fcn from source voltage to A1

Tightened bolts on N duct
compensator Support Plate

5:00 PM

-TF from H to H weld H brace

TF23

TF24

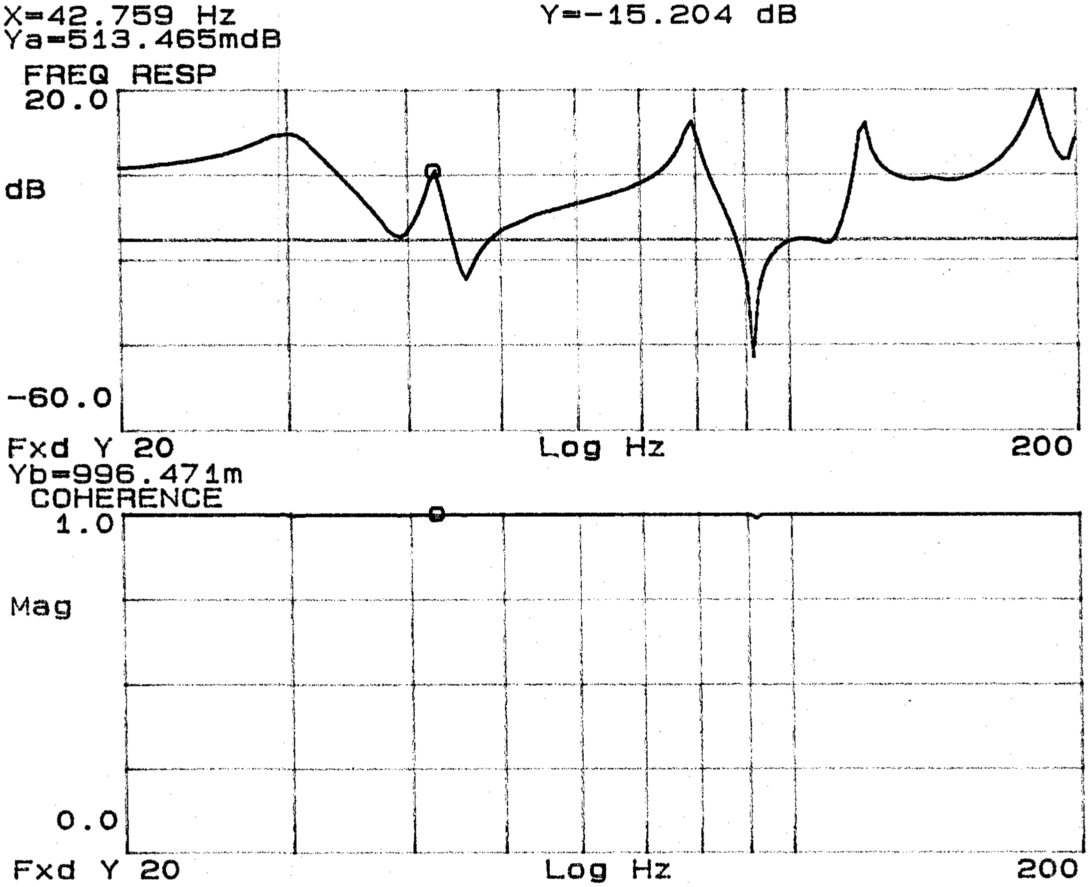

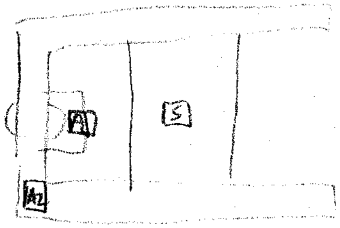

Bottom accel = A1

Top Accel = A2

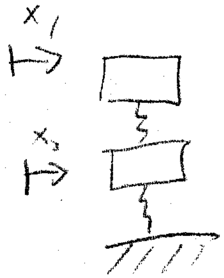

TF from H-to H with
H drive

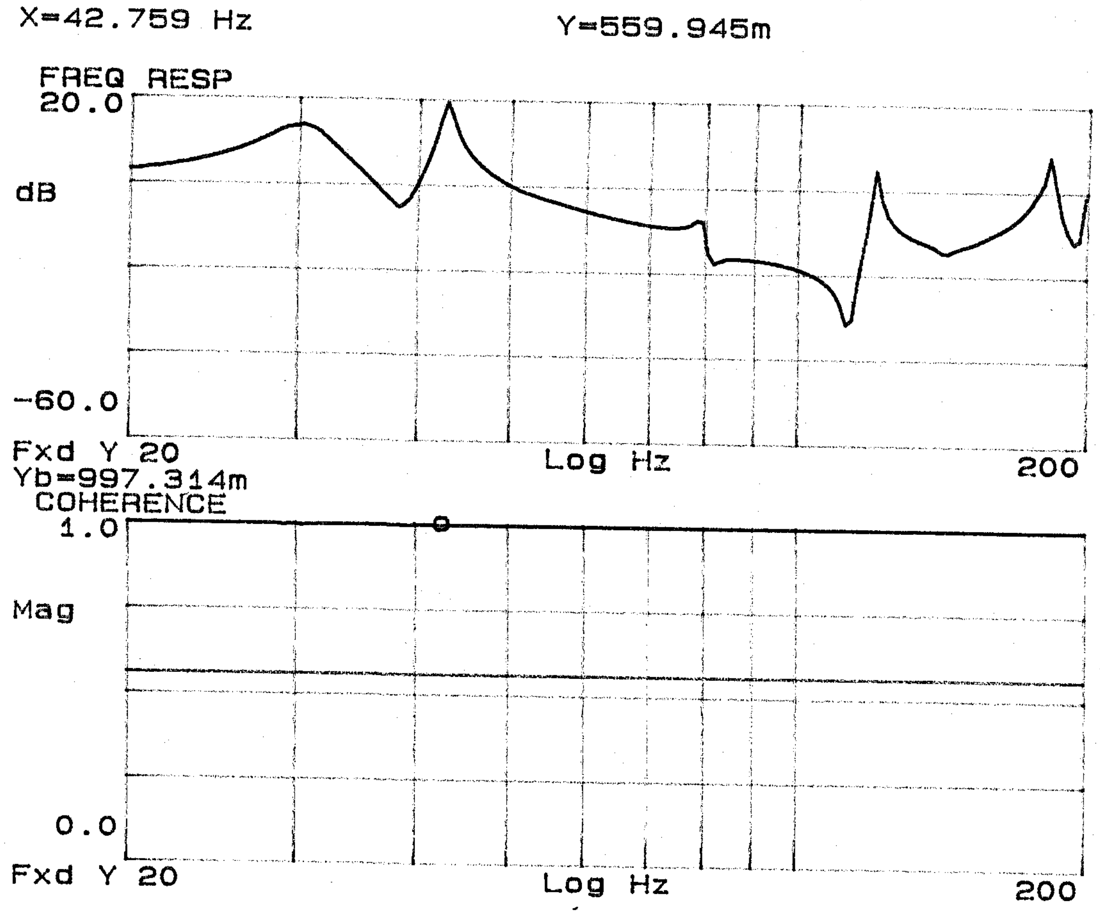

TF25

TF26

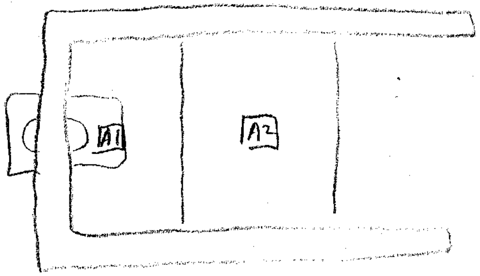

Bottom accel = A1
Top accel = A2

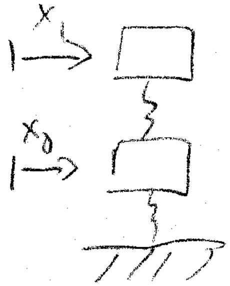

- Transfer fctn from longitudinal to vertical

TF27

F28

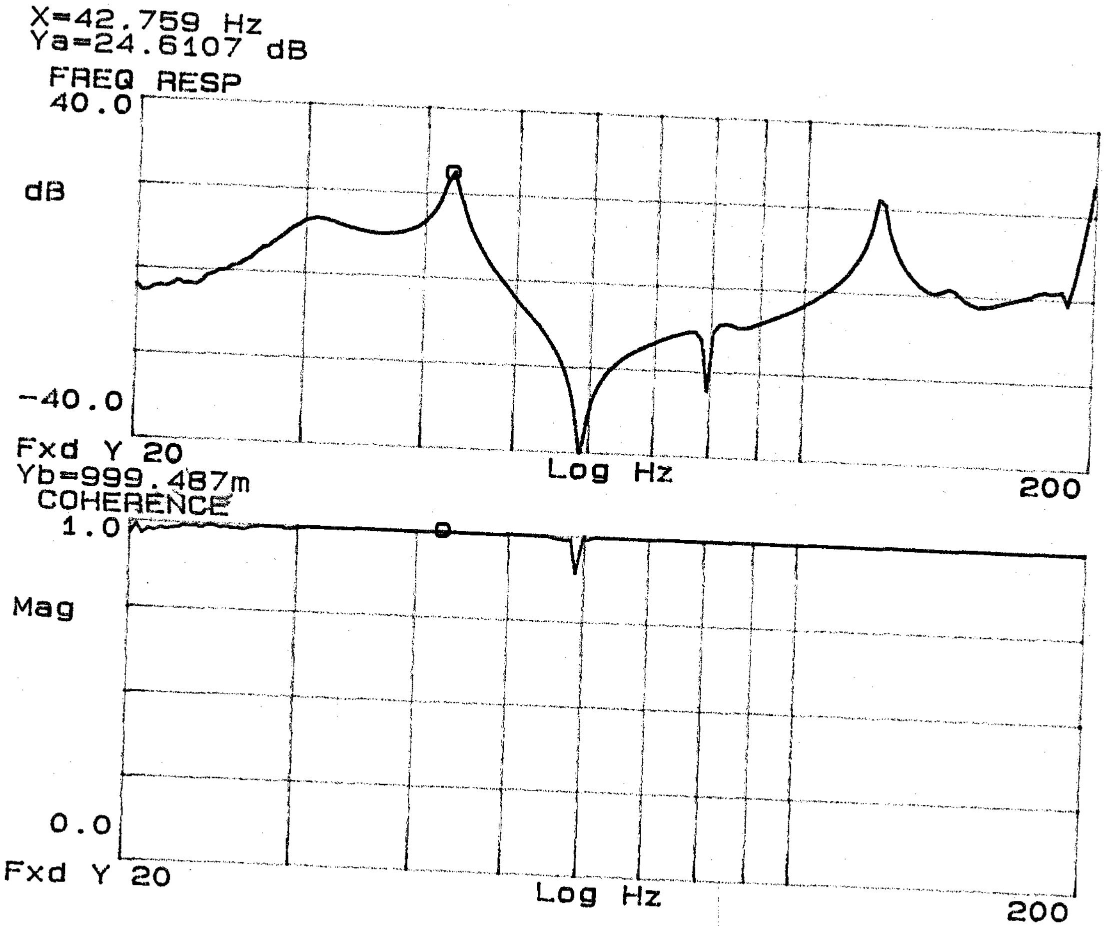

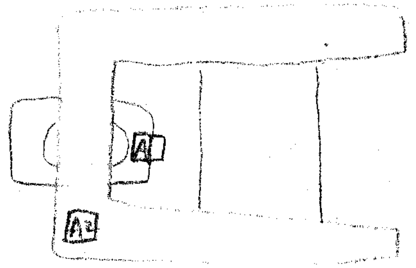

Source level = 100 mV rms
gain (amp) = full

Bottom accel = A1
Top accel = A2

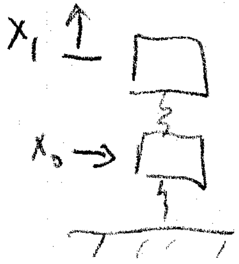

- Transfer Fcn from horiz to vertical

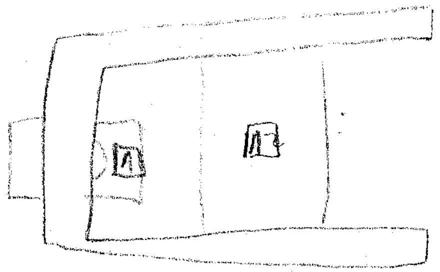

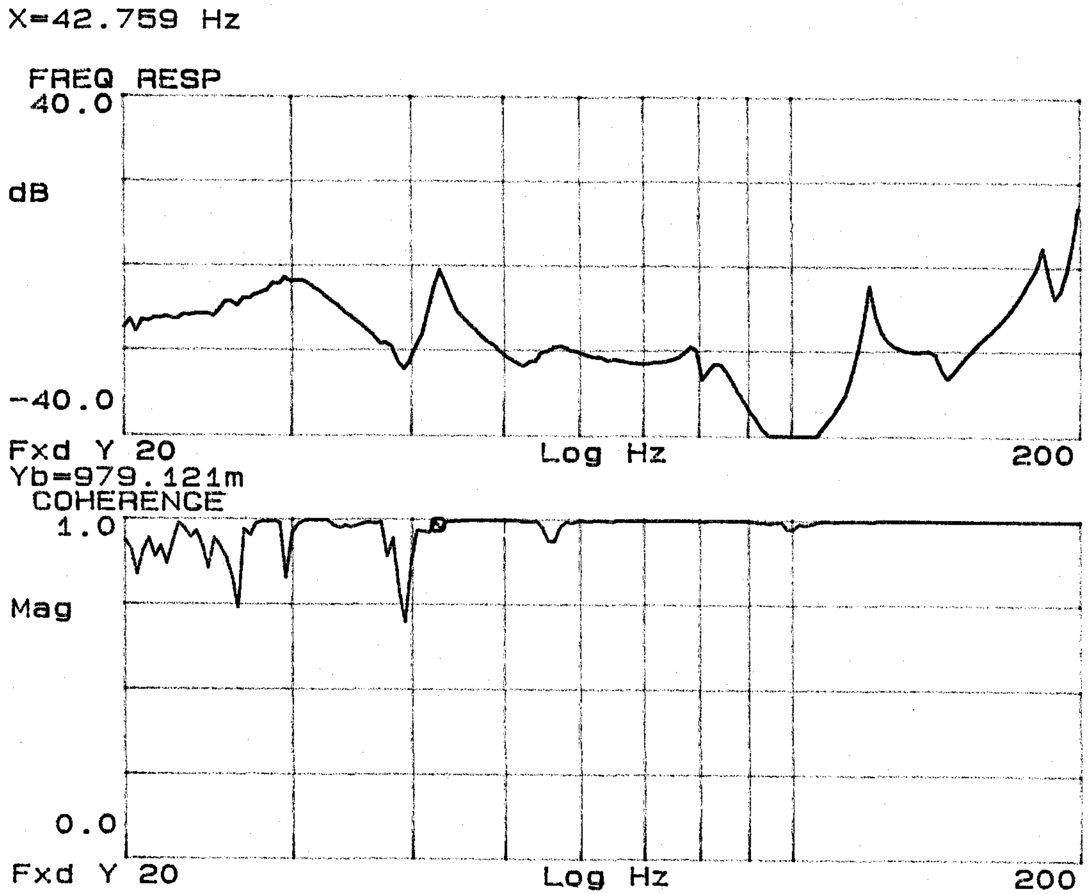

TF29

TF30

Source level = 100mV$_{rms}$
gain (amp) = full
Bottom accel = A1
Top accel = A2

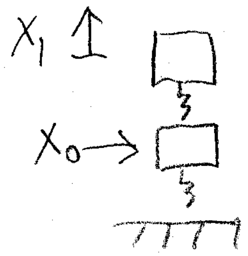

Conclusions From Test:

1) There are a number of floor resonances in both the V + H directions

2) The SS and the optics table interact dynamically below 100 Hz but the table doesn't bend at these frequencies.
- The transfer functions from S to H are identical from shaker source voltage to each of the support points
- The transfer functions from S to V are identical from shaker source voltage to each of support points

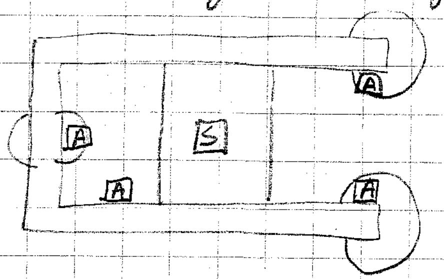

The conclusion from this is that we should be able to get an accurate picture of how the ground shakes the shake by only looking at the accelerometer at 1 site on the table

3) Internal resonances

	Expected	Measured (I think these are the correct resonances?)
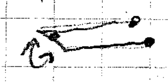	33 Hz	30 Hz
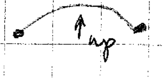	53 Hz	40 Hz
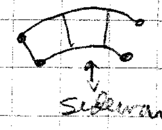	72 Hz	42.7 Hz

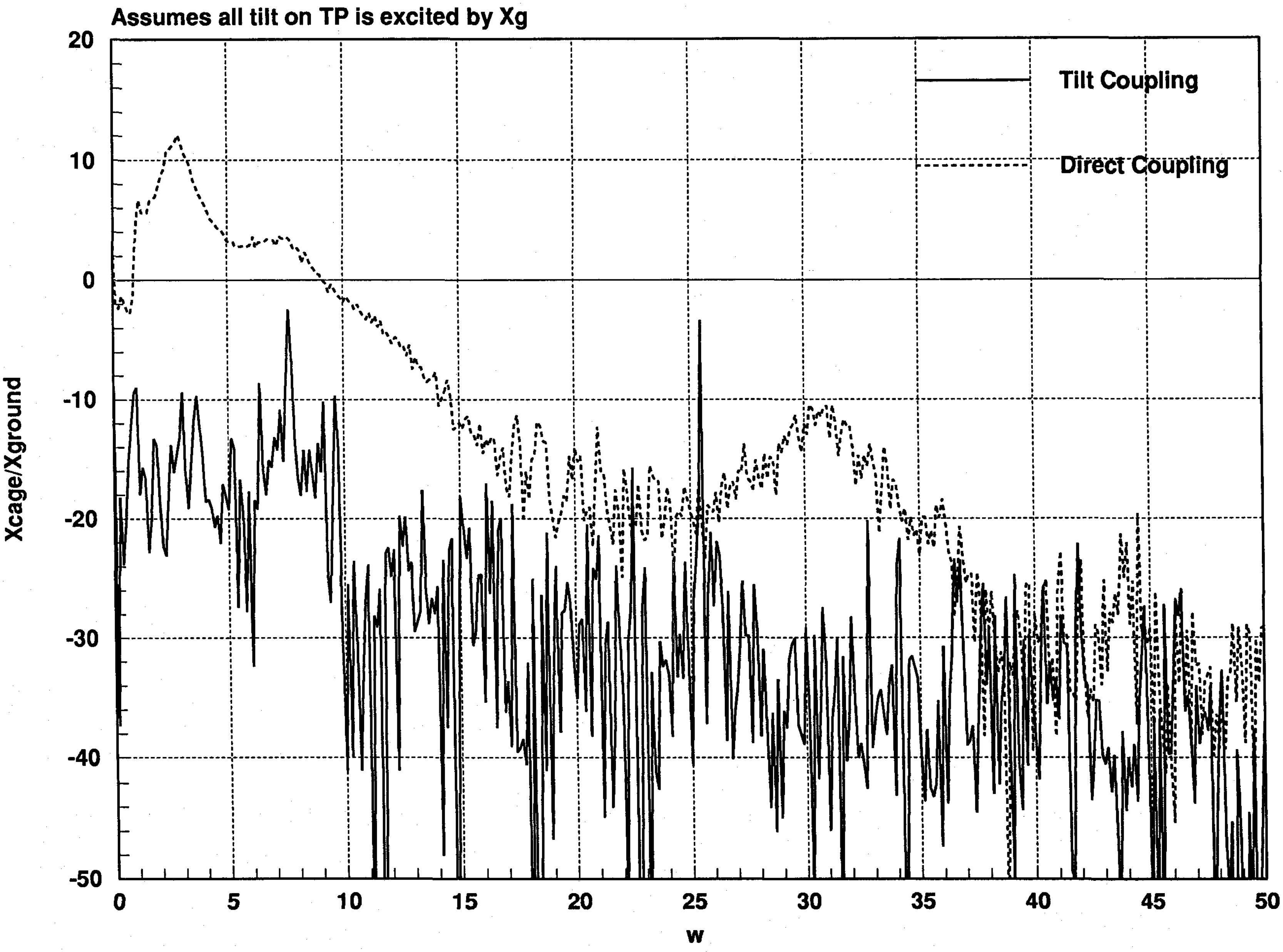

Upper Bound on H Transfer Functions Assuming Direct and Tilt Coupling

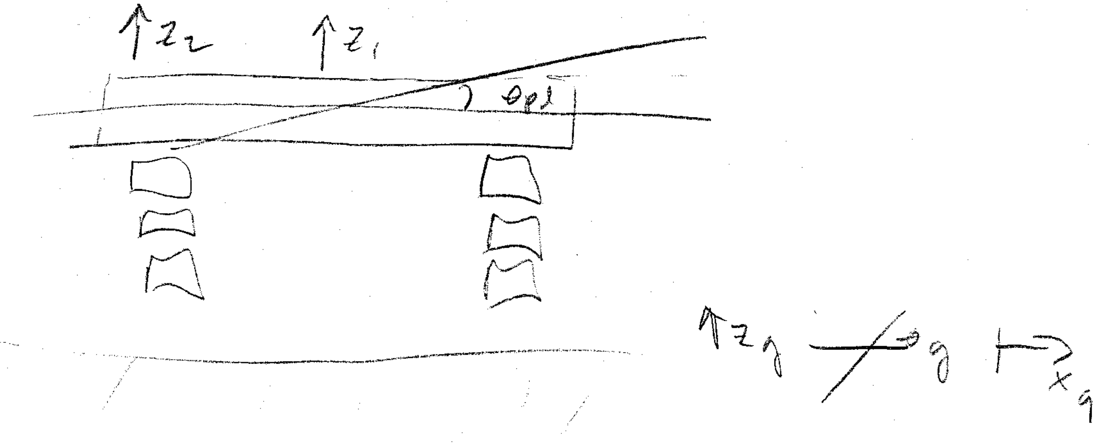

ground

(1) $\left| z_2 - z_1 \right| < \left| \frac{1}{10} z_1 \right|$ ⟵ from data

(2) $\left| \theta_{pl} \right| \approx \frac{(z_2 - z_1)}{R_{plate}} < \frac{\left| \frac{1}{10} z_1 \right|}{R_{plate}}$ from 1

~~(3) $\left| \frac{\theta_{pl}}{ground} \right| < \left| \frac{\frac{\frac{1}{10} z_1}{R_{plate}}}{ground} \right| \sim \frac{1}{10} \frac{1}{R_{plate}} \left| \frac{z_1}{z_{ground}} \right|$~~

~~(3) $z_1 = \frac{z_1}{x_g} x_g + \frac{z_1}{\theta_g} \theta_g + \frac{z_1}{z_g} z_g \approx \frac{z_1}{z_g} z_g$~~

~~$\Rightarrow \left| \theta_{pl} \right| < \frac{\left| \frac{1}{10} \frac{z_1}{z_g} z_g \right|}{R_{pl}}$~~

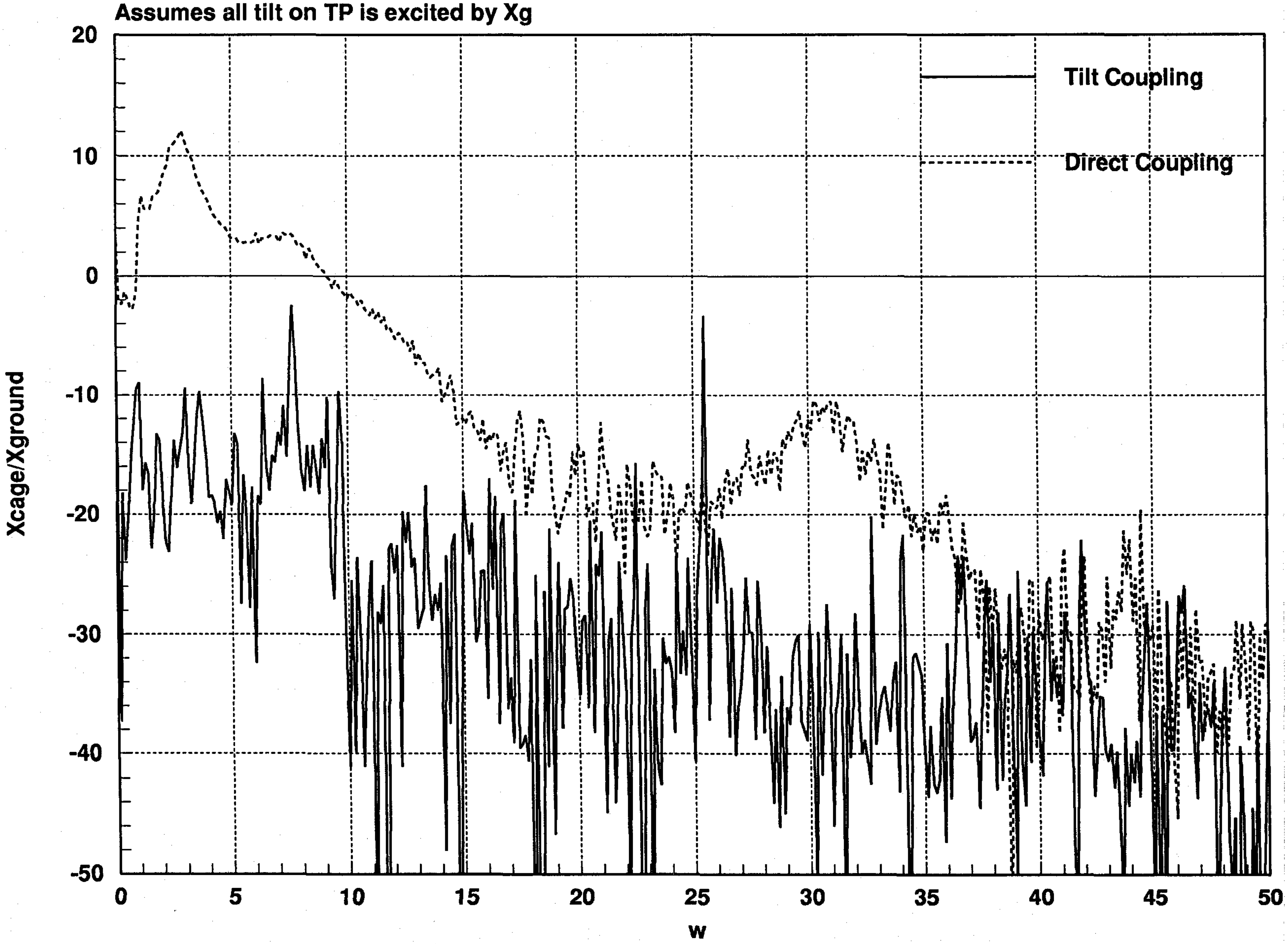

Upper Bound on H Transfer Functions Assuming Direct and Tilt Coupling

$$\frac{\theta}{\text{ground excitation}} = \left(\frac{z}{\text{ground}}\right)\frac{1}{10}\,\frac{1}{R_{\text{plate}}}$$

$$\frac{X_{\text{due to tilt}}}{\text{ground excitation}} = \frac{\theta\, R_{\text{cage}}}{\text{ground excitation}}$$

$$\frac{X_{\text{due to tilt}}}{\text{ground excitation}} = \left(\frac{z}{\text{ground}}\right)\frac{1}{10}\,\frac{R_{\text{cage}}}{R_{\text{plate}}}$$

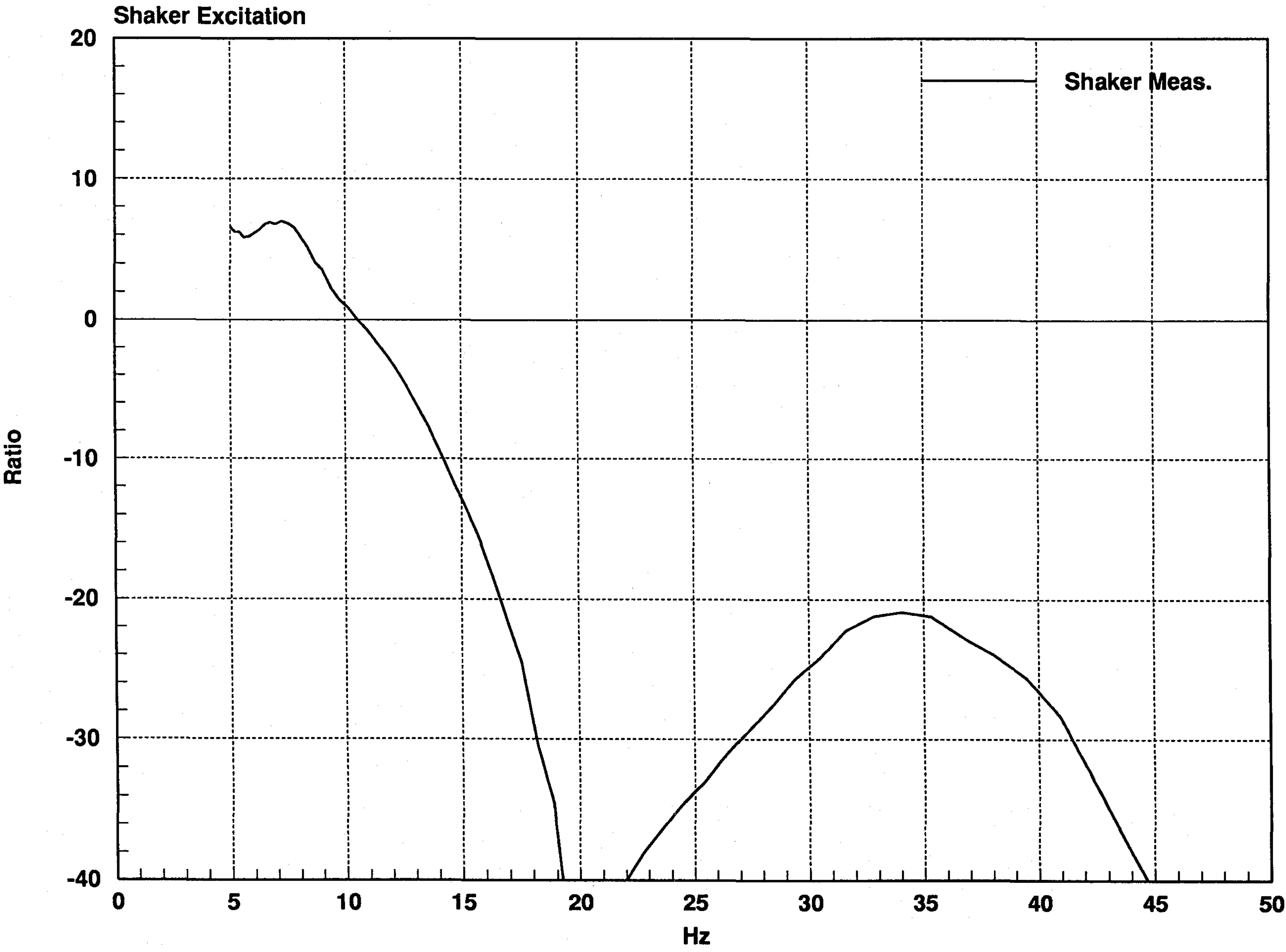

H to H TFs of Stack on Support Structure (vst)

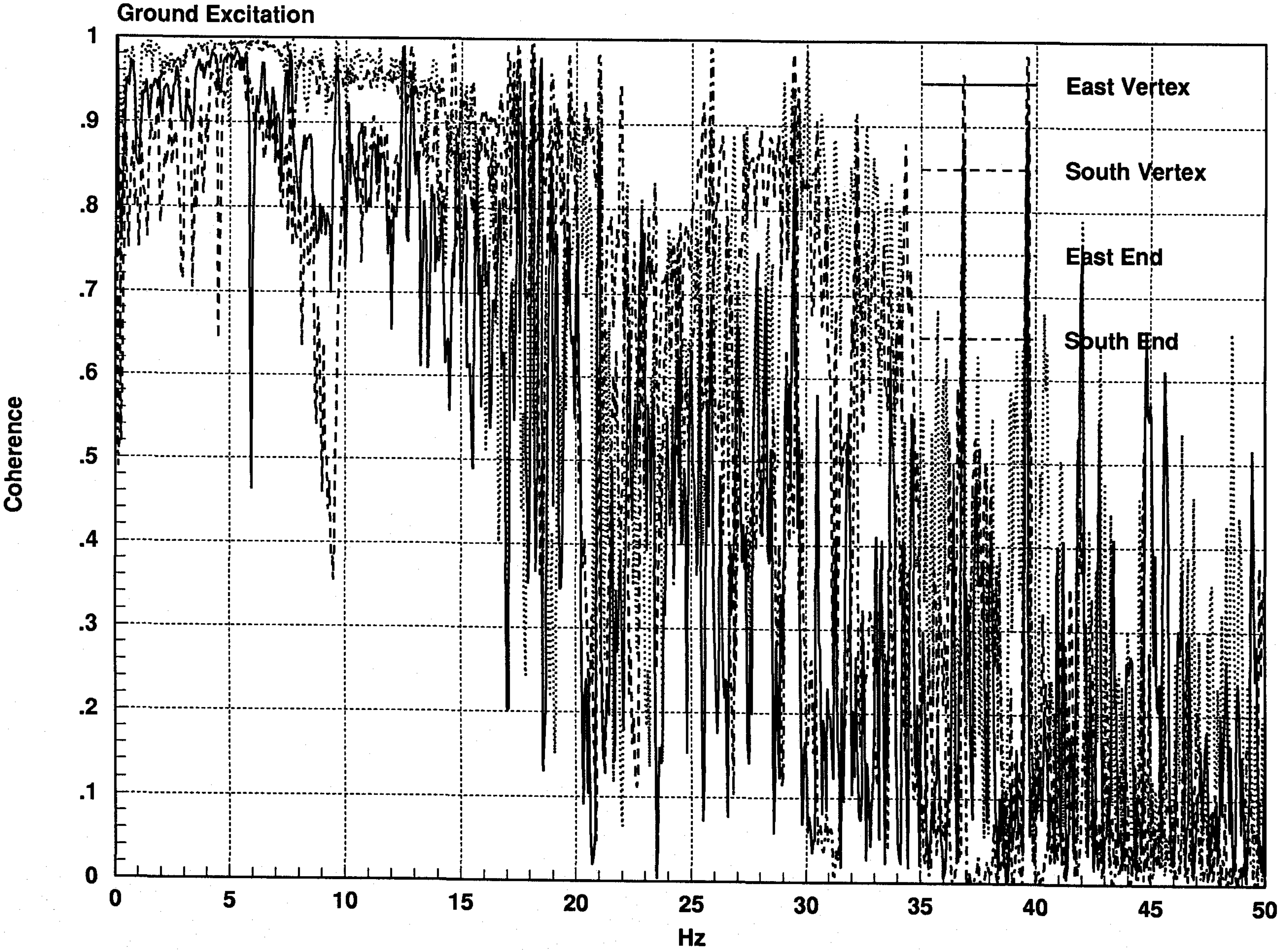

Coh of Vertex & End (seis_sv1 seis_sv9 tiltse29 eept10)

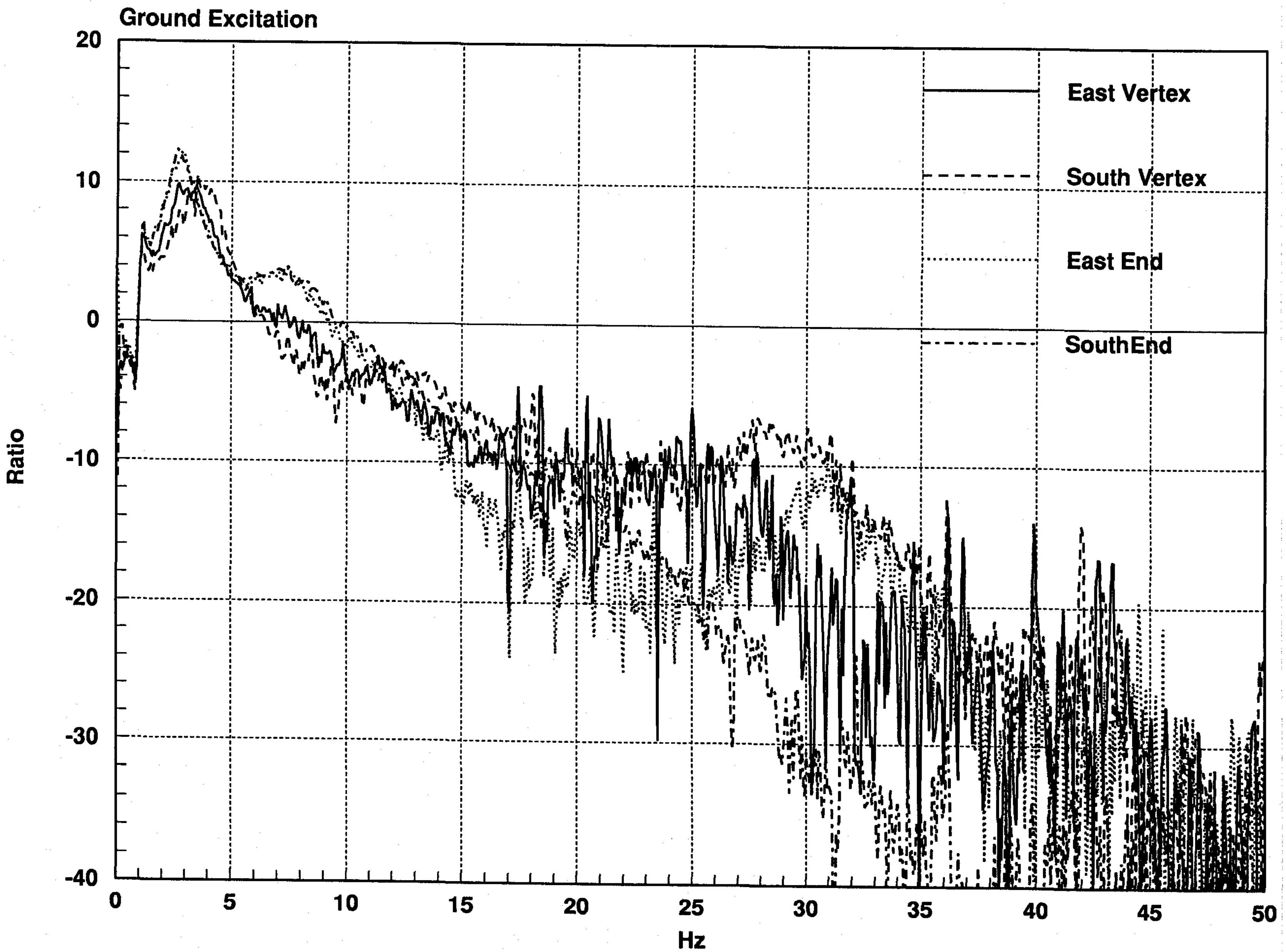

H to H TFs of Vertex & End Stacks (seis_sv seis_sv8 tiltse28 eetp9)

Analysis of (1)

If a-b with R=0 & R=38" are equal
⇒ at noise level of tilt on top plate
Since a-b should scale with R

Analysis of (2)

Same as (1)

Analysis of (3)

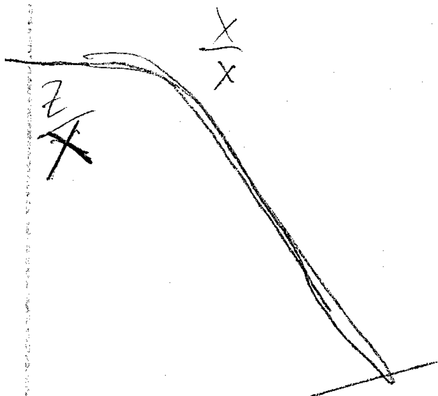

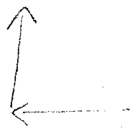

Want a handle on
$\frac{\theta_{TP}}{X_g} + \frac{\theta_{TP}}{\theta_g}$

Want to figure out if
$\frac{\theta_{TP}}{X_g} X_g$ or $\frac{\theta_{TP}}{\theta_g} \theta_g$ dominates

Check in Joe's gauge $\frac{\theta}{\theta}$ & $\frac{\theta}{X}$ ←

has a measurement
⇔ see if this dominates

$\left(\frac{Z}{X}\right)_{TPF} = \left(\frac{Z}{X}\right)$ common mode $\pm \boxed{\frac{R\theta}{X}} Y \approx \frac{Z}{X}$ common mode

Believe $R\theta/X$ small compared

then $\frac{\theta}{X}$ is small compared to

$c = \lambda \nu$

<u>air</u> $\nu = 1$ hz $\Rightarrow \lambda = 331$ m

$c = 331$ m/sec $\nu = 50$ Hz $\Rightarrow \lambda = 6.6$ m $= 21.6$ ft

$\nu = 30$ Hz $\Rightarrow \lambda = 11$ m $= 36$ ft

<u>concrete</u> $\nu = 1$ hz $\Rightarrow \lambda = 3100$ m~~/sec~~ =

$c = 3100$ m/sec $\nu = 50$ hz $\Rightarrow \lambda = 62$ m.

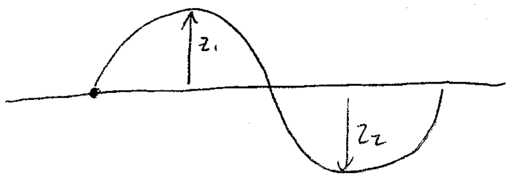

$\frac{1}{2}\lambda$ get $z_1 - z_2 = 2 z_1$

$\frac{1}{4}\lambda$ get $z_1 - z_2 \sim z_1$

$\frac{1}{8}\lambda$ get $z_1 - z_2 \sim \frac{z_1}{2}$

concrete $\frac{1}{4}\lambda \geq 15$ m at 50 Hz

air $\frac{1}{4}\lambda \sim 5.4$ ft

$\frac{1}{8}\lambda \sim 2.7$ ft $= 32.4''$

Tests for T.I.s

*

1) Measure tilt on top of stack

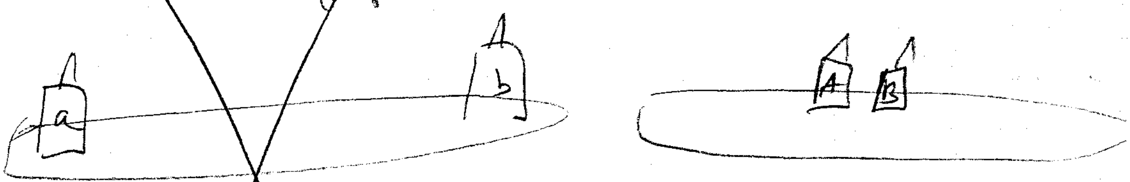

a) want to get a-b + a simultaneously
b) also want $\frac{a}{b}$ + coherence

2) Want to get better idea of tilt on floor

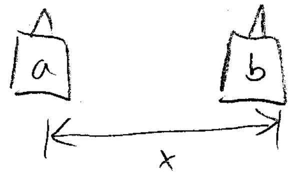

x = 5"
= 10"
= 20"
= 40"

a) a-b + a simultaneously
b) $\frac{a}{b}$ + coherence

*

3) Want to get coherence between vert + horiz ground motion

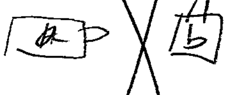

a) $\frac{a}{b}$ + coherence

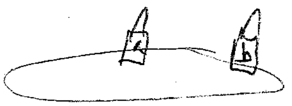

b) If no coherence do $\frac{X_{TP}}{Z_g}$ + $\frac{Z_{TP}}{X_g}$

~~If there is coherence [illegible] still do $\frac{Z_{TP}}{X_g}$ + get upper bound~~

If there is coherence do $\frac{Z_{TP}}{X_g}$

4) Do $\frac{X_{TP}}{X_g}$ over night + see what data looks like

* (5)

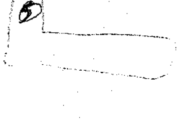

try to do tilt transfer fctn (V1) (V2)

would for the ground noise drive expected in the intended application.

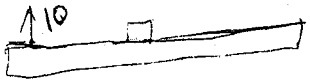

1/17

2. *Low-frequency ground-noise-driven measurements:*

At low frequencies, the stack's response is strongly influenced by the exact shapes and frequencies of the rigid-body modes, which range in frequency from approximately 1.5 to 25 Hz. The configuration we wished to characterize, and the one we modeled on the computer, was with the base fixed to a very large reaction mass. When the stack's base table is placed on springs, as was done for the high-frequency measurements, these low-frequency modes change frequency and shape because the table is a very different reaction mass than the floor-mounted posts. This doesn't greatly affect the high frequency measurements, but would distort any low frequency data taken with the base ungrounded. At frequencies below about 20 Hz, there is sufficient ground noise to drive the stack when rigidly attached to our vacuum tank mounting posts. Only two transfer functions were taken in this frequency range, the ratio of vertical motion on top to vertical motion at the base, and the same for horizontal motion. These two sets of data approximate T_{zz} and T_{xx}, but do not take into account the contribution of the cross coupling terms on the signal on top. Since we have no easy way of making the measurement with two different drive vectors of ground noise, which is what would be necessary to discriminate the four components, only two traces appear below 20 Hz in the transfer function plot of the all-Fluorel stack, Fig. 2(a). The Fluorel-RTV stack has somewhat lower normal mode frequencies, and begins to isolate well at lower frequencies, as can be seen in Fig. 2(b), so the cutoff for these low-frequency measurements was lower.

3. *High-frequency cantilever measurements:*

due to [illegible]

In the highest frequency range, above 90 Hz for the all-Fluorel, and 60 Hz for the Fluorel-RTV, it becomes difficult to take data using the first method. The accelerometers we use (Endevco model 7707-1000) exhibit a slight response to magnetic fields; this becomes important when we wish to measure transmission of 10^{-5} or lower, due to pickup from the motor coils. In addition, the noise floor of our accelerometer amplifiers becomes significant at about this level. We solve this problem by providing mechanical amplification at the accelerometer mounting on the top table, by mounting the accelerometer on the end of an aluminum cantilever. The length (and thus the resonant frequency) is adjusted while under vacuum via remote-control motors. This assembly was mounted on the top table, in place of the simple accelerometer. For each frequency point, the cantilever length was adjusted to the correct length, and clamped. The appropriate

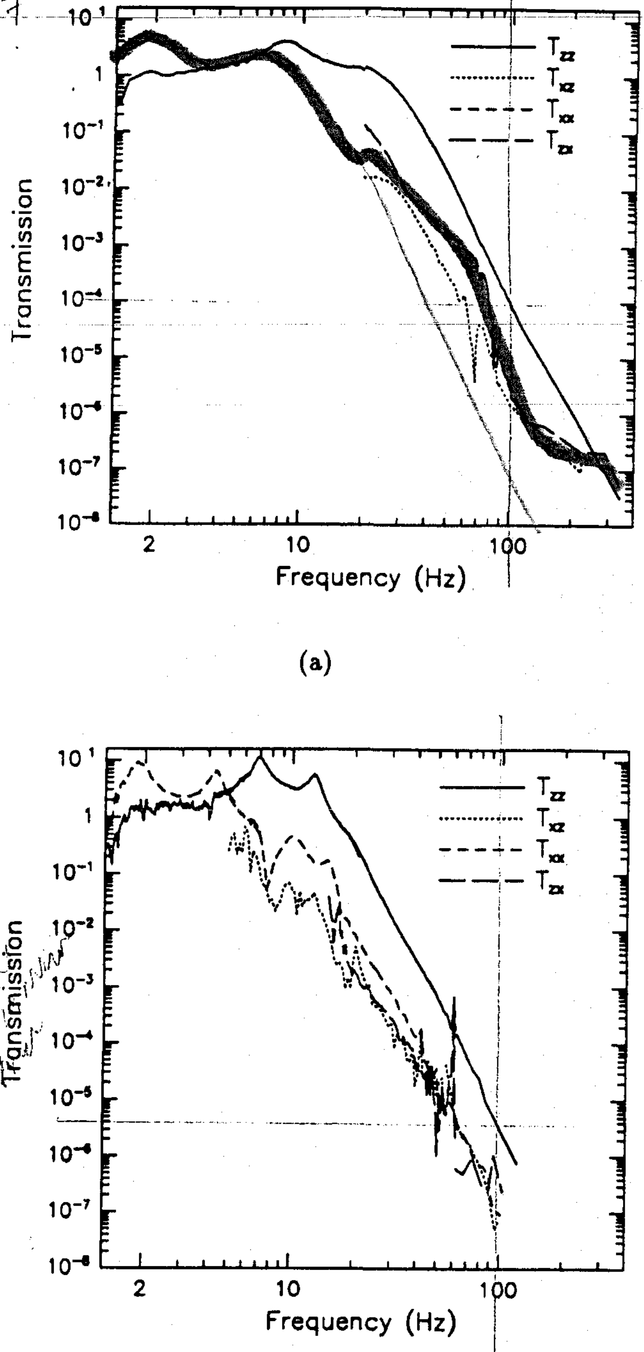

(a)

(b)

FIG. 2. Measured transmission matrix elements for (a) the stack built with all Fluorel springs, and (b), built with two lower layers of Fluorel springs and two upper layers of RTV springs.

Top Plate

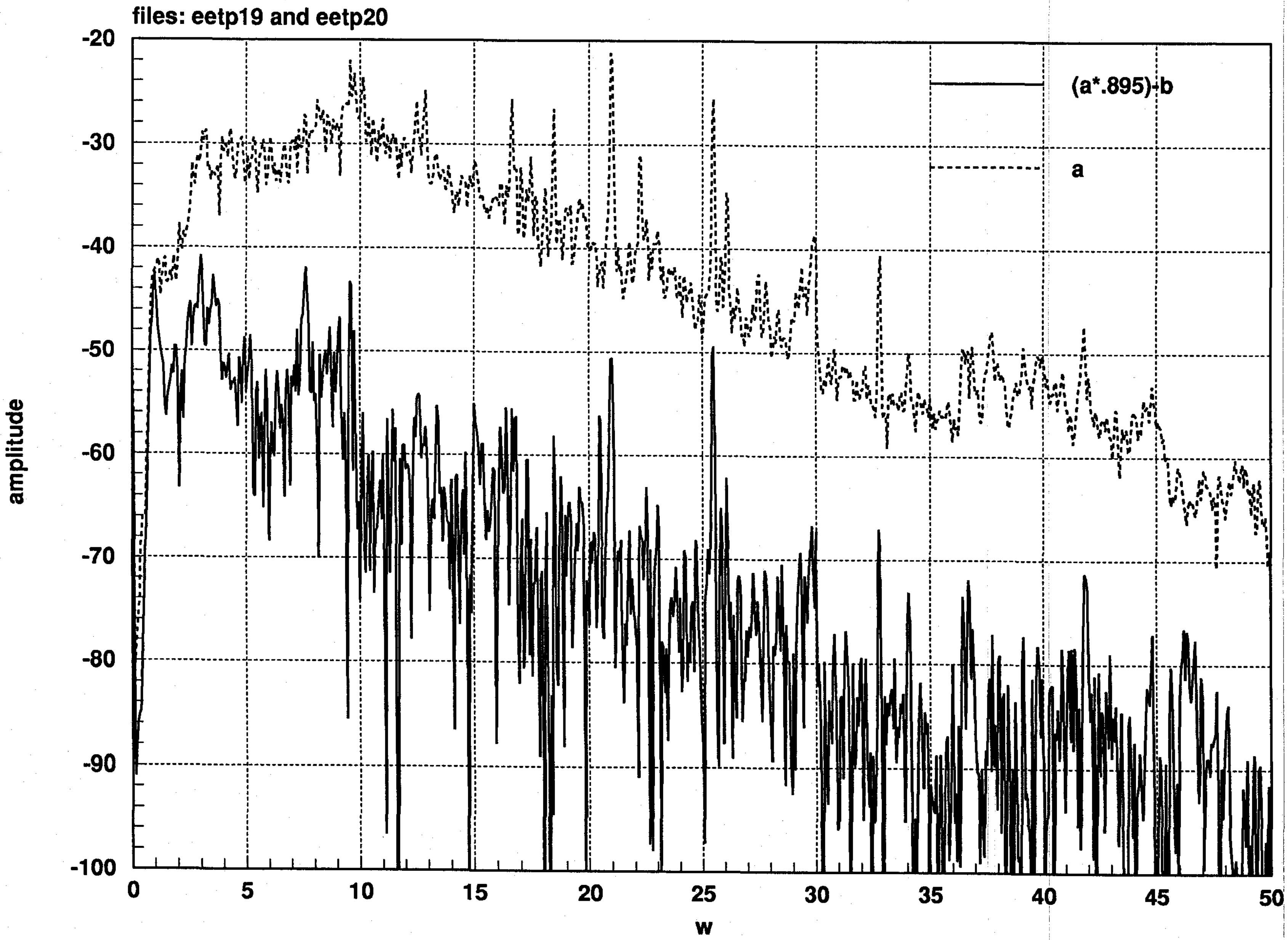

plots of a and (a*.895-b)

Top Plate

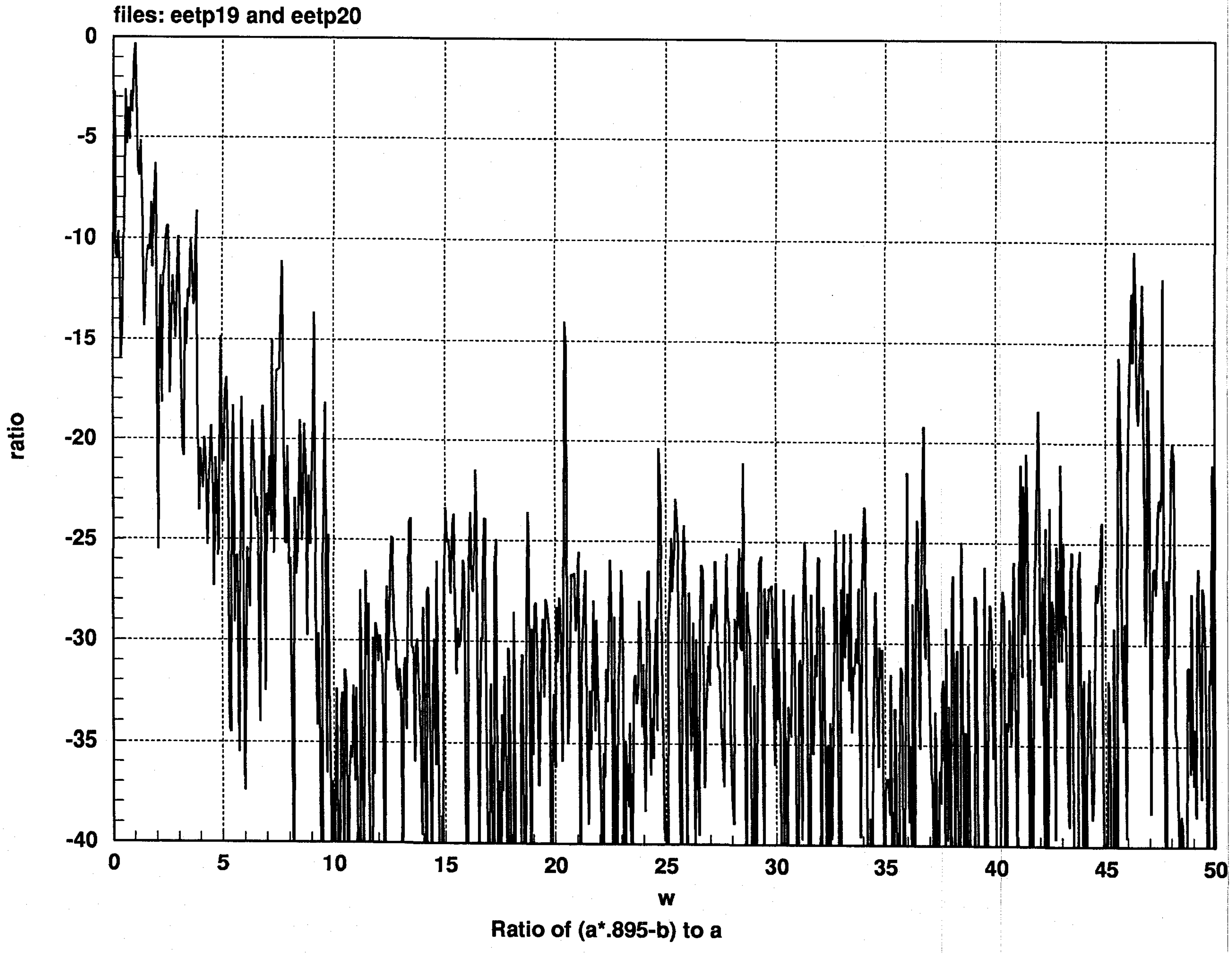
files: eetp19 and eetp20
ratio
0
-5
-10
-15
-20
-25
-30
-35
-40
0
5
10
15
20
25
30
35
40
45
50
w
Ratio of (a*.895-b) to a

Top Plate

b2b-odb

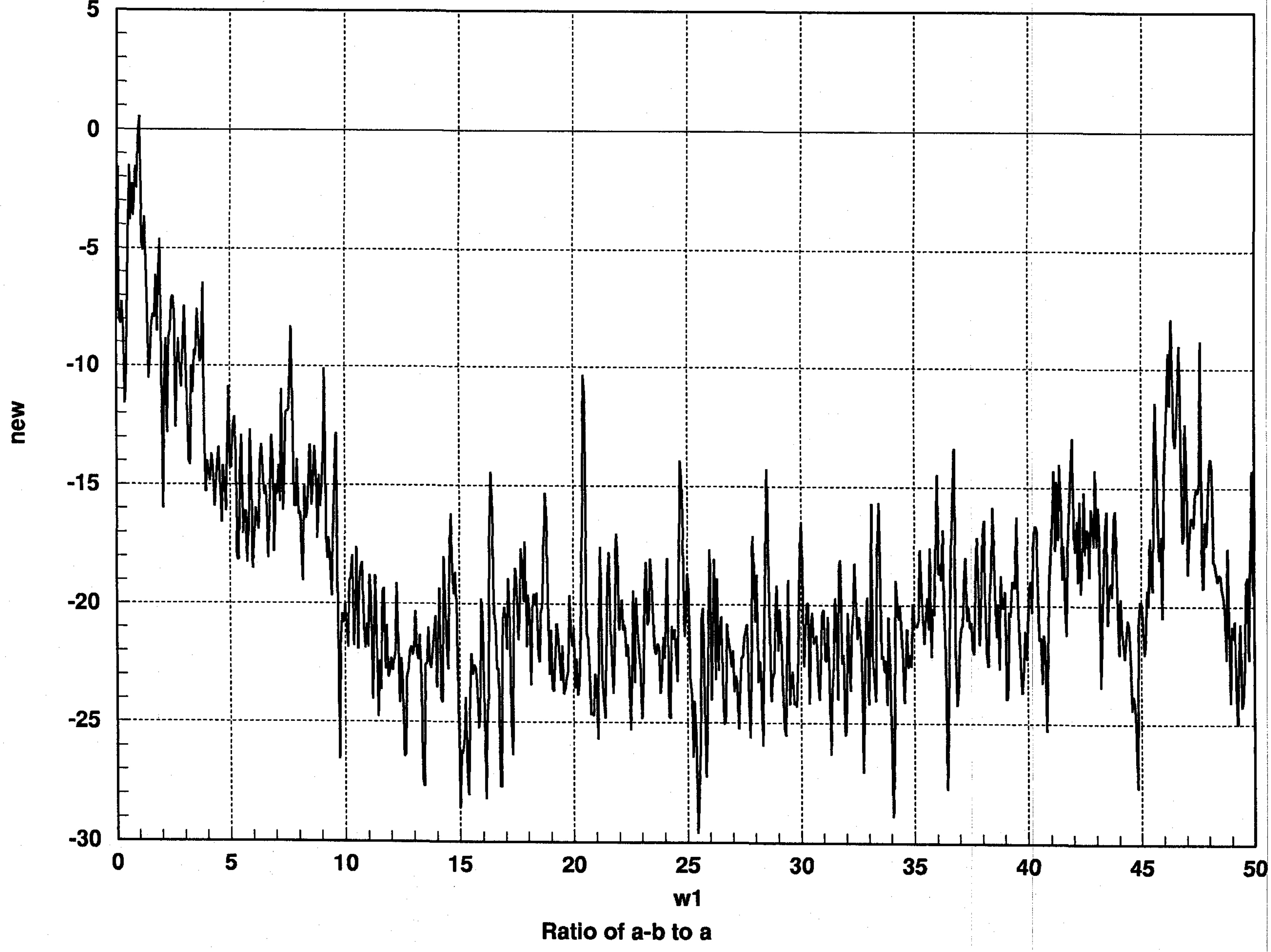
Ratio of EETP20 to EETP19

Ground Noise

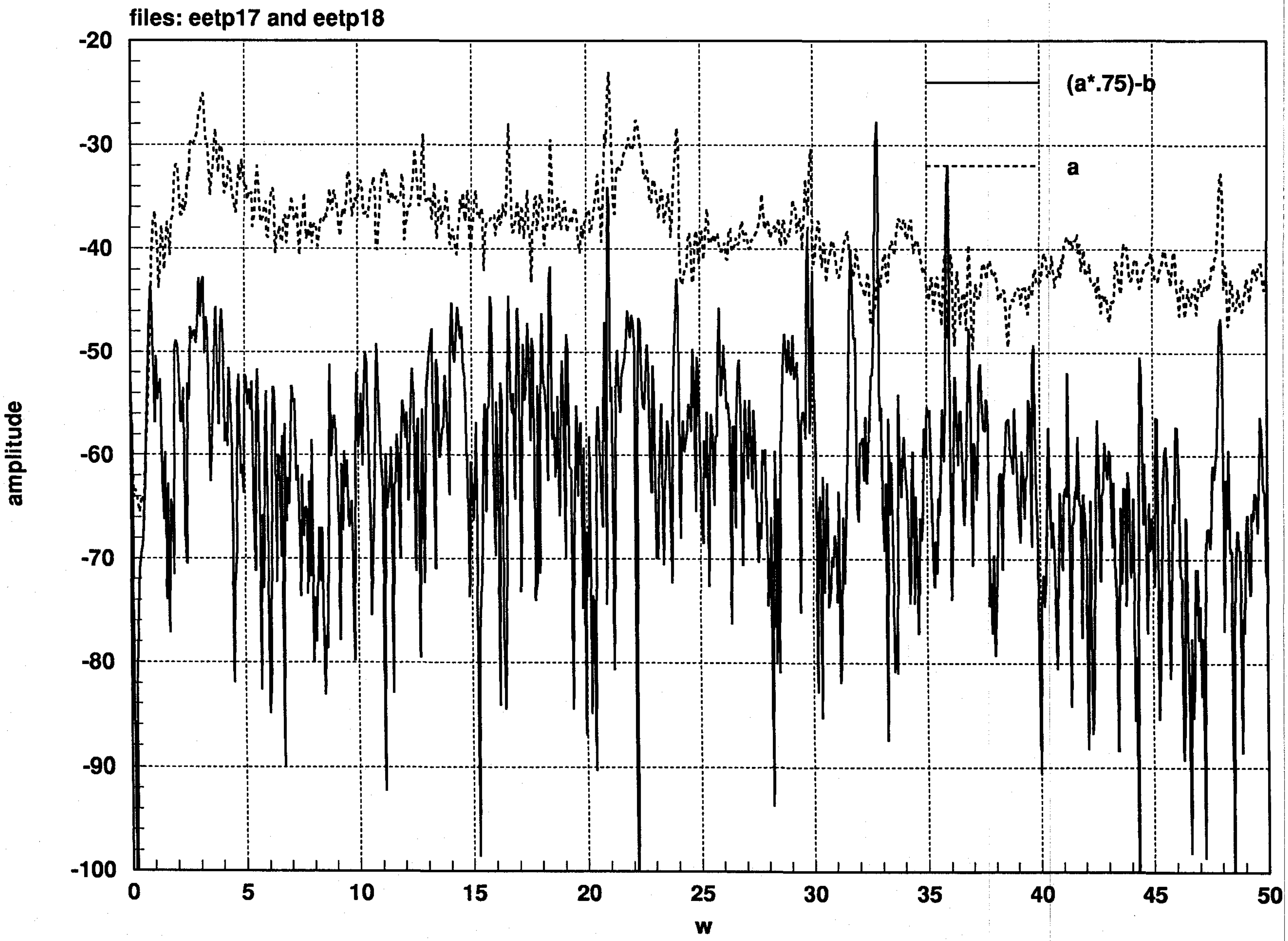

plots of a and (a*.75-b)

Ground Noise

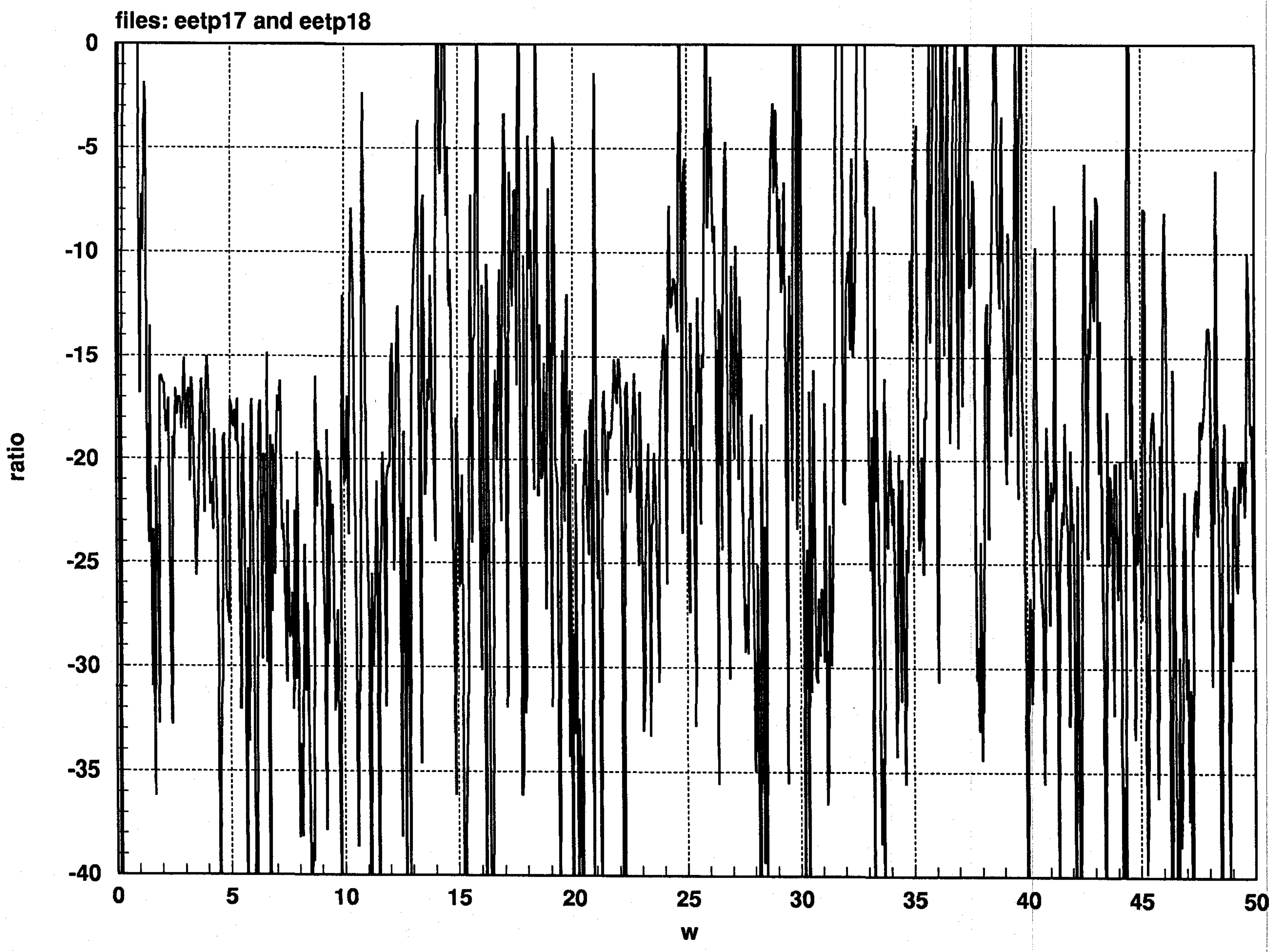

Ratio of (a*.75-b) to a

$S = \theta R$

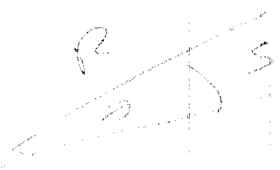

$$\frac{X_{Tilt}}{XR} = \frac{Z_1 - Z_2}{D}$$

$Z_1 - Z_2 = R_g \theta_{g}$

$Z_{MP} - Z_{MP} = R_{MP} \theta_{MP}$

$$\frac{\theta_{TP}}{\theta_g} = \left(\frac{R_G}{R_{TP}}\right) \frac{Z_{MP} - Z_{TP}}{Z_G - Z_G}$$

Seismic isolation and suspensions
(Giaime, Shoemaker, Spero, Raab, Gillespie,
Sievers, Saulson, Stebbins)

a) Overview of the seismic isolation and suspension requirements for the initial LIGO interferometer: seismic noise contribution to the test mass motion, rms motion permitted, long term length and tilt stability required.
Overview of the thermal noise requirements for the initial interferometer; pendulum and test mass internal modes.
(Raab, 40 min)

b) Passive vibration isolation stacks: analysis, transmssion measurements, transmssion by cabling, adaptation for 40 meter system, improvements with rtv springs. (Giaime, Shoemaker, Sievers, 30 min)

c) Vacuum and contamination compatibility of elastomers: rga measurements, optical contamination cavity measurments
(Raab or equivalent, 20 min)

d) Measurements of suspension isolation in 40 meter suspensions
Anticipated seismic spectrum in Mark II 40 meter system
(Spero, 20 min)

d') Visit 40 m stacks and suspensions (Sievers/Spero, 30 min)

e) Thermal noise studies: Pendulum string modes and predictions for pendulum thermal noise in suspension for mark II 40 meter system.
(Gillespie, Raab, 30 min)

f) Test mass thermal noise: current state of analysis and Q measurments, projections for 40 meter system, (information on the low Q modes?) losses from magnets, losses from wires, losses at attachments.
(Gillespie, Raab, 30 min)

g) Off resonance thermal noise studies in fused quartz (Kovalik experiment)
(Shoemaker, 10 min)

ef') Visit to Optics lab suspension development (Gillespie/Raab, 30 min)

h) Work at Syracuse (Saulson, 40 min)

i) Summary of work by Braginsky (Spero, 20 min)

j) Active isolation systems (Stebbins, 40 min)

k) Summary of progress and plans to meet requirements for vibration isolation and thermal noise (suspension and test mass modes) for the initial interferometer. (Raab, 20 min)

Total time 6 hours

Measured in AIR

$\phi_x \rightarrow$ rock

$\phi_z \rightarrow$ twist

ϕ_x $\underline{vs}$ x

ϕ_z^{top} $\underline{vs}$ x^{bot}

ϕ_x^{top} $\underline{vs}$ z_E^{bot}

ϕ_z^{top} $\underline{vs}$ z^{bot}

black – NS77 - 40dB
blue – NS78 - 40dB
red – NS 58 - 40dB
brown – NS 59 -40dB

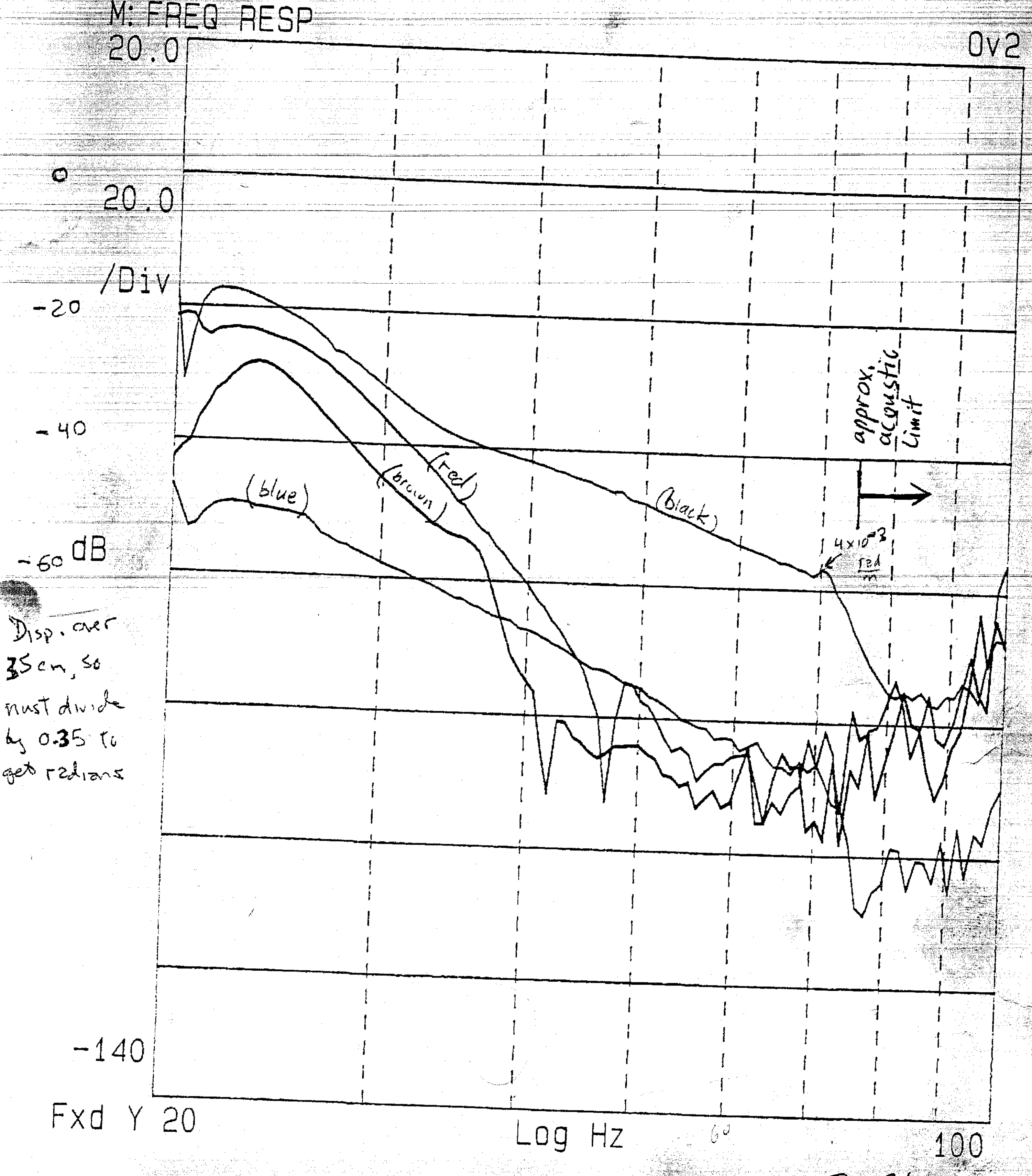

Disp. over 35cm, so must divide by 0.35 to get radians

J. Giaime
11-5-91

MASSACHUSETTS INSTITUTE OF TECHNOLOGY
Gravitation and Cosmology Research Group
Cambridge, Massachusetts 02139

MIT GRAVITY GRP. FAX #617-253-7014
CONFIRMATION # 617-253-4824

Facsimile Cover Sheet

DATE: 11-5-91 **TIME:** 5 PM (E.T.)

TO: LISA SIEVERS **FAX#:**

ADDRESS:

NUMBER OF PAGES (including this cover sheet): 4

FROM: Joe Giaime **OFFICE #:** (617)253-0203

Massachusetts Institute of Technology
Room 20B–145
Cambridge, Massachusetts 02139

NOTES:

(see next page)

- electrical cross talk
- magnetic coupling
- vacuum not tight enough

11-5-91

Lisa,

Here are some of the data.

The first plot, from 20 - 200 Hz, shows the four transfer function elements, measured at the outer edge of the top table & drive table. These were measured in vacuum, and the electronic noise floor was ≈ -100 dB

The second plot runs from 20-100 Hz, and was from air measurements. I have marked the approximate point where the acoustic coupling became important. These transfer functions were of the setup drawn below, shown for each ϕ. The "lever arm" between A & B was ~15 cm

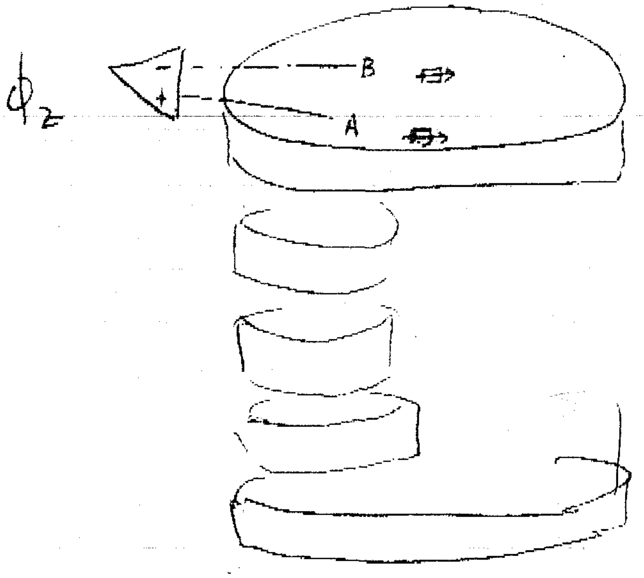

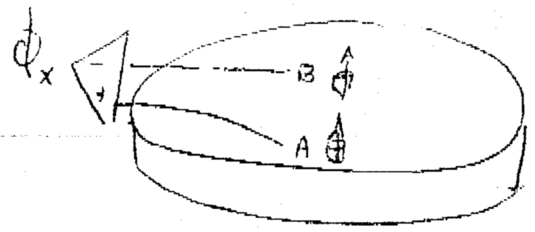

— Joe

Measured in AIR

ϕ_x → rock

ϕ_z → twist

ϕ_x vs x^{bot} black — NS77 -40dB

ϕ_z^{top} vs x^{bot} blue — NS78 - 40dB

ϕ_x^{top} vs z_z^{bot} red — NS 58 -40dB

ϕ_z^{top} vs z^{bot} brown — NS 59 -40dB

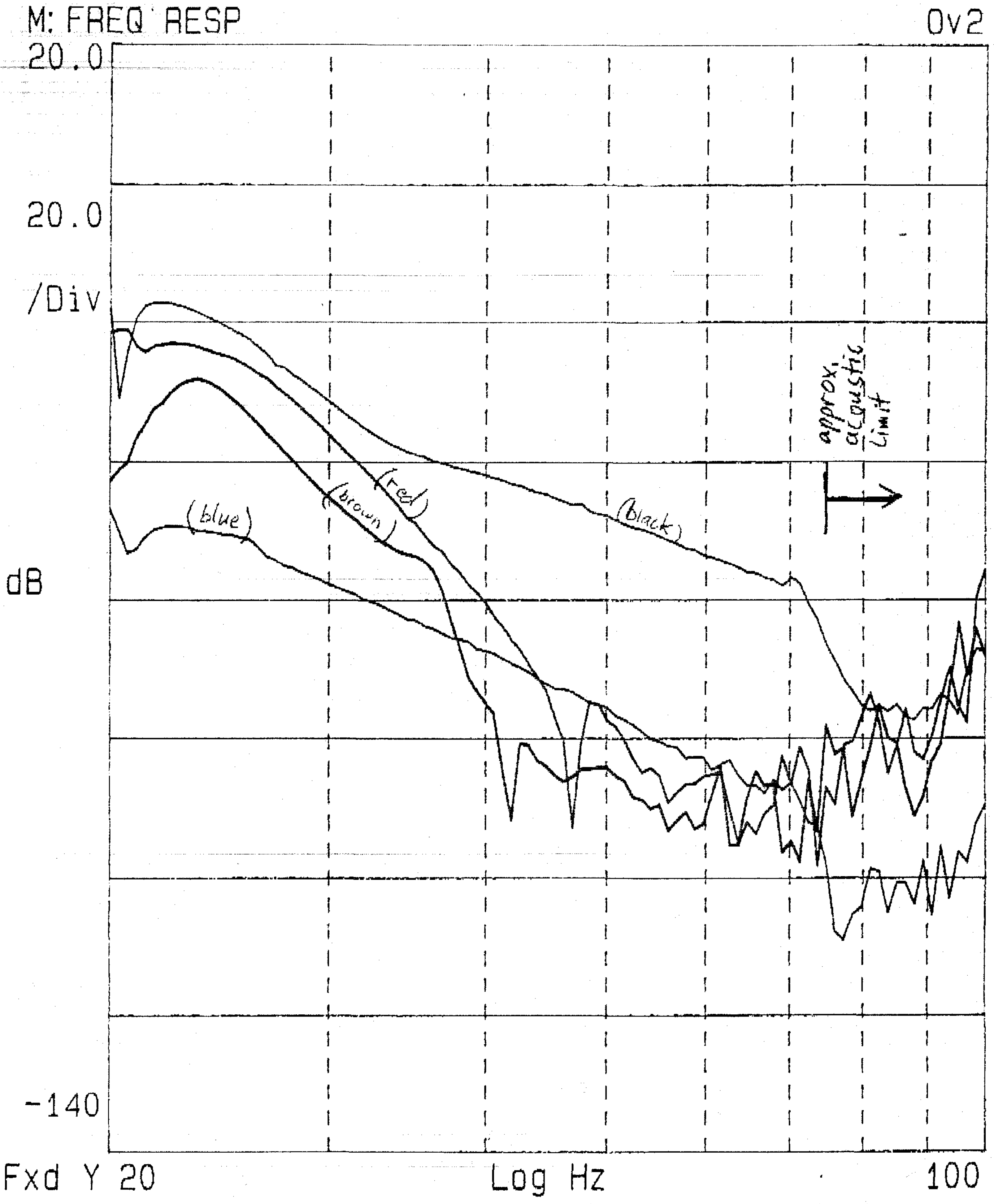

J. Giaime
11-5-91

BATCH
START

STACKS BOOK 2

STAPLE
OR
DIVIDER

2/11/93 4:50 PM

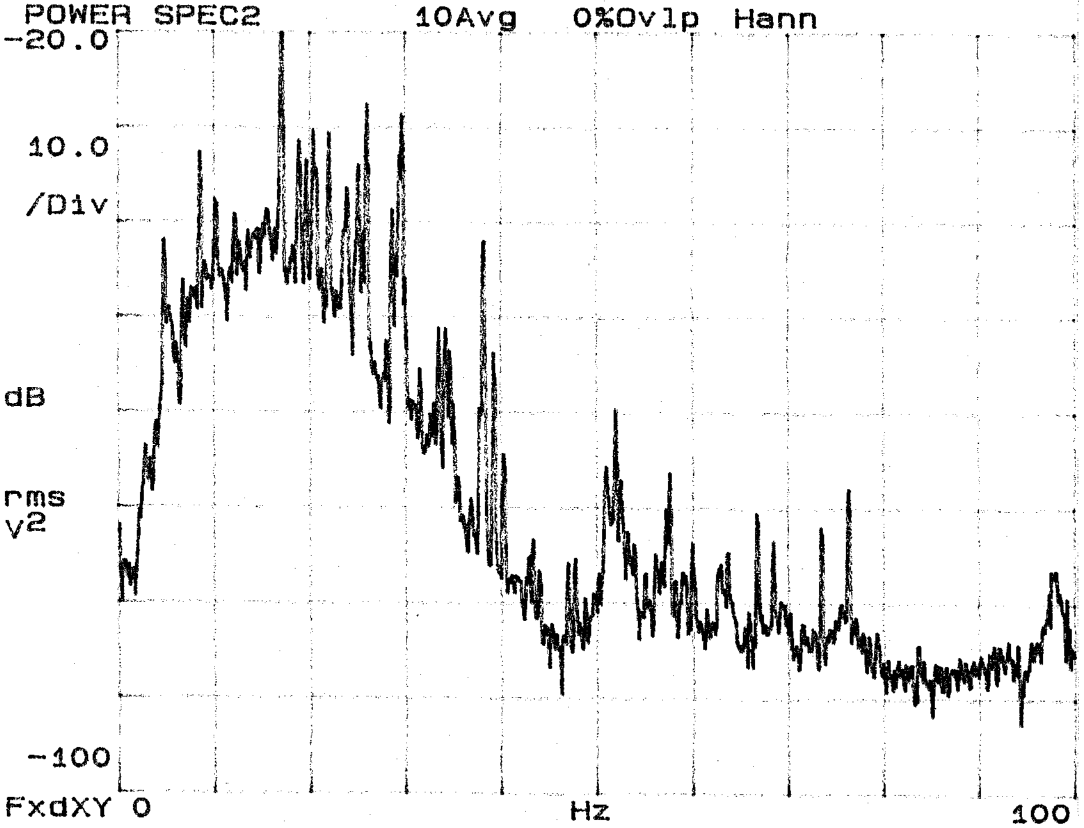

Q5

Power Spectrum of accel in vertical position on Al Plate

- All rotor stack (8,2,46)
- Used gray noise excitation

2/11/93 4:50PM

Power spectrum of accel in vert. and in horiz position on Al plate

- All viton stacks (8-6-4-2)
- Used ground noise excitation

Q6

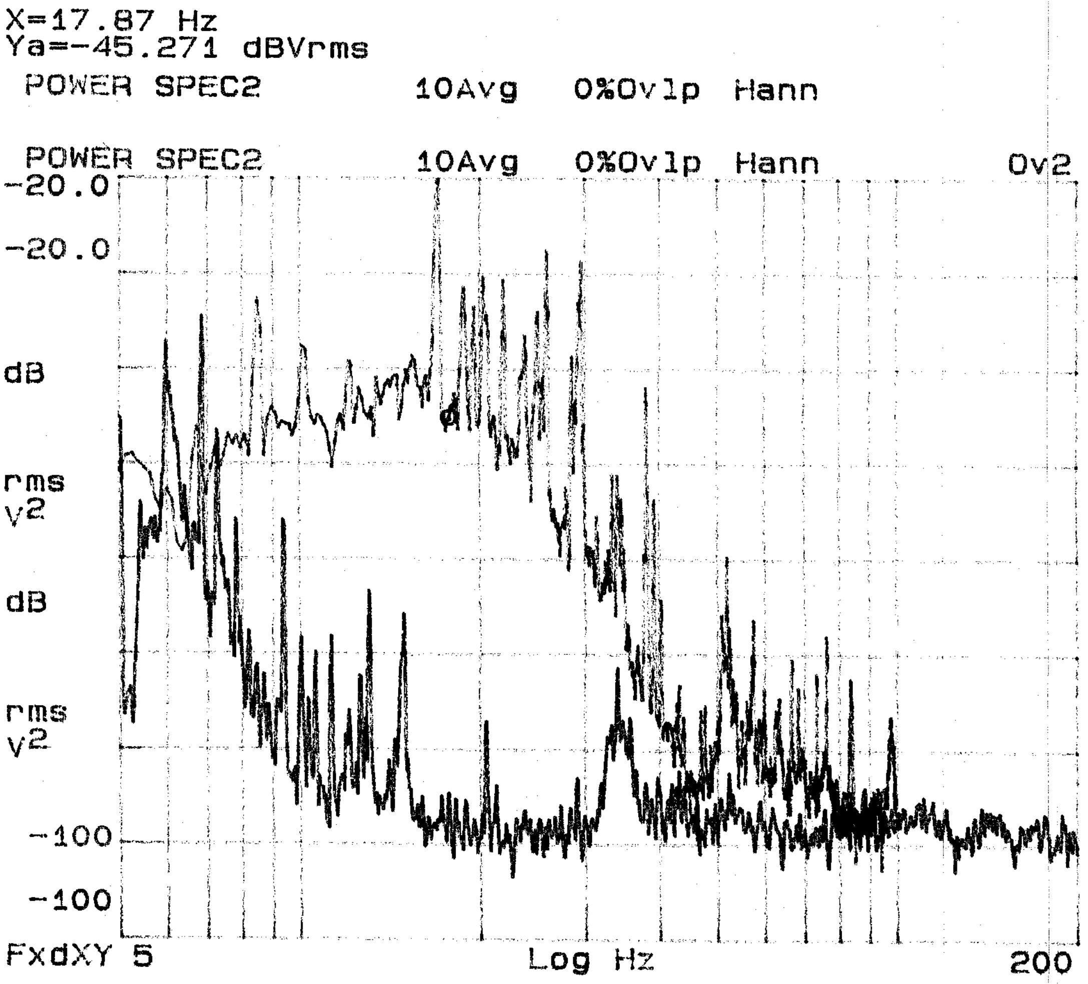

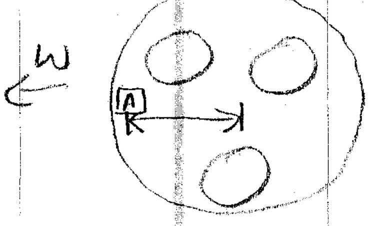

Oct. 21, 1992

RTU Springs tests to determine stiffness
under different loading

springs are compressed by 8%

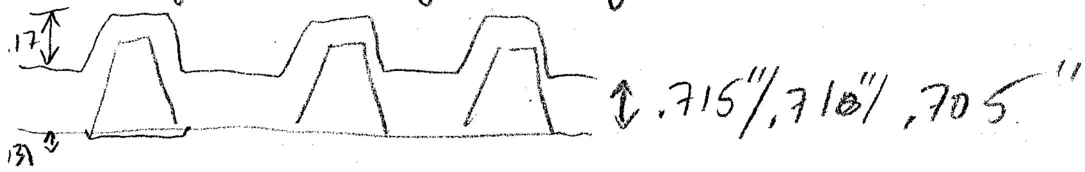

V-V Transfer function
of spring mass for RTV
Oct 21, 1992
3:45 PM

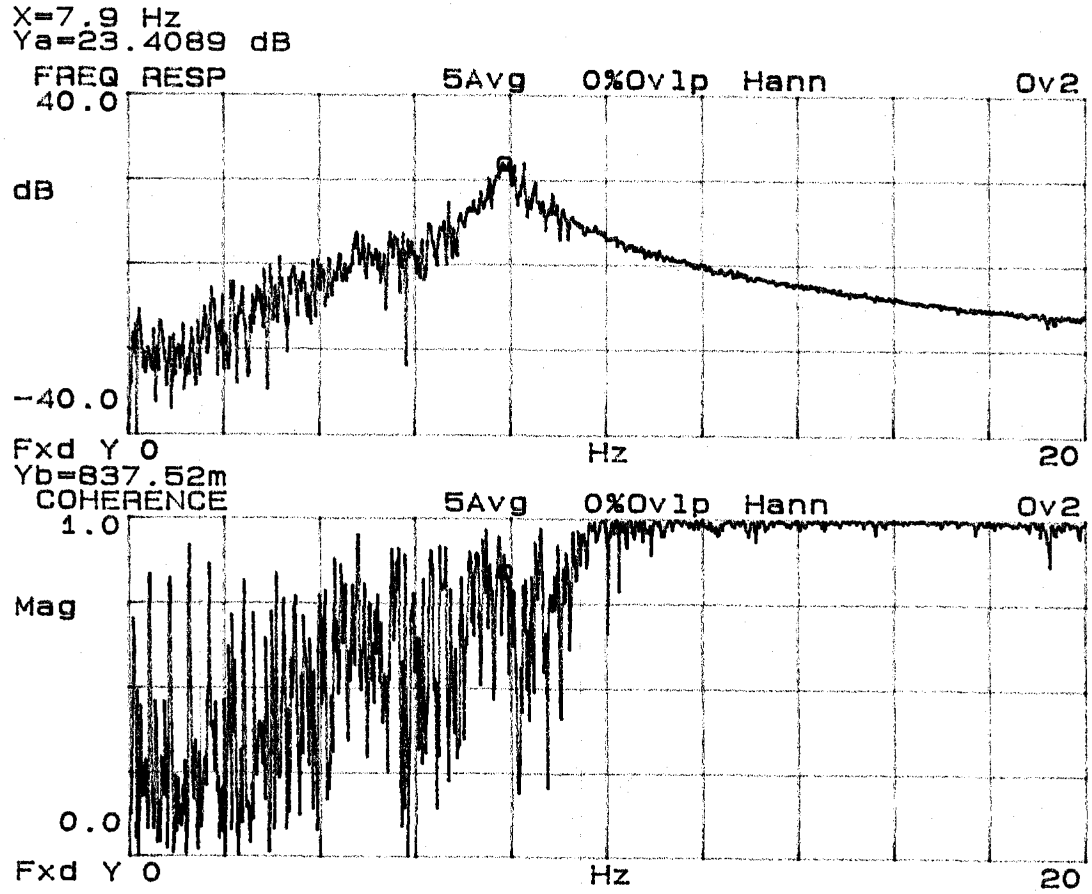

- ground noise excitation

springs:
conical design to be used in
Mark II

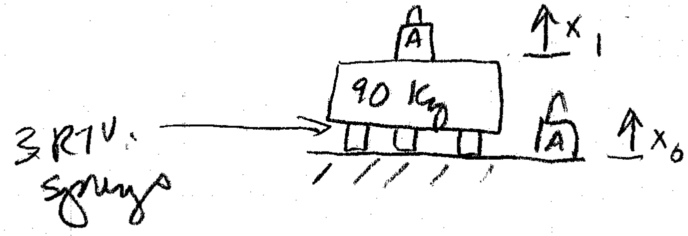

V-V transfer fctn of
spring mass for RTT
Oct 21, 1992
4:00 PM

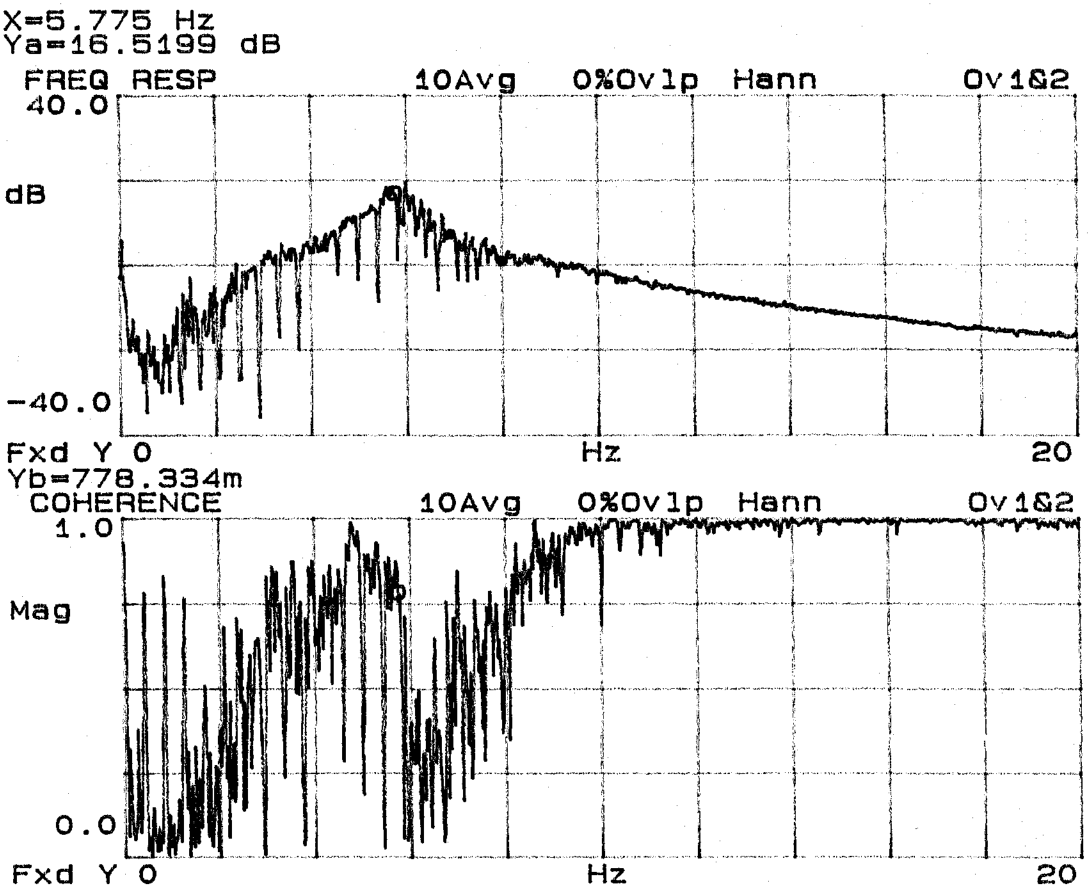

- Testing conical springs to be used in Mark II

- ground noise excitation

- Springs are compressed by 17%

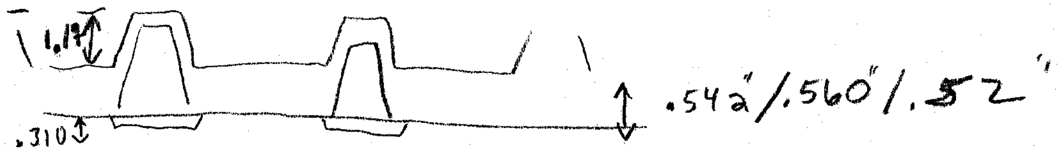

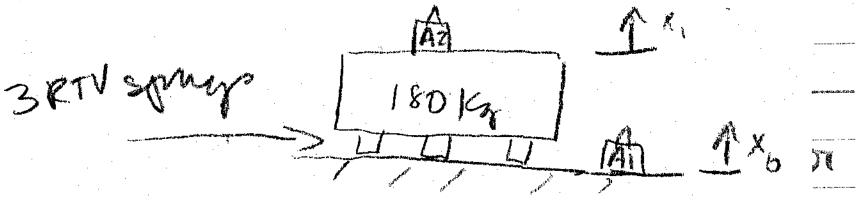

Transfer function of spring-mass for RTV

Oct 21, 1992
3:30 PM

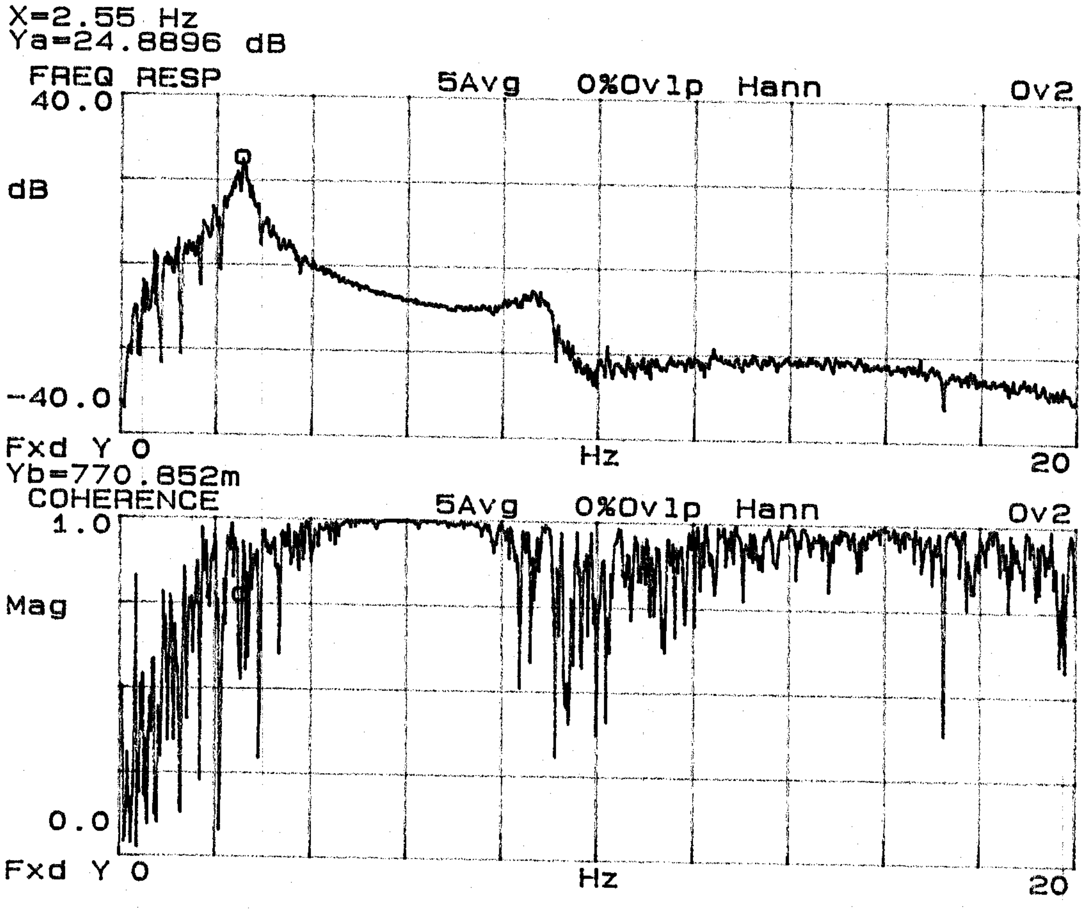

- ground noise excitation

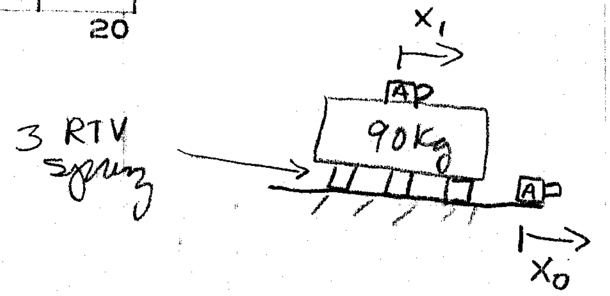

mzp:
Conical design to be used in Mark II

Transfer function of
spring-mass for RIV

Oct 21, 1992

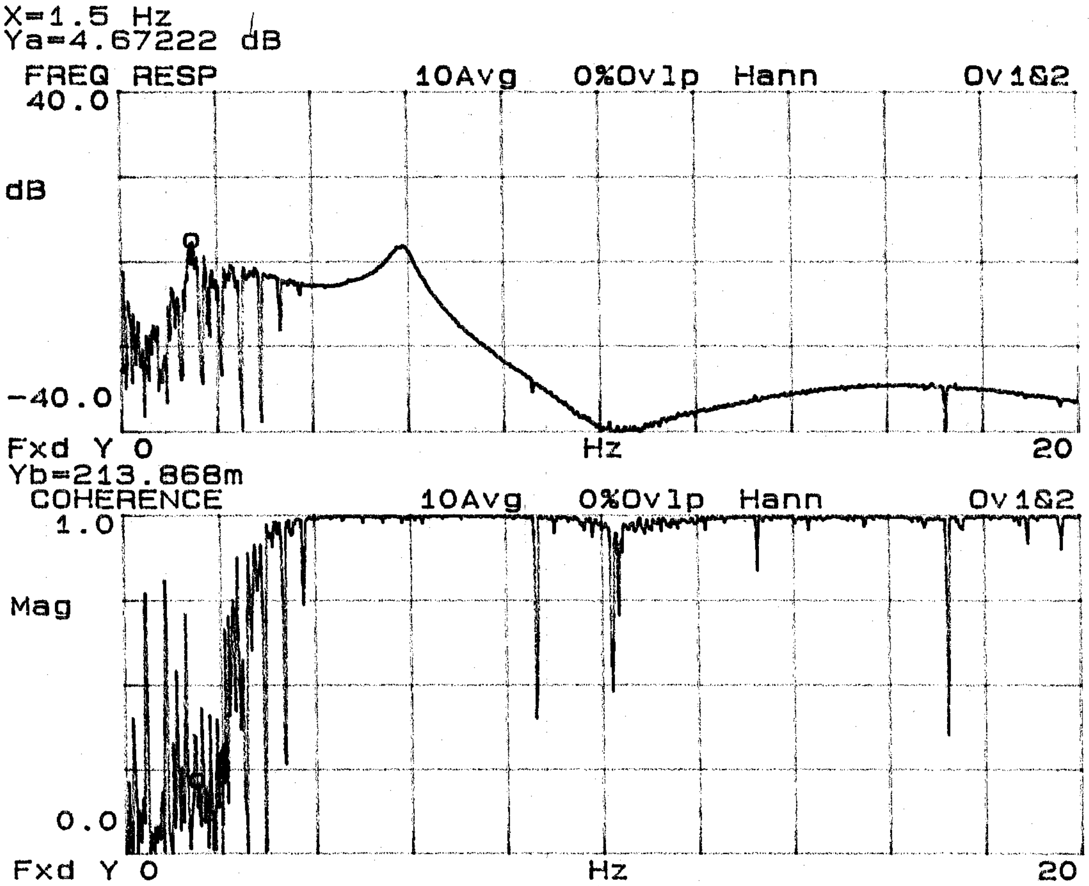

— ground noise excited

springs:
Conical design to be used in Mark II

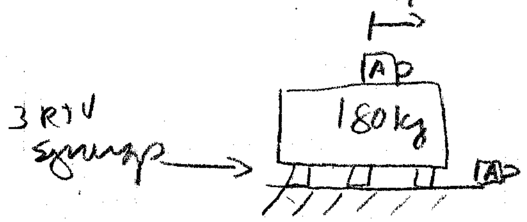

Stack Tests

Set up stacks with 4 layers of viton

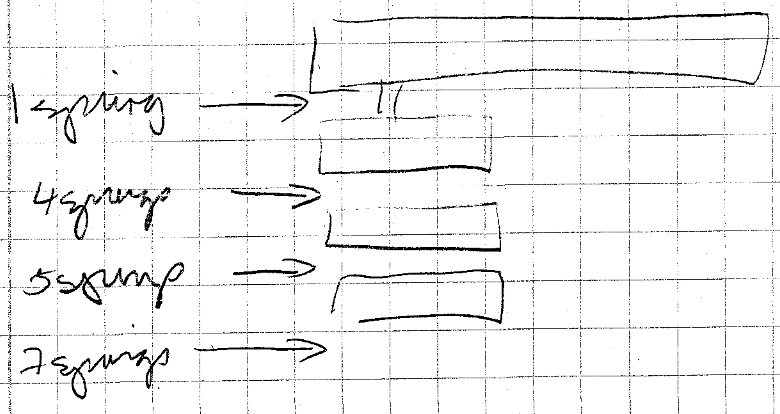

Height of stack

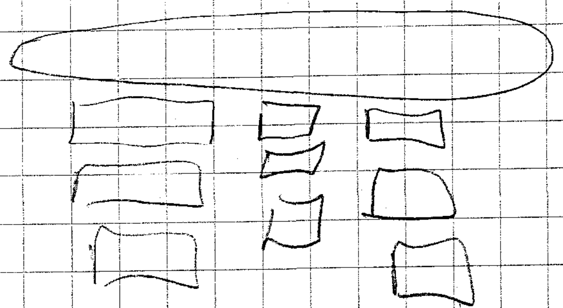

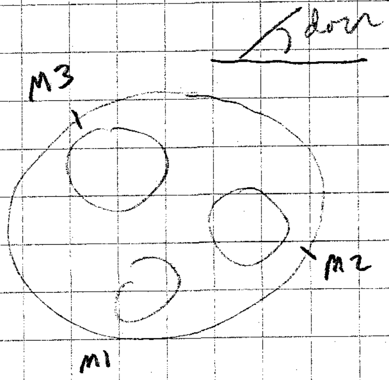

	M1	M2	M3
Oct 22	20 13/16	20 13/16	20 14/16
Oct 26	20 6 5/16	20 9/16	20 7/16
Nov 3	20 1/4	20 5/16	20 6/16

Horizontal Tests

1) Do transfer functions to see effect of loading on Support structure

2) Do transfer functions to make sure optics table remains rigid structure with load on top

3) Do transfer functions to see attenuation of stack + SS H-H, H-V, V-V, V-H

also rotation + tilt

(Could do H-T, V-T, T-T, T-H, T-V, rot, + tilt) resonances of S.S. when loaded

10:40AM

STV

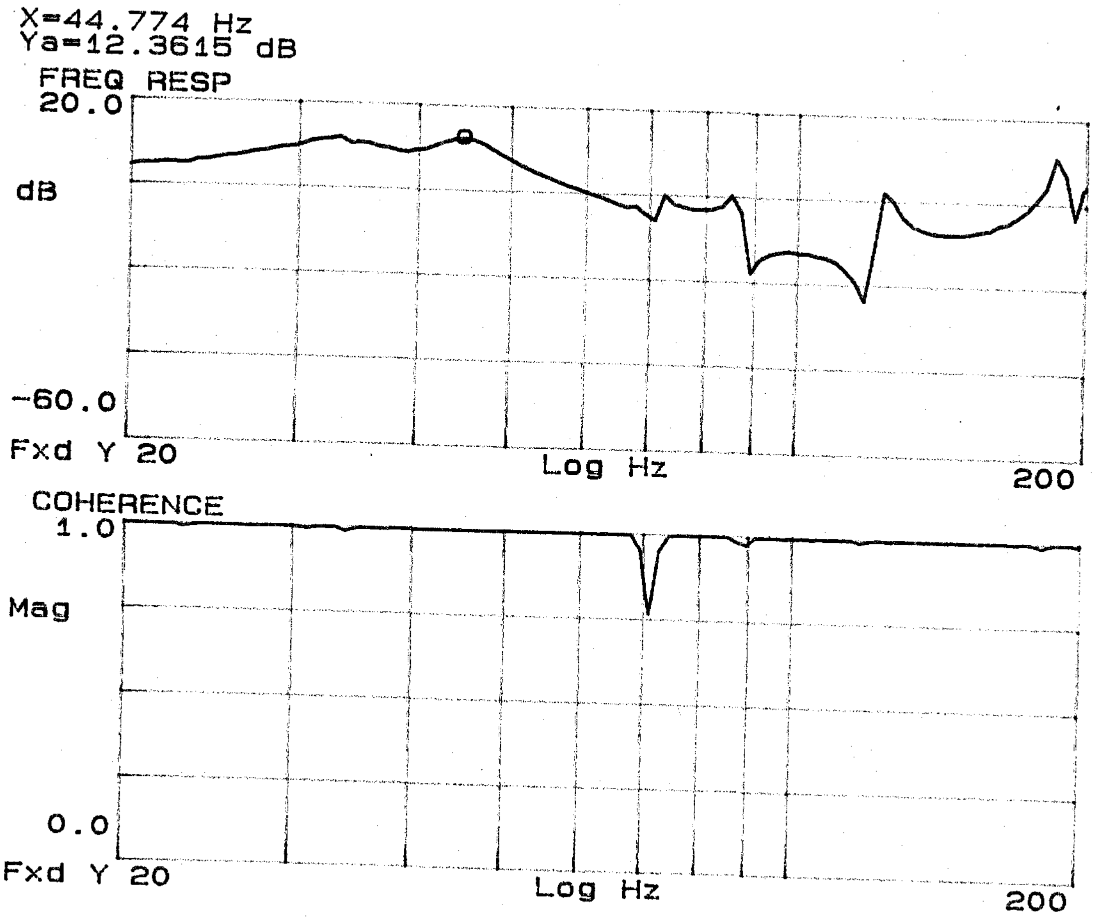

- 4 Layer Viton stack
- Measurement on support Structure with nelon Ste

Ave = 2

Integ time = 200 msec

Resln = 100 pt/dec

Source level = 100mV$_{rms}$

Crown Amp Gain = full

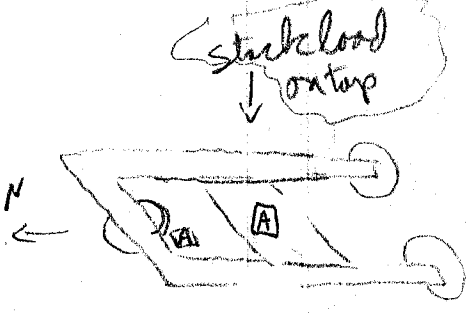

- Bottom accel at base of N support point
- Top accel at center of S.S.

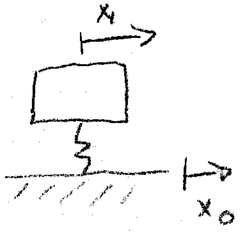

11:30

Comparison of Horizontal S.S modes with a stack on top and no stack

Blue : TF25 - no stack

Black : STV - stack

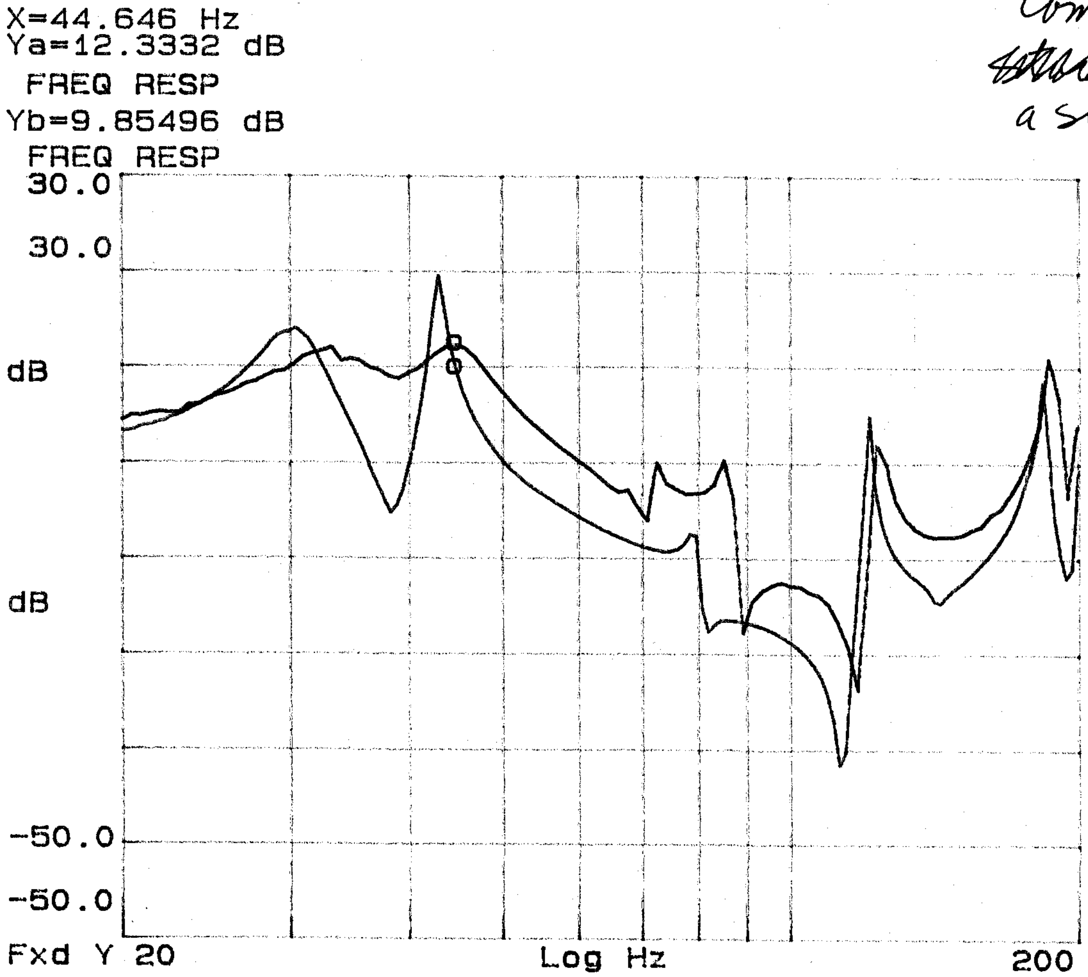

- Stack only damps modes
- Also increases frequencies slightly

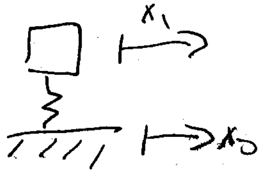

1:30 PM

Same as STV but with top accelerometer in vertical position

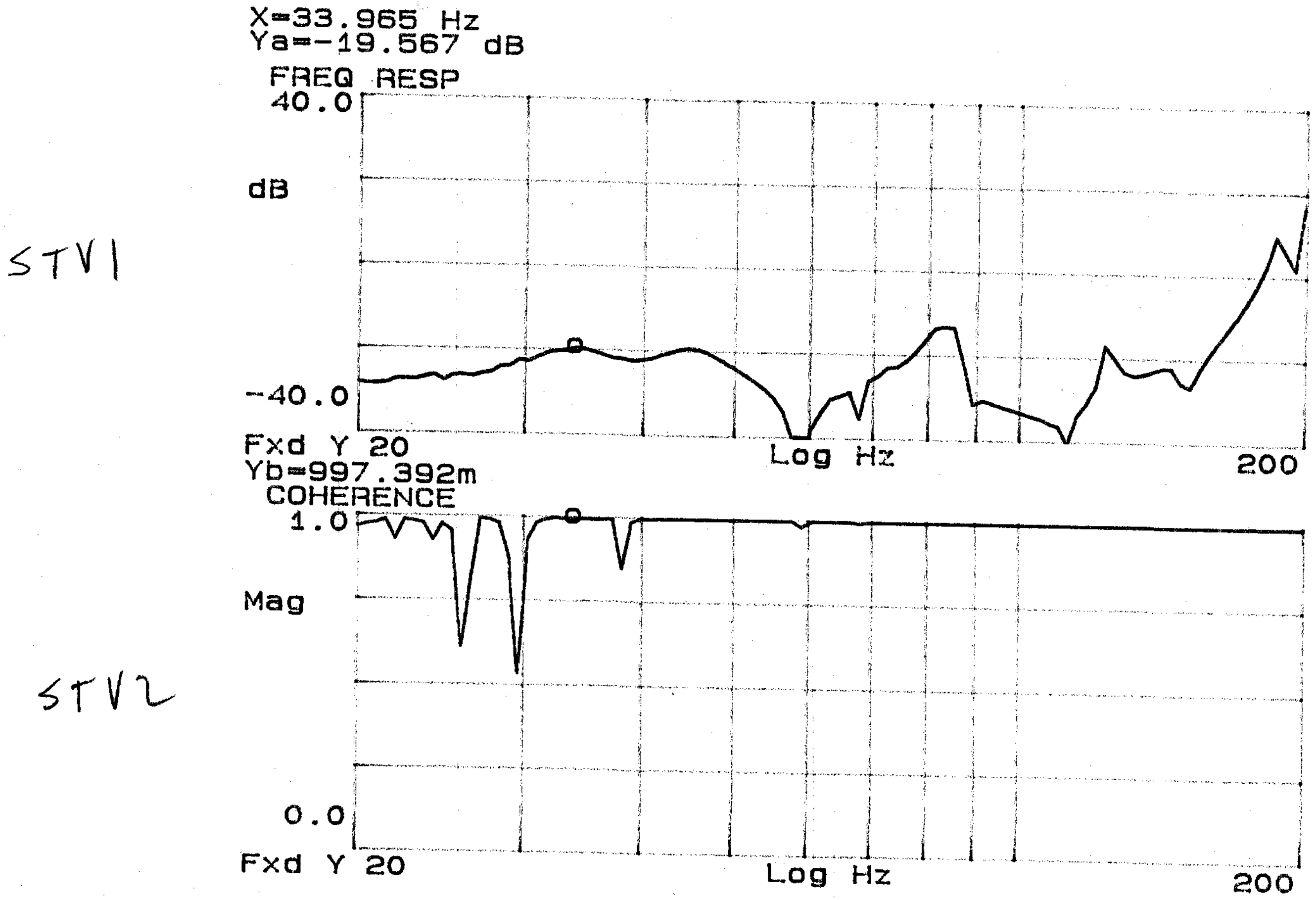

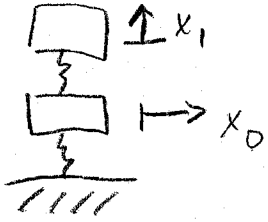

Oct 27, 1992
2:30 PM

STV3

STV(L)

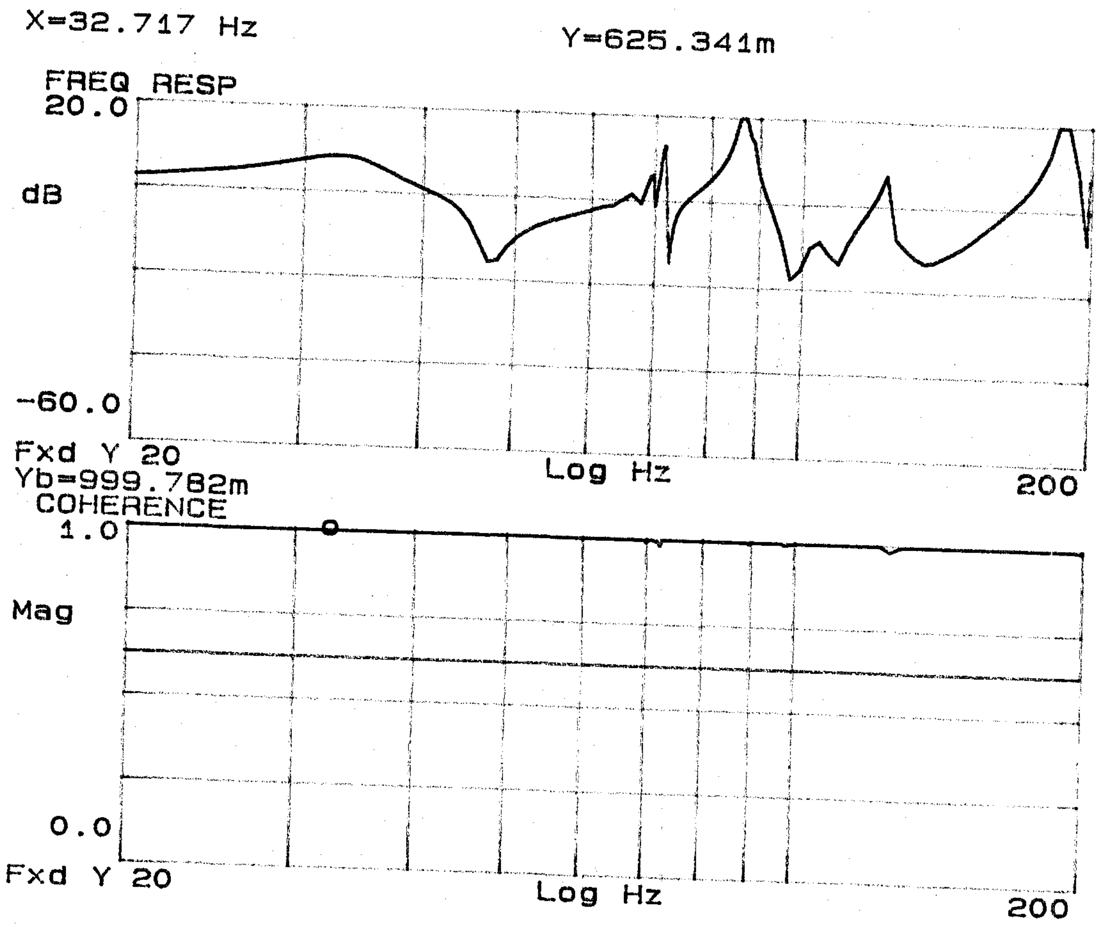

- 4 Layer Viton stack

Ave = 5

Integ time = 2 sec

Resln = 400 pt/sec

Source level = 400 mV$_{rms}$

Brown Amp Gain = full

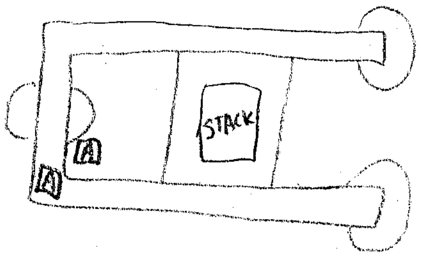

- Bottom accel in H position at base of N support point

- Top accel at N-W point on S3

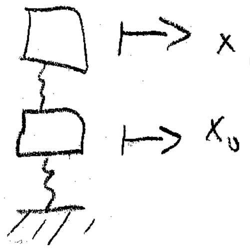

2:40 PM

Same as STV3 & STV4 except that upper accelerometer is in vertical position

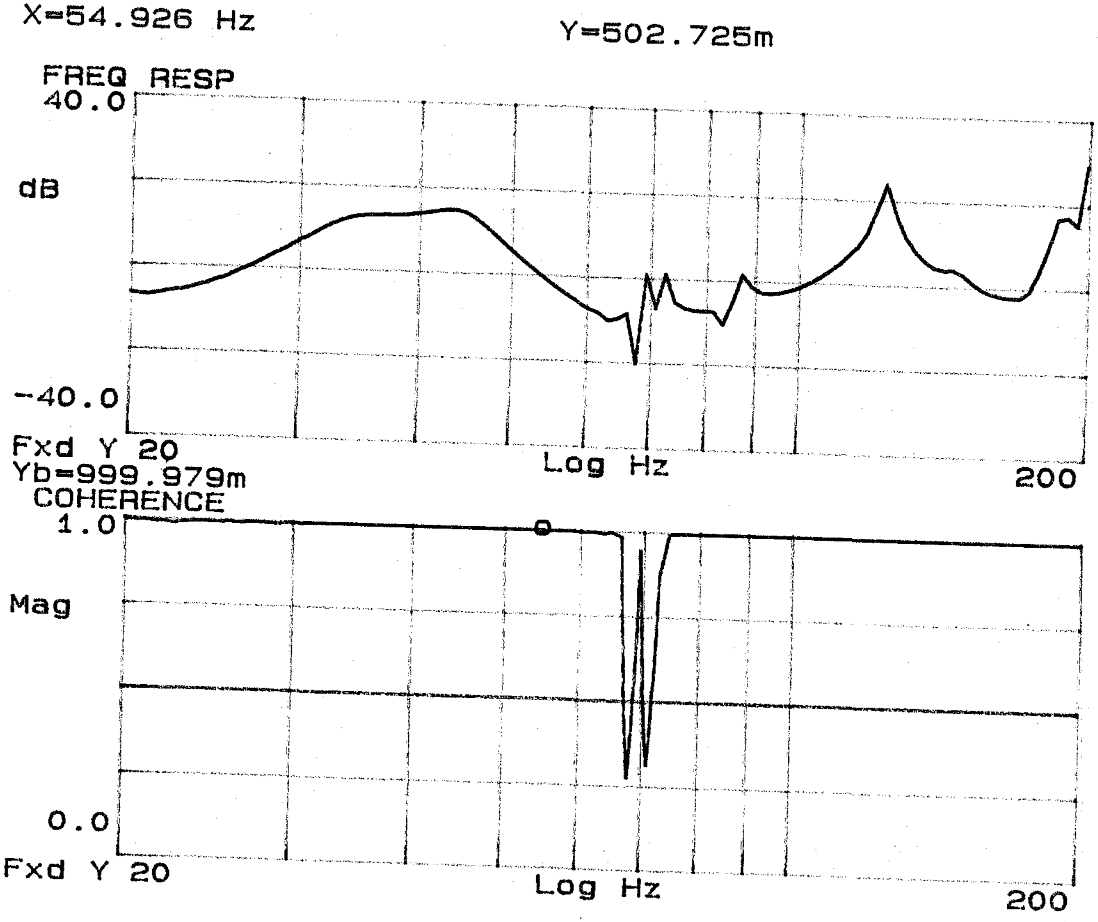

STV8

STV9

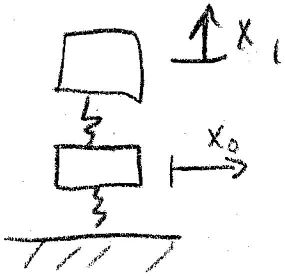

Oct 27, 1992
2:50 PM

- Transfer function from source voltage to horizontal acceleration on optics table
- Shaker is in H position

STV6

STV7

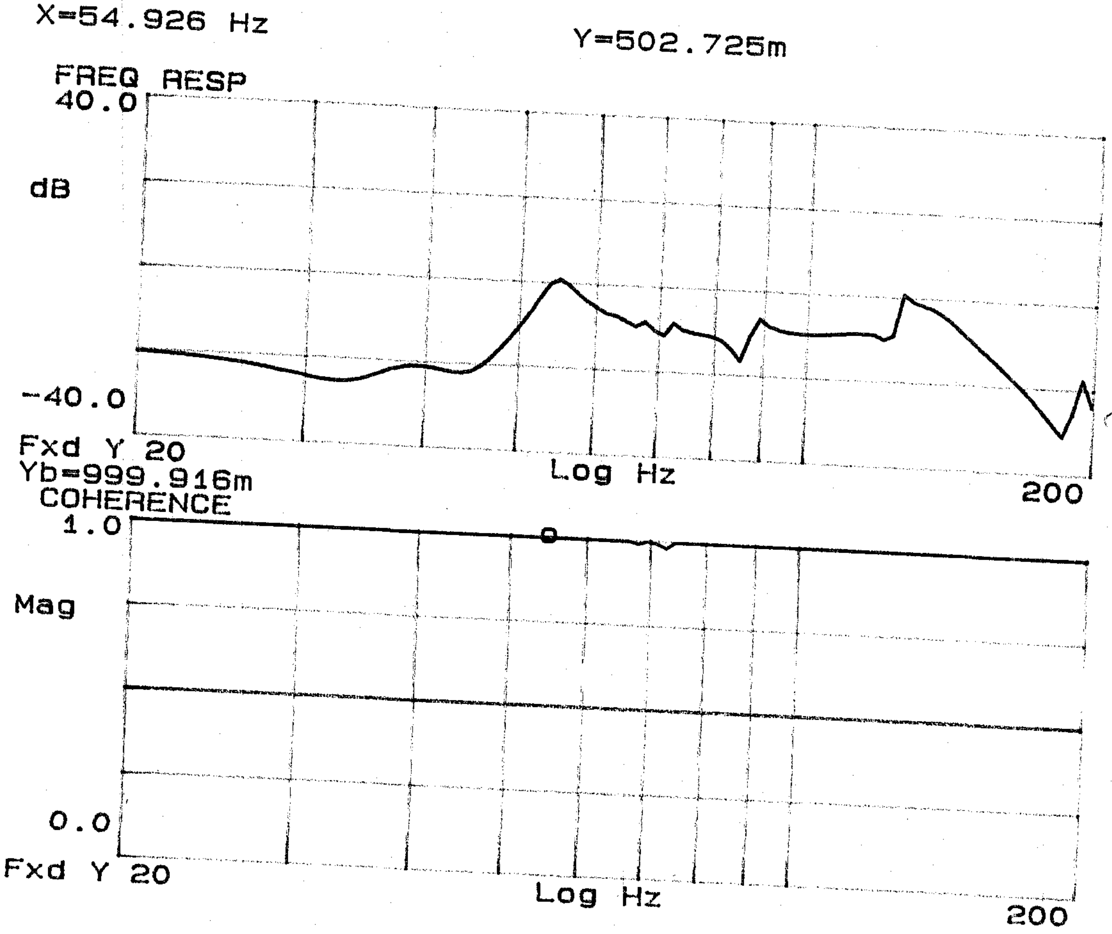

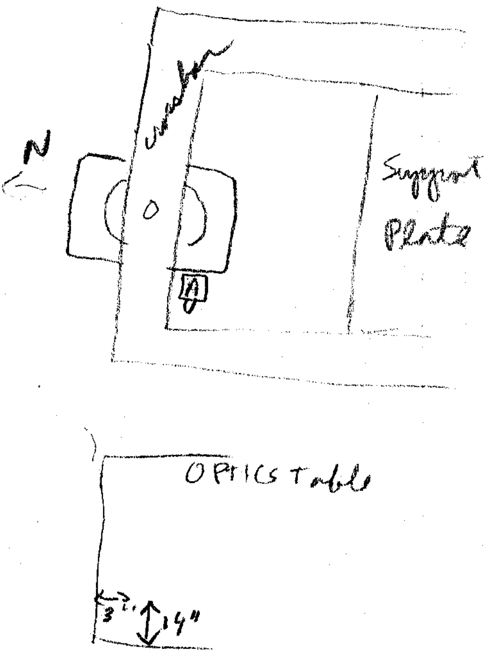

- Accel at North support point

Oct 27, 1992
3:15 PM

- Transfer fctns from source voltage to horizontal acceleration on optics table
- Shaker in H position

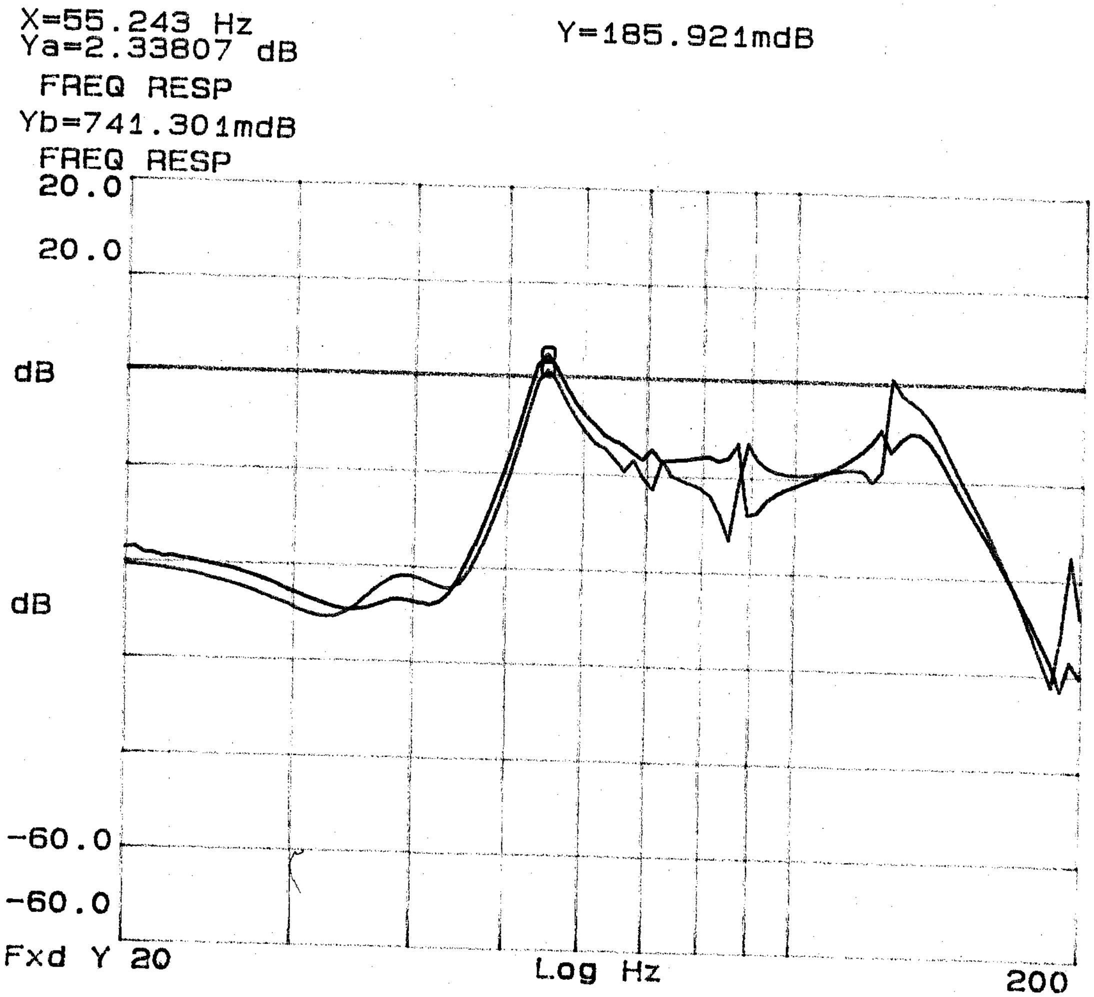

lack: STV10
rometer mounted
SW corner of optics
- close to SS
port point)

lue: STV6
elerometer mounted
l side of optics
e - close to
support point

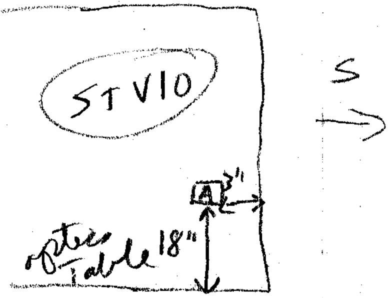

The 2 transfer fctns are close enough in value that it is reasonable to assume that when shaking in the H direction, each support point is moving with the same amount of motion. (i.e. all 3 support points are equivalent)

- Did Sine transfer fcn ~~in~~ H-H direction
- Could get data down to 5 Hz

5-10 Hz	10-17 Hz	17-20 Hz	20-50 Hz	50-200 Hz
20 mVrms	50 mVrms	100 mVrms	400 mVrms	600 mVrms
2 sec integ	2 sec integ	2 sec	500 msec integ	500 msec integ

400

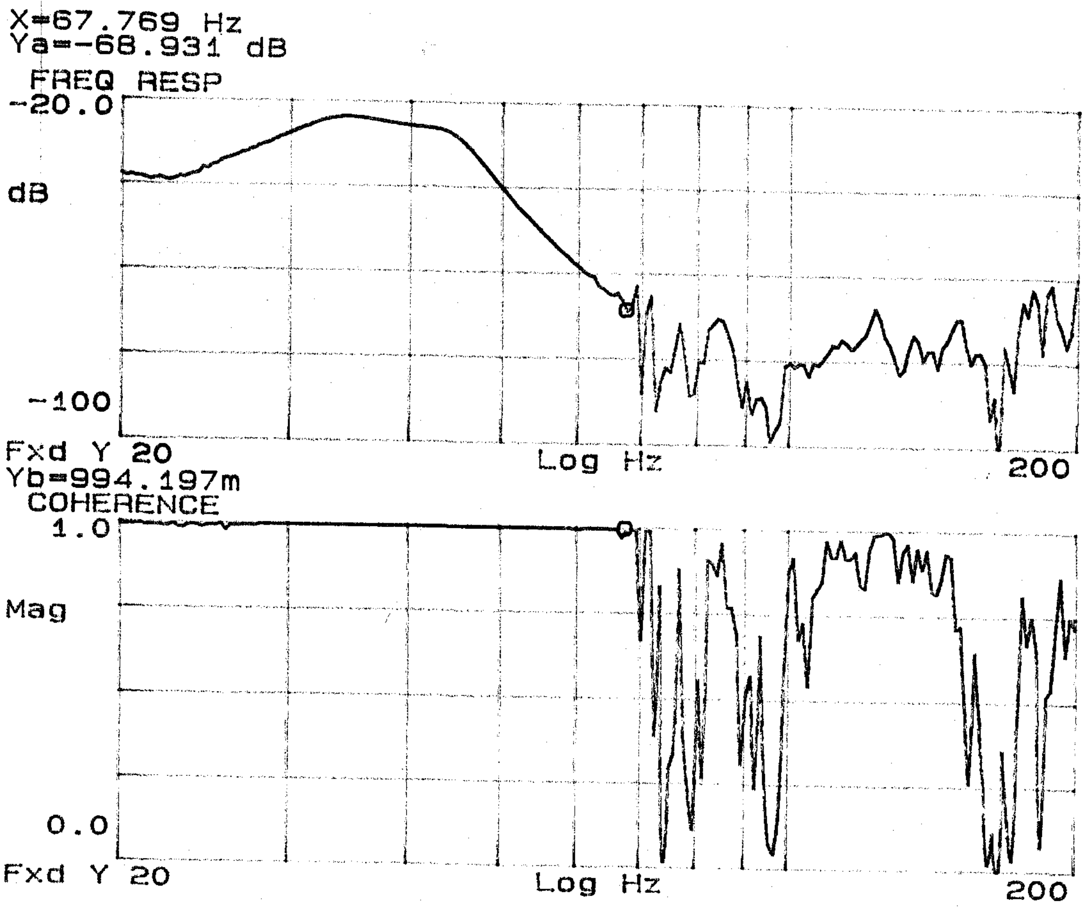
X=67.769 Hz
Ya=-68.931 dB
FREQ RESP
-20.0
dB
-100
Fxd Y 20
Log Hz
200
Yb=994.197m
COHERENCE
1.0
Mag
0.0
Fxd Y 20
Log Hz
200

Oct. 30, 1992
11:30 AM

Transfer Fcn from H-H

Source	Sweep
20mV$_{rms}$	5-10 Hz
50mV$_{rms}$	10-17 Hz
100mV$_{rms}$	17-20 Hz
400mV$_{rms}$	20-50 Hz
600mV$_{rms}$	50-200 Hz

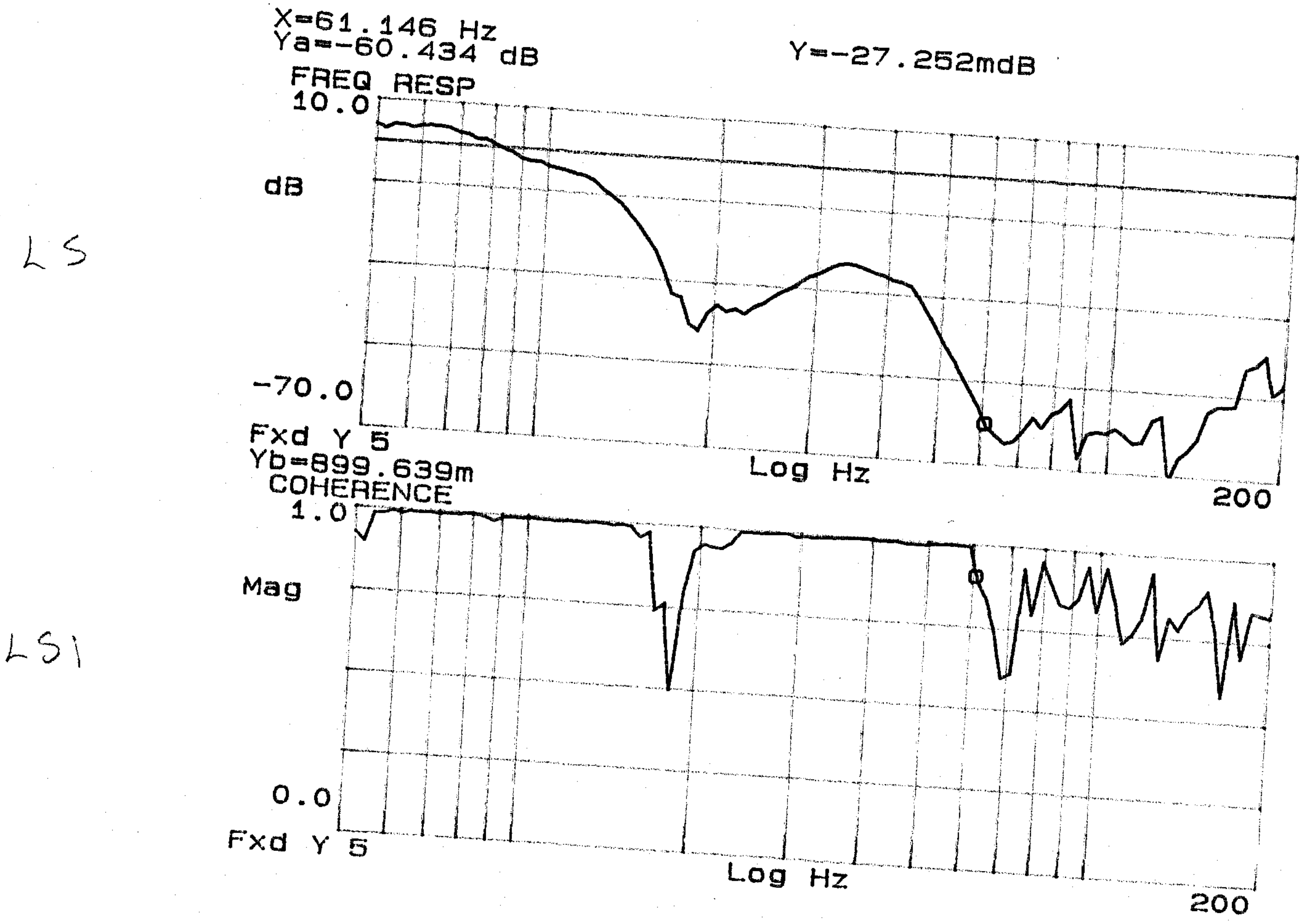

integ time = 500msec - 2 sec
Resln. = 50 pts/dec
Ave = 5

- Top accel on center of slab in Horiz position.
- Shaker is Horiz
- bottom accel by base of N drift compensator

inp 8-6-4-2

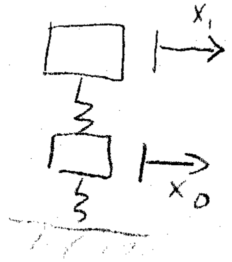

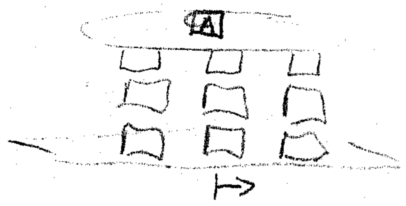

Oct 30, 1992
4:00 PM

Transfer Fcn from H-H
with top accel on edge of top
plate

Same setup as LS
except top accel on edge
of plate (18" from center)

LS2

LS3

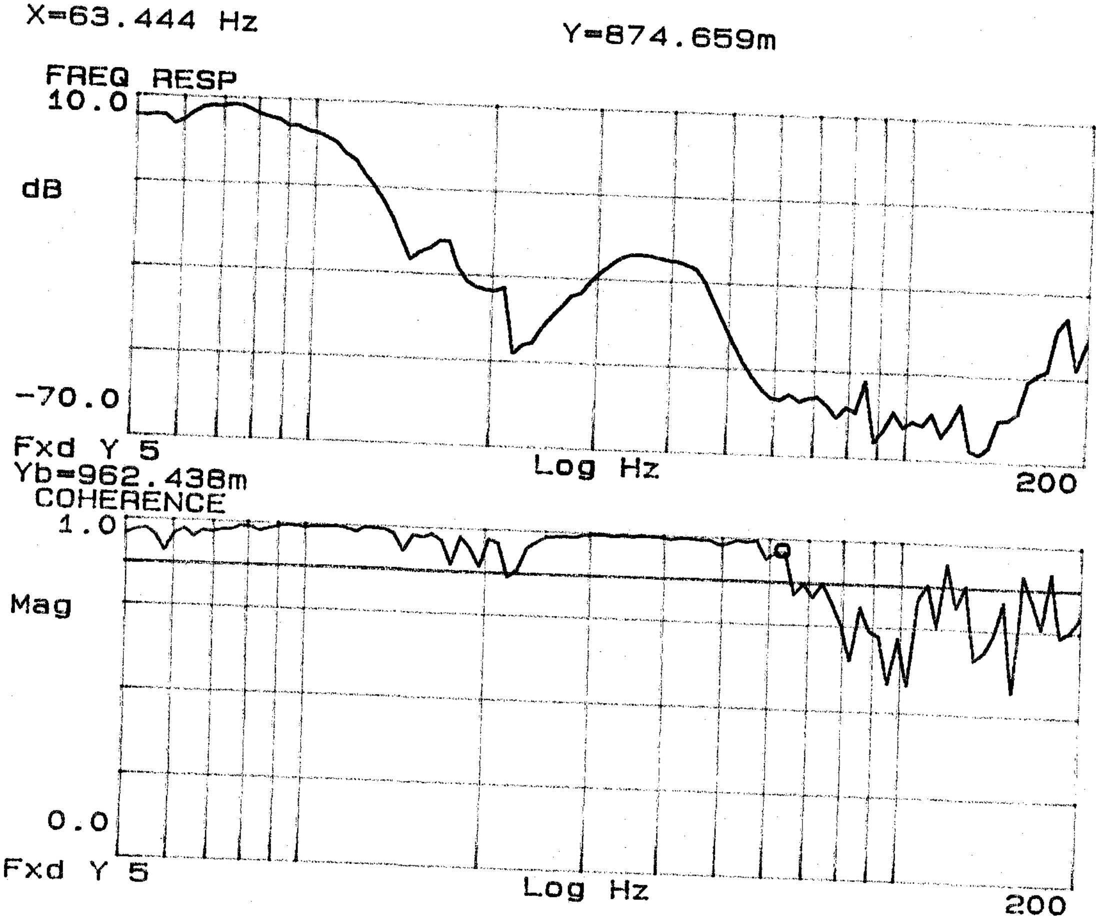

sideview

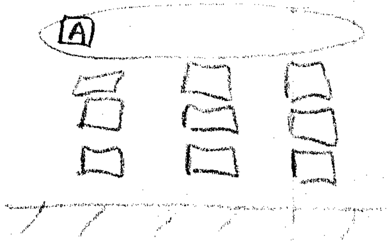

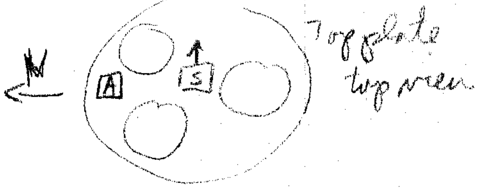

Top plate
top view

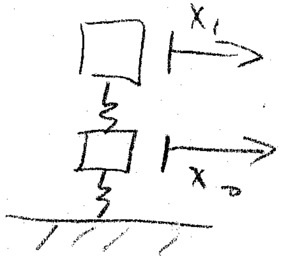

Oct 30, 1992
4:30 PM

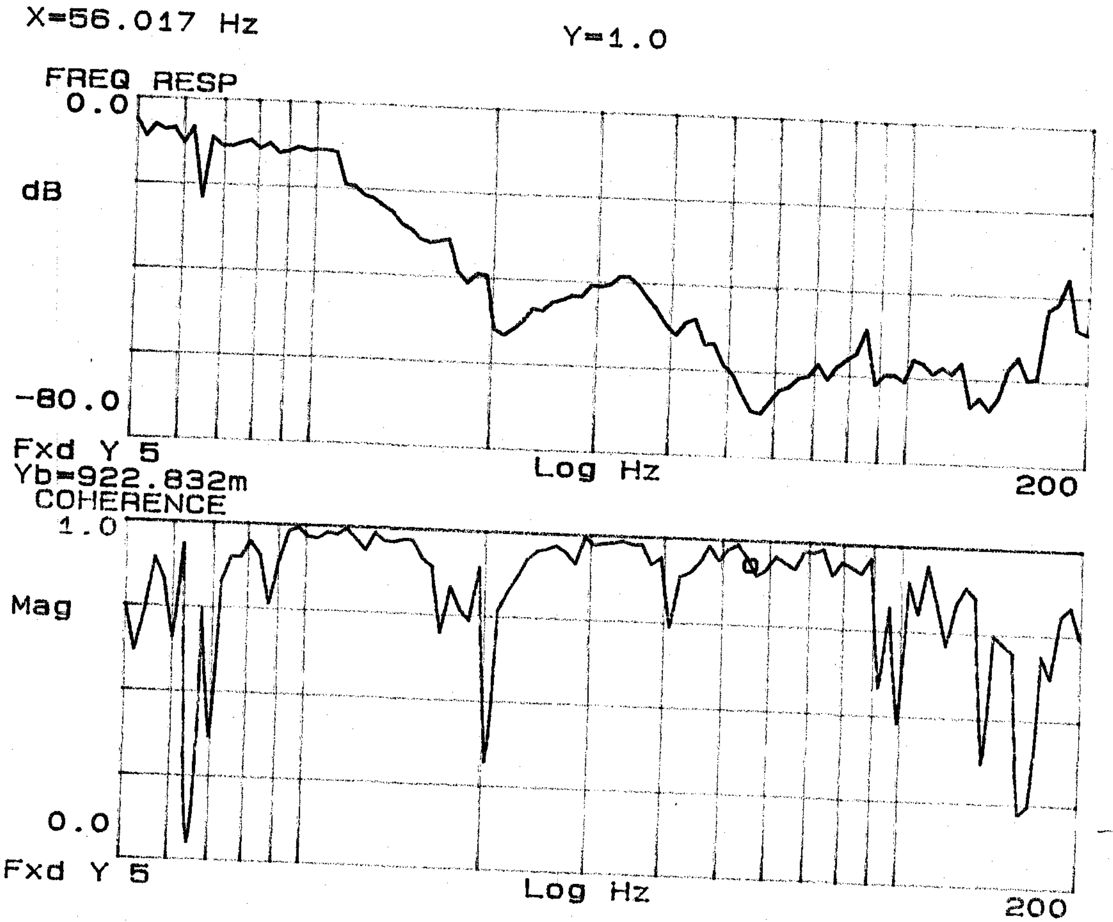

LS11

LS5

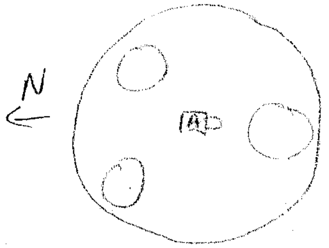

- Shaker was in Horizontal orientation
- Top accelerometers in transverse orientation
- Bottom accel in long orientation near N drift compensator

Transfer fctn

Nov. 5, 1992
4:20 PM

Transfer fctn from Horizontal to vertical on center of plate

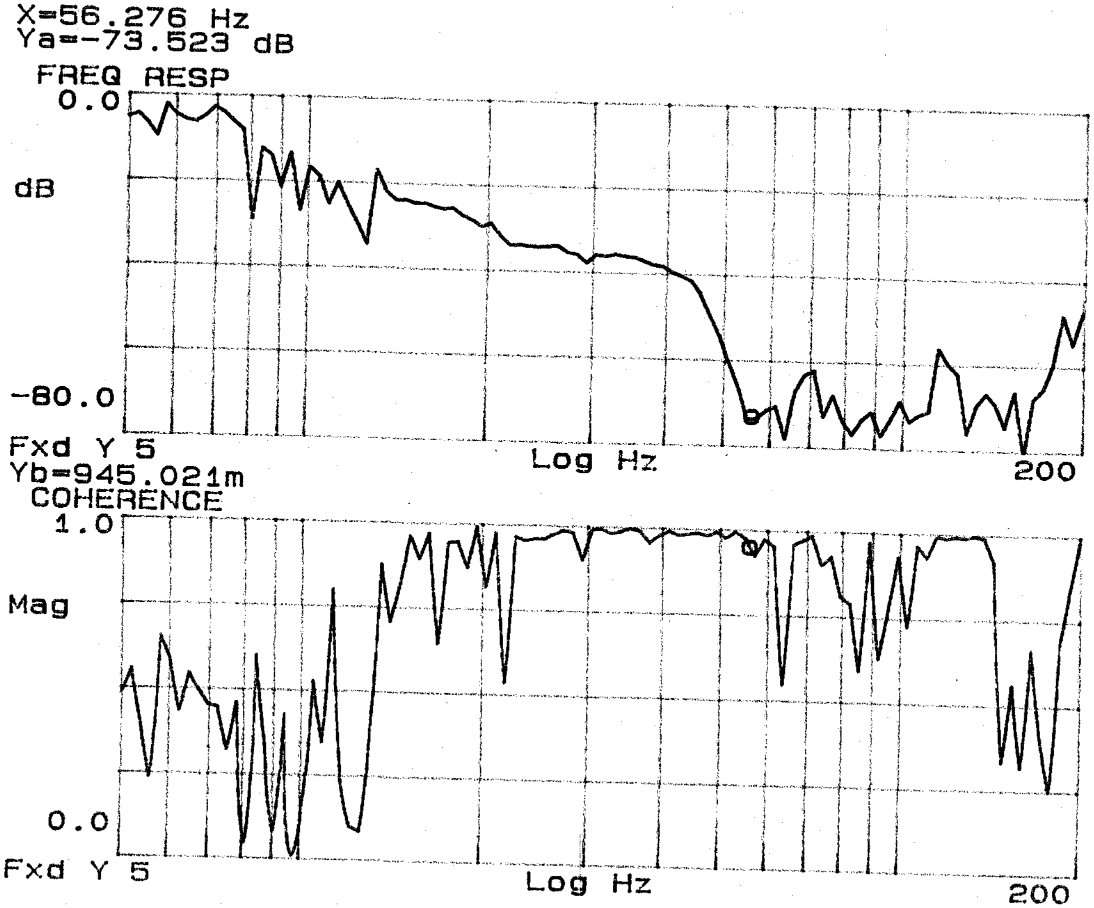

LS8

LS9

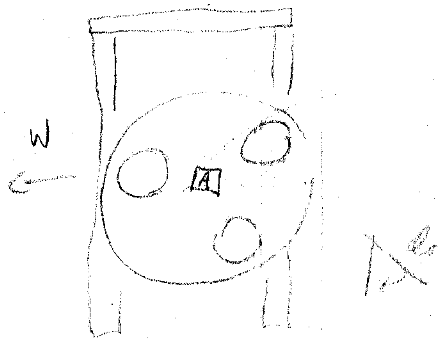

- Shaker in Horizontal position
- 1 op accel at center of plate

5 Av

5-7Hz	20mVrms	3sec integ
7-12Hz	50mVrms	3sec integ
12-17Hz	100mVrms	3sec integ
17-50Hz	400mVrms	2sec integ

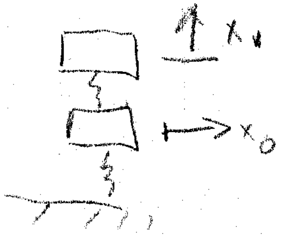

4:50 PM

Transfer Fctn from Horiz
to vertical on edge of plate

LS10

LS11

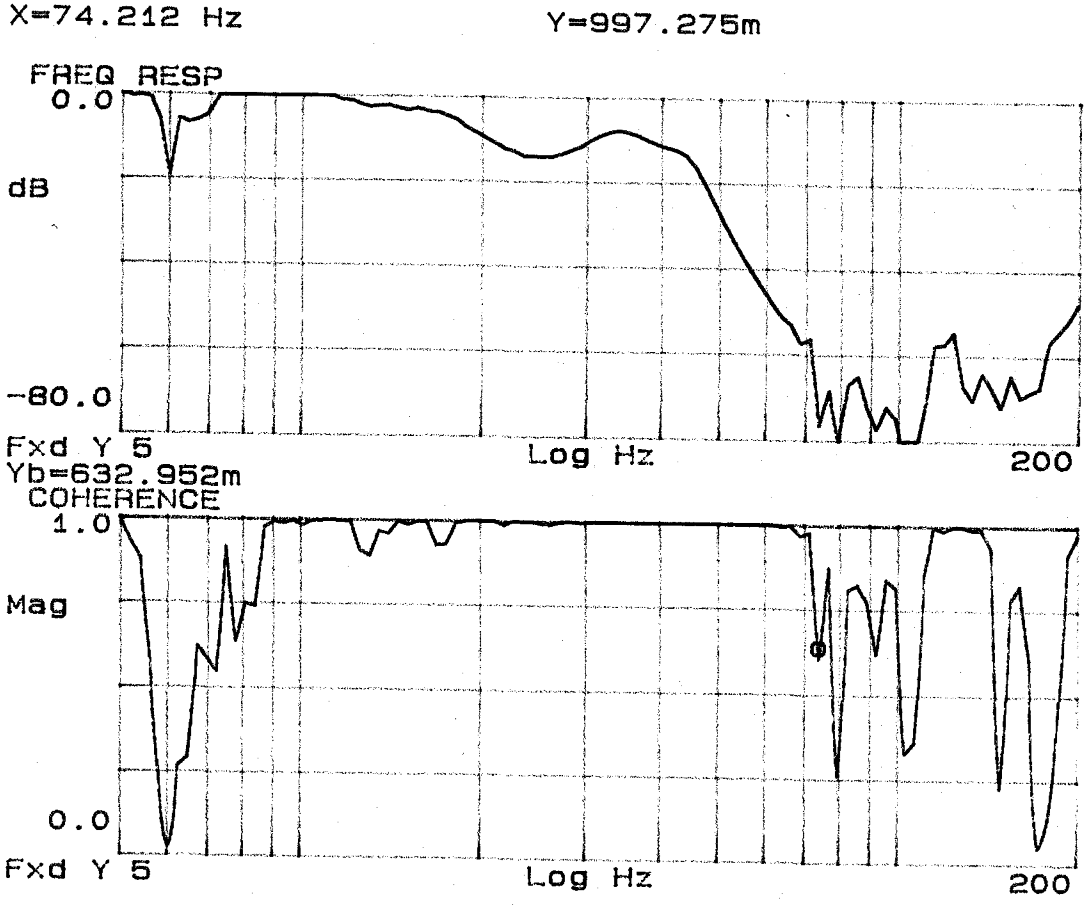

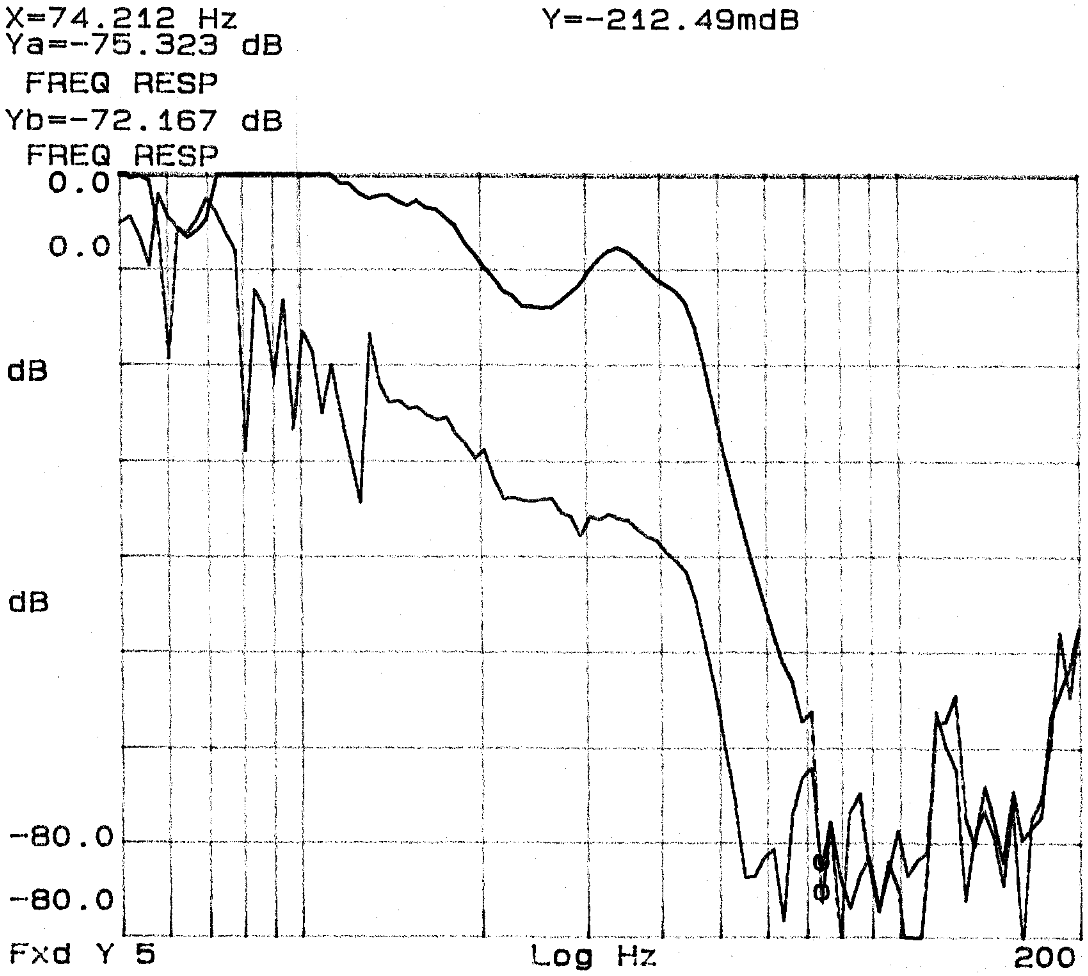
X=74.212 Hz
Ya=-75.323 dB
FREQ RESP
Yb=-72.167 dB
FREQ RESP
Y=-212.49mdB
0.0
0.0
dB
dB
-80.0
-80.0
Fxd Y 5
Log Hz
200

Top plate drifted way over to side so took top plate off to see what springs had done. They had drifted to one side. Top + bottom of spring were perfectly parallel. Shape looks distorted

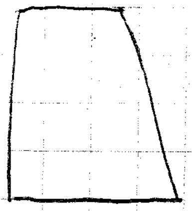

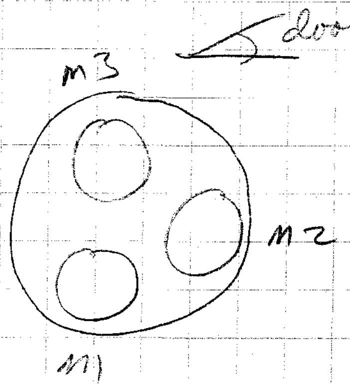

1 spray first layer

	M1	M2	M3
height	max 1.838" min 1.835"	max 1.838" min 1.830"	max 1850" min 1.842"

lly skewed

nearly as skewed

ge ||

4 springs	M1 leg 2nd layer	S1	S2	S3	S4
	height	max 1.856" min 1.848"	max 1.877" min 1.894"	max 1.8904 min 1.882"	max 1.874" min 1.862"

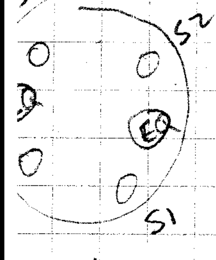

v ↓

- rubber has small surface cracks
- probably due to air pockets close to surface bursting under load

- Reassembled stack with better centered EQ stops
- This time we leveled bottom plate (not top plate)
- We decided to measure drift of EQ relative to EQ stops

Nov 4, 1995
5:00PM

	~~M1-1~~		~~M2-3~~		~~M3-5~~	
	~~1~~	~~2~~	~~1~~	~~2~~	~~1~~	~~2~~
~~distance from EQ stop to plate~~	~~.295~~	~~.268~~			~~.2~~	

~~M1-2~~		~~M2-4~~		~~M3-6~~	
~~1~~	~~2~~	~~1~~	~~2~~	~~1~~	~~2~~

Nov. 4, 1992 5.00 PM

Measurements on side
drift of stack

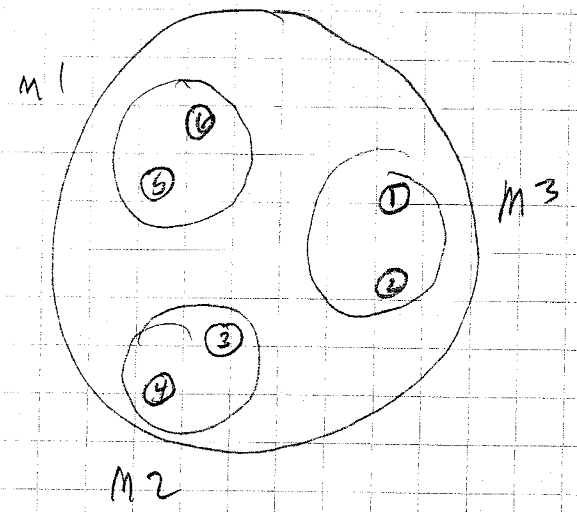

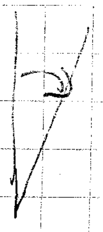

Nov. 4, 1995
5.00 PM

	1		2		3		4		5		6	
	1	2	1	2	1	2	1	2	1	2	1	2
distance from EQ stop to plate	.295	.268	365	.320	.311	.323	.300	.302	.272	.306	.241	.278

Nov. 9, 1992

The stack drifted back onto the earthquake stops so decided to change springs out. The M1 leg second layer had one of the springs collapse.

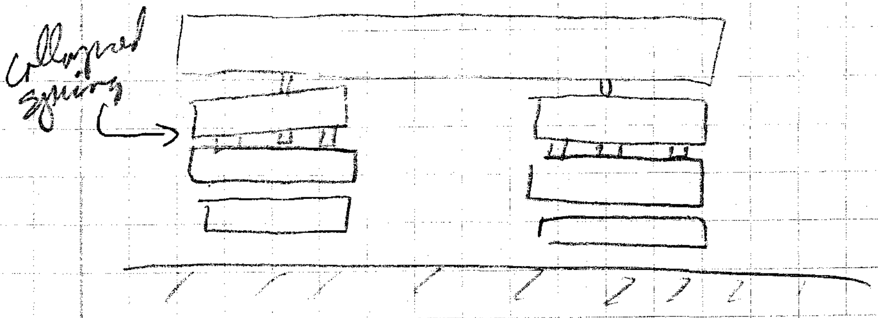

- Brand new springs (springs that had been in spring compressor) that had been post-cured at 260°C for 24 Hrs were put in the bottom layer
- Layer 4 springs were used in layer 3
- Layer 3 springs were used in layer 2
- Top layer: Outer springs come from layer 2 (3 springs) of M2
  Inner springs come from layer 3 (3 springs) of M3
- The remaining springs were marked and put in bags

The level of the top of the stack was measured and was as follows

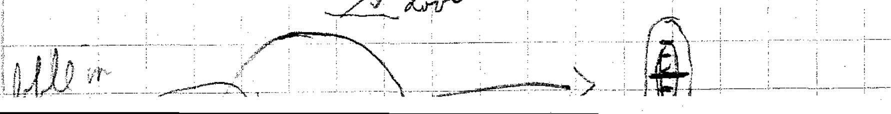

We left the 3 guide pins in with the hope that the stack would have a chance to drift down and would stop it from drifting sideways

Old Stack Spring Composition (#1)

1st layer - 1 - 55 Kg/spring
2nd " - 4 - 36 Kg/spring
3rd " - 5 - 47 Kg/spring
4th " - 7 - 47 Kg/spring

New Stack Spring Composition (#2)

1st layer - 2 - 27.5 Kg/spring
2nd layer - 4 - 36 Kg/spring
3rd layer - 6 - 39 Kg/spring
4th layer - 8 - 42 Kg/spring

Nov. 12, 1992

Took the 3 guide pins out and replaced with EQ stops

The level was the same as Nov. 9

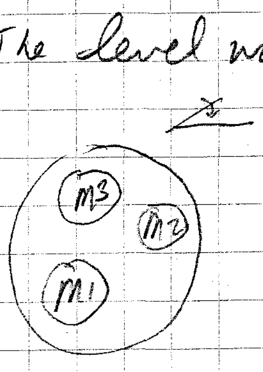

Height of stack: M1 - 20 $\frac{9.5}{16}$
M2 - 20 10/16
M3 - 20 10/16

Measurements of where EQ Strips are in each socket in the top plate:

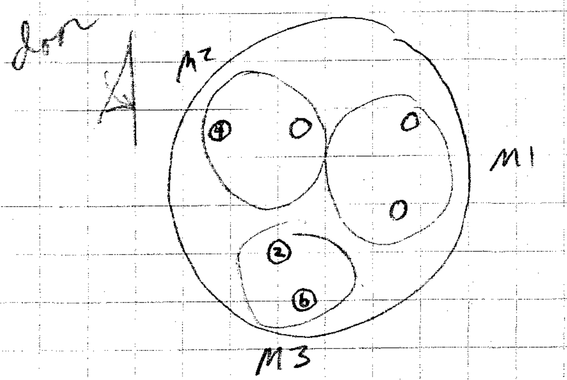

6		2		4		3		1		5	
1	2	1	2	1	2	1	2	1	2	1	
2.75	4.04	4.28	4.51	3.80	3.40	3.67	3.93	3.23	3.58	4.96	3.17

vv.14,1992
12.00 PM

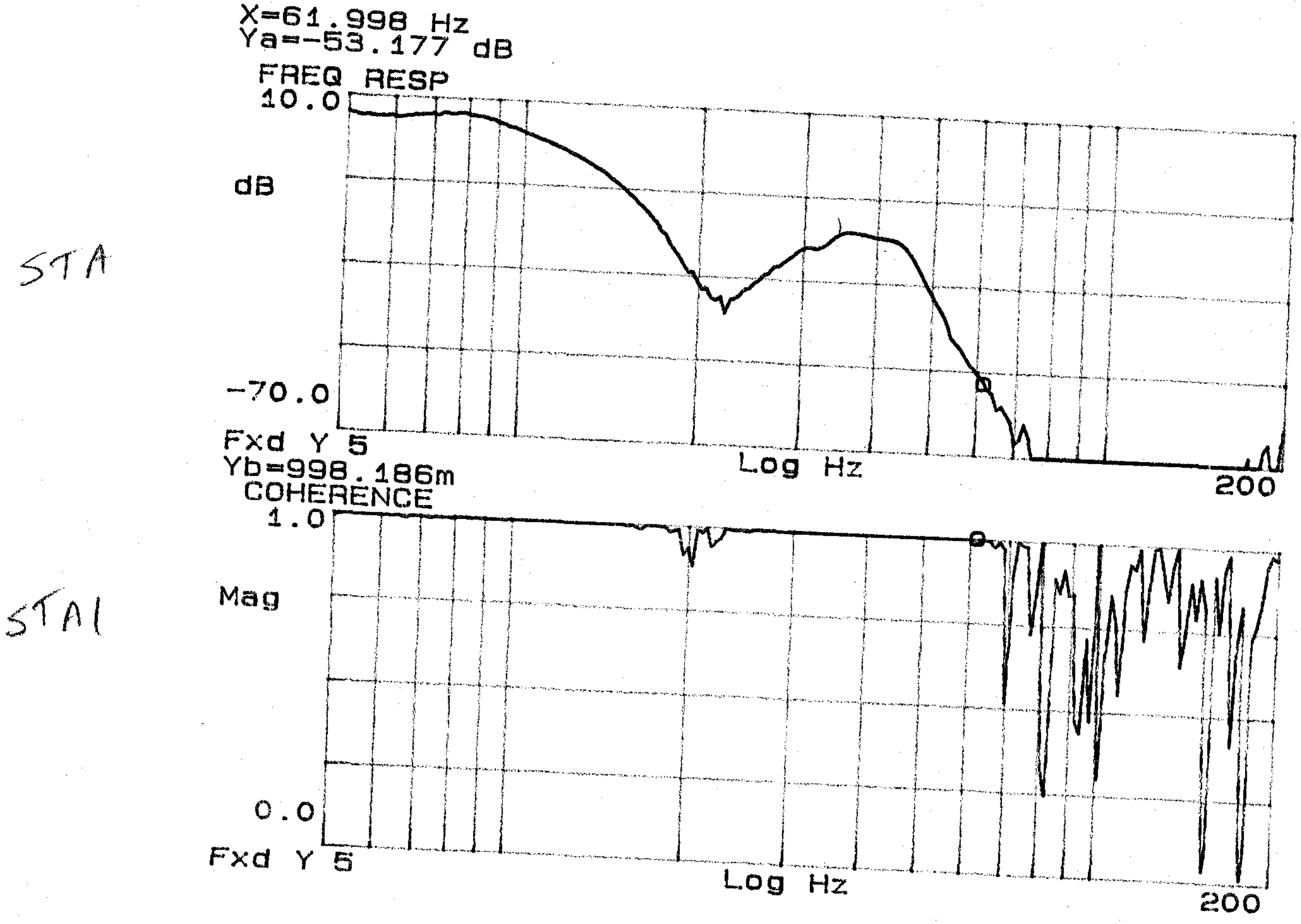

HtoH Transfer Fcn

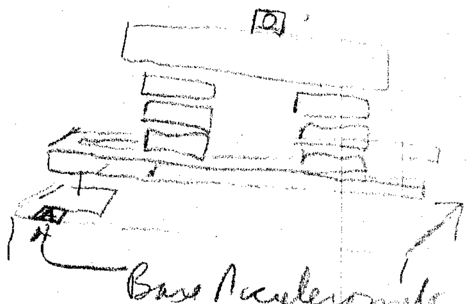

Base Accelerometer next to N drift compensation pad

Top accel in center of plate. Oriented to the east (toward the door)

ouce level = 100mVrms 5-20Hz
= 406mVrms 20-200Hz

Vg = 2
integ time = 300msec
sln = 125 pt/dec

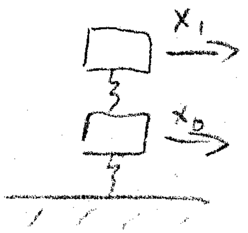

This stack was rebuilt after trying stack with cracked springs. Added an extra spring to layer 1 (top), 3, + 4. Shifted roll-off by ~6Hz => stiffness changed by ~20%

We found out that bringing the temp of the rotor from 0-230°c over a short period of time cracked the springs. We did a step + ramp post-cure over 2 + 3 day time periods that didn't crack springs. We reassembled stack with springs from MIT that had been ramp post-cured

Dec. 30

- Assembled stack 8-6-4-2
- Finished assembly at 3:30 PM
- Top Layer has springs from all batches so we can check & see mechanical properties
- Left guide pins in since EQ stops were too tall since stack hadn't drifted significantly

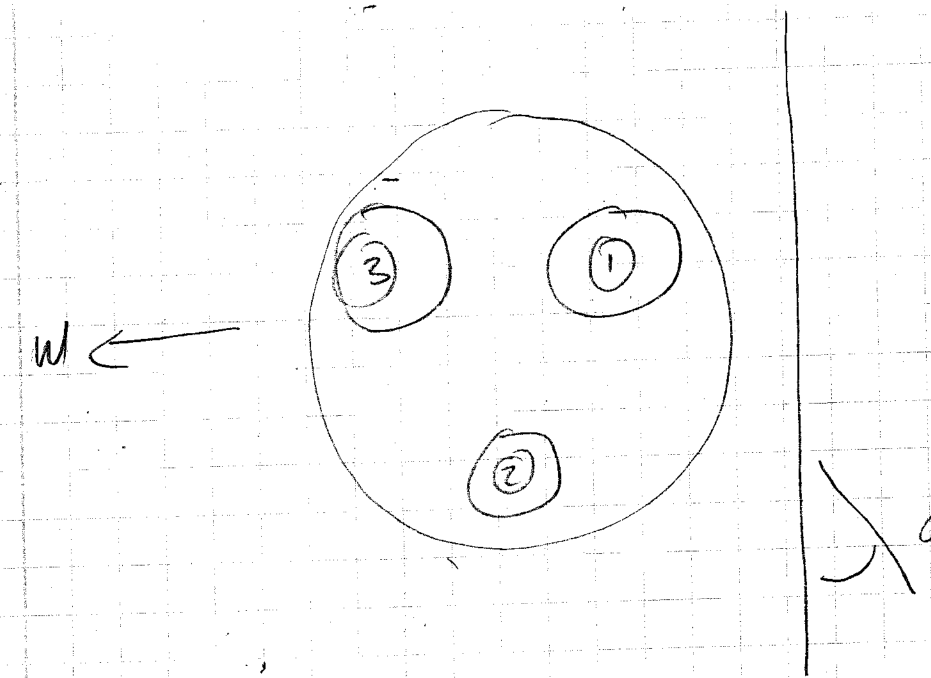

stack height (vs) Time

		①	②	③
12/30	3:50 PM	21¼"	21⅛"	21⅛"
	4:50 pm	21 1/32"	21 1/16"	21 1/32"
1/2	11:05 AM	20 15/16	20⅞"	20 15/16"
1/4	11:20 AM	20 15/16	20⅞"	20 29/32"
1/5	10:50 AM	20 29/32"	20 29/32"	20 29/32"

1/2/92 Lifted top plate to see if any springs had cracked on first layer (visibly)

Batch 1 - maybe a crack, maybe OK (1 spring)
Batch 2 - not visibly cracked (1 spring)
Batch 4 - not visibly cracked (2 springs)
Batch 5 - not visibly cracked (1 spring)
Batch 6 - not visibly cracked (1 spring)

EQ stop height = 19.81"
stack height - recess = $20\frac{15}{16}$" - .8268" = 20.11"
Needs to drift .3" = .76 cm for EQ stops to fit

Load/spring given 2 Spring Configurations

(Al plate = 164 Kg
Steel leg = 91.3 Kg)

	# springs	with no optics load	with 40 Kg optics load
1	2	27 Kg/spring	34 Kg/spring
2	3	49 Kg/spring	53 Kg/spring
3	5	47 Kg/spring	50 Kg/spring
4	7	47 Kg/spring	48 Kg/spring
1	2	27 Kg/spring	34 Kg/spring
2	4	36 Kg/spring	40 Kg/spring
3	6	40 Kg/spring	42 Kg/spring
4	8	41 Kg/spring	43 Kg/spring

2:10 PM

Transfer fcn from H-H

Source	Freq
100mV$_{rms}$	5-18Hz
400mV$_{rms}$	18-40 Hz
600mV$_{rms}$	40-100 Hz
200mV$_{rms}$	> 100 Hz

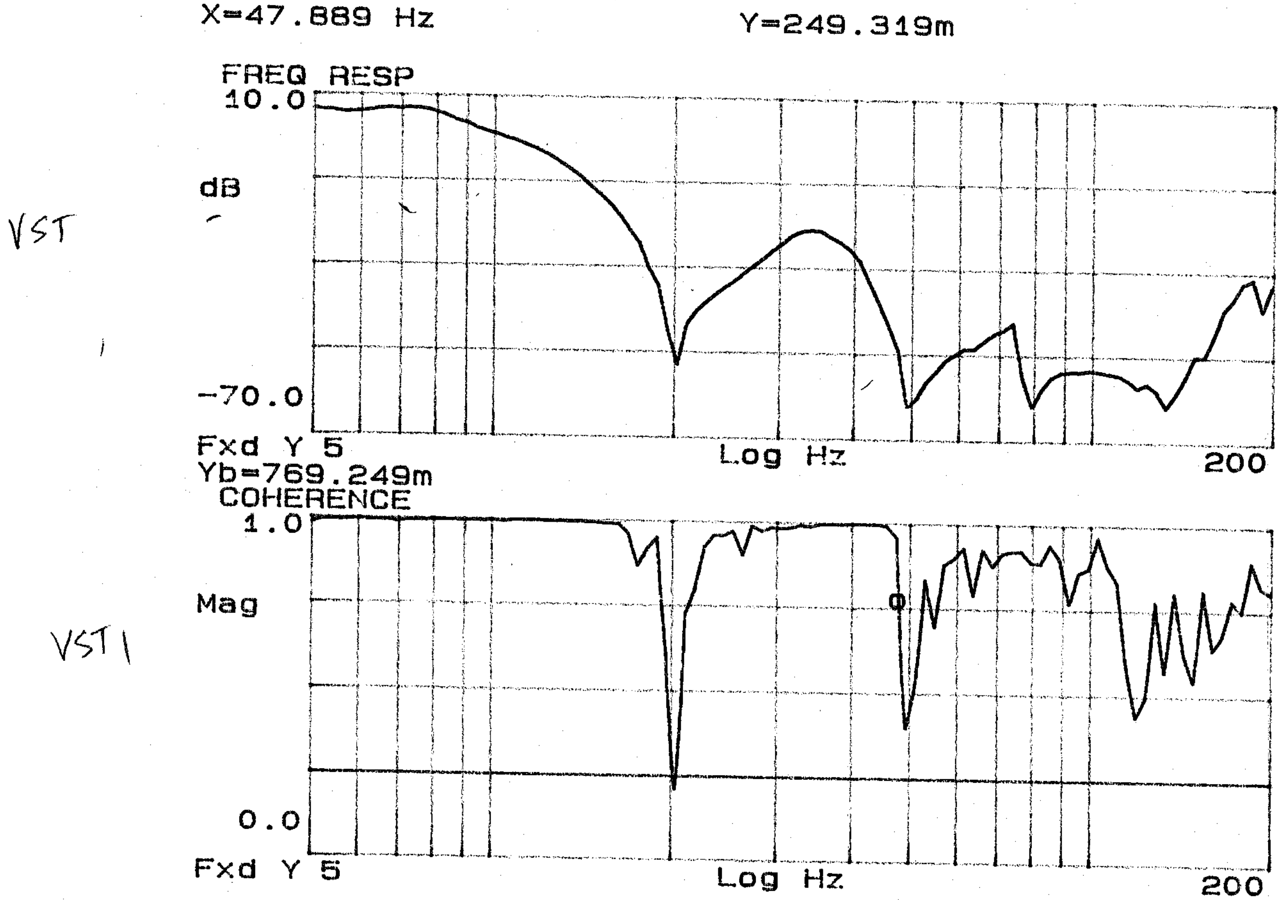

Ave = 5
Integ time = 284ms
Resln: 62.4 pts/dec

Top accel on edge of slab in H position

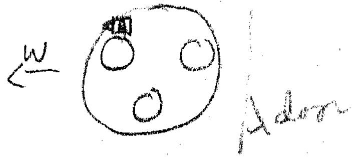

- shaker in H
- bottom accel by base of N drift compensator

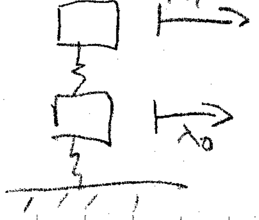

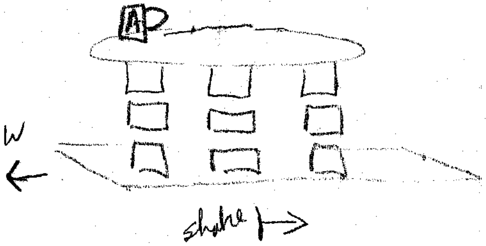

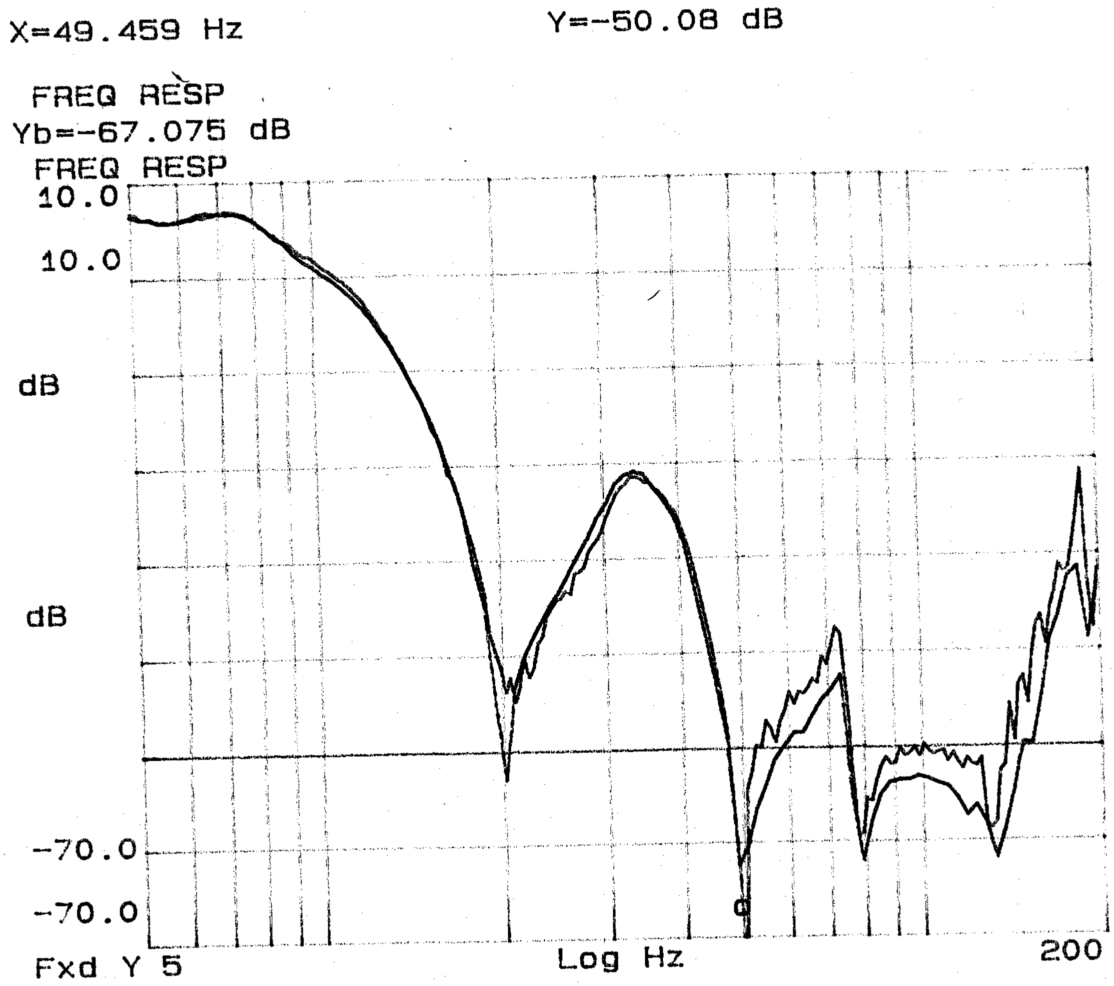

Black VST

Blue - VST 2

Essentially no rotation when shake horizontally

Jan 6, 1992
3:10 PM

Transfer Fcn from H to

Source	Freqn
100 mV$_{rms}$	5-18 Hz
400 mV$_{rms}$	18-40 Hz
600 mV$_{rms}$	40-120 Hz
200 mV$_{rms}$	>120 Hz

VST 2

VST 3

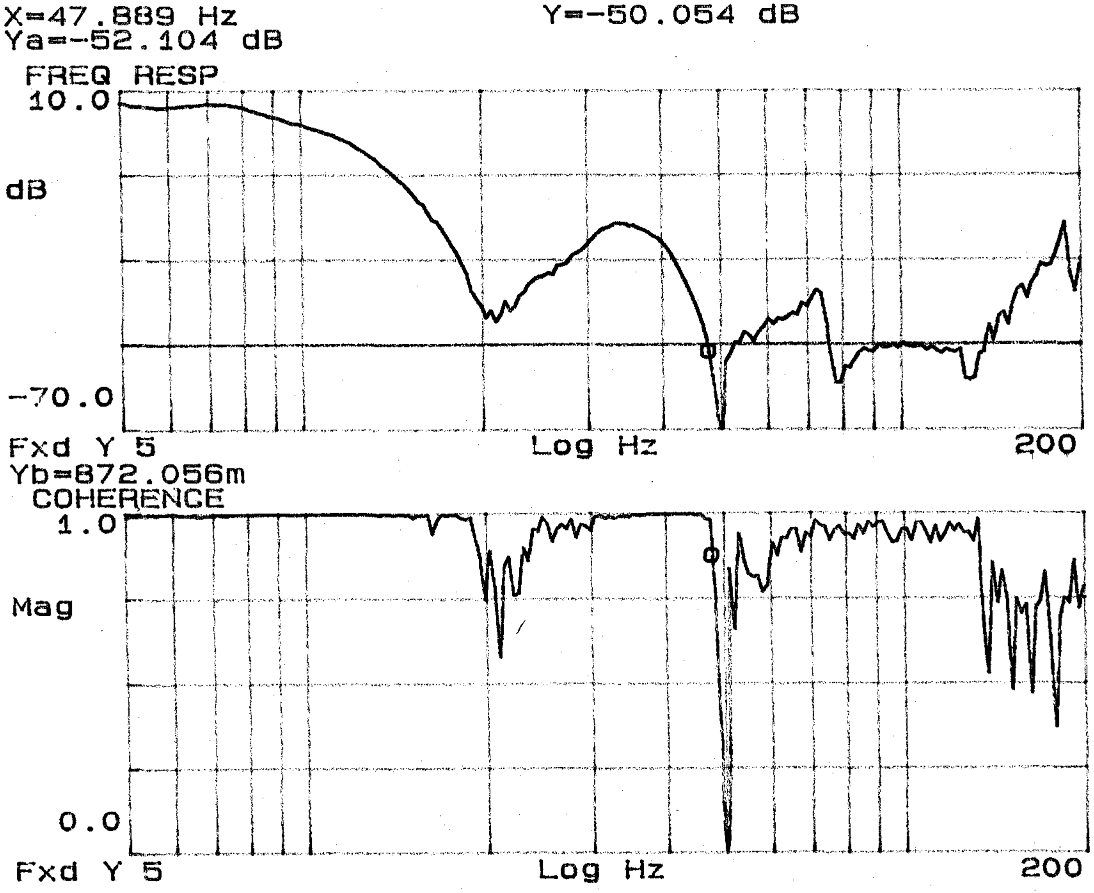

Ave = 5
Integ time = 284 msec
Resln = 125 pts/dec

Tripaxial on center of plate in H gondola

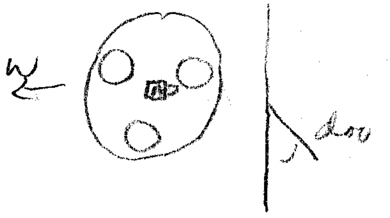

Shaker in H bottom accel by base of N drift compensation

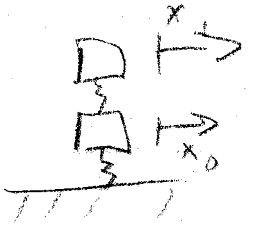

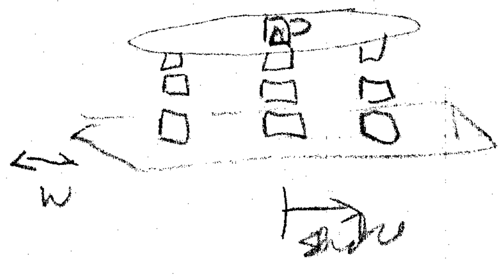

Slack Springs
2-3-5-7

Jun 6, 1992
3:10 PM

e accelerometer
er spectrum of
ST2

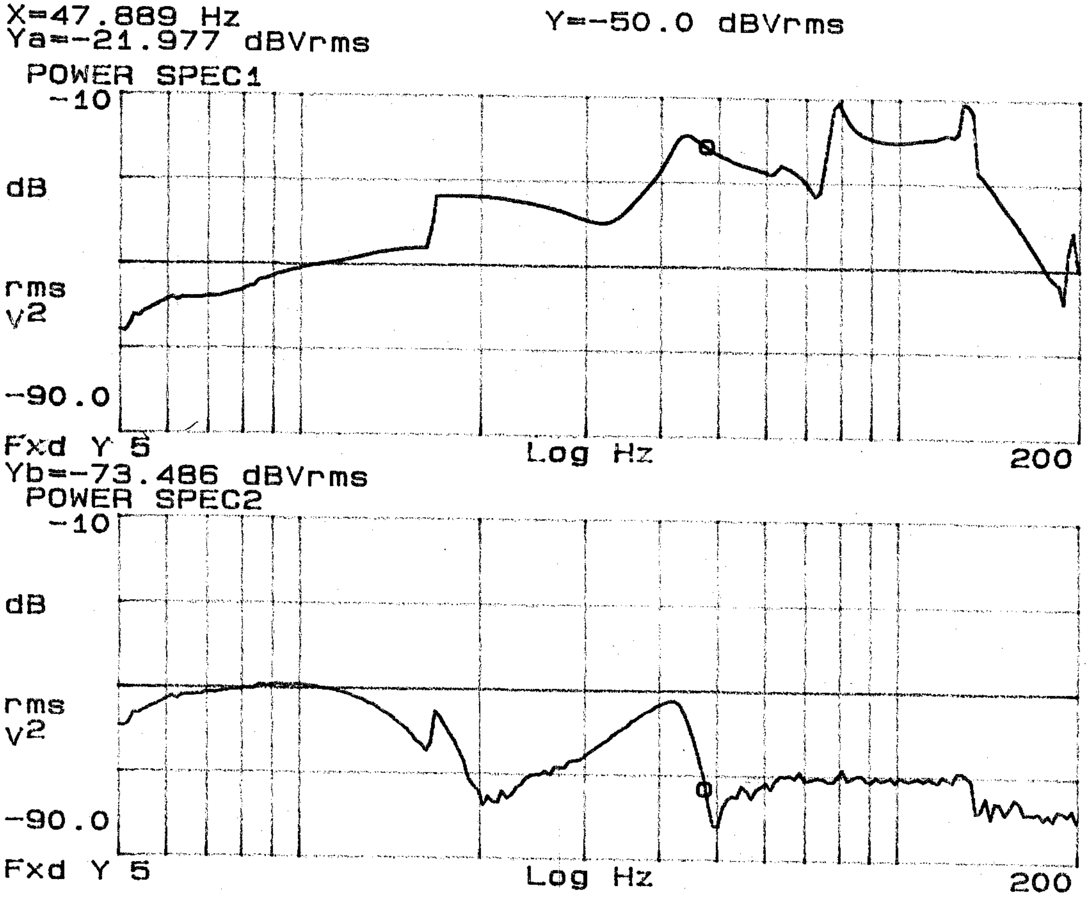

Power Spectra
of accelerometers
taking transfer
fctns

Top plate
accelerometer of
VST2

See VST2

Transfer function from

Source voltage to top H accelerometer

VST4

VST5

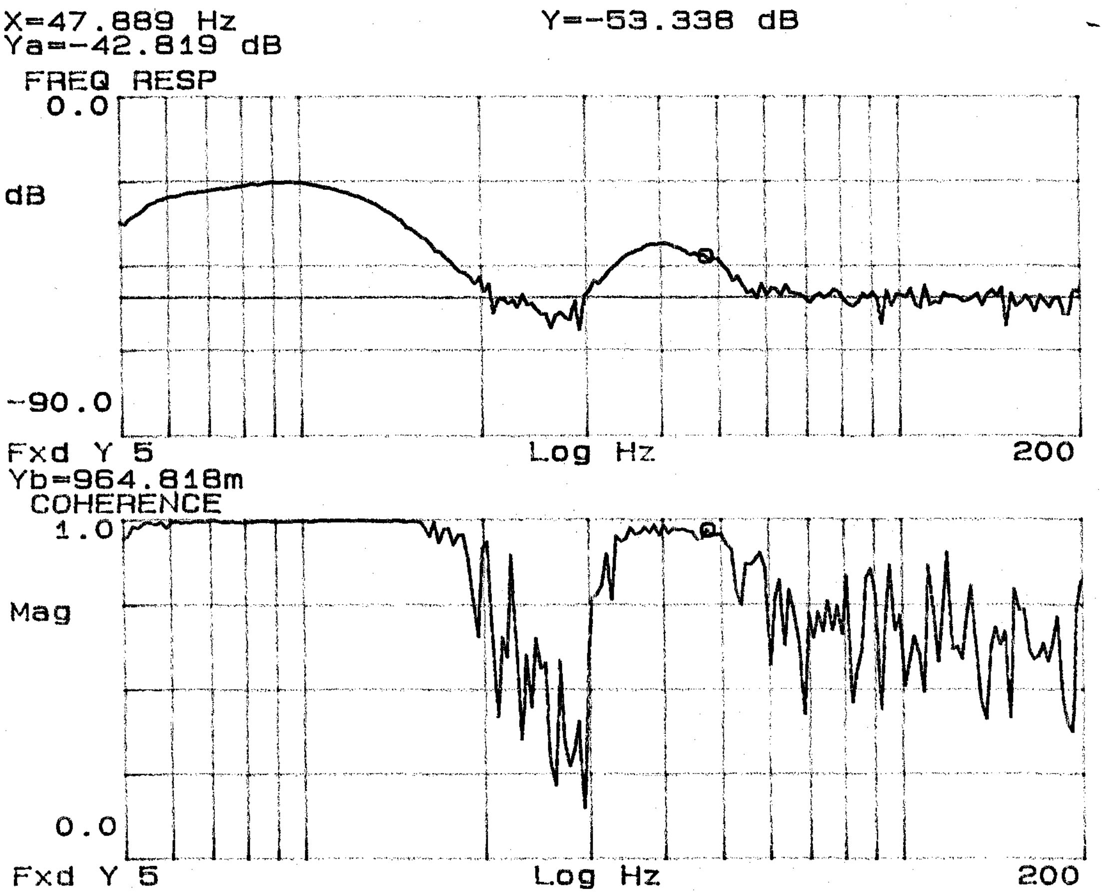

- This was done to check that the data above 50 Hz was due to acoustic noise.
- Since the data above 50 Hz is flat, we concluded that the noise must be due to acoustic excitations from the shaker. If it would have been due to mechanical excitation we should have seen the curve roll-off
- The accelerometer was at the center of the top plate in the H position
- Shaker was in H position

source level = 100 mVrms

Ave = 5

Integ time = 125 pts/dec

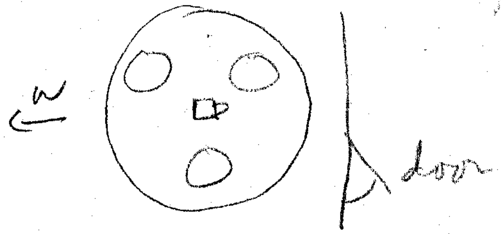

Transfer function from source voltage to top H accelerometer

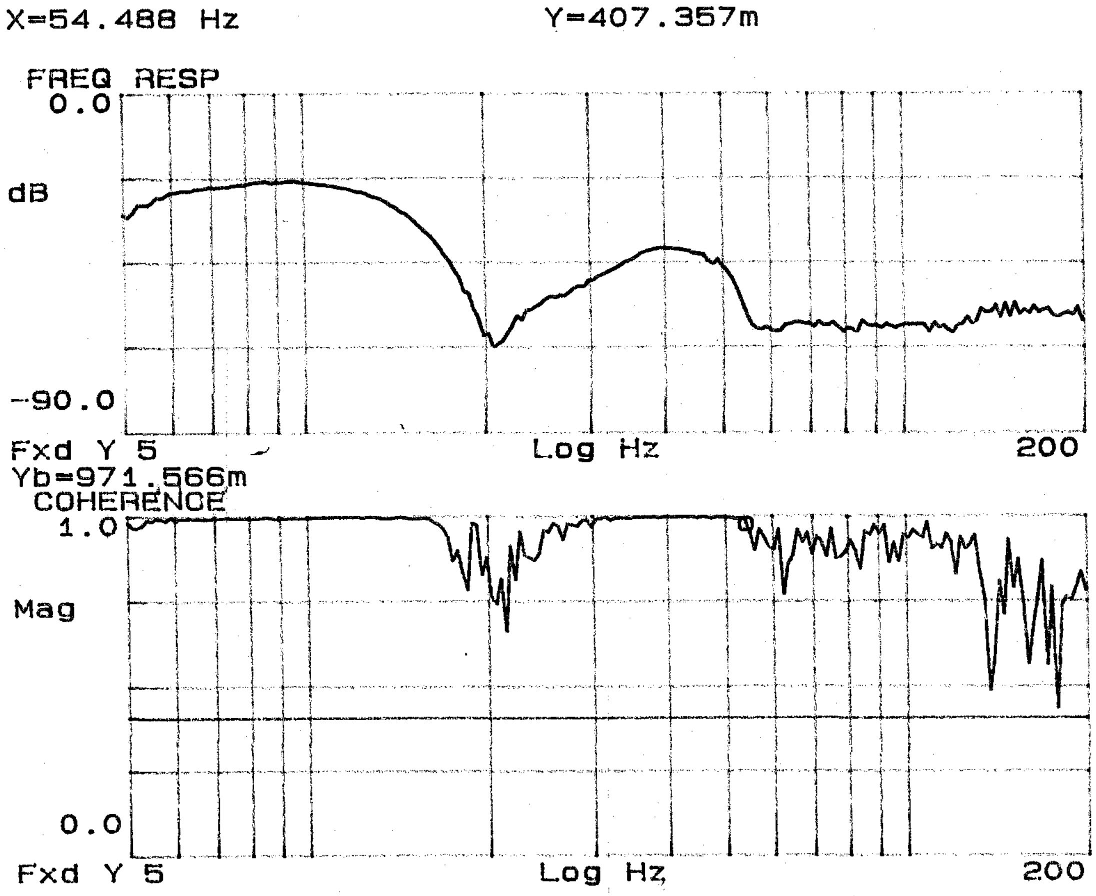

VST6

VST7

Same as VST4 + VST3 but changed source level

Source	Freq
100 mVrms	5-18 Hz
400 mVrms	18-40 Hz
600 mVrms	40-120 Hz
200 mVrms	>120 Hz

Check for Acoustic Coupling

JAN

JAN1

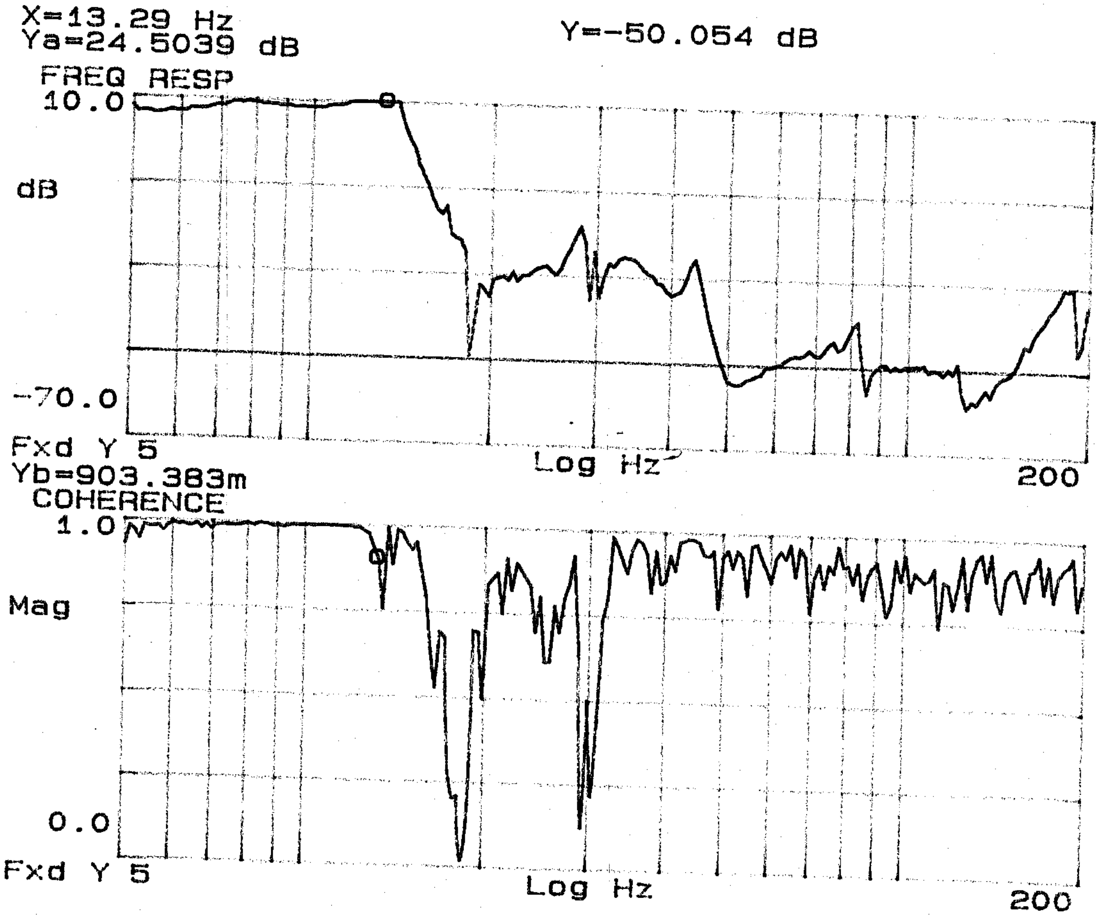

- Transfer function from H base accelerometer to H top accelerometer
- Shaker in H position

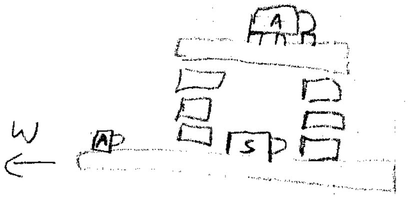

- Frequencies above 50 Hz match up pretty well with data in VST 2 above 50 Hz — I believe data above 50 Hz is acoustic noise due to shaker

Conn Amp on full gain
AV = 5

Integ = 284 msec
Resln = 125 Pt/Dec
Source level = $100 mV_{RMS}$ <18 Hz
= $400 mV_{RMS}$ >18 Hz

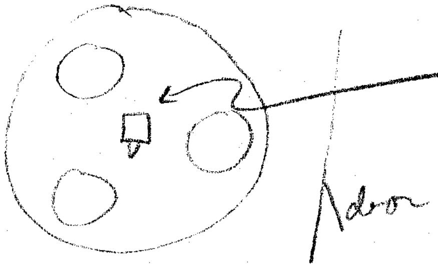

accelerometer is on soft rubber cubes

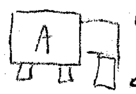

accel

rubber cubes

Power Spectra of JAN.

Lower Accel. (JAN2)

Upper Accel (JAN3)

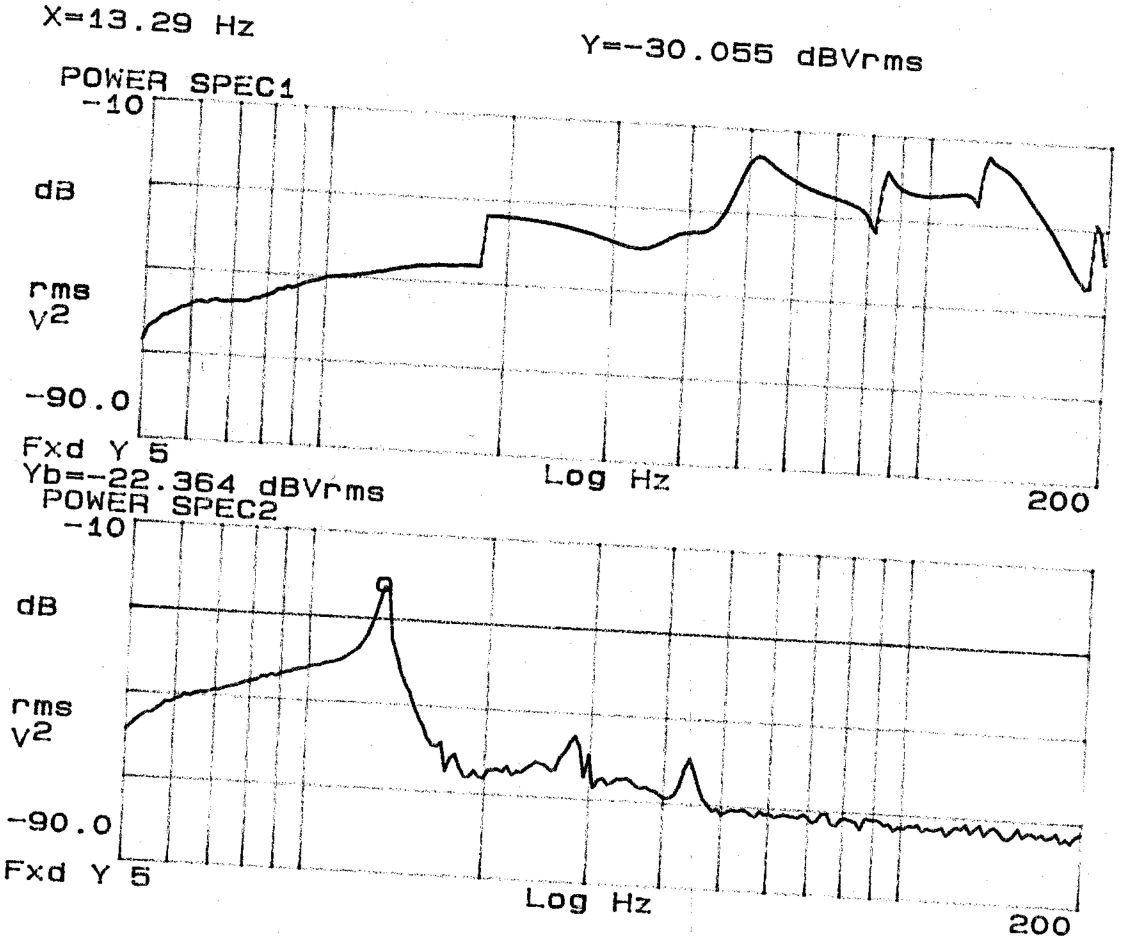

JAN 2

JAN 3

Transfer function from Horizontal base accel to vertical top accelerometer where top accelerometer is on RTV spring

JA4

JANS

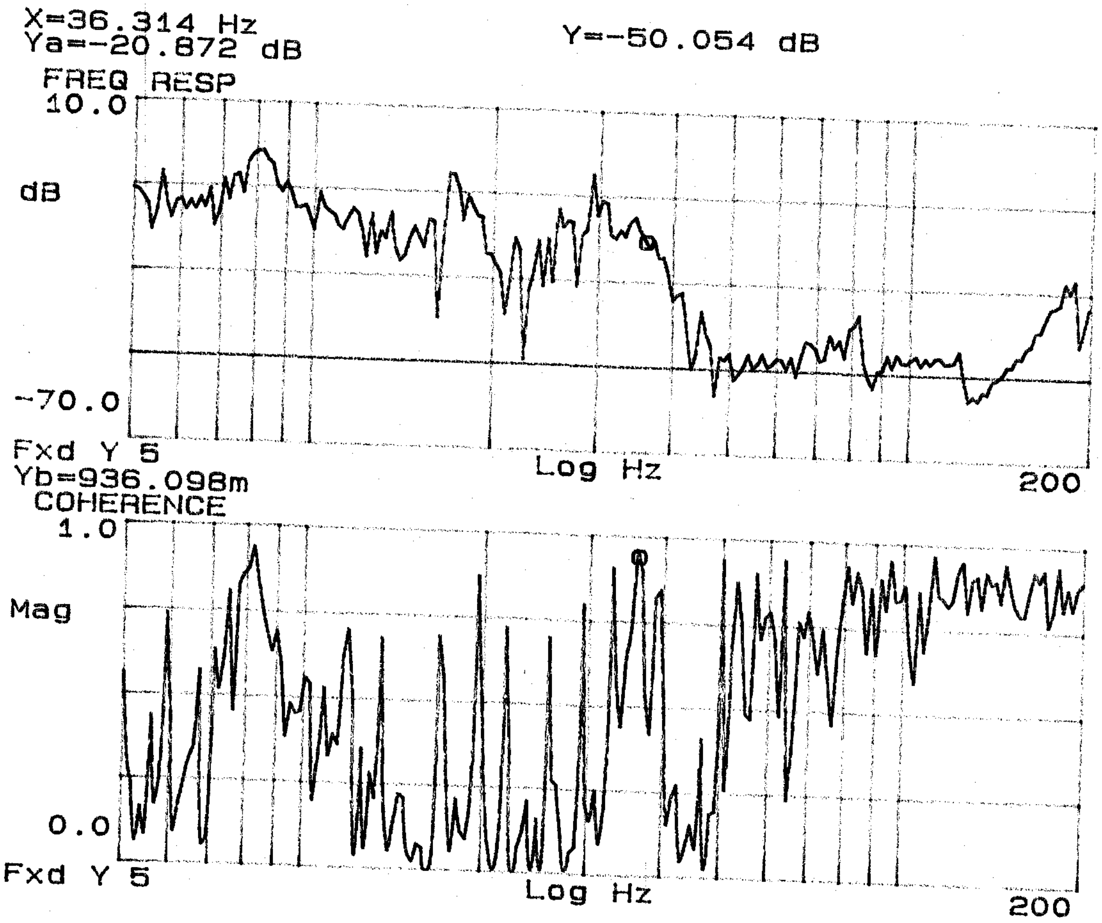

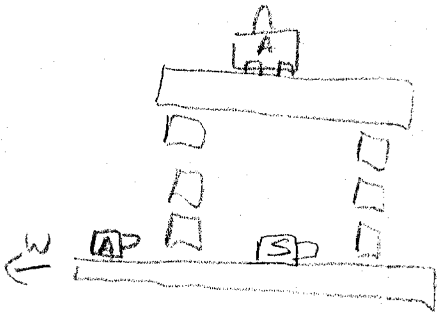

Test to check for acoustic noise

- Top accel is in center
- Base accel is close to N drift compensator

Transfer fctn from H to V where V accel is on center of top plate

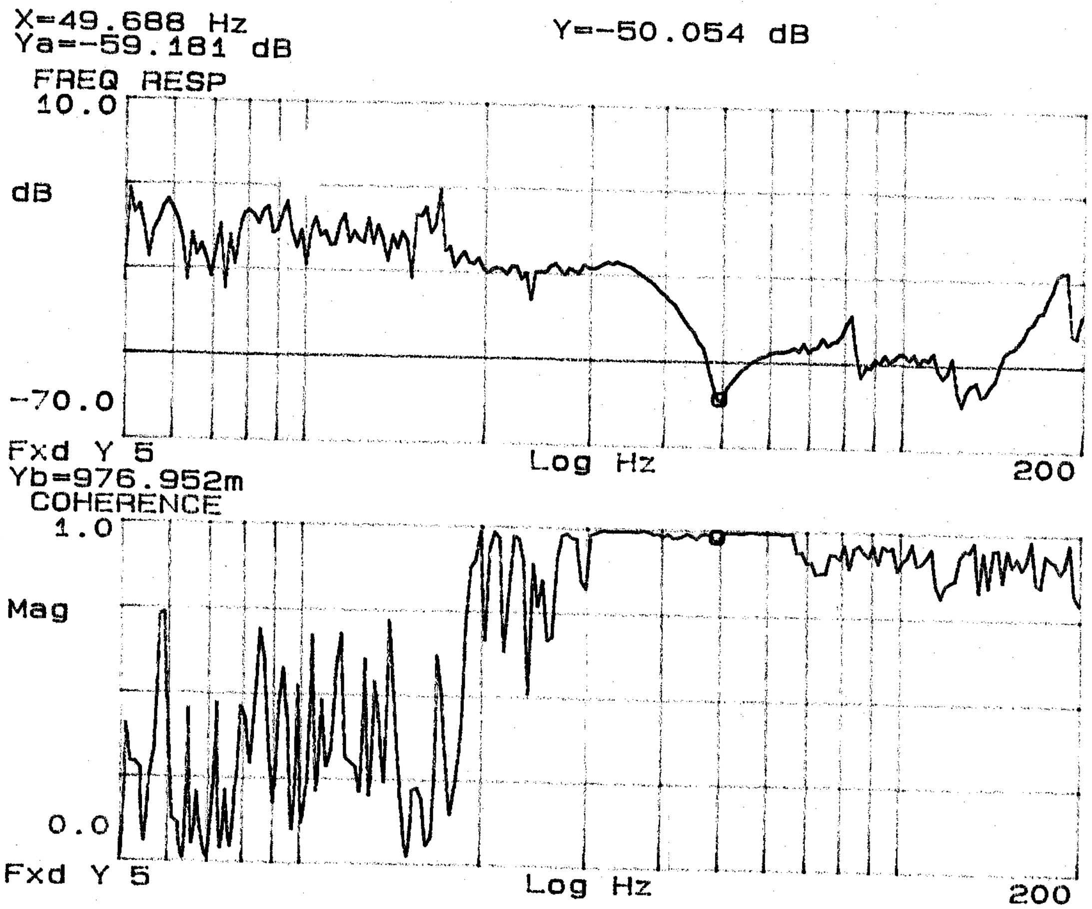

JAN 6

JAN 7

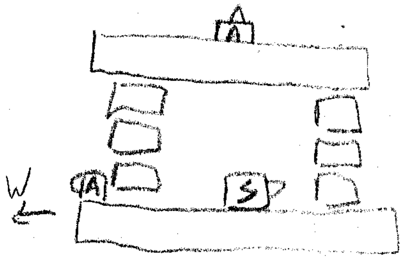

- Top accel on center of Al plate
- Bottom accel near North drift compensator

gain: full scale on crown

Source level = 100 mVrms f<18 Hz
400 mV$_{RMS}$ f>18 Hz

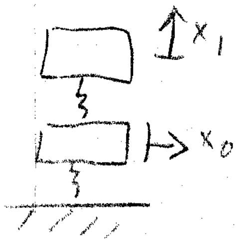

Integ time = 300 ms f < 20 Hz f > 60 Hz
2 sec 20 < f < 60

Resln = 125 Pt/dec

Transfer function [illegible]

V where Vaccel is on edge of top plate

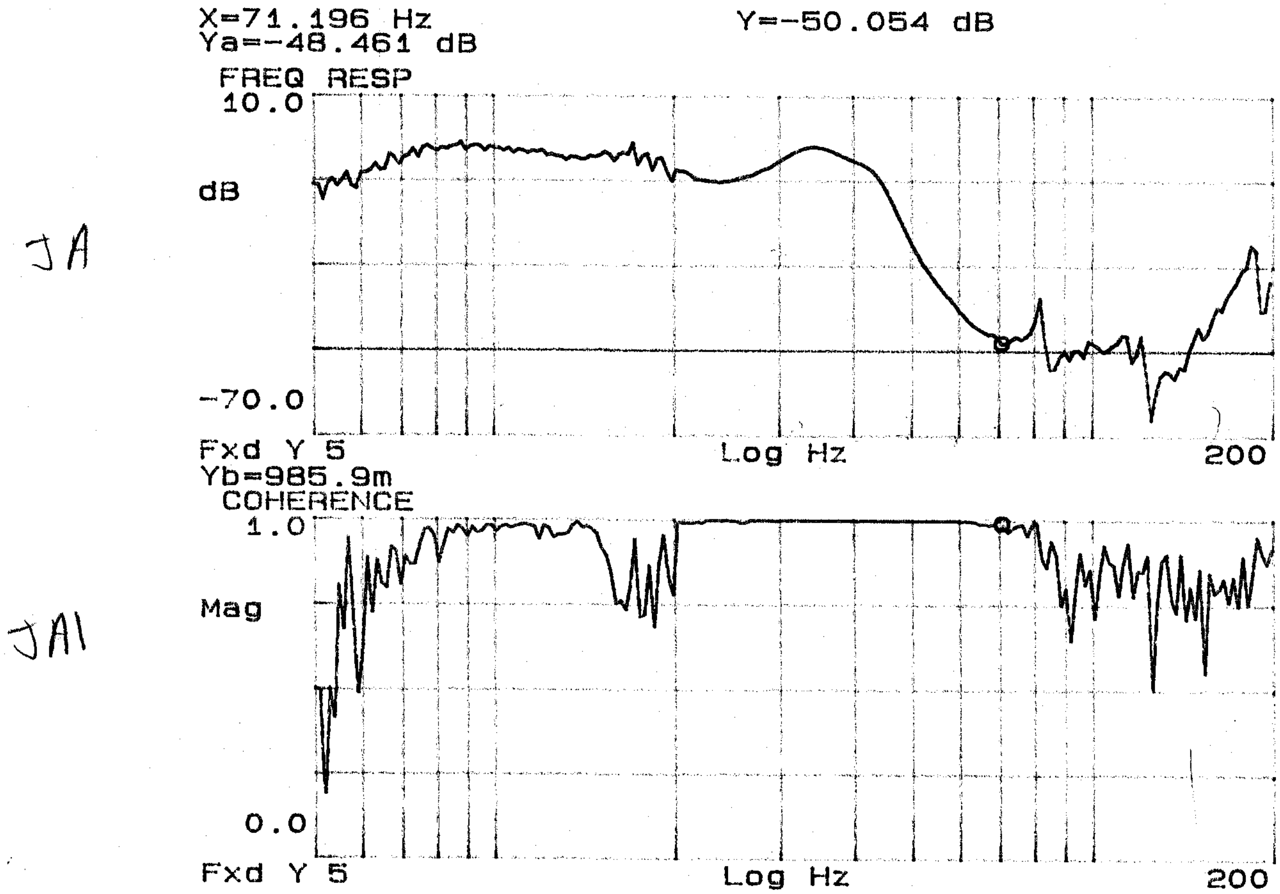

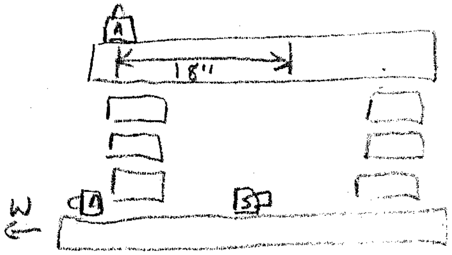

- Top accel on edge of Al plate

- Bottom accel near North drift compensator

gain = full scale on chan

source level: 100mVrms f<18 Hz
400mVrms f>18Hz

integ time = 300 msec f<20Hz, f>60Hz
2 sec 20<f<60

Resln = 125 Pt/dec

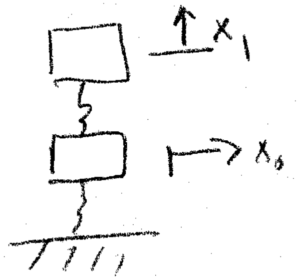

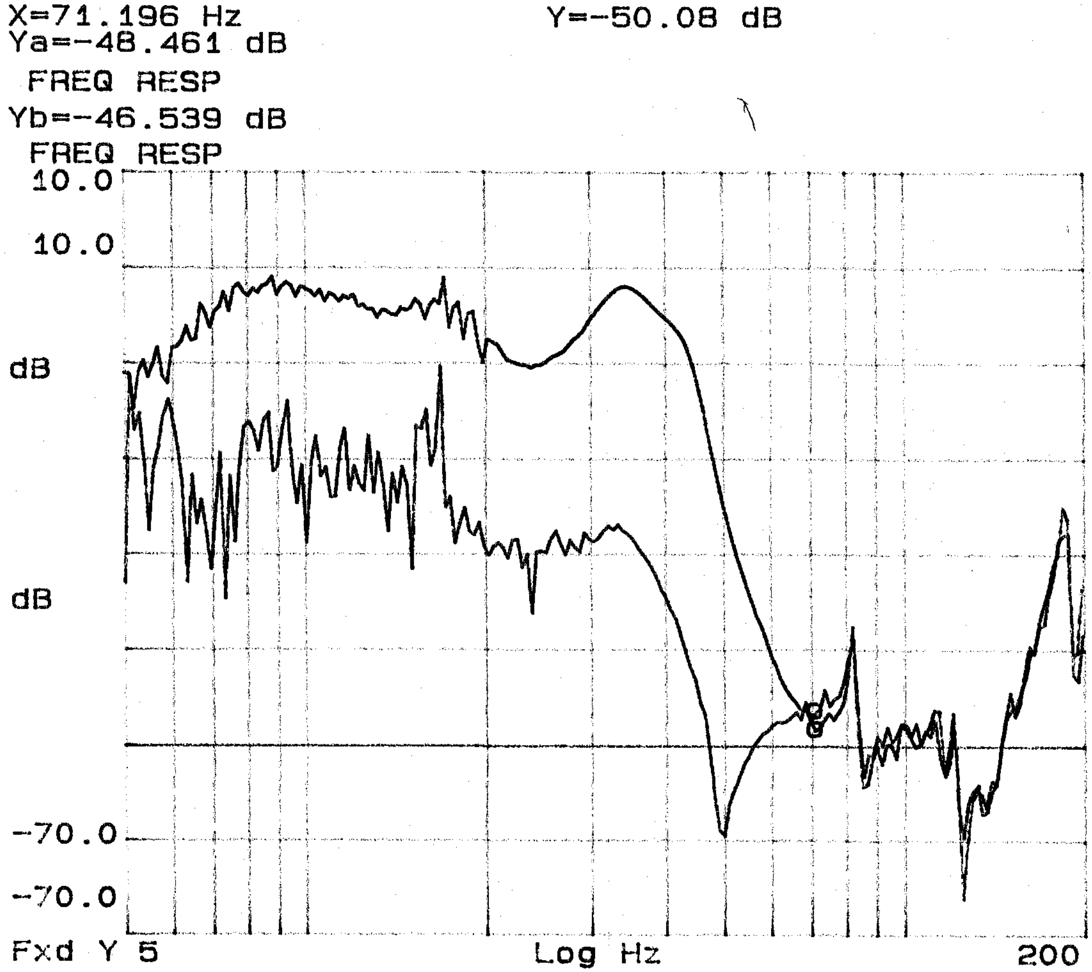

Black is JA
Blue is JAN6

Transfer fctn from V to V

0dB
-10dB
-20dB
-30dB
-40dB

12dB
6dB
1dB
-8dB
-22.5dB
-36dB

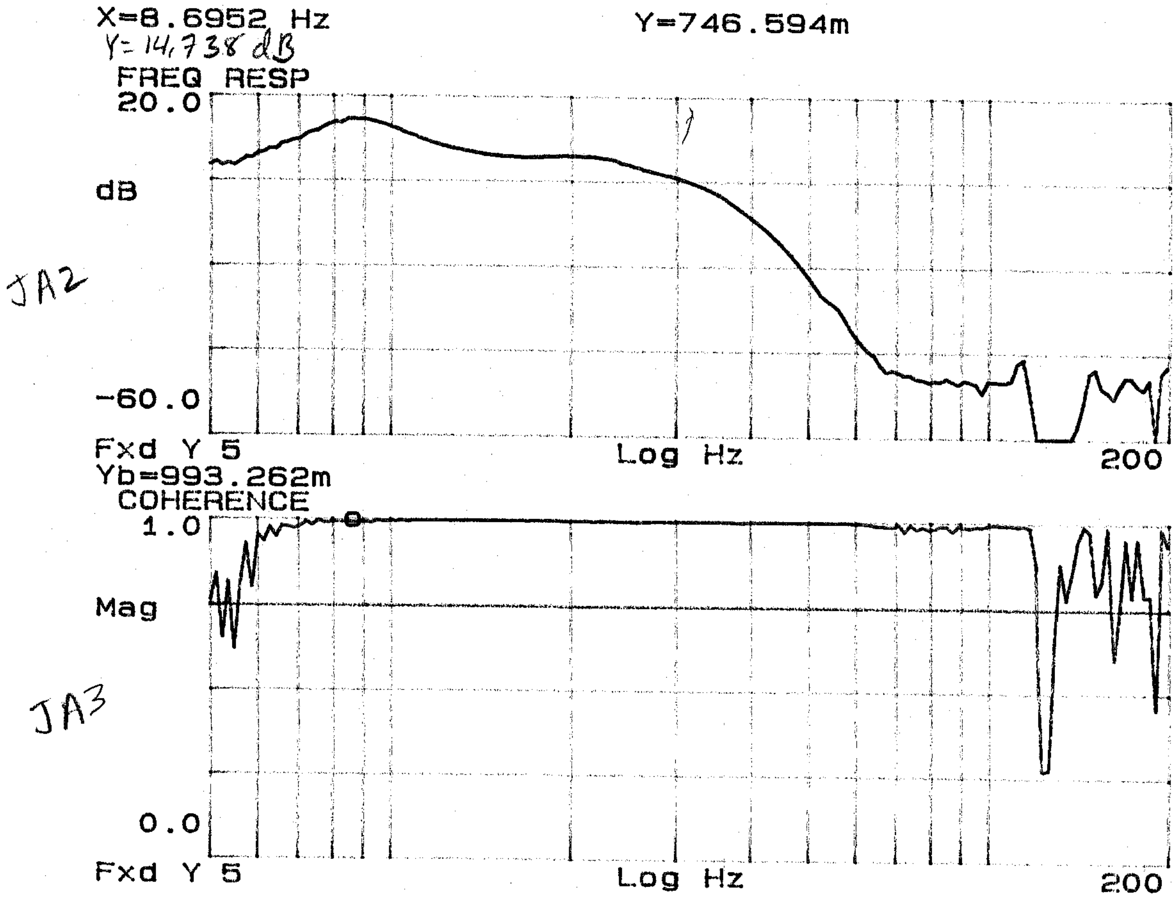

<20 Hz
Ave=8
Integ time = 1sec
Resln = 100 pt/dec
Source level = 150 mVrms

>20Hz
Ave = 8
Integ time = 300 msec
Resln = 100 pt/dec
source level = 300mVrms

>100 Hz
Source level = 100mVrms

- Bottom accel near North diff config
- Top accel on edge of plate

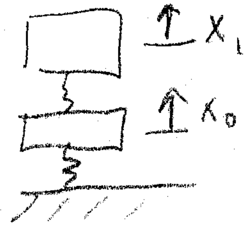

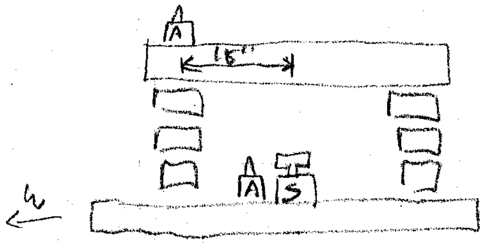

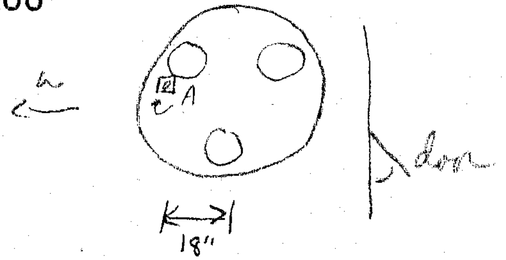

Transfer Fcn from V to V

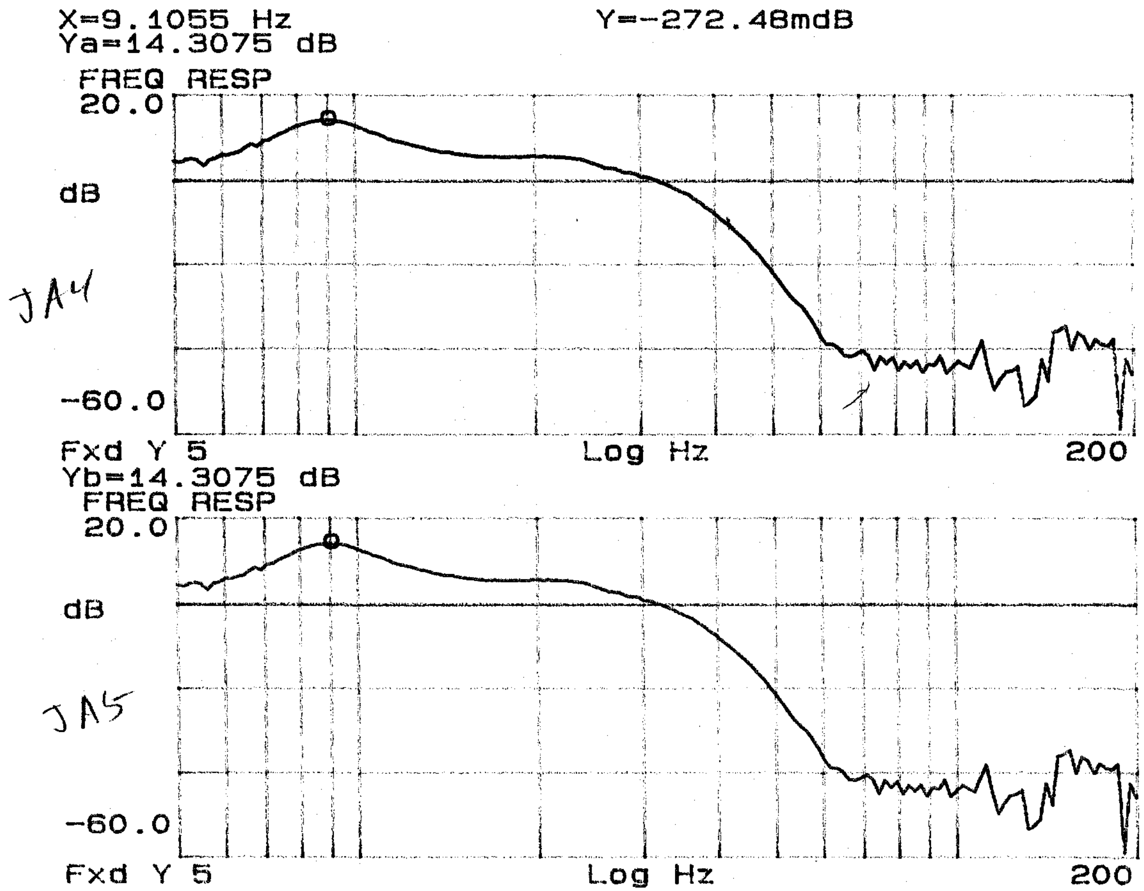

- Same settings as JA2
- Plot is almost identical to JA2

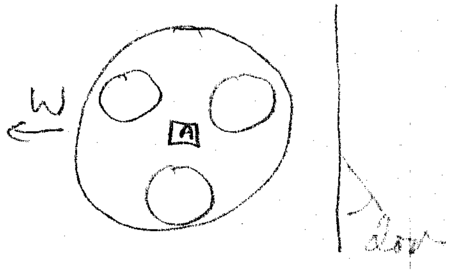

- Bottom accel near N drift compensator
- Top accel at center of plate
- Shaker in V position

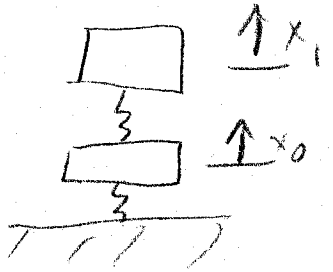

Transfer Fctn from V to H

- shaker in V position
- lower accel in V position by N drift compensator
- Upper accel in H position in center of Al plate

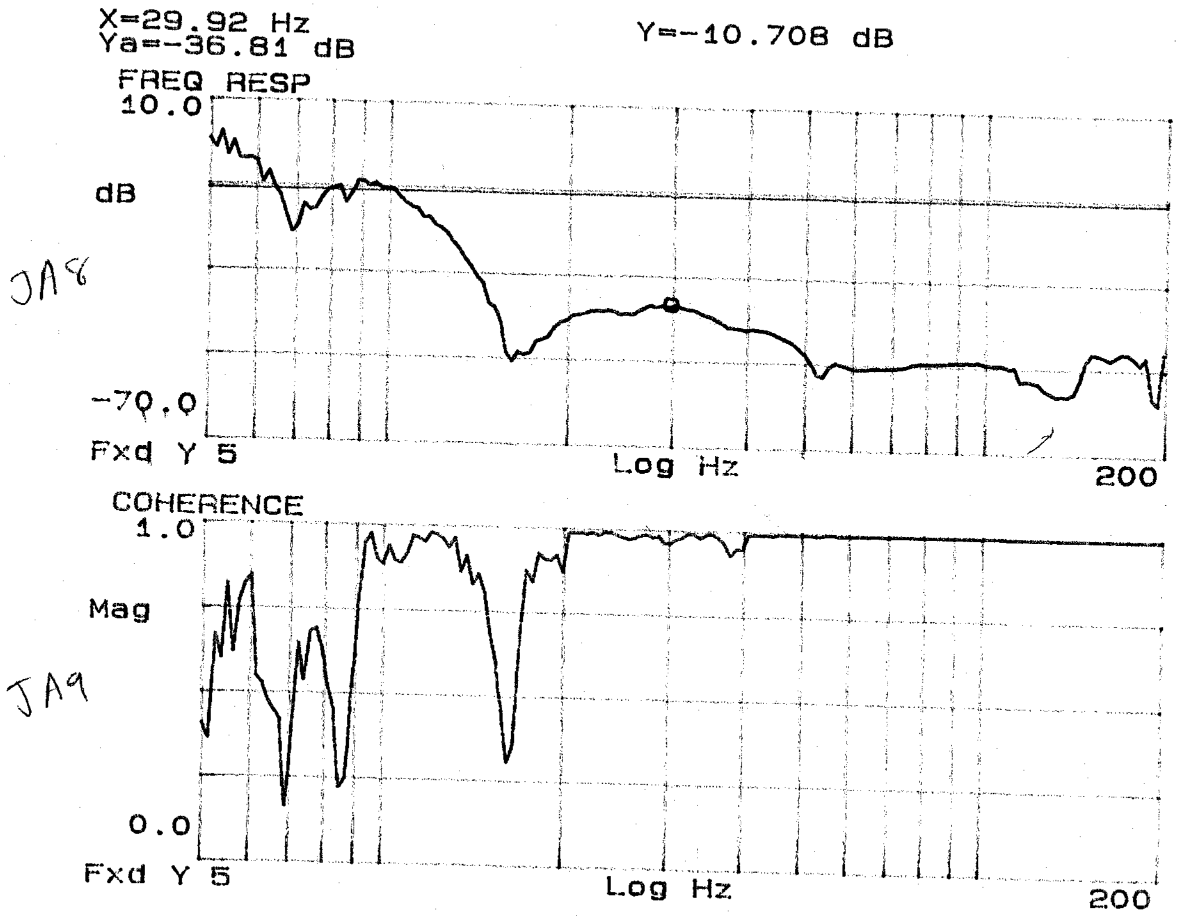

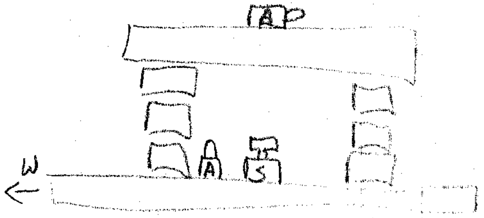

<20 Hz

Ave = 8

Integ = 1sec

Resln = 100pt/dec

Source = 150mV rms

>20 Hz

Ave = 8

integ = 300msec

Resln = 100pt/dec

Source = 300mV RMS

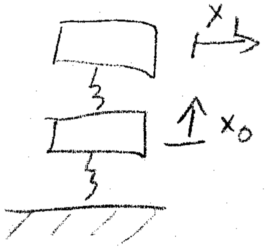

[illegible] transform V to H
with top accel on rubber

- Same as JA8 but with [illegible] accel on rubber cubes

JA10

JA11

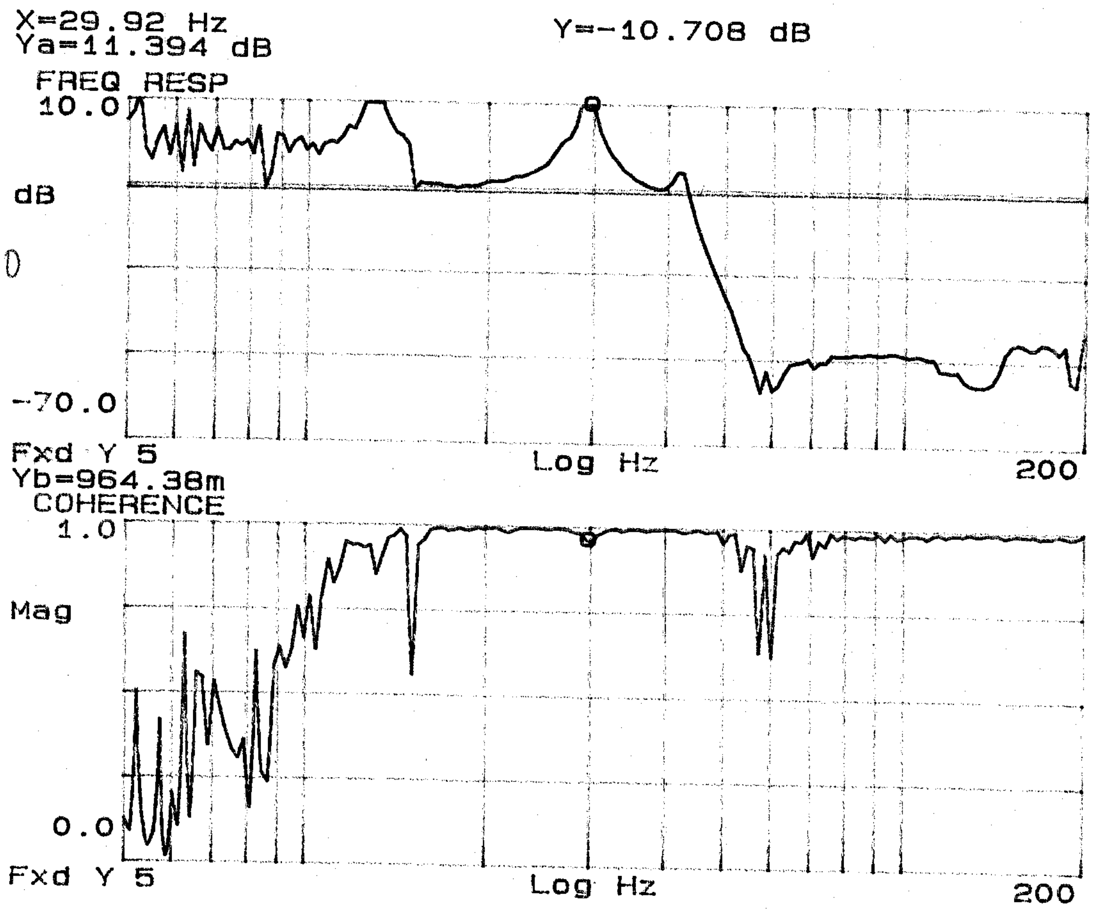

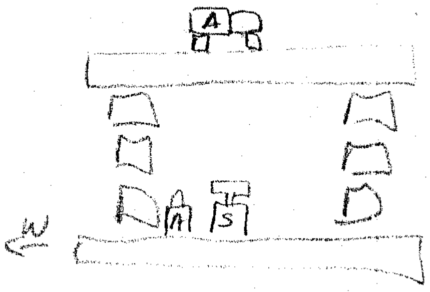

Transfer Fctn From V-tot

- shaker in V position
- lower accel in V position by N drift compensator
- Upper accel in || position on edge of plate

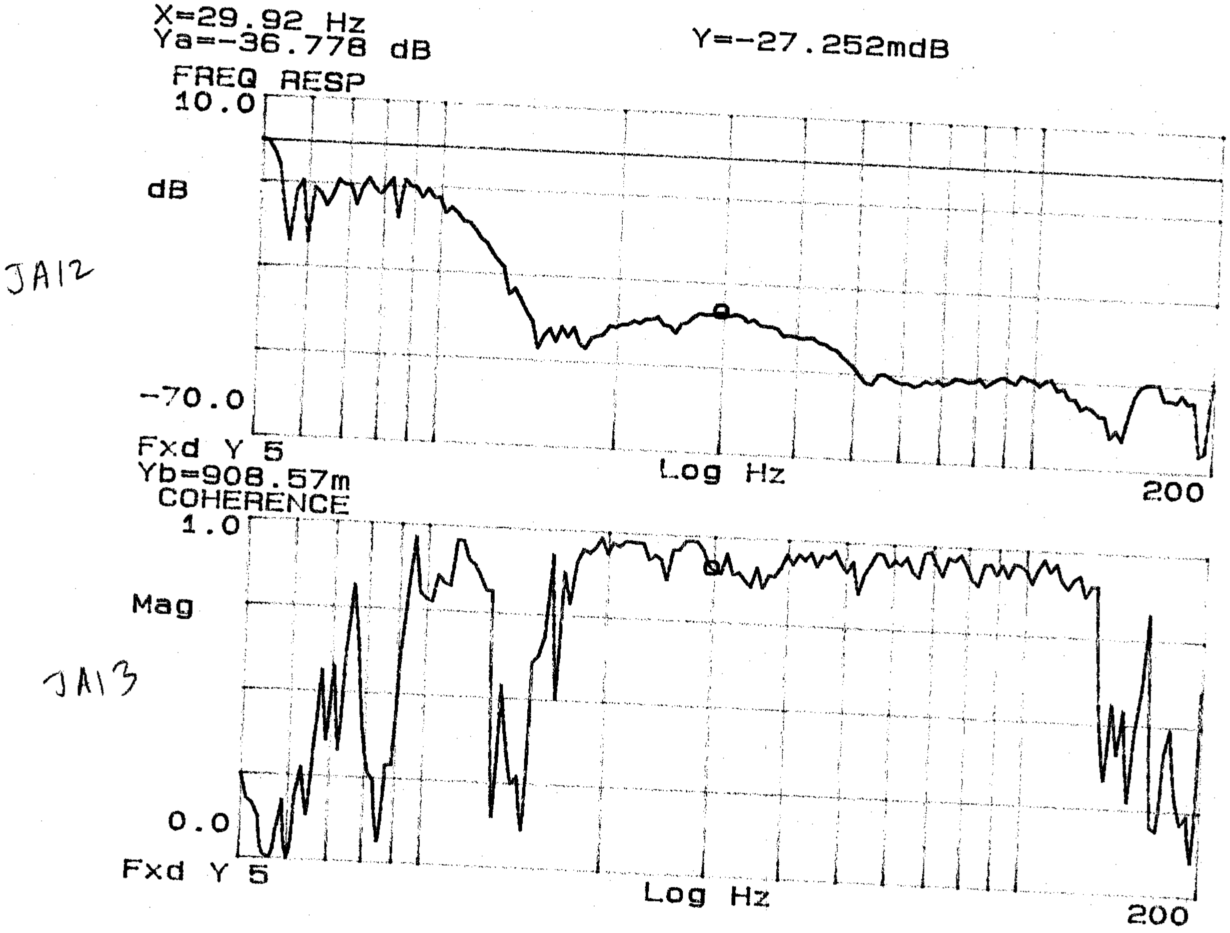

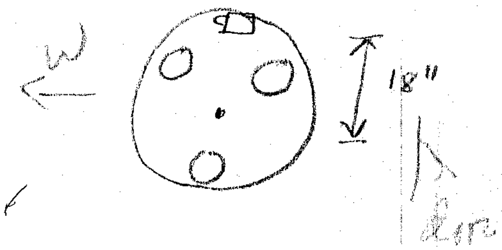

<20 Hz

AV=8
Integ=1sec
Source=150 mV
resln=100 pts/dec

>20Hz

Ave=8
Integ=300 msec
Source=300 mV rms

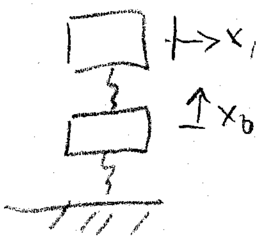

Vertical Orientation on top plate of Stack.
Noisy lab
Accel. outputs directly → S.A

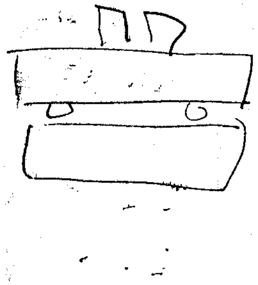

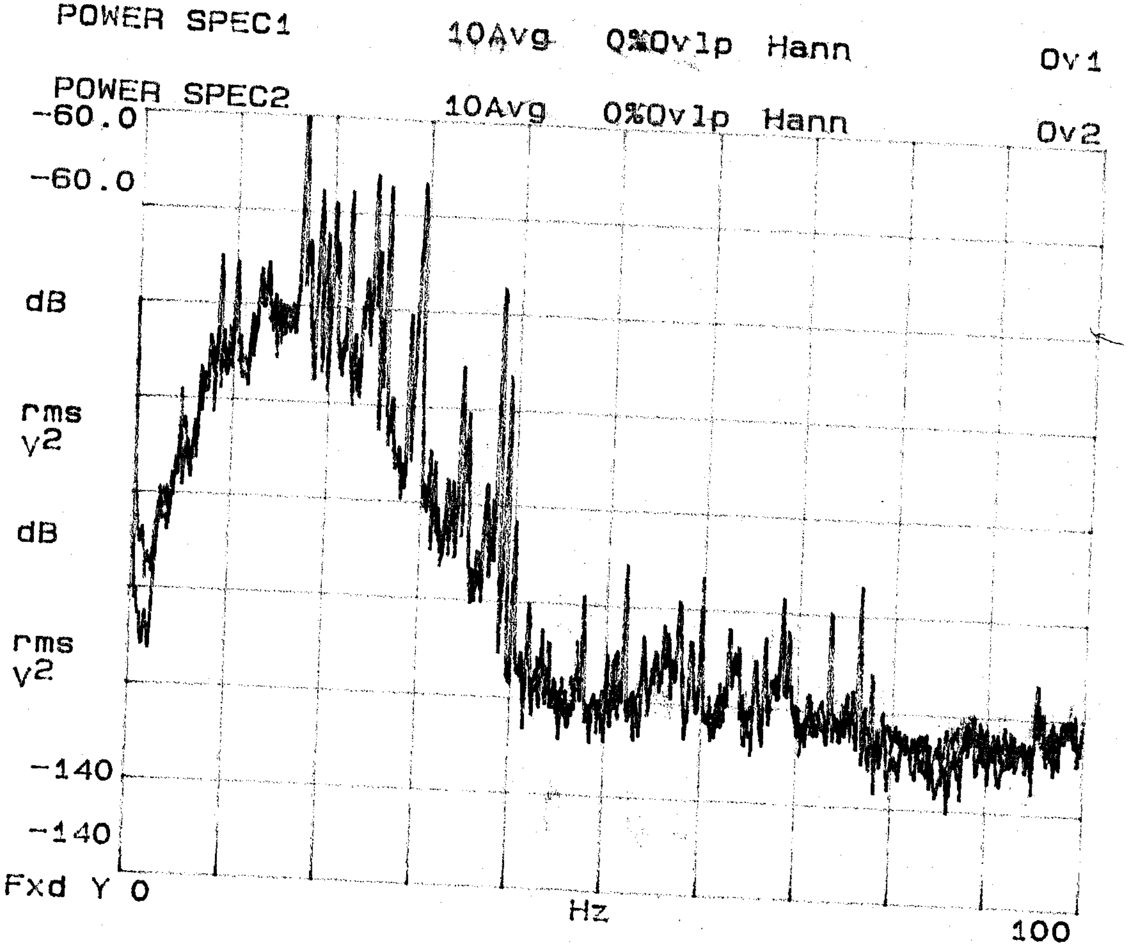

Black; #886910
"GREEN"

Blue · #886909
"Red

ke - JA14
urve of Black is JA15)

urve is JA4
nsfer Fctn from V to
th top accelerometer
d mounted on top
e

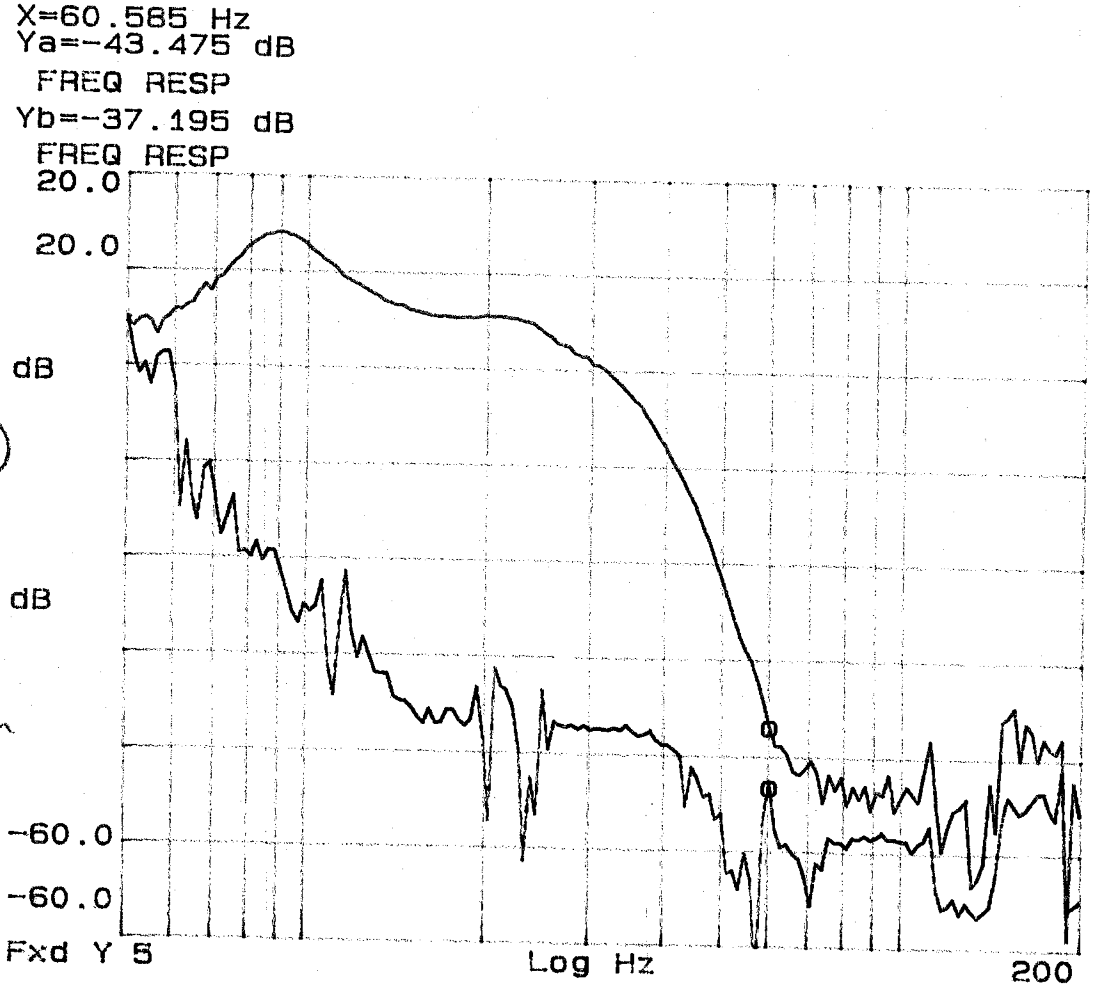

JA14 is Transfer Fctn from
V to V with upper accel
Suspended above Al plate

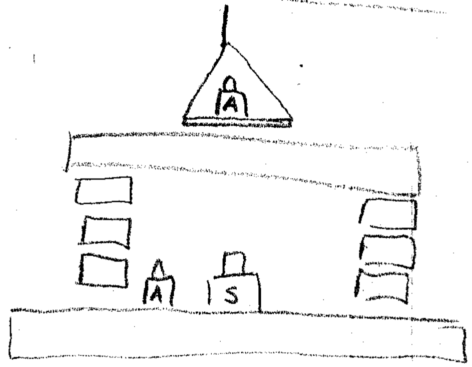

- Test to see what part of signal is acoustic
- Result is that above 60 Hz we see acoustic pickup

ck - JA16

lacence of JA16 is
, JA17)

line is - JA8

nsfer Fctn from
, H with top H
celerometer
d mounted on
, plate

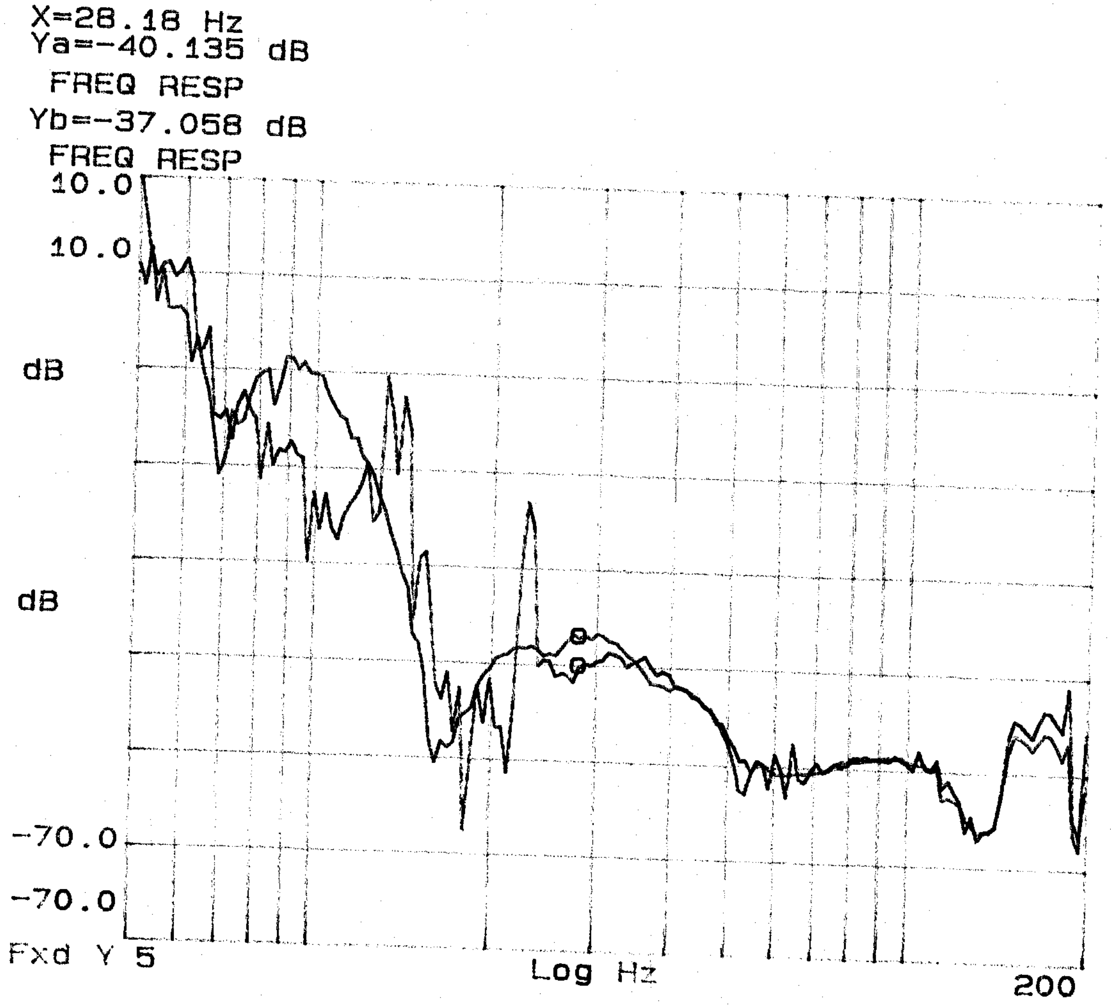

JA16 is transfer Fctn
from V to H with upper accel
Suspended in H position
above A1 plate

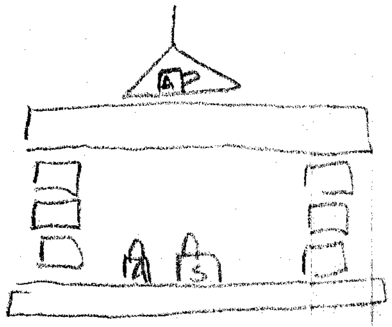

- Test to see what part of signal is acoustic

- Result is that most of signal is acoustic

1/13/93
4:00 PM

Changed # of springs in Stack to

2-3-5-7

Stack height (vs) Time

		①	②	③
1/13/93	4:00 PM	$20\frac{13}{16}$"	$20\frac{3}{4}$	$20\frac{13}{16}$"
1/14/93	12:35 AM	$20\frac{11.5}{16}$"	$20\frac{11}{16}$"	$20\frac{11.5}{16}$"
1/15/93	9:20 AM	$28\frac{11}{16}$"	$20\frac{11}{16}$"	$20\frac{11}{16}$"

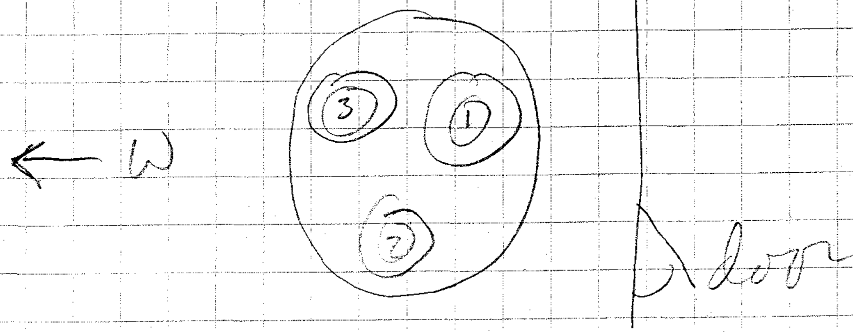

Power Spectrum on top of Al plate with springs in 2 different configurations

(Power Spectra taken 15 min from each other)

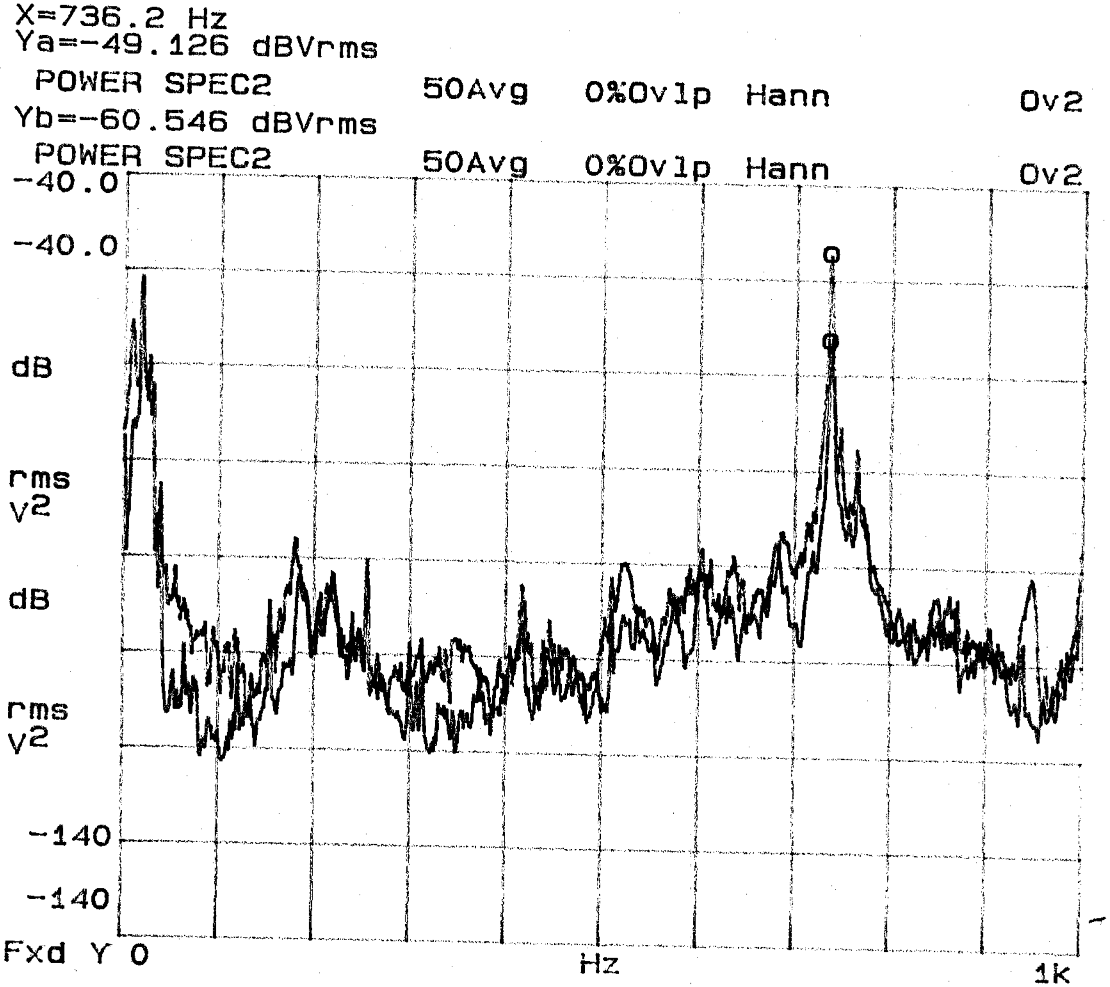

```
X=736.2 Hz
Ya=-49.126 dBVrms
 POWER SPEC2          50Avg   0%Ov1p  Hann       Ov2
Yb=-60.546 dBVrms
 POWER SPEC2          50Avg   0%Ov1p  Hann       Ov2
```

b JA19

e JA20

l accelerometer
der of plate

JA19

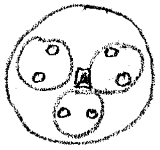

Springs in tangential configuration

JA20

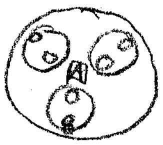

Springs in radial configuration

- Believe the springs damp first drumhead mode in radial configuration by factor of 3 better than in tangential configuration at 736 Hz

Believe springs are on nodal line so don't provide as much symmetry

Did a visual ringdown looking at oscilloscope

Tangential ~ 1sec to get to ½ amp. ⇒ Q ≈ 3000

Radial ~ ½-⅓ sec to get to ½ amp ⇒ Q ≈ 1000

- First resonant of Al plate should be ~483 Hz for ⊕ mode
- Next is at 780 Hz for ⊙ mode

Power Spectra on Al plate

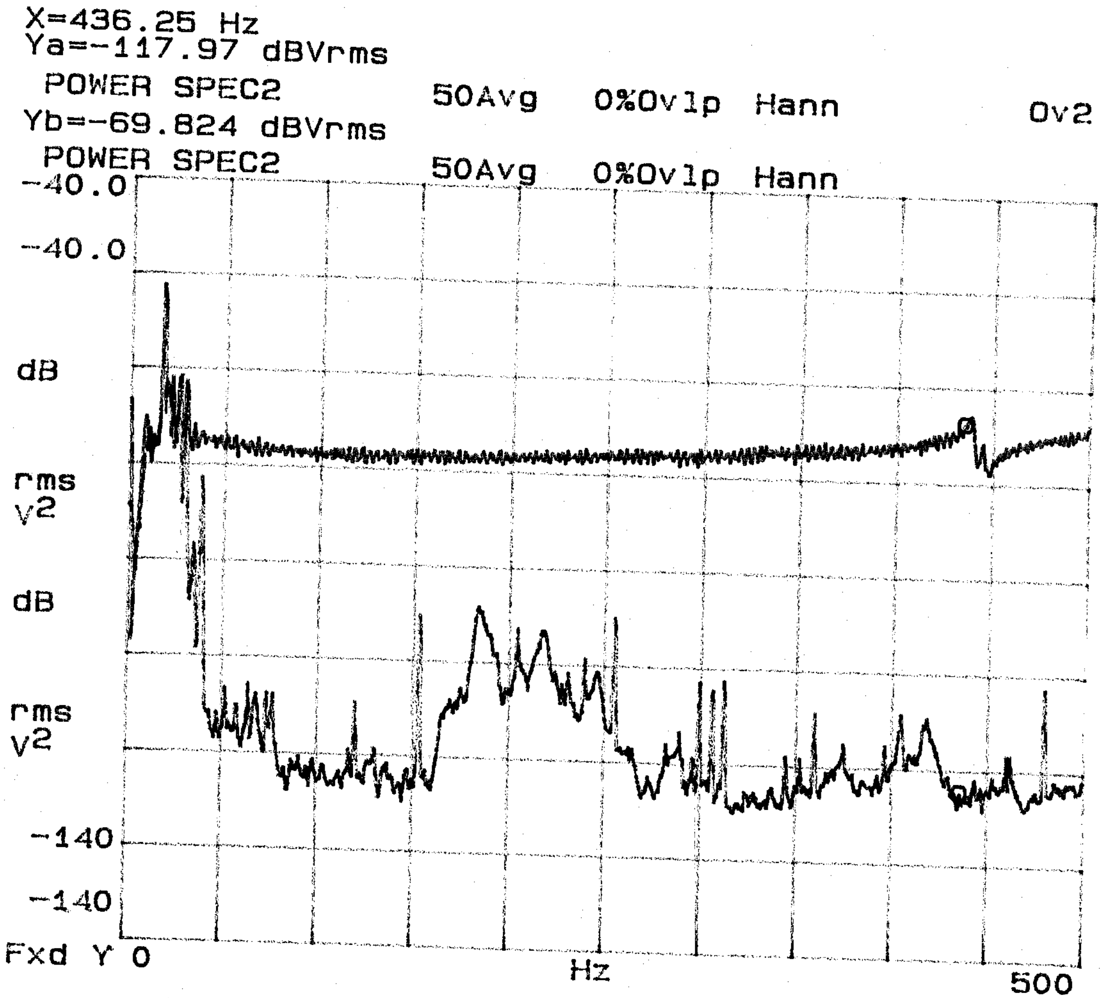
X=436.25 Hz
Ya=-117.97 dBVrms
POWER SPEC2 50Avg 0%Ovlp Hann Ov2
Yb=-69.824 dBVrms
POWER SPEC2 50Avg 0%Ovlp Hann

l - JA21

ack - JA22

Blue - tapped with hammer over 50 Ave

Black - power spectrum with no tapping

Al plate

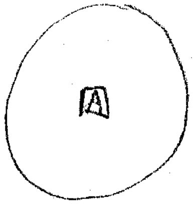

vertical accelerometer in center of plate

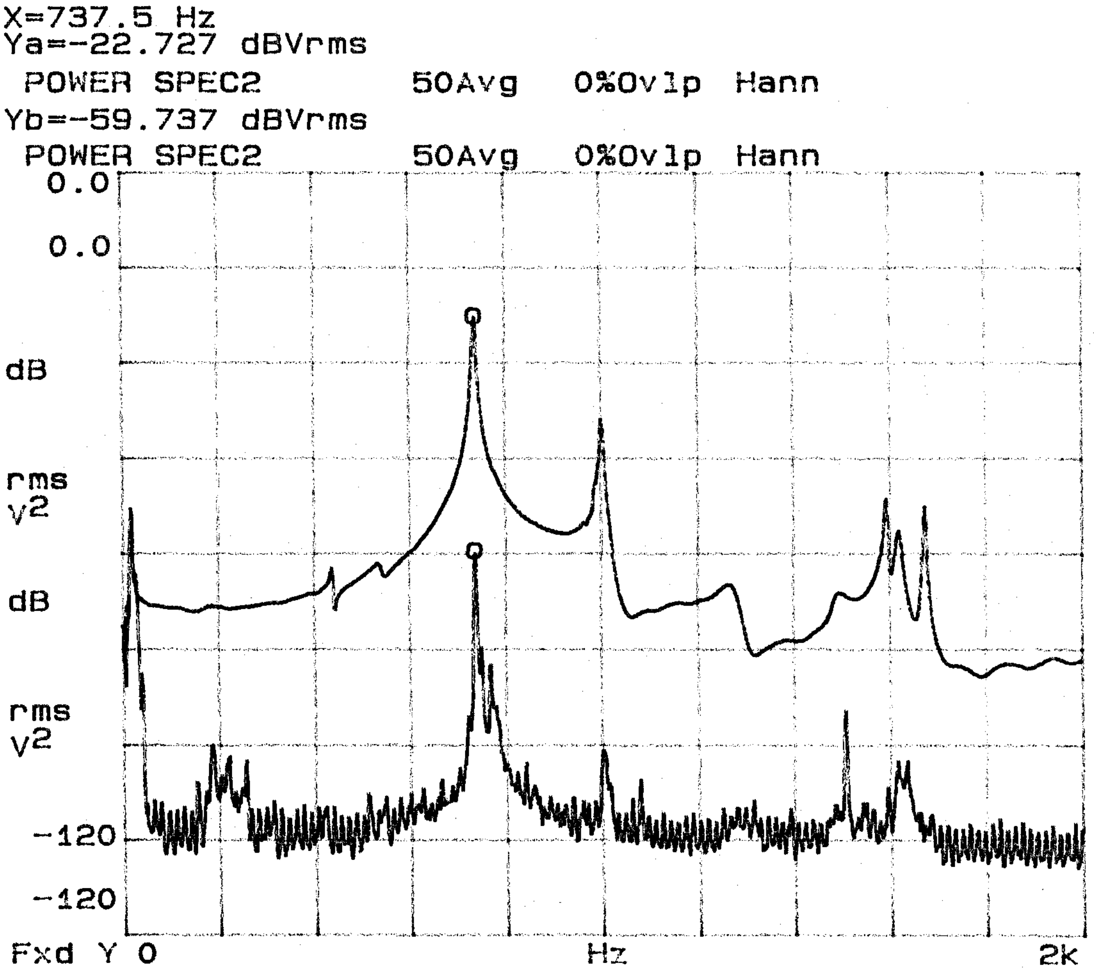

```
X=737.5 Hz
Ya=-22.727 dBVrms
 POWER SPEC2         50Avg   0%Ovlp  Hann
Yb=-59.737 dBVrms
 POWER SPEC2         50Avg   0%Ovlp  Hann
```

Power Spectra of 38" Al plate that is 3.5" in Length

Black - Power spectrum taken while tapping plate

Blue - Power spectrum with natural background noise

Al plate

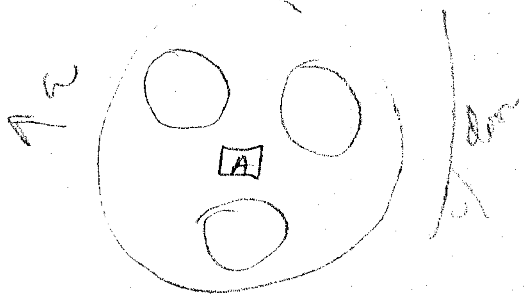

V A accelerometer in center of plate

Power Spectra of 38
Al plate that is 3.5" thick

Power spectrum taken while tapping the underside of the plate

SORE5

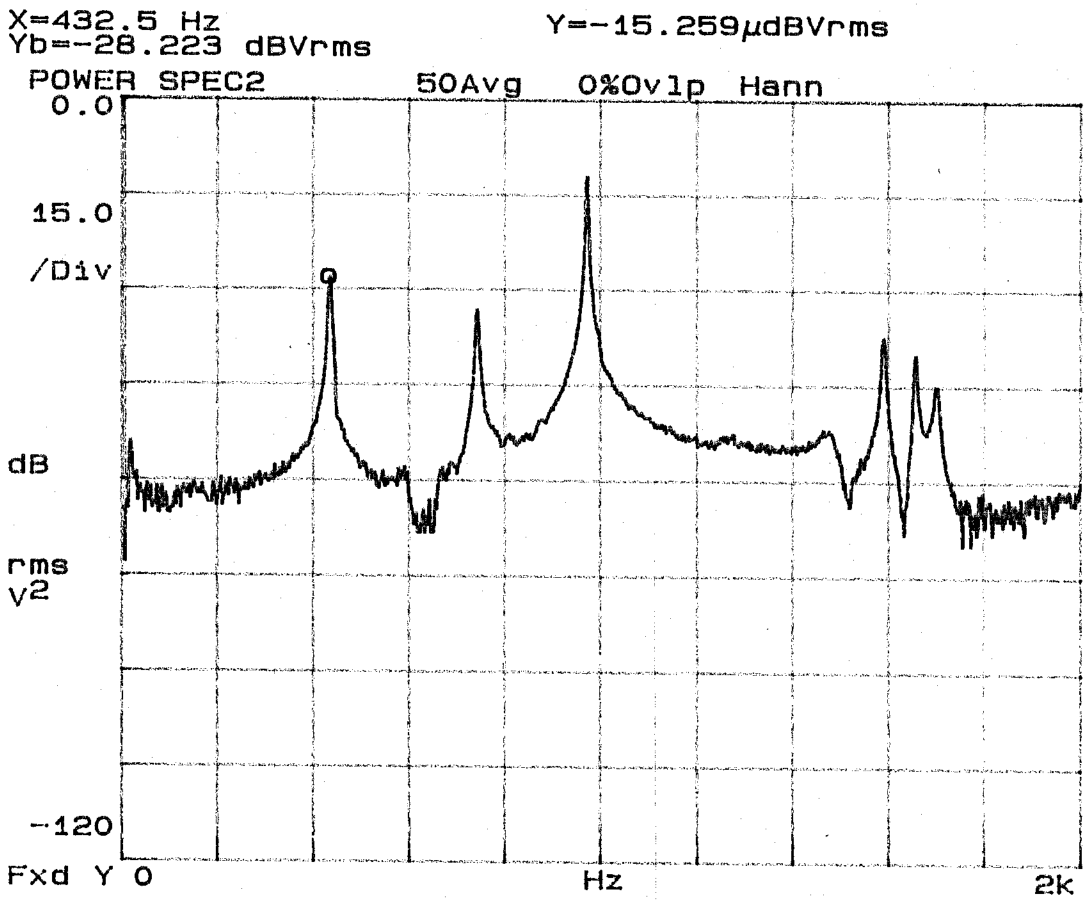

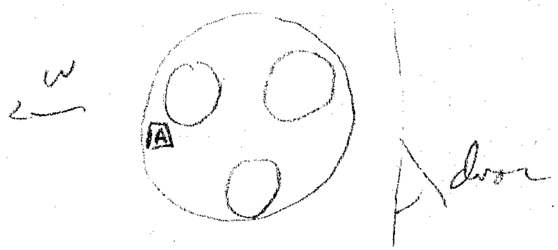

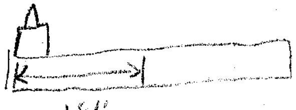

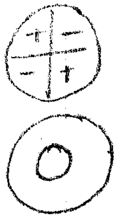

432Hz peak

737Hz peak

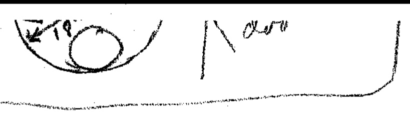

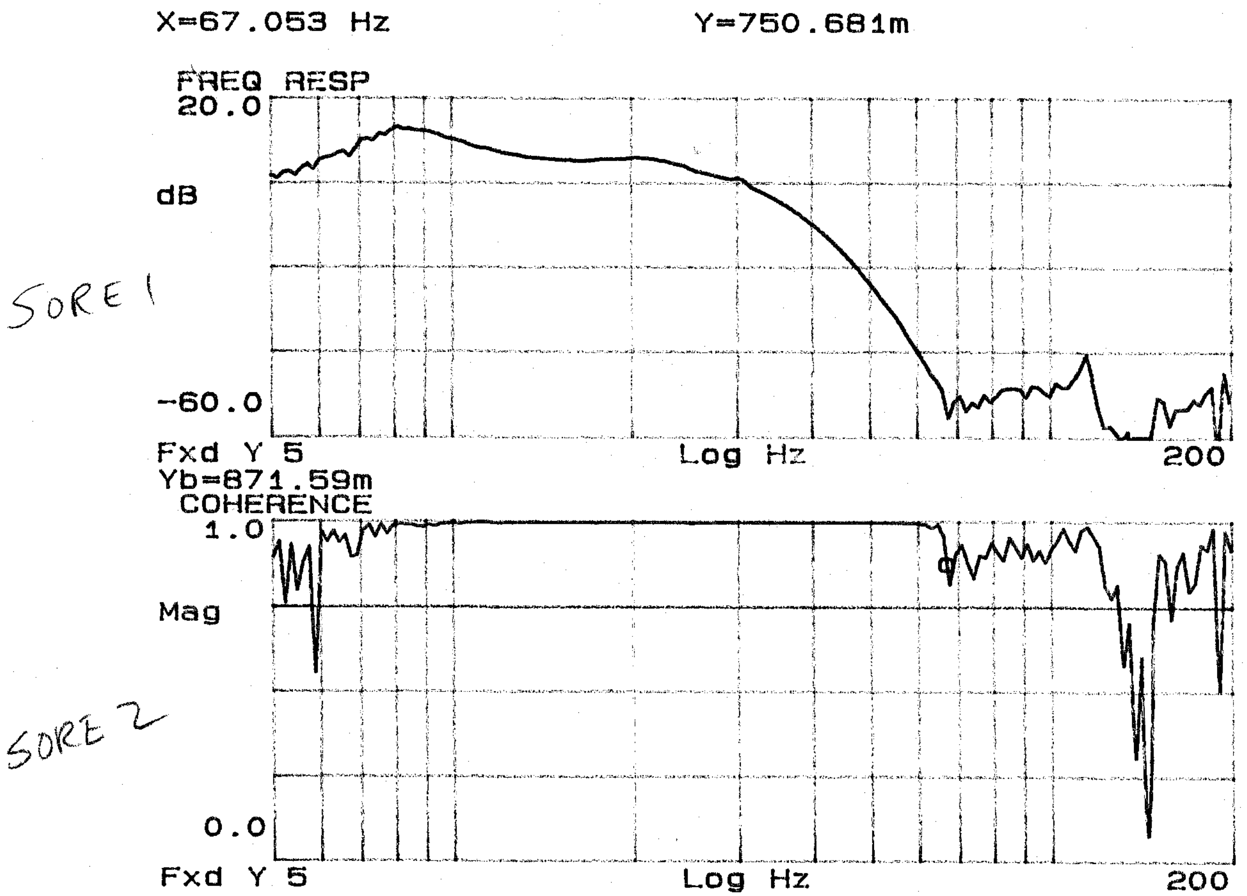

< 20 Hz
Av = 5
Integ time = 1 sec
Resln = 100 pts/dec
Source level = 150 mV RMS

> 20 Hz

Source level = 300 mV RMS

- Bottom accel near N drift compensator
- Top accel on center of plate
- All accel and shaker in V position

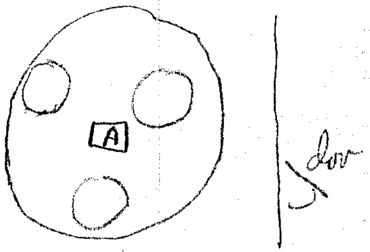

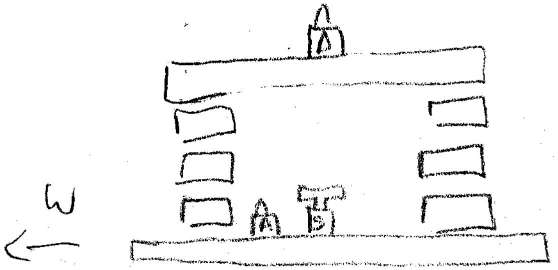

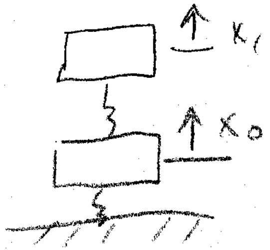

Transfer Fctn from V&V

Same as SORE1
but with much longer
integration time

SORE

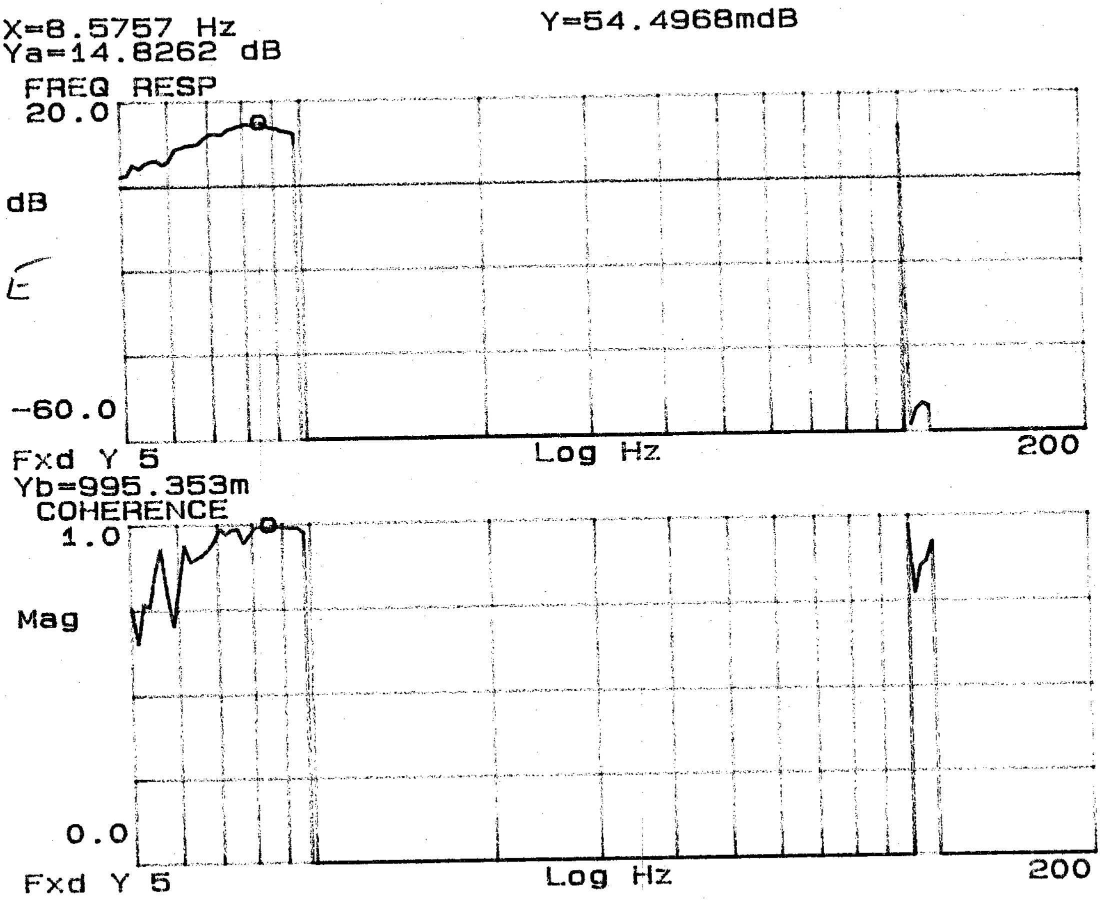

V to H transfer fcts

- shaker in V position
- lower accel in V position
- upper accel in H position on top of slide (center

Black - SORE 6

(reference SORE 7)

Blue - JA16

see page 101)

acoustic pickup from shaker

X=37.853 Hz
Ya=-39.529 dB
FREQ RESP
Yb=-40.54 dB
FREQ RESP

Y=-79.681mdB

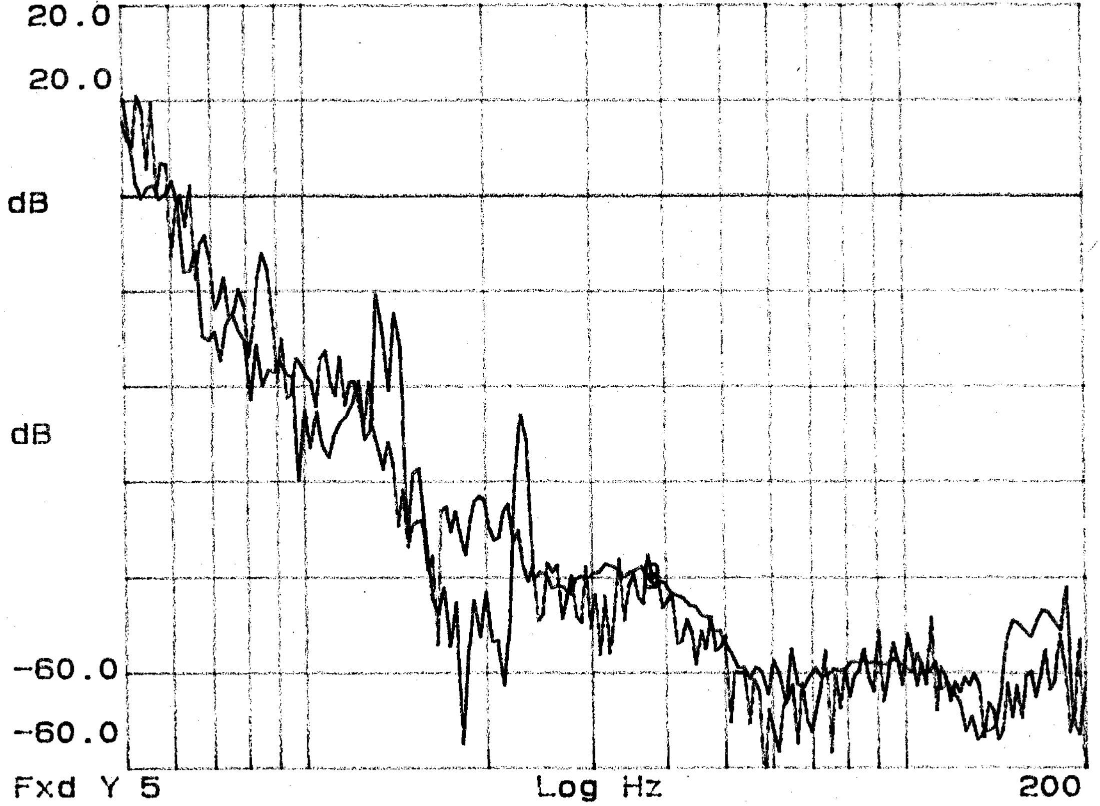

< 20Hz

Ave=8

Integ=300msec

Resln=100pts/dec

source=150mV rms

>20 Hz

Source=300mV rms

This shows the signal is limited by acoustic pickup due to shaker

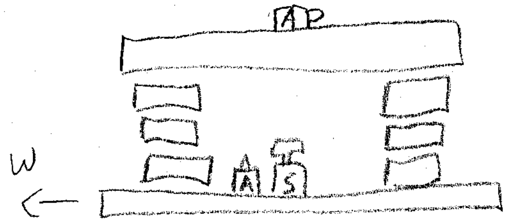

Transfer Fdn from
H to H

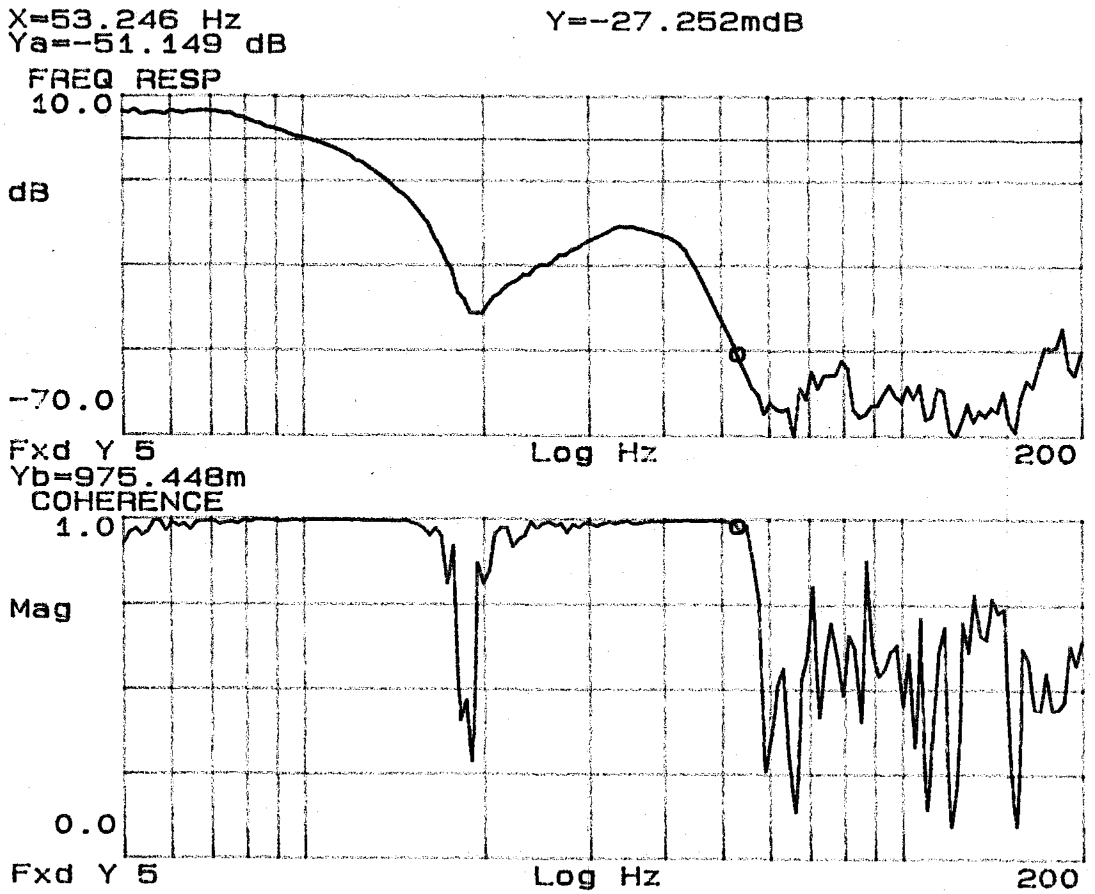

SORE 8

SORE 9

Source	Freq
100mV rms	5-18Hz
400mV rms	18-40Hz
600mV rms	>40Hz

Ave = 5
Intg time = 300msec
Reln = 100 pts

Top accel on center of plate

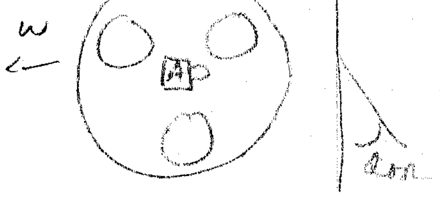

- Shaker in H
- bottom accel in H next to N diff compen.

10:45 1/15/92

Block-SORE10:

Transfer Fctn from H accel to H accel suspended

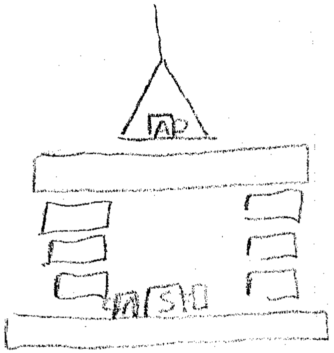

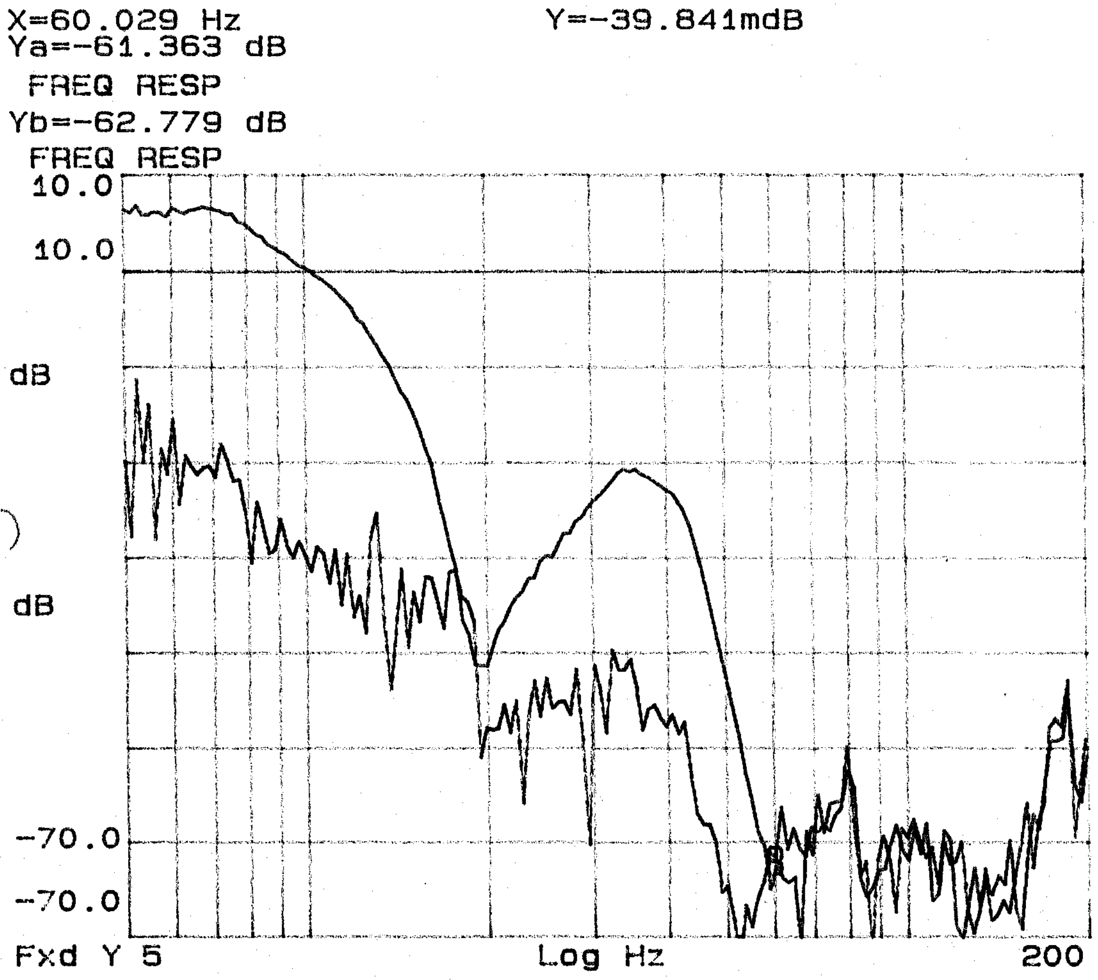

Blue : Sore 8 (H to H transfer fctn)

lock: Sore 10 (Sore 11)

to H transfer fctn tested for acoustic coupling

- Shows that there is acoustic coupling at frequencies above 60 Hz
- Did similar test with accel on springs rather than hanging and got same result (Sore 12 + SORE13)

Transfer Fctn from H to H with top accel on edge of Al plate

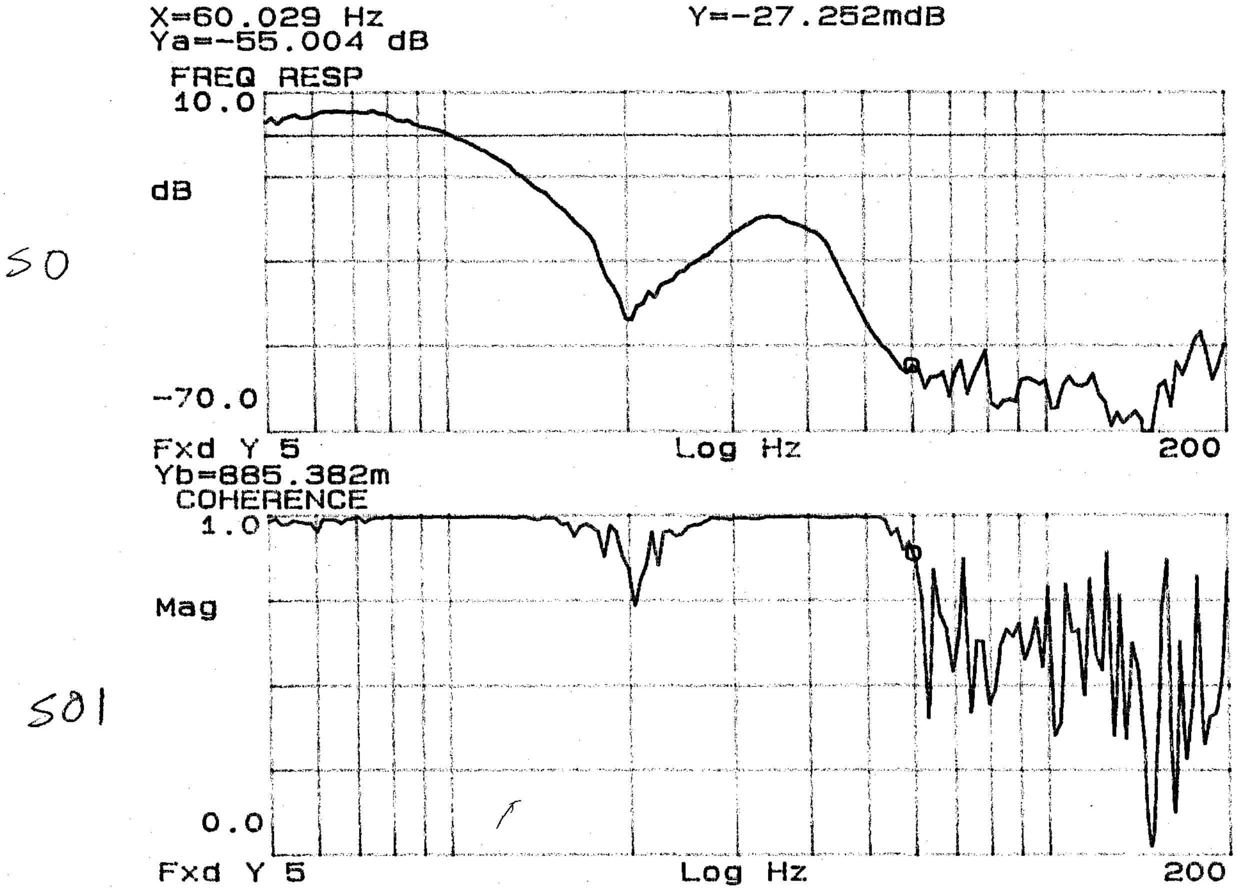

Same settings as SORE8

- Top accel on edge of Al plate

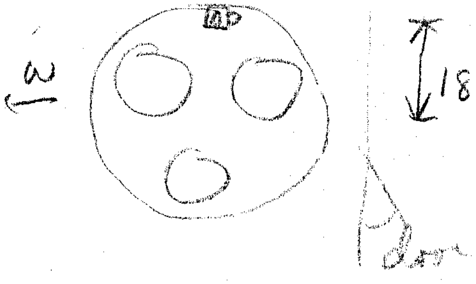

Essentially identical to SORE8 — see no rotational coupling

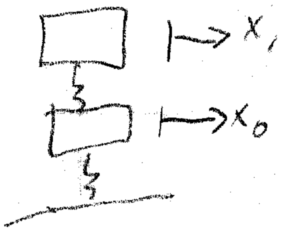

1/15/92

Transfer Fctn from H to V (accelerometer of Al plate)

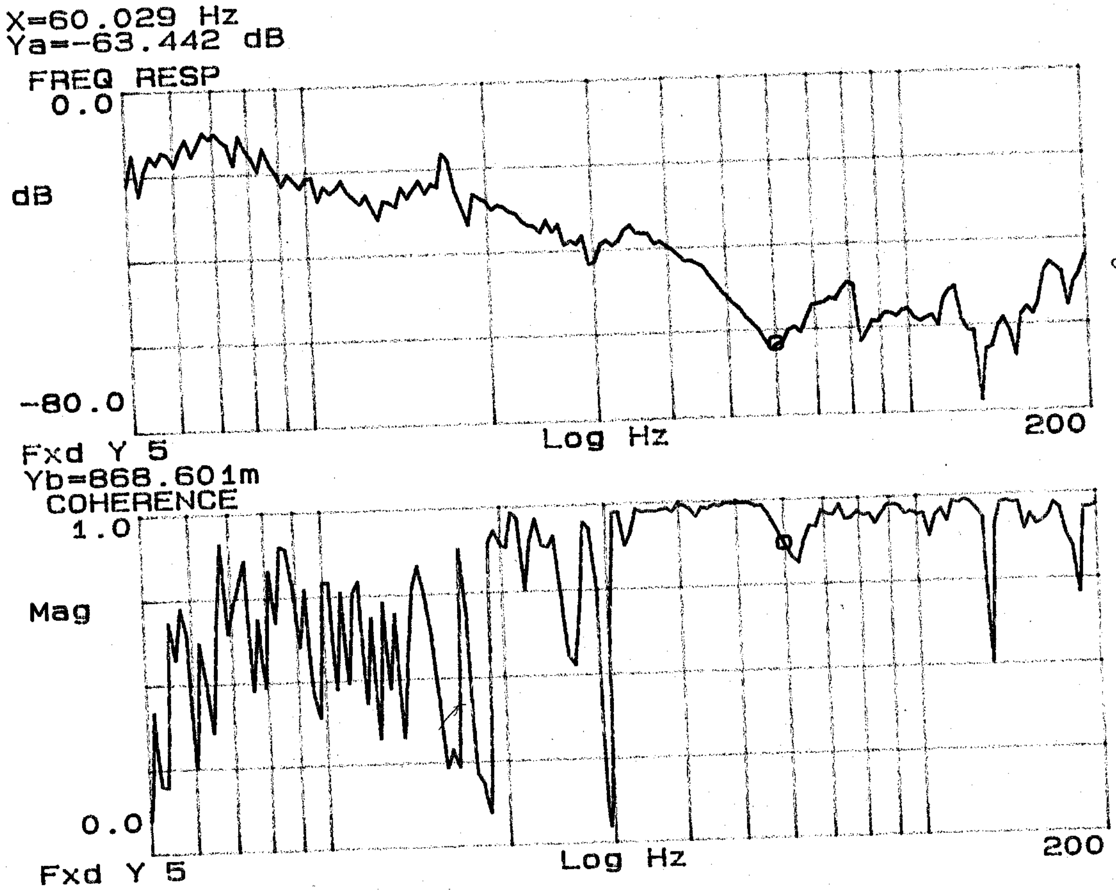

SOR

SORI

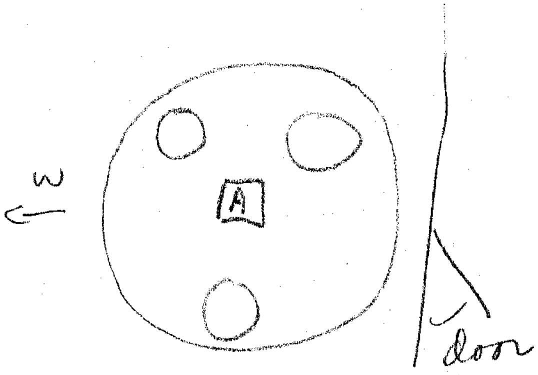

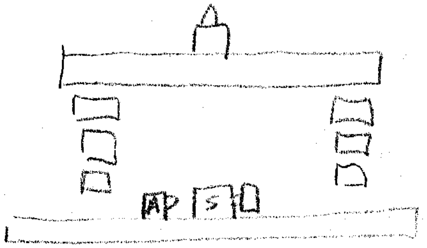

Source level = 100 mV$_{rms}$ f≤18Hz
400 mV$_{rms}$ f>18Hz

Integ time = 300ms f<18Hz
2 sec f>18Hz

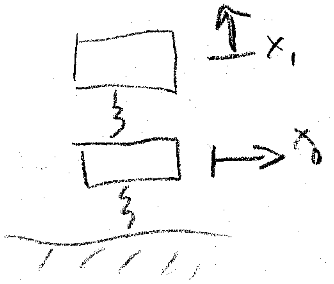

- Shaker in ‖ position
- Bottom accel next to N draft compensator
- Top accel on center of plate

Transfer . . .

II to V (accel on edge of Al plate)

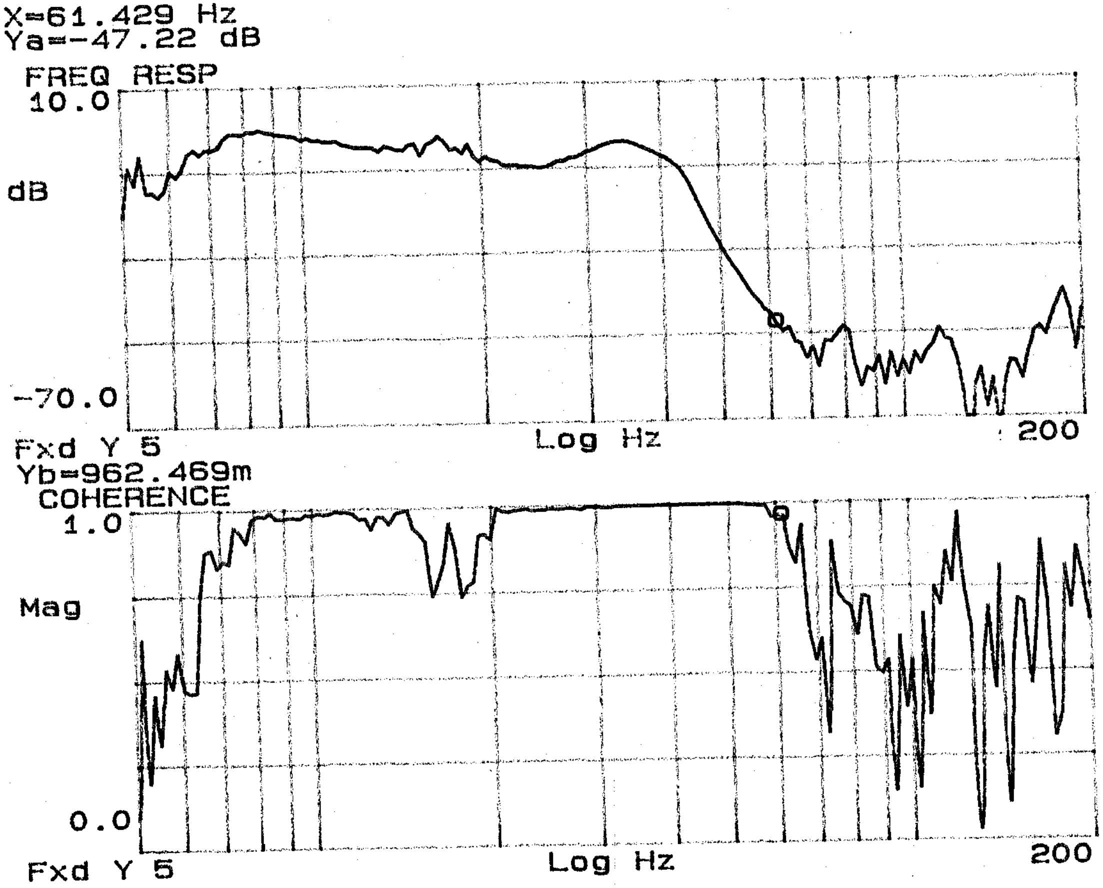

SOR2

SOR3

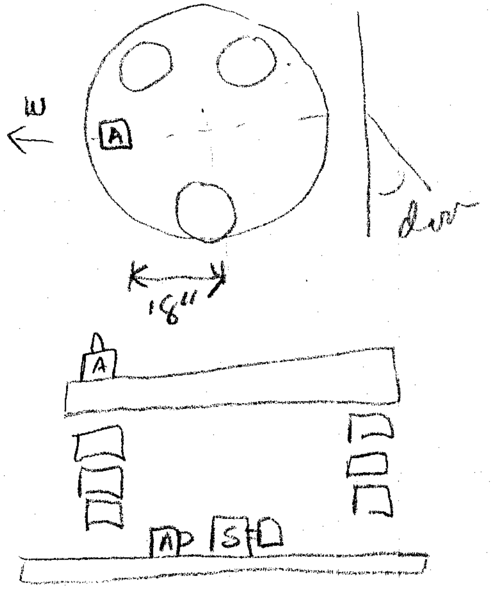

source level = 100mVrms f < 20Hz
400mVrms f > 20Hz

integ time = 300m sec
Ave = 5

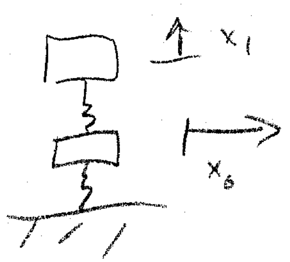

1/15/93 Setup (accel/shaker)

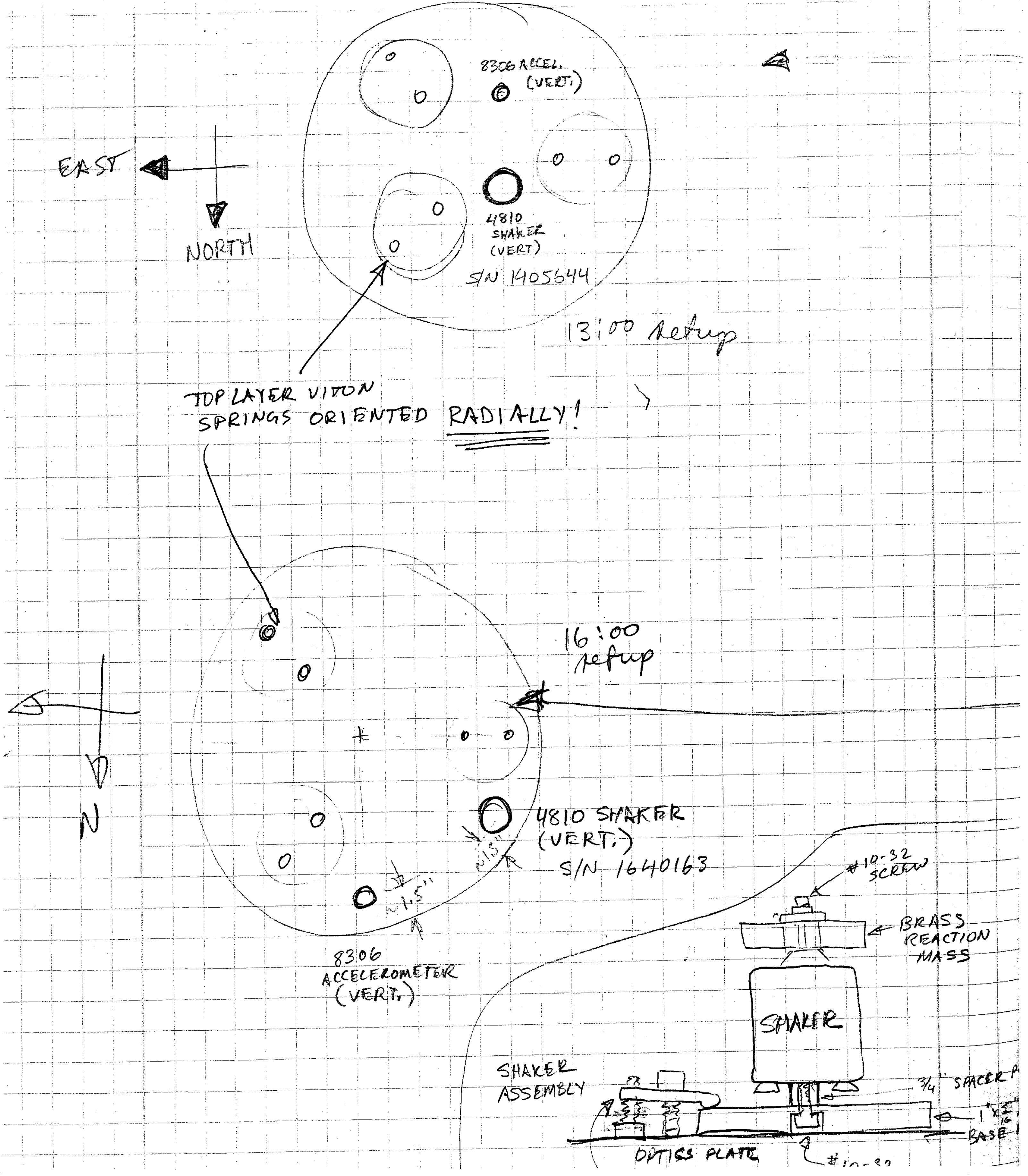

1/15/93
~13:00

Ringdowns of major top plate modes

mode A   736.5 Hz $\tau_{1/2}$ = 39.8 ms   8-4   Trial 1
36.2 ms   4-2

$\tau_{1/2}$ = 33.2 ms   8-4   Trial 2
31.4 ms   2-1

mode B   445.25 Hz   SIGNAL TOO SMALL –

$Q = 4.53 f \tau_{1/2}$

FOUND SHAKER, S/N 1405644 WAS NOT OPERATING PROPERLY – ARMATURE BENT, FRICTION VERY HIGH.

SWITCHED TO OTHER 4810 SHAKER, S/N 1640163

FOUND BETTER S/N BUT Q'S APPEAR LOWER THAN ESTIMATED VALUES FROM PLAYING AROUND ON ~~FP~~ 1/14 – SUSPECT MOUNTING OF SHAKER IS ALTERING MODES + DAMPING. MOVED SHAKER + ACCELEROMETER TO EDGE ~~E~~ OF PLATE

Mode B
accel + shaker @ edge
f_0 = 434.05 Hz (experimental maximum response with shaker/accel in these pos'ns)

$\tau_{1/2}$ = 86 ± 5 ms   8-4 div
92 ± 5   6-3 div.
83 ± 5   4-2 div.
} $\bar{\tau}_2$ =   ⇒ Q =

MODE A
same setup, found peak freq. f_0 = 738.2 Hz now

$\tau_{1/2}$ = 51.4 ms   8-4 div.
52.4 ms   1-2 $\bar{\tau}$ =   ⇒ Q =

1/15/93 LS/MEZ

Summary of Q measurements w/ drive + sense as shown on p. 124 (i.e. near edge of optical plate)

MODE	f_0	Q_{RD}	Q_{XF}
B	434.0 Hz	160	140
A	738.2 Hz	170	160
C	943.3 Hz	470	410

FORMULAS;

$$Q_{RD} = \frac{\pi}{\ln(2)} f_0 \tau_{1/2} = 4.53 f_0 \tau_{1}$$

$$Q_{XF} = \frac{f_0}{\Delta f_{-3dB}}$$

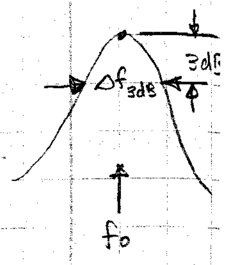

Electrical Setup for Ringdown

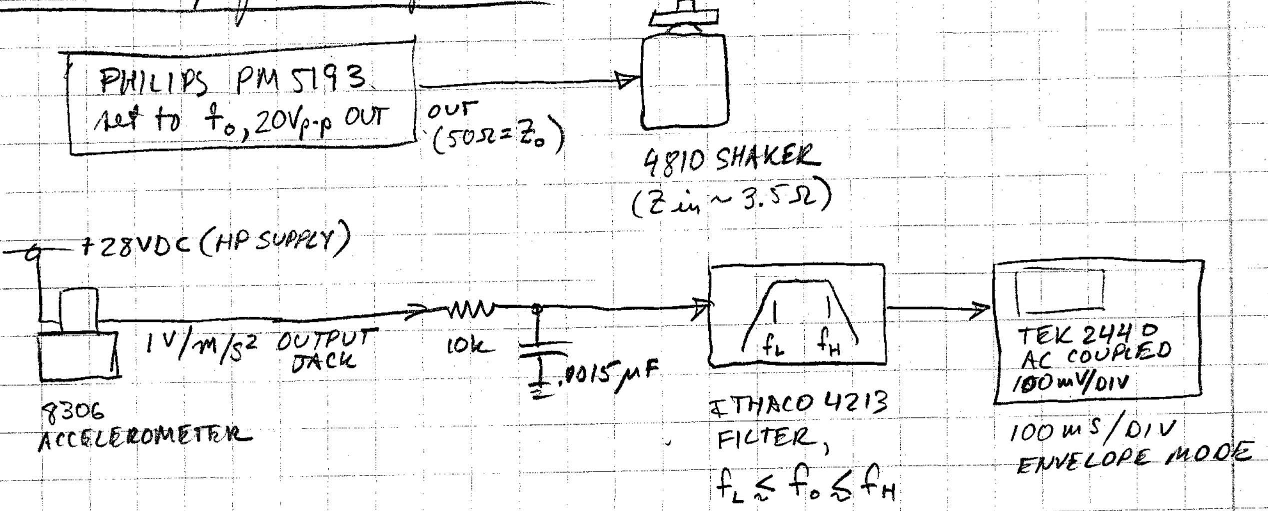

PROCEDURE; HIT "ACQUIRE", PLUG IN 5193 TO SHAKER; WHEN AMPLITUDE IS BUILT UP, UNPLUG 5193 & HIT "SAVE" ON SCOPE TO FREEZE DECAYING ENVELOPE.

Electrical Setup for Transfer Function (XF)

MODE = "LINEAR RES."

MEAS. = "FREQ. RESP."

NOTE; 1 VRMS NOISE IS BAND LIMITED AUTOMATICALLY to FREQUENCY SPAN SELECTED
.E. SET START

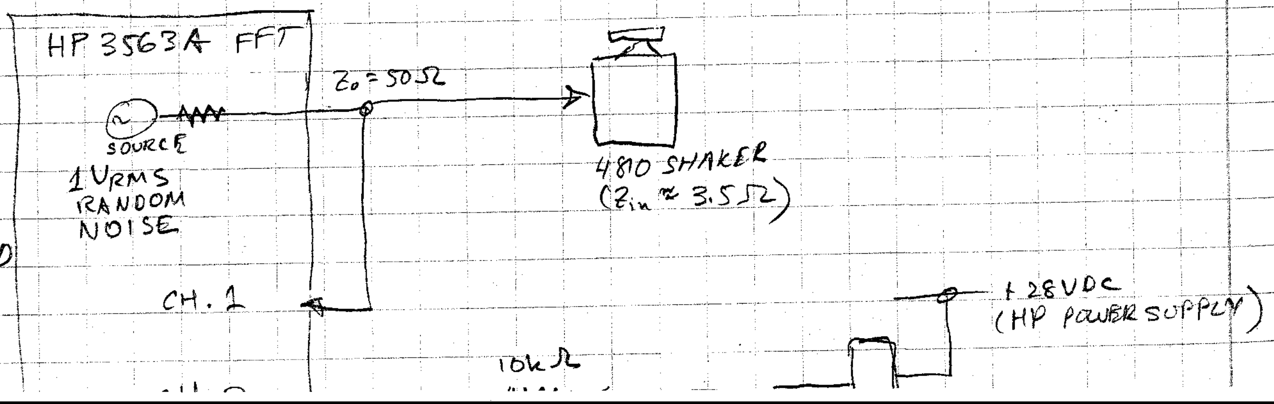

TRANSFER F'N, SHAKER → ACCEL,
1 VRMS RANDOM NOISE
EXCITATION

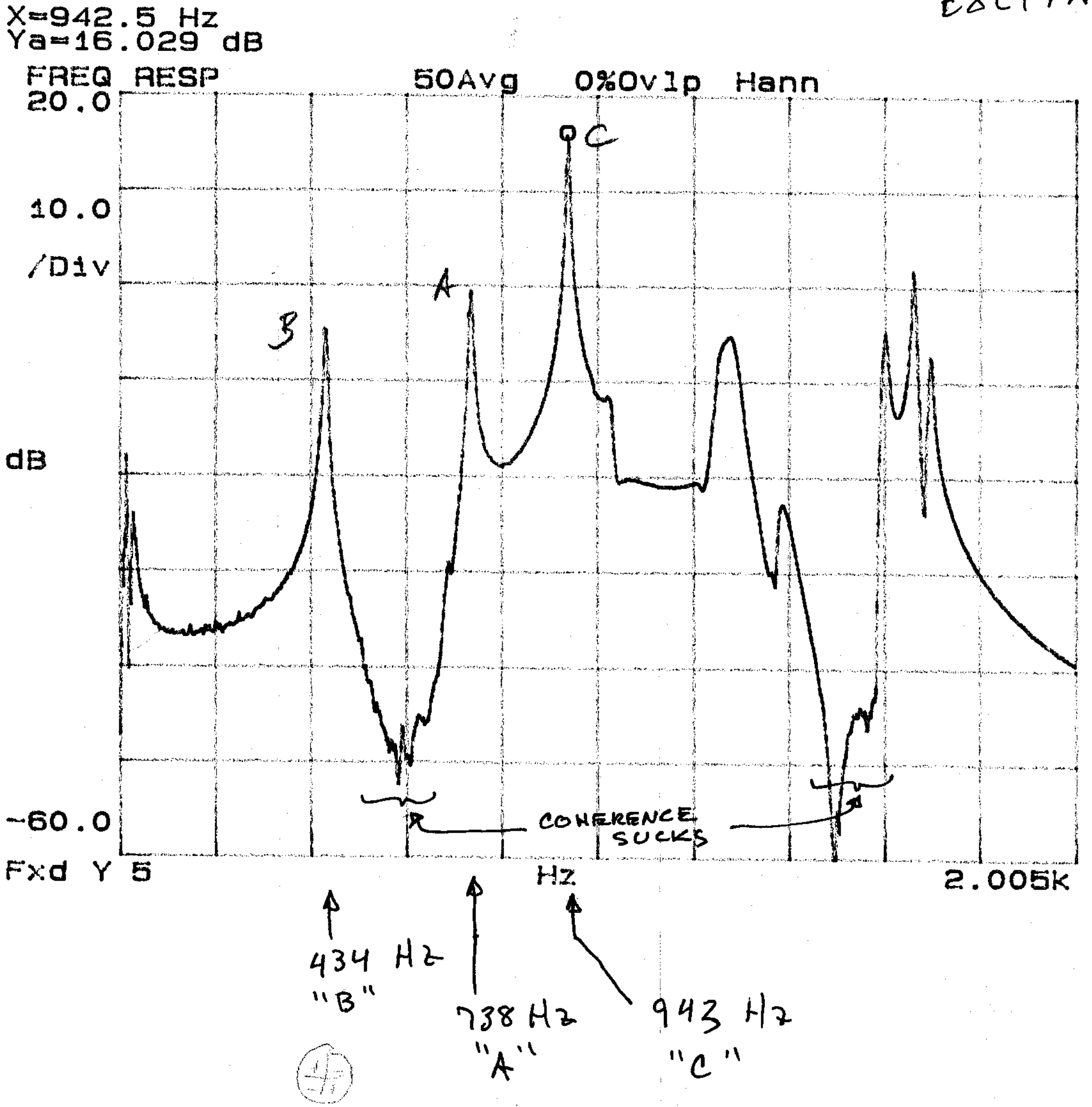

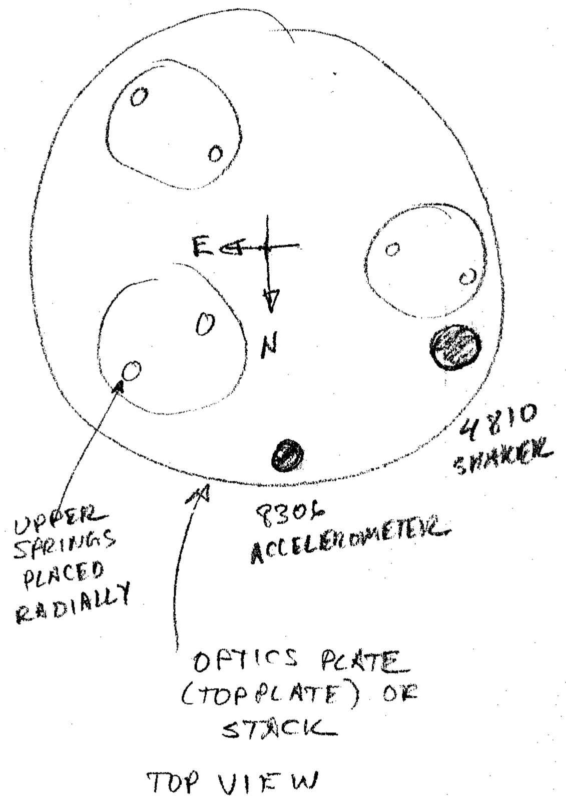

1/15/93 LS/M2 16:50
STACK OPTICS PLATE
738.2 Hz MODE ("A")
RINGDOWN

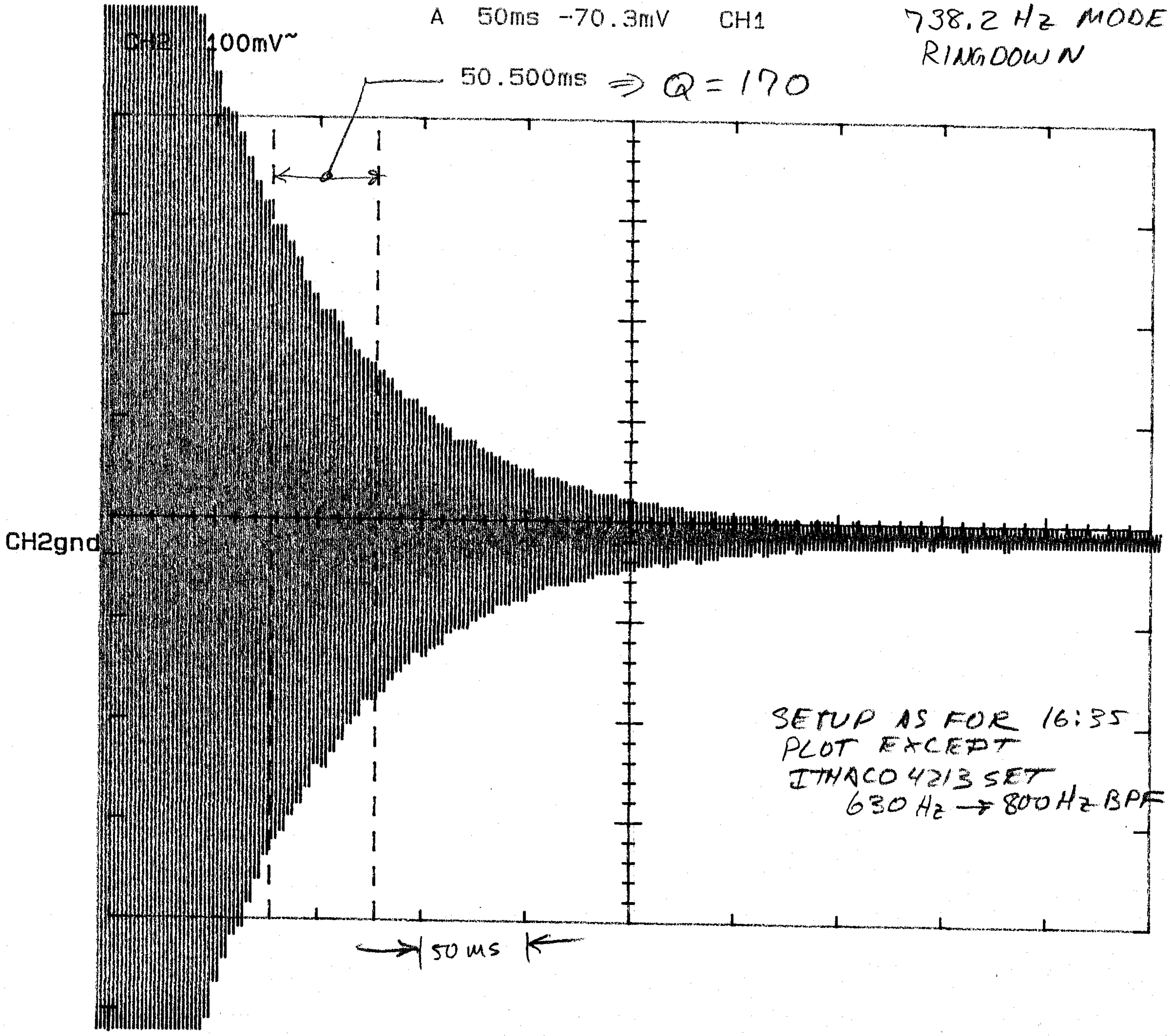

50.500ms ⇒ Q = 170

50 ms

SETUP AS FOR 16:35
PLOT EXCEPT
ITHACO 4213 SET
630 Hz → 800 Hz BPF

17:00

TRANSFER F'N,
B&K 4810 DRIVE VOLTAGE
↓
B&K 8306 OUTPUT VOLTAGE,
near 738.2 Hz OPTICS PLATE
RESONANCE "A"

⇒ $Q = 160 = \frac{740}{4.5}$

```
X=740.82 Hz  ΔX=4.5 Hz       Y=1.7697 dB
Ya=-1.2562   ΔYa=75.14mdB
 FREQ RESP              27Avg    0%Ovlp  Hann          Ov1
```

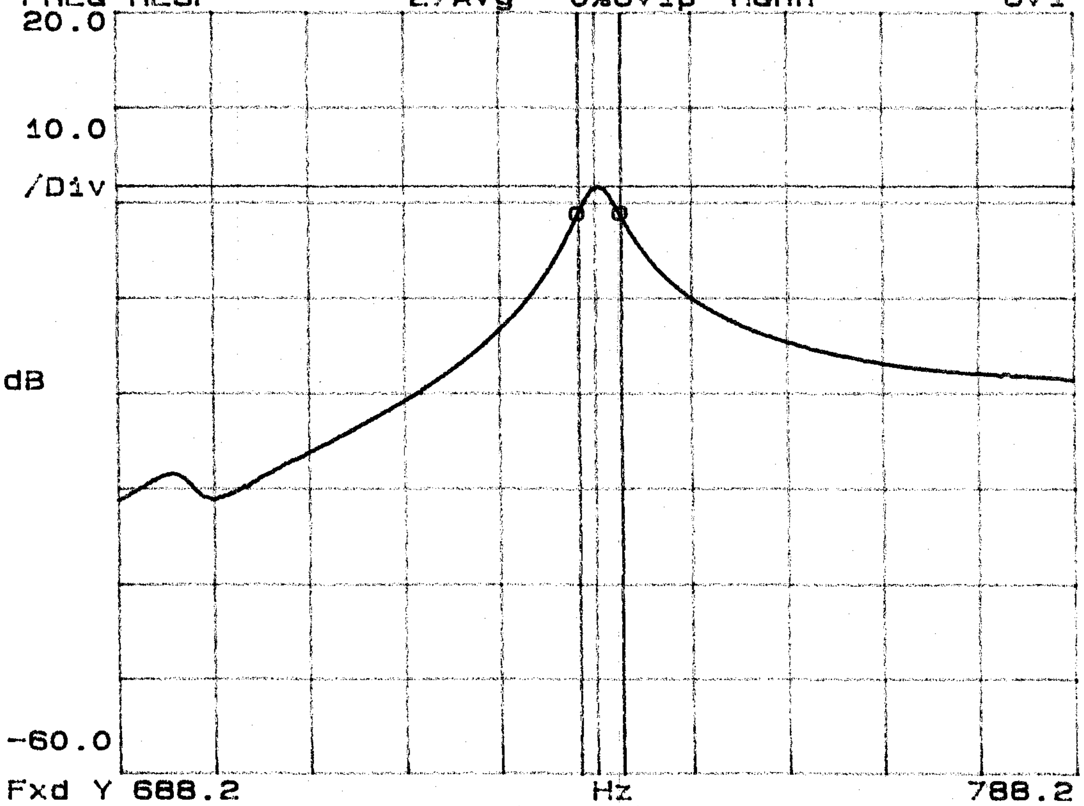

COHERENCE = 100%
EVERYWHERE

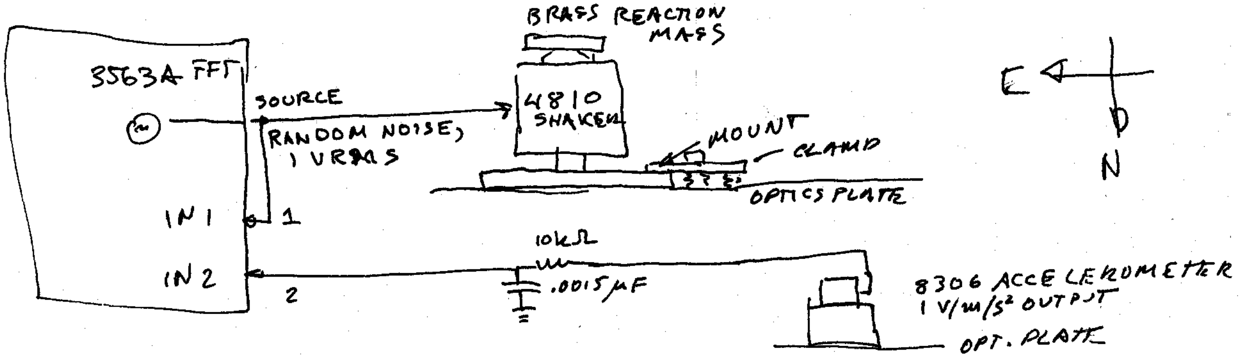

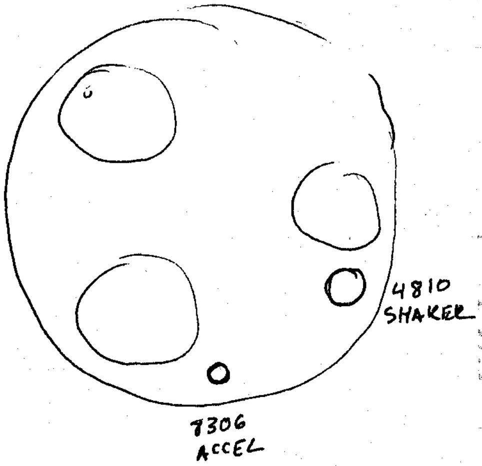

1/15/93 LS/MEZ 16:35

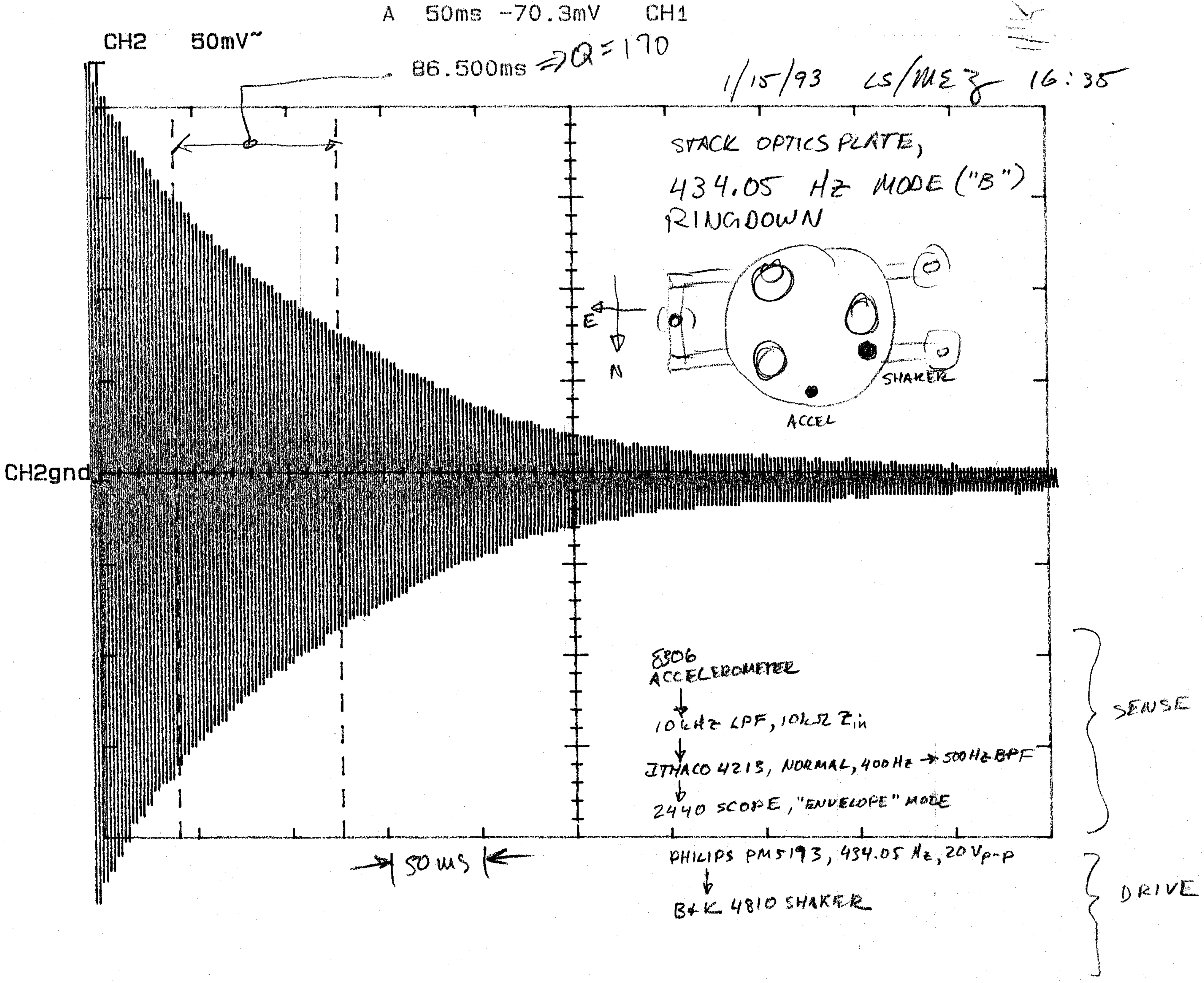

STACK OPTICS PLATE,
434.05 Hz MODE ("B")
RINGDOWN

86.500ms ⇒ Q = 170

8306 ACCELEROMETER
↓
10kHz LPF, 10kΩ Z_{in}
↓
ITHACO 4213, NORMAL, 400 Hz → 500 Hz BPF
↓
2440 SCOPE, "ENVELOPE" MODE

SENSE

PHILIPS PM5193, 434.05 Hz, 20 V_{p-p}
↓
B+K 4810 SHAKER

DRIVE

XF, 4810 DRIVE V

8306 OUTPUT

near 434.0 Hz

OPTICS PLATE RESONANCE "B"

SETUP SAME

AS 17:00

Q = 140

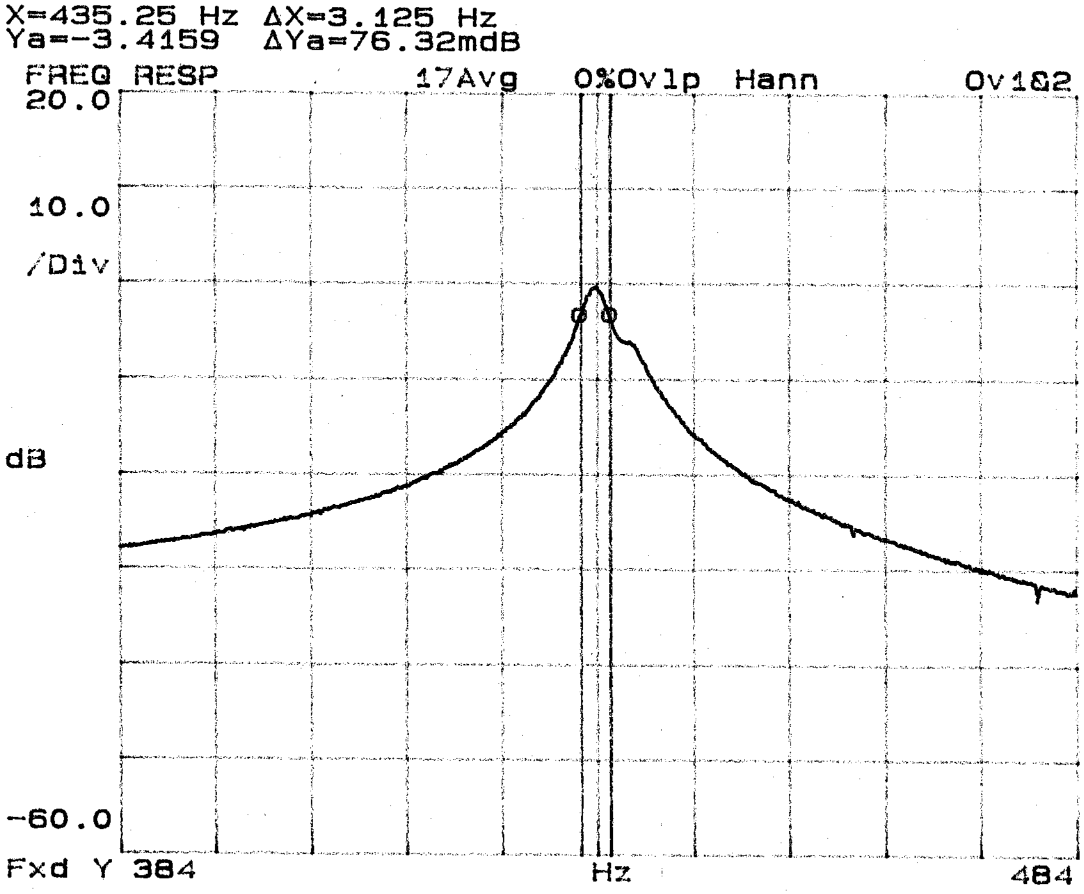

1/15/93 WE 2(C)

17:40

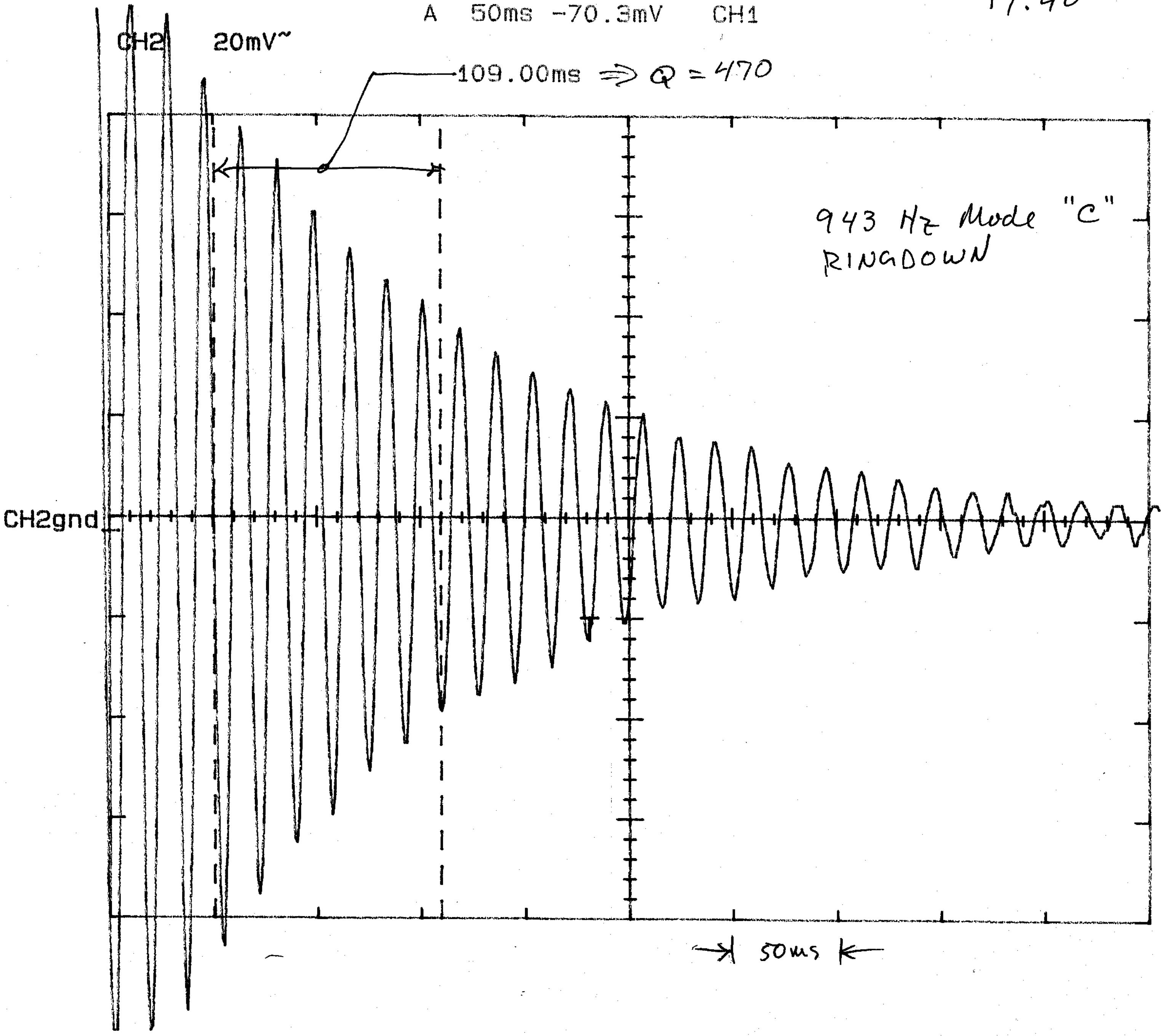

943 Hz Mode "C"
RINGDOWN

OPTICS PLATE RESONANCE "C"
943.3 Hz @ PEAK

Q=410

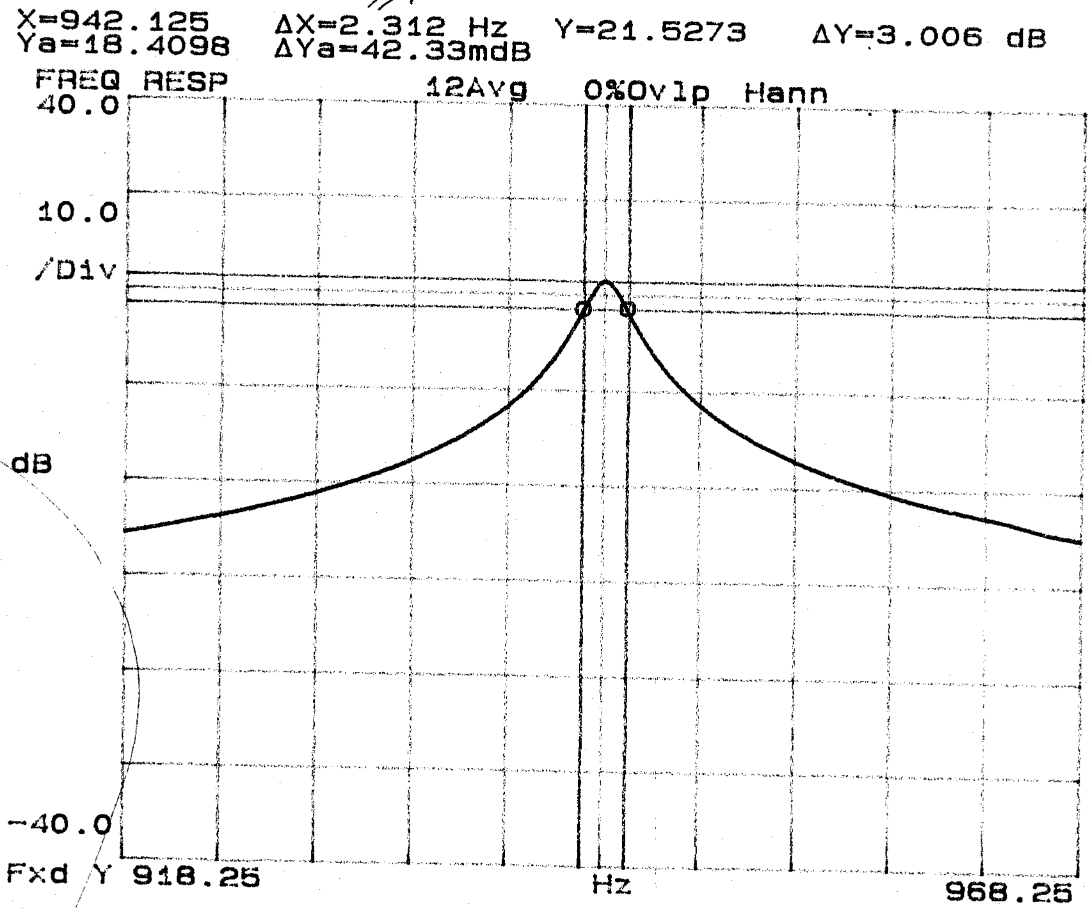

1/18/93 M.E.Z.

STACK HAS BEEN REBUILT WITH SILICONE SPRINGS IN UPPER 2 LAYERS. TOP LAYER HAS 2 SPRINGS IN EACH LEG, ORIENTED "RADIALLY" (SEE P. 124 THIS BOOK)

SETUP SAME AS 1/15.

NEW RESULTS (PLOTS ON FOLLOWING PAGES)

MODE	f_0	Q	comment
A	738.7	450	
B	433.1	1,100	now clearly a doublet, $f_0' = 436.8$ Hz
C	949.1	620	

used on test in CES
(want to use 1 less spring)

SPRING LENGTH	2.03 in	2.03 in	2.03 in	2.03 in	2.03 in	2.03 in
SPRING RATE	409.7 lb/in	409.7 lb/in	409.7 lb/in	409.7 lb/in	409.7 lb/in	409.7 lb
LONG TERM DRIFT (in/lb)	0.0013 in/lb	0.0013 in/lb	0.0013 in/lb	0.0013 in/lb	0.0013 in/lb	0.0013 in
WEIGHT ON TABLE TOP	0 lb	44.1 lb	88.2 lb	0 lb	44.1 lb	88.2 lb
WEIGHT OF TABLE	362.2 lb	362.2 lb	362.2 lb	362.2 lb	362.2 lb	362.2 lb
NO SPRINGS/LEG	2 27kg spring	2	34 2	2 27kg spring	2	34 2
TOTAL SPRINGS/LAYER	6	6	6	6	6	6
SPRING COMPRESSION	0.147 in	0.165 in	0.183 in	0.147 in	0.165 in	0.183 in
LONG TERN DRIFT	0.078 in	0.088 in	0.098 in	0.078 in	0.088 in	0.098 in
TOTAL SPRING COMP %	11.1 %	12.5 %	13.8 %	11.1 %	12.5 %	13.8 %
TOTAL STACK EL SEP.	0.603 in	0.576 in	0.548 in	0.603 in	0.576 in	0.548 in
WEIGHT OF 3 LEG EL.	602.5 lb	602.5 lb	602.5 lb	602.5 lb	602.5 lb	602.5 lb
NO SPRINGS/LEG	3 49kg. spring	3	3 53kg spring	4 36kg spring	4	4
TOTAL SPRINGS/LAYER	9	9	9	12	12	40kg 12
SPRING COMPRESSION	0.262 in	0.274 in	0.286 in	0.196 in	0.205 in	0.214 in
LONG TERN DRIFT	0.139 in	0.146 in	0.152 in	0.105 in	0.109 in	0.114 in
TOTAL SPRING COMP %	19.8 %	20.7 %	21.6 %	14.8 %	15.5 %	16.2 %
TOTAL STACK EL SEP.	0.428 in	0.410 in	0.391 in	0.528 in	0.515 in	0.501 in
WEIGHT OF 3 LEG EL.	602.5 lb	602.5 lb	602.5 lb	602.5 lb	602.5 lb	602.5 lb
NO SPRINGS/LEG	5 47.4 spring	5	5 50kg spring	6 39.5kg spring	6	41.7 6
TOTAL SPRINGS/LAYER	15	15	15	18	18	18
SPRING COMPRESSION	0.255 in	0.262 in	0.269 in	0.213 in	0.218 in	0.224 in
LONG TERN DRIFT	0.136 in	0.140 in	0.143 in	0.113 in	0.116 in	0.120 in
TOTAL SPRING COMP %	19.3 %	19.8 %	20.3 %	16.0 %	16.5 %	16.9 %
TOTAL STACK EL SEP.	0.438 in	0.427 in	0.416 in	0.503 in	0.494 in	0.485 in
WEIGHT OF 3 LEG EL.	602.5 lb	602.5 lb	602.5 lb	602.5 lb	602.5 lb	602.5 lb
NO SPRINGS/LEG	7 47kg spring	7	7 48kg spring	8 41kg spring	8	43 8
TOTAL SPRINGS/LAYER	21	21	21	24	24	24
SPRING COMPRESSION	0.252 in	0.257 in	0.262 in	0.221 in	0.225 in	0.230 in
LONG TERN DRIFT	0.134 in	0.137 in	0.140 in	0.118 in	0.120 in	0.122 in
TOTAL SPRING COMP %	19.0 %	19.4 %	19.8 %	16.7 %	17.0 %	17.3 %
TOTAL STACK EL SEP.	0.443 in	0.435 in	0.427 in	0.491 in	0.484 in	0.477 in
TOTAL COPMRESSION	1.404 in	1.469 in	1.533 in	1.190 in	1.248 in	1.305 in
PLATE TO TABLE TOP HT	20.412 in	20.347 in	20.283 in	20.626 in	20.568 in	20.511 in
DEV FROM IDEAL (20.5)	-0.088 in	-0.153 in	-0.217 in	0.126 in	0.068 in	0.011 in
COMP. DUE TO DRIFT	0.487961 in	0.510438 in	0.532915 in	0.413698 in	0.433604 in	0.45351 in

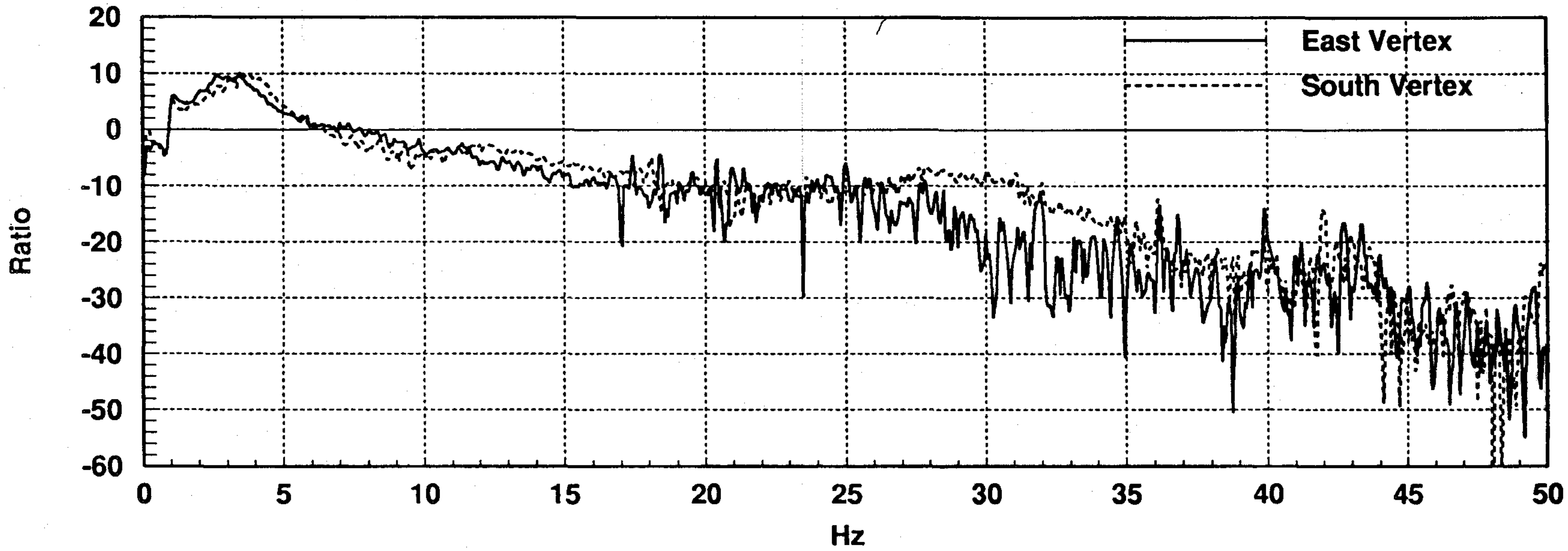

H to H TFs of Vertex Chamber Stacks (seis_sv & seis_sv8)

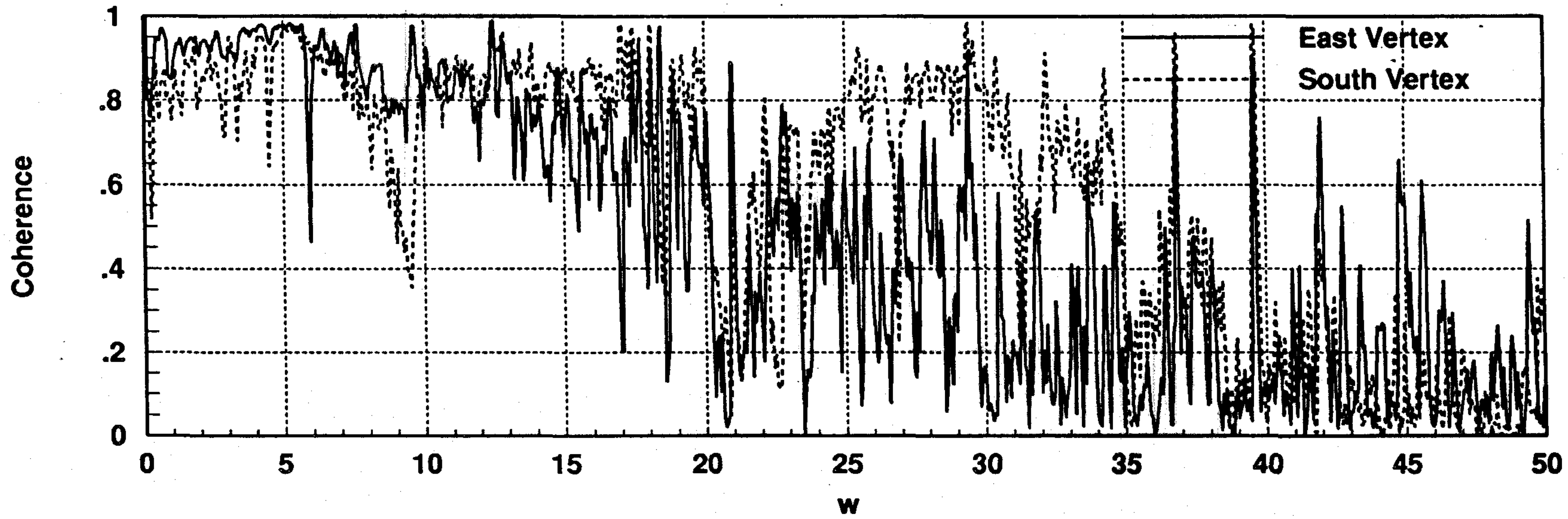

Coherence of Vertex Chamber Stack TFs (seis_sv1 &seis_sv9)

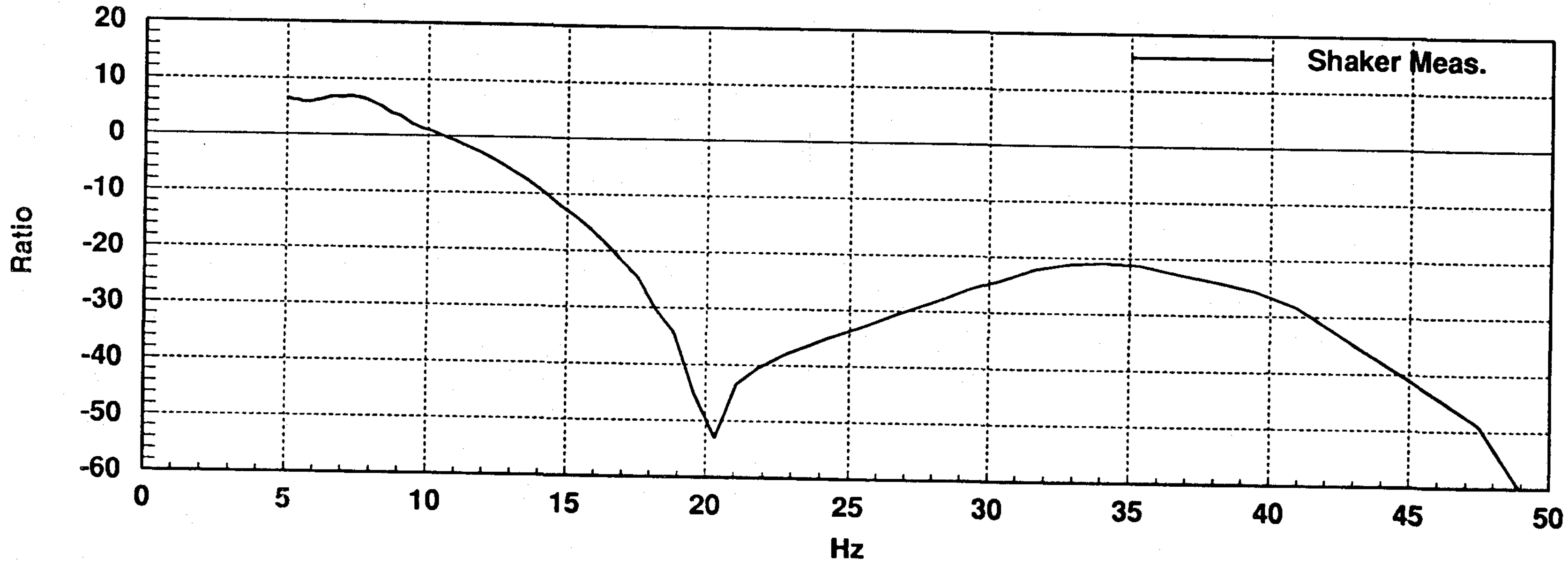

Shaker H to H TFs of Stack on Support Structure (vst)

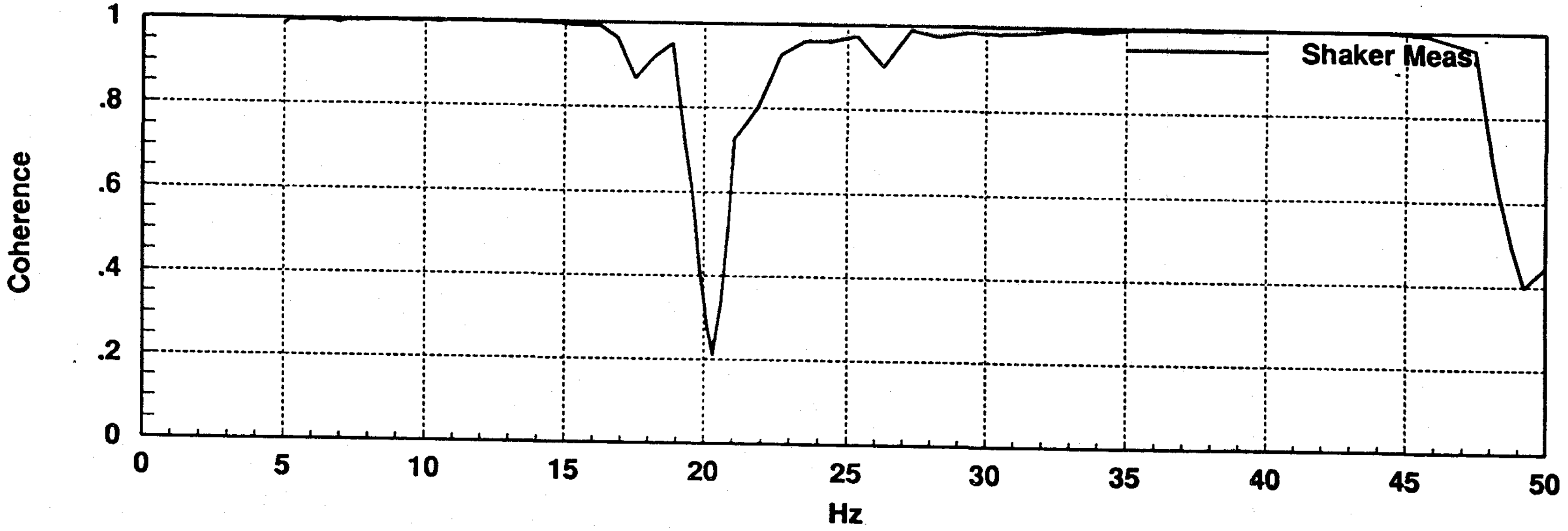

Shaker Coherence of Stack on Support Structure (vst12)

☆ 6) Check $\frac{X}{X_g}$ + $\frac{Z}{Z_g}$ for consitency

- Save X, X_g, Z, + Z_g power spectra

A Passive vibration isolation stack for LIGO: design, modeling, and testing.

Joseph Giaime, Partha Saha, David Shoemaker
Department of Physics, Massachusetts Institute of Technology, Cambridge, Massachusetts

Lisa Sievers
California Institute of Technology, Pasadena, California

(February 27, 1993)

Multiple-stage seismic vibration isolation stacks, which consist of alternating layers of heavy and soft materials, are widely used in mechanical-noise-sensitive experiments. They provide passive, reliable, ground noise filtering so that measurements may be made of the tiny motions that result from gravitational waves. This work describes a four-stage rubber/stainless steel stack, designed for use in the laser interferometer gravitational-wave observatory (LIGO). The stack's transmission of vertical and horizontal base motion to vertical and horizontal top motion were measured, with a sensitivity to transmission of 10^{-7}. In a stack with a combination of Fluorel and RTV rubber springs, the largest transmission component was measured to be 10^{-6} at 100 Hz. 3D finite-element models were studied to understand the limits to the use of such models and to our measurement techniques.

123.234.456.look.up.soon

I. INTRODUCTION

Future interferometric gravitational wave (GW) detectors will use suspended mirrors as gravitational test masses to measure the local strain perturbation in the gravitational metric. [1,2] At the frequencies of interest, from less than 100 Hz to several kHz, the non-gravitational forces on the test masses must be kept as low as possible. Our goal has been to develop a seismic isolation system for the LIGO [2] GW detector that, when used with an appropriate test mass suspension, transmits ground vibration at a level which is small compared with other expected noise sources. Other instrumental applications are possible, for example as a quiet platform for scanning tunneling microscopes. [3]

There have been a number of approaches taken to the seismic isolation problem for GW detectors. Multiple pendulums in series [4,5] attempt to gain isolation by suspending the test mass with wire from a series of similarly suspended masses. There have been experiments with actively controlled suspension elements [6], in which the effective resonant frequency of the isolating harmonic oscillator is lowered using a servo loop.

A straightforward approach, and the one followed here, is the use of a stack consisting of alternating layers of dense stiff material and light compliant material, which may be roughly described as cascaded simple mass-spring oscillators. Such stacks are widely used in GW detector designs, but have often been built by intuition and only partially characterized. As the scale and sensitivity of GW detectors grows, it becomes increasingly important to thoroughly understand the seismic isolation system and to have a design procedure in place. Recently, significant progress has been made on this front [7–10]; we report here on the development of the prototype seismic isolation system for the LIGO detector.

This paper describes the design, finite-element modeling, and laboratory testing of two similar four-layer stacks of fluorocarbon and silicone elastomer springs between sets of stainless steel cylinders. First there is a discussion of the requirements and constraints in designing a stack for use in a laser interferometer gravitational wave detector.

Next, we describe the two designs, one using all Fluorel springs, and one of two layers of Fluorel and two of RTV, and the laboratory tests of them. The experimental tests were carried out in vacuum for dynamic response to vertical and horizontal excitation and vertical and horizontal response. The vibration transfer functions were measured with a sensitivity to transmission of below 10^{-7}.

Finally, there is a comparison of the experimental tests of these stacks with finite-element models of them in order to better understand the limitations of both the modeling process and the measurement techniques.

II. STACK DESIGN REQUIREMENTS.

There are a number of requirements which constrain our design choices: Some constraints follow from the seismic isolation needed in our system, which determines our vibration transmission requirement. Others result from the stack's physical properties, including its spring material's behavior in vacuum, and long term drift.

A. Notation for stack motion coordinates:

To explain the isolation requirements, we first set the notation: Let z describe vertical, and x and y horizontal displacement. We will assume the system's dynamic response is sufficiently linear that one can pick a drive point at the bottom of the stack and a measurement point at the top of stack and express the vibration transmission,

$T_{ij}(f)$, from bottom to top as a 3x3 matrix of complex functions of frequency.

For simplicity, and taking into account the roughly cylindrical symmetry of the stack being considered, these transfer functions are written in terms of only the vertical coordinate, z, and and an arbitrary horizontal coordinate, x. Although the finite-element (FE) analysis was done in three dimensions and, of course, the experimental stack was 3D, the transmission of vibration will be written simply as

$$\begin{pmatrix} x_{\rm top}(f) \\ z_{\rm top}(f) \end{pmatrix} = \begin{pmatrix} T_{xx}(f) & T_{xz}(f) \\ T_{zx}(f) & T_{zz}(f) \end{pmatrix} \begin{pmatrix} x_{\rm drive}(f) \\ z_{\rm drive}(f) \end{pmatrix}, \quad (1)$$

$$\text{or,} \quad X_{\rm top} = T\, X_{\rm drive}, \quad (2)$$

where the drive and top displacement vectors represent the spectral density of displacement noise applied to the bottom of the stack and measured at the top of the stack, respectively. In the steady-state sinusoidally-driven case, T_{ij} is also the transfer function for acceleration and velocity. We actually measure the acceleration.

If the stack rests on a structure that is rigid over the frequency span being considered, and whose tilt motions are sufficiently small, then $X_{\rm drive}$ is that structure's displacement spectral density. If these conditions are not met, the 2×2 matrix notation is insufficient to completely describe the transfer function. As we will describe below, our drive platform can couple horizontal motion to tilting. One might therefore wish to use the tilt angle of the lower table, θ, as a dynamic variable to supplement the description in terms of x and z under certain circumstances. Similarly, the motion of the top table induced by horizontal motion below could be written in terms of a combination of translation and tilt, if one desires a more complete description than the x and z displacements at a chosen point. For simplicity, we will describe in terms of x and z, except when we point out certain important tilt effects.

With this framework, we can discuss the requirements for the seismic isolation system:

B. Attenuation in the gravity wave band:

The seismic noise that drives the stack is modeled here as isotropic along the x, y, and z axes, and with the following spectral density: $10^{-9}/f^3\,\mathrm{m}/\sqrt{\mathrm{Hz}}$ from 0.1 to 1 Hz, $10^{-9}\,\mathrm{m}/\sqrt{\mathrm{Hz}}$ from 1 to 10 Hz, and $(10^{-7}/f^2)\mathrm{m}/\sqrt{\mathrm{Hz}}$ from 10 Hz to 10 kHz. This spectrum is based on measurements in a number of laboratories and ground-noise surveys [11,2].

A complete isolation and suspension system for our application in interferometric GW detectors consists of an isolation stack and a pendulum suspension for the test mass. The pendulum suspension offers some isolation in both the vertical and horizontal axes [8,5]. The GW detector is principally sensitive to motion along an x (horizontal) axis (thus constraining T_{xx} and T_{xz}). The earth's curvature over the 4 km length of the LIGO GW detector gives a internal coupling in the pendulum suspension from motion in the z axis to motion along the x sensing axis of at least 3×10^{-4} (constraining T_{zz} and T_{zx}); additional cross-coupling in the test-mass suspension is likely. The mechanical support structure between the stack and the pendulum also converts tilting motion of the stack top plate (around the y axis) into motion along the x axis, as will be disussed. This can be related to the T_{zx}.

The noise contribution from the native ground noise, filtered by the stack and pendulum transfer functions, must be substantially less than the expected noise from the thermal excitation of the mirror pendulum suspension [2,12] in the LIGO. This leads to a requirement for the stack isolation. Since the pendulum transfer function and the ground noise should be falling rapidly with frequency in the vicinity of 100 Hz, the minimum isolation requirement is specified as a required attenuation of the various isolation system transfer functions at a single frequency. Above that frequency, even if the stack's response levels off, the overall seismic noise contribution should still decrease.

The maximum seismic transmission for our application is 10^{-5} at frequencies above 100 Hz for T_{xx} and T_{xz}, which couple to horizontal motion, and approximately a factor of 10 less for T_{zx} and T_{zz}, which couple to the vertical. Improvements beyond this requirement may improve the sensitivity of the GW detector, either directly or by reducing indirect contributions from cross-couplings, and are highly desirable.

C. Noise amplification at rigid-body resonances:

Rigid-body resonances are those for which the solid masses of the stack behave as perfectly rigid bodies applying forces to one another through the low-mass spring elements. The transmission peaks due to rigid-body stack resonances, in the high-ground-noise region from 1 to 10 Hz, must be damped well enough that the RMS motion on top does not exceed the gravity wave antenna servo system's ability to suppress this motion because of dynamic range or gain-bandwidth limitations. Since the sub-hertz motion dominates the integral to calculate $x_{\rm rms}$, it would seem that high-Q peaks at several hertz wouldn't contribute very much to the displacement noise, if one only considers 'stationary' random ground noise. However, impulse or step excitations might excite high-Q resonances. The optical and control systems contain non-linearities, which can lead to upconversion of the motion at low frequencies to signals at GW frequencies (roughly 50 Hz to 5 kHz); Or, if noise is coupled to the mirrors through magnetic fields, which push the small control magnets to be glued on them, any eddy current sites on the isolation stack would contribute in proportion to their velocity, not position, enhancing the contribution from the rigid-body modes. These considerations suggest against a design with transmission peaks greater than of order ten.

D. Other constraints.

a. Static characteristics: The top of the stack needs to support a load of up to 150 kg, consisting of various suspension, test mass/mirror, and control elements for the interferometer. With this load, the stack must have a long-term drift consistent with the ability of the rest of the isolation/suspension system to compensate. A stack drift of several mm per year, beginning a few months after assembly, is acceptable. In addition, short-term temperature drifts must not result in motions of the stack which exceed the interferometer servo system's short-term dynamic range.

b. Vacuum compatibility: Since interferometric gravity wave detectors will operate in the very high to ultra high vacuum, and since the large size of the systems precludes high pumping capacity, the materials used for the stack must have low outgassing properties. In addition to the simple outgassing rate, the contamination of nearby low-loss optics must be held to an acceptable level.

III. THE DESIGN

A. Design concept

The basic stack design can be thought of as four cascaded harmonic oscillators. The lower three oscillators consist of layers of three, 100 kg stainless steel cylinders above layers of 70 durometer Fluorel or RTV rubber springs, forming three 'legs' of three cylinders each. The final layer is a single 78 kg circular aluminum table supported through three rubber springs on the three legs below. To predict the response of the stack to horizontal motion, it was necessary to do numerical simulation. However, the vertical response to vertical excitation, $T_{zz}(f)$, can be accurately described as four cascaded one-dimensional oscillators: At frequencies well below a single oscillator's resonance, there is unity transmission. Near the resonance, the transmission is enhanced by approximately the Q of the oscillator. Well above the resonance, the transmission falls with frequency as $1/f^n$, where n lies between 1 and 2 and depends on the dissipation mechanism in the springs and on the Q. When four such layers are cascaded, the resonance peaks in $T_{zz}(f)$ will be spread in frequency and will correspond with the frequencies of the four rigid-body modes that have predominantly vertical mode shapes. Well above the resonances, $T_{zz}(f)$ will fall approximately as the product of the individual stages' responses.

The stack's response to horizontal excitation is not as easy to predict with simple arguments as the vertical response, since this kind of drive couples into complicated modes involving both tilts and translation of the solid elements; the numerical analysis used to describe the horizontal motions will be discussed below.

There are also high frequency internal modes in the solid mass and spring elements. The approach we took in this design was to make the rigid-body modes low Q, and below the frequencies where we needed high isolation, and to make all of the internal modes high enough in frequency that they would be well filtered by the rest of the stack, despite their high Q. This requirement led to compact structures of steel to be used as the masses, and rubber as the springs.

B. Selection of spring materials.

A major design concern was to find a material for the springs compatible with vacuum use, which could be incorporated in a stack design which meets the above criteria. Two will be discussed: Fluorel, and RTV.

Fluorocarbon elastomers, often known by their trademarked names Viton and Fluorel, for example, are widely used as seal materials for high vacuum systems. We investigated the dynamic properties of injection molded 3M-Fluorel 2176 by measuring the real and imaginary parts of the elastic modulus over the range of interesting frequencies. For the frequency region in which we expect resonances, the ratio of real to imaginary modulus is near 3. This means that a harmonic oscillator using this as the spring element will have resonance Q's of that order as well. We found that the elastic modulus grows with excitation frequency, and that the imaginary part of the modulus grows faster, as approximately the square root of frequency. A system consisting of a viscous (velocity-proportional) damper in parallel with a hooke-law spring, if analyzed in terms of a complex spring constant, would have a imaginary part linearly proportional to the drive frequency. The behavior of the Fluorel is typical of visco-elastic damping found in various materials. The advantage of this form of damping to our application is that while the modal resonance peaks are well damped, well above these frequencies the transmission falls nearly as $(f_0/f)^2$ per oscillator stage, where f_0 is the oscillator's resonance frequency. The transmission of a viscously damped system with a similar resonance Q would fall less steeply, providing less high frequency isolation.

We also characterized GE RTV615 silicone rubber, for which we also had experience in preparation for vacuum use. The RTV's modulus was lower than that of the Fluorel, and mostly real, indicating that a mechanical oscillator made with RTV springs would have a considerably higher Q than one with Fluorel. The use of a combination of these materials allows a tradeoff between the high

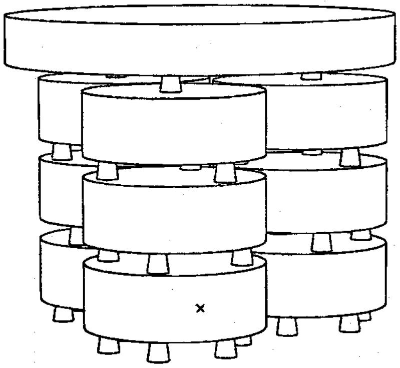

FIG. 1. Perspective drawing of the isolation stack.

damping and low rigid-body-mode resonant frequencies we desire.

Although the modulus vs. frequency data allow the prediction of the system's dynamic response, it is important to note that lossy elastomers such as Fluorel strain over time in response to constant stress. For very long times, of order at least hundreds of seconds, these materials often exhibit a creep described by $\delta l/l \sim \log(\text{time})$. We also observed a short-time relaxation of the material, which occurs over tens of seconds after loading. Experimentally, we determined that the overall strain on the springs should not exceed about 20% to limit the creep to acceptable levels; this initial deformation limits the load capacity of the Fluorel. This long-term behavior is not well described by the modulus vs. frequency data.

IV. EXPERIMENTAL TESTS.

A. Configurations Tested.

With some lessons learned from preliminary element analysis (to be described below), and our spring materials selected, two full-scale isolation stacks were tested. The tests were performed in a vacuum chamber which was pumped down to less than 10^{-4} mbar for all measurements requiring sonic isolation.

The stack is drawn in perspective in Fig. 1. The leg elements were made from 5 in. (12.7 cm) long by 14 in. (35.6 cm) diameter cylinders of type 304 stainless steel. These pieces were approximately 100 kg each, and we calculate that all of their internal resonances lie above 3 kHz. The table, made of Aluminum alloys, measures 78.49 cm in diameter and 9.52 cm in height, and consists of a 2.54 cm thick top plate welded to a 7.0 cm by 7.6 cm ring, with 2.54 cm wide radial webbing welded inside, for stiffness. Another of these tables was used as the platform on which the entire stack was constructed. The only table resonances below 1 kHz were measured at 467 Hz and 825 Hz, with Qs of approximately 500.

We present results from tests of two spring configurations: The first stack was assembled with springs made with Fluorel [13], held in place with friction. These springs measure 5.08 cm high, uncompressed, and after compression and settling measured, by layer from top to bottom, 4.52, 4.19, 4.04, and 4.07 cm in height. The number of springs per layer, per leg, top to bottom, was 1-3-4-6, making a total of 42 spring in the stack. The second configuration was identical to the first in the lower two layers, but used similarly shaped RTV springs for the upper layers. The RTV springs measured approximately 3.4 cm long uncompressed, and 2.7 cm compressed on both layers.

B. Dynamic Measurements:

In order to characterize each stack's dynamic response over the frequency range of 1-350 Hz, three methods were used.

1. Mid-frequency measurements:

The most straightforward measurements were made in the frequency range of approximately 20 to 90 Hz, covering the part of the transfer function over which the vibration transmission drops from about a few tenths to about 10^{-4}. For this series of measurements, the stack was built on a base table which itself was resting on three stiff springs. Two electromagnetic shakers were used to excite motion in the base: one mounted horizontally on the drive table side, and one oriented vertically, mounted on the center of the table's underside. Accelerometers were attached to reference points chosen for the lower table and top table, with an accelerometer in each location for each of the directions defined by the two drivers. These reference points were near each table's edge, in order to make them sensitive to both tilt and translation of the tables, so that phenomena involving one or both of these motions would not be missed. We then applied a frequency-swept sinewave drive of approximately 5 N_{rms} to the bottom, vertically, and recorded the transfer functions T_{zz} and T_{xz}, by taking the vector ratios of the signals on the top to those on the bottom. Similarly, horizontal drive was used to measure T_{xx} and T_{zx}. This drive level produced very small motions in the drive table, less than a micron at 100 Hz, so we have assumed that the elastomers are behaving approximately as they would for the ground noise drive expected in the intended application.

2. *Low-frequency ground-noise-driven measurements:*

At low frequencies, the stack's response is strongly influenced by the exact shapes and frequencies of the rigid-body modes, which range in frequency from approximately 1.5 to 25 Hz. The configuration we wished to characterize, and the one we modeled on the computer, was with the base fixed to a very large reaction mass. When the stack's base table is placed on springs, as was done for the high-frequency measurements, these low-frequency modes change frequency and shape because the table is a very different reaction mass than the floor-mounted posts. This doesn't greatly affect the high frequency measurements, but would distort any low frequency data taken with the base ungrounded. At frequencies below about 20 Hz, there is sufficient ground noise to drive the stack when rigidly attached to our vacuum tank mounting posts. Only two transfer functions were taken in this frequency range, the ratio of vertical motion on top to vertical motion at the base, and the same for horizontal motion. These two sets of data approximate T_{zz} and T_{xx}, but do not take into account the contribution of the cross coupling terms on the signal on top. Since we have no easy way of making the measurement with two different drive vectors of ground noise, which is what would be necessary to discriminate the four components, only two traces appear below 20 Hz in the transfer function plot of the all-Fluorel stack, Fig. 2(a). The Fluorel-RTV stack has somewhat lower normal mode frequencies, and begins to isolate well at lower frequencies, as can be seen in Fig. 2(b), so the cutoff for these low-frequency measurements was lower.

3. *High-frequency cantilever measurements:*

In the highest frequency range, above 90 Hz for the all-Fluorel, and 60 Hz for the Fluorel-RTV, it becomes difficult to take data using the first method. The accelerometers we use (Endevco model 7707-1000) exhibit a slight response to magnetic fields; this becomes important when we wish to measure transmission of 10^{-5} or lower, due to pickup from the motor coils. In addition, the noise floor of our accelerometer amplifiers becomes significant at about this level. We solve this problem by providing mechanical amplification at the accelerometer mounting on the top table, by mounting the accelerometer on the end of an aluminum cantilever. The length (and thus the resonant frequency) is adjusted while under vacuum via remote-control motors. This assembly was mounted on the top table, in place of the simple accelerometer. For each frequency point, the cantilever length was adjusted to the correct length, and clamped. The appropriate drive table shaker was swept in frequency over an interval of approximately 3 Hz around the cantilever resonance, and a transfer function was recorded, with reference to the drive table motion. One such response function ap-

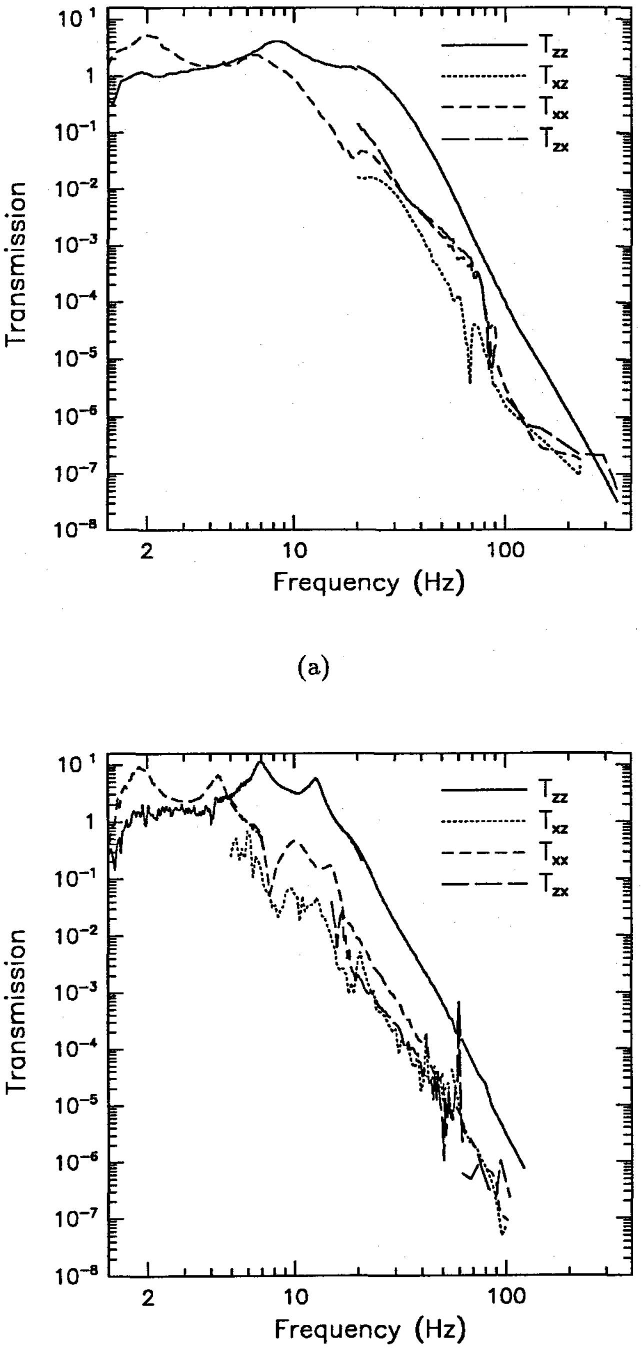

(a)

(b)

FIG. 2. Measured transmission matrix elements for (a) the stack built with all Fluorel springs, and (b), built with two lower layers of Fluorel springs and two upper layers of RTV springs.

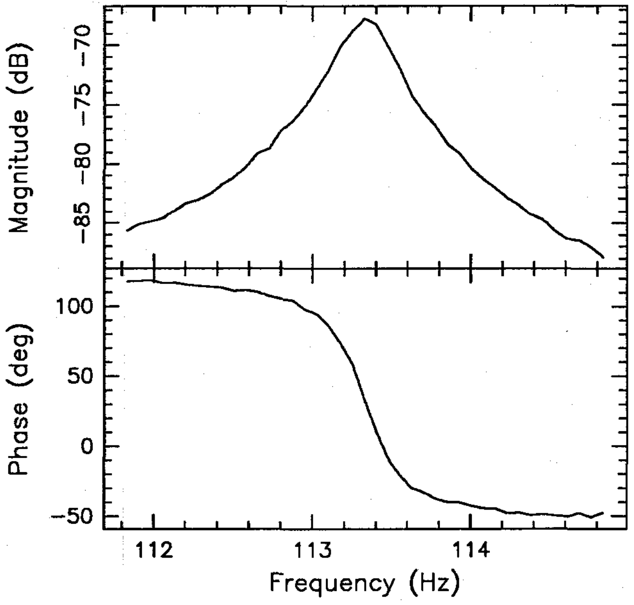

FIG. 3. Transfer function of the signal from the cantilever-mounted accelerometer versus that from the drive table accelerometer. The response closely follows the form of a simple harmonic oscillator at the cantilever oscillator frequency despite the four intervening mass-spring layers.

pears in Fig. 3. The Q of the cantilever, and therefore its mechanical amplification factor on the resonance peak, could not be reliably measured at atmospheric pressure (due to sonic coupling and atmospheric drag on the cantilever), so the response as driven through the stack was used to calculate the Q. This Q was taken to be the mechanical amplification factor. The stack isolation at that frequency was calculated as the measured transfer function of the top accelerometer signal divided by the bottom accelerometer signal, and then divided by the cantilever Q. The accuracy of this procedure was verified by comparison with direct measurements at the lower frequencies. Data were taken at enough points to deduce the stack's response shape, typically 8 for each of the T_{ij}.

C. Summary of measured transfer functions.

The largest transmission component, in each spring configuration, is T_{zz}. After two visible resonance peaks, T_{zz} falls slightly less steeply with frequency than $1/f^{-8}$. T_{xx} also appears to have at least two low frequency resonances before dropping at higher frequencies with about the same rate as T_{zz}, displaced downward in magnitude by a factor of about 20. The cross-terms, T_{xz} and T_{zx}, are somewhat more complicated. In the Fluorel stack, T_{zx} levels off and then drops suddenly just below 100 Hz, while in the mixed (Fuorel and RTV) rubber stack it has two low peaks between 90 and 150 Hz. T_{xz} lurks just below the other components in each case. The rolloff frequencies for the mixed rubber stack are typically about 2/3 of those for the all Fluorel case.

The peak T_{xx} transmission due to a resonance is 5.3, at 2 Hz for the all Fluorel stack, and 9.4 at 1.8 Hz for the mixed stack. T_{zz} peaks at 4.2 at 8.5 Hz in the Fluorel, and 11.3 at 6.9 Hz for the mixed. It can be seen that substituting RTV for the Fluorel in the top layers significantly enhances the isolation, while only increasing the resonance amplification by a factor of order 2. Most of the improvement in isolation is a result of the RTV springs lower modulus magnitude, rather than their lower loss. The initial deformation under load of the Fluorel, which was mentioned above, limited the weight capacity per spring to be about that of the RTV springs despite their higher stiffness.

D. Drift Measurements.

The stack exhibits creep due to the loading of the Fluorel elastomers. To characterize this creep and its temperature dependence, the stack was instrumented with position sensors to measure the distance between the top and bottom plate at three points around the circumference of the stack. Data were taken for an approximately 10 day period, about 90 days after the initial construction of the stack. The natural ambient temperature changes (which were recorded as well) were sufficient to allow a robust fit of the data to a sum of a linear drift with time of 1.3×10^{-10} m/sec plus a linear response to temperature of 3.2×10^{-5}m/°C (the stack becomes shorter with increasing temperature) See Fig. 4.

Previous research [cite Rai references] indicates that a logarithmic drift (i.e., a change in height δh of the stack which evolves with time t as $\delta h = C \log(t)$ with C a constant related to the initial deflection and material properties), is a good model for many elastomers that are not strained beyond their elastic limit. In this case, we calculate that the drift after an additional year would be < 2 mm; a linear drift (the likely worst case) would lead to a drift of $\approx$4.1 mm/year.

V. ABAQUS MODELING AND COMPARISON WITH DATA:

A. Pre-experiment model

Our stack design was modeled using a finite element analysis software package. We chose ABAQUS [14], running on MIT's Cray X-MP EA/464. We needed a package which allowed slightly modified versions of a single geometric model to be used to test static stability against buckling and to determine the system's response to dynamic excitation. In addition, we wished to model the

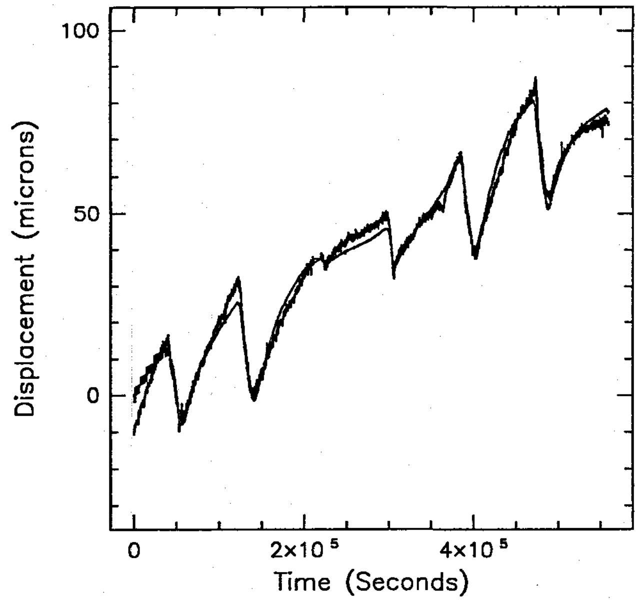

FIG. 4. Drift in the overall height of the stack, data (jagged line) and fit. Daily variations in temperature ($\approx 1^\circ$C peak-to-peak) lead to $\approx$ 25 micron height changes. In addition, over the roughly 7-day period shown, a monotonic shortening of the stack is evident. The fit is described in the text.

rubber with its actual frequency-dependent complex elastic modulus taken from a lookup table assembled from the material test data.

A preliminary model was constructed using a geometry different from the stack which we eventually built. The solid blocks in the legs, as well as the top table, were composed in this model of arrays of quadratically interpolated solid isoparametric elements taken from the ABAQUS element library. A sufficient number of elements were used, 9 each for the blocks, and 81 for the top table, to allow the block and table resonances to influence the stack's dynamic response. Because of this, calculations using this model were quite time consuming.

The results of this preliminary model were the following: The visco-elastic rubber springs damped the rigid-body modes of the stack well; most had Qs of less than three. The transfer function component T_{zz} dominated the others for most frequencies above a few hertz. The overall transfer function could be made to meet the isolation specification, with reasonable choices of spring distributions among the layers. The internal resonances of the leg blocks were above the frequencies of interest, so were not studied in detail, but were seen to produce a leveling of the frequency response as they became important. The top table's resonances, which in this model began at a few hundred hertz, resulted in high-Q spikes in the transfer function, only slightly damped by the table's contact with the rubber. With the geometry used, the isolation criteria were not compromised, but it was clear that we must be careful to make a final stack design with a small and stiff table, so that any resonances occur where there is significant isolation, and with leg elements with resonances well away from the interesting frequencies.

This pre-construction model was also tested for the effects of non-vertical gravity loading, in order to see if the design could be toppled over easily. No such instability was found. The gravity loading simulation was also useful, but not necessary, in predicting the percentage compression of the various springs.

B. Post-experiment model

After the data were taken, we rewrote the ABAQUS code to reflect the geometry and spring placement and properties of the stacks as built. Also, since we had constructed the stacks with structures whose internal resonance frequencies were well above the measured frequencies, this model was written to treat them as nearly rigid bodies. Because of this, the second model required a small fraction of the execution time of the pre-construction model. These after-the-fact predictions are plotted in Fig. 5, and reflect an idealized model in which identical spring elements and identical intermediate mass elements are placed symmetrically below the top table. Also, the bottoms of the bottom springs were mathematically contrained to move together with driven base mass, which eliminates the possible effects of a rocking drive table.

We have attempted to relax these symmetries in additional simulations. These models of imperfections in the system, rather than being useful in exactly duplicating our specific experimental circumstances, which would be nearly impossible, may be viewed as a measure of the robustness of such a system to the various defects mentioned. For brevity, we only present these perturbation model results for the Fluorel/RTV stack.

1. Stiffness variations:

In the naive model (Fig. 5) T_{xz}, the modeled coupling of vertical drive to horizontal motion on top, is nearly zero. In the real stacks, slight variations among the springs' stiffnesses break this symmetry. We expect this additional coupling to be larger in the Fluorel springs because some machining had to be done on each spring, and their final sizes varied slightly. The possible effect of this first type of imperfection is modeled by introducing normally distributed Fluorel elastic modulus magnitudes. The predictions of a model with a stiffness standard deviation of 5% are shown in Fig. 6. We also tried 2%, and note that the contribution to T_{xz} is linearly proportional to the standard deviation. T_{xz} here is not negligible, as it is in the 'perfect' model.

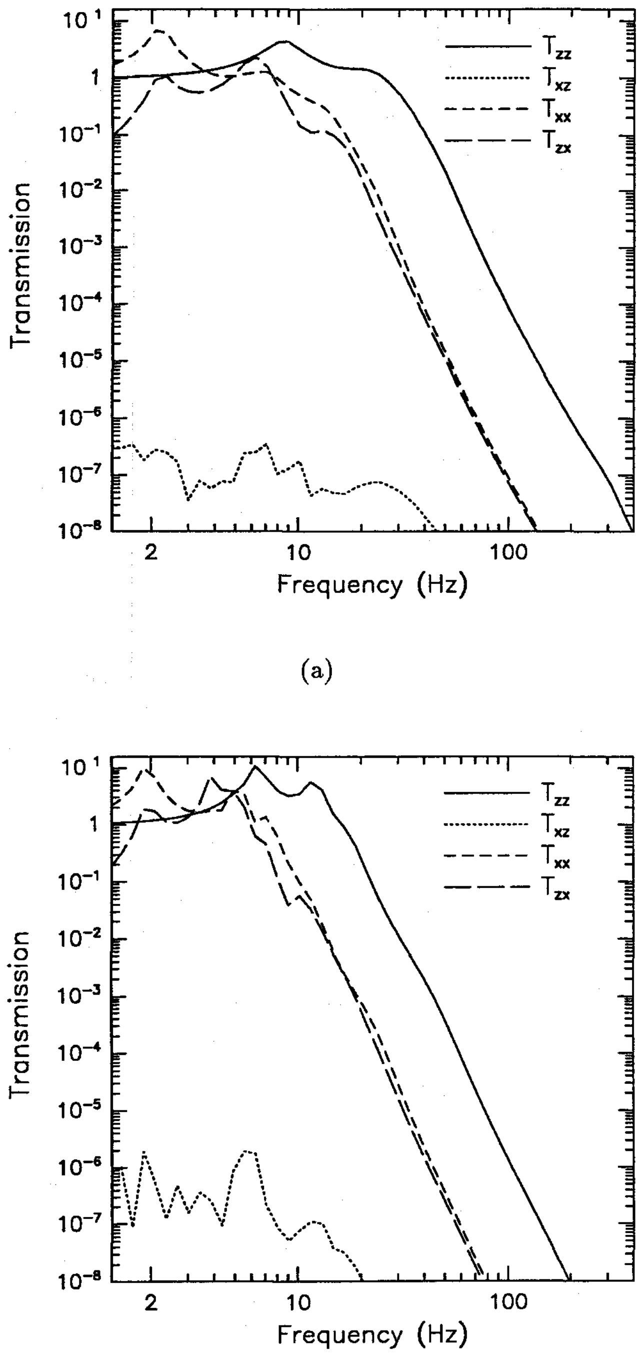

(a)

(b)

FIG. 5. Naive ABAQUS model of (a) the all Fluorel, and (b) the Fluorel/RTV spring stack. This model neglects various imperfections that may exist in the real stack.

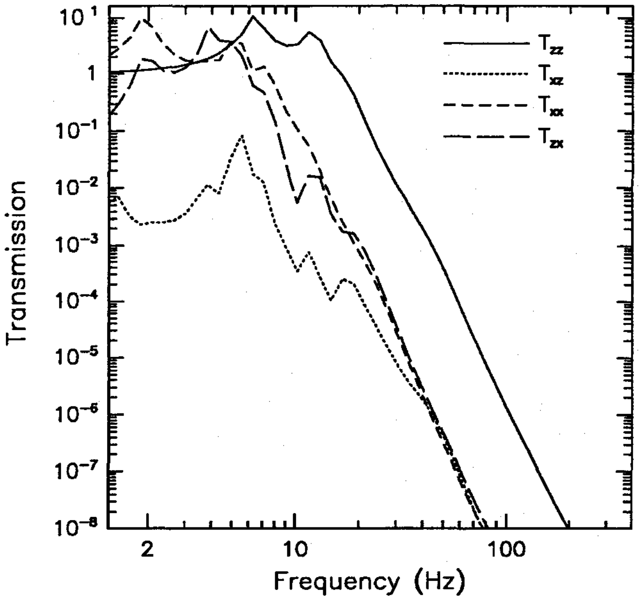

FIG. 6. ABAQUS model of the Fluorel/RTV spring stack with normally distributed spring stiffnesses introduced in the Fluorel stages. The standard deviation is .05 the average stiffness.

2. Response to tilting

Another naive-model simplification is the drive method. The lower table is mathematically constrained not to rock or twist; in other words, the nodes at the base of each of the lowest springs move together with a 100 Ton reaction mass. A force applied to the reaction mass results in an acceleration of the base nearly perfectly aligned with the force vector. In our lab tests, we measured the response of the base table to the drive motors, and found that a nominally horizontal excitation gave rise to a slight tilting motion (rotation about the x or y axis) of the base table, causing vertical motion at the table edge approximately 10^{-1} of the intended horizontal motion. This would mean that the measured T_{zx} and T_{xx} may be at most a factor of ten or so below T_{zz} and T_{xz}, respectively.

We performed a simulation of the effects of pure tilting of the lower stage on the motion above. For this model, the lower faces of the base springs are constrained to lie on a flat, rigid surface which tilts about the an axis in the y direction that lies on the surface with the spring bottoms. We plot two types of response to these conditions in Fig. 7: the coupling of rocking angle, θ, to rocking on the top table, $T_{\theta\theta}$, and the coupling of rocking below to x displacement above, $T_{x\theta}$. $T_{\theta\theta}$ is dimensionless, but $T_{x\theta}$ converts θ through a 34 cm lever arm to the x motion in cm. This apparently odd convention is helpful because 34 cm is the half width of the model's drive table, so $T_{x\theta}$ multiplied by the z motion resulting from the

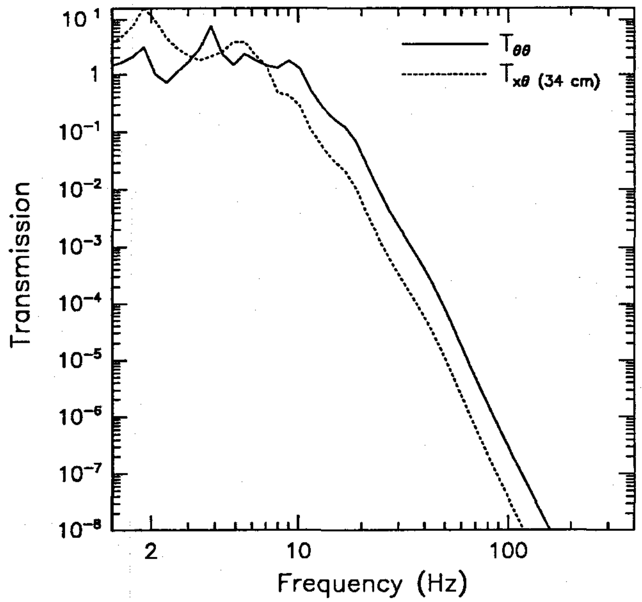

FIG. 7. Fluorel/RTV stack ABAQUS model response to pure tilt of the drive table. The two curves represent the coupling to tilt and horizontal displacement, as is explained in the text.

x shaker drive should give the x motion coupled through this mechanism to the top table.

3. *Spring alignment precision:*

Finally, the naive model's fidelity to the stack might be compromised because the individual springs are all mounted in the exact design alignment. In the real stacks, there were variations among the face angles of the springs, since one side had to be machined to remove traces of the mounting lug. Also, springs may be horizontally stressed during assembly. These things can result in individual springs cross-coupling x strain to z force and vice-versa.

The simulation of the possible influence of crooked springs was carried out quite differently than the random modulus simulation. Rather than attempt to somehow randomly orient springs, we added one specific cross-coupling spring to each of three of the layers (thus modifying 3 out of 42 springs). These springs had non-zero off-diagonal terms, but zero diagonal ones. That is, these perturbation springs caused a force in the z direction for x or y displacement, and vise-versa, but didn't apply additional forces in the direction of displacement. To see a clear effect, the magnitude of these three perturbation springs was chosen to be about the same size as the z component of the regular spring's force constant, and all were oriented so that T_{xz} would be enhanced. Fig. 8 shows the stack model's results with these springs added. Two values for the strength of cross coupling are used:

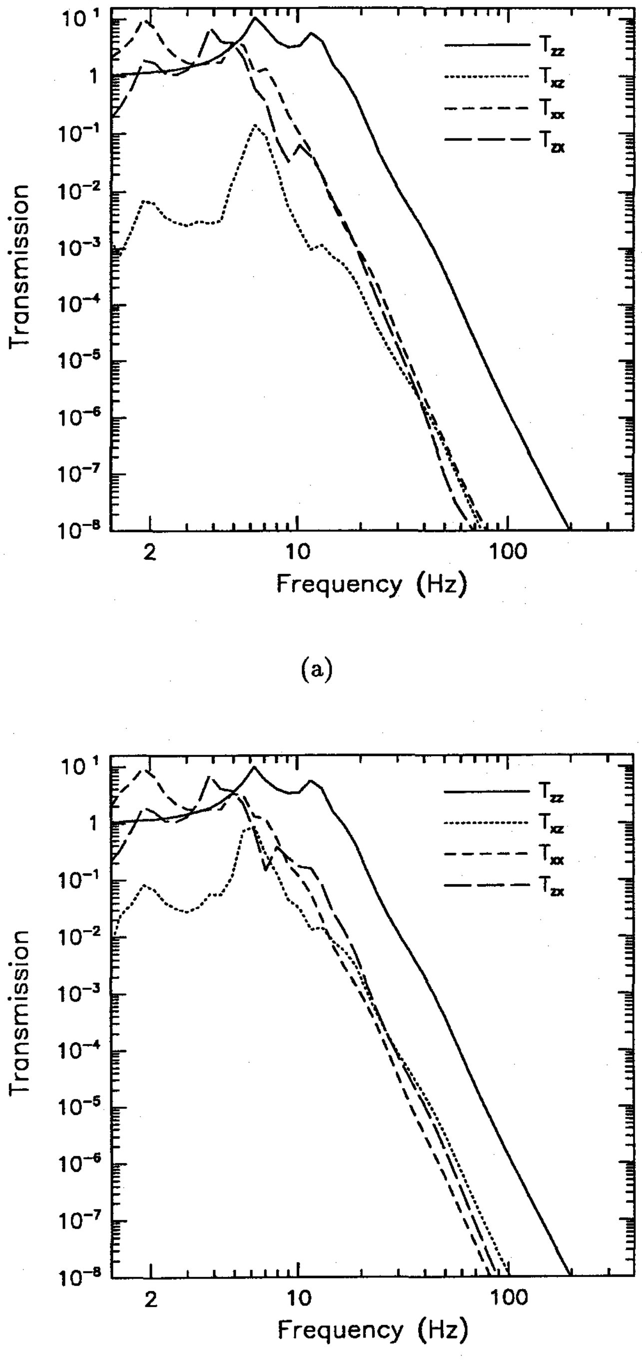

(a)

(b)

FIG. 8. Fluorel/RTV stack ABAQUS model with extra springs that couple vertical force to horizontal strain and vise-versa. (a) shows results with three cross-coupling springs of strength .05 of the vertical stiffness, and (b) shows the results for .5.

.5 and .05 of the regular vertical stiffness.

C. Model agreement with data:

In writing these finite element models of the LIGO stack prototype, we have the opportunity to evaluate the usefulness of such models in designing seismic isolation stacks. There are four aspects of these models that may offer advantages over analytic modeling. One is the use of a frequency-dependent complex elastic modulus for the spring materials. In the Fluorel, for example, the modulus's imaginary part is of the same order as the real part, so is would be tricky to simulate its properties with some series-parallel combination of springs and dashpots. Another case for which finite element modeling is valuable is the analysis of mechanical systems containing parts with internal normal modes that might affect the overall system response. Third, these models can be very helpful when there are important aspects of the modeled system that are affected by 3D motion. And, finally, we relied on the FE model in testing our design for stability against buckling before actually building it.

The success of the visco-elastic modeling can be judged by how well the vertical-vertical transfer function prediction, T_{zz}, which is less complicated by other effects, matches the data. We need to compare both the Qs of the low-frequency stack modes, which reflect how loss and restoring force compare at the resonance frequencies, and the high-frequency transfer function slope, which reflects the same far above the resonances. The data and models, we believe, agree well over the entire T_{zz} curve.

The second result sought from the FE modeling is a prediction of how the stack transmission is influenced by internal modes in the leg and table elements. The qualitative predictions of the pre-construction models, described above, indicate that the internal modes should not appear in the frequency band of interest; to the extent that no unexplained features were seen, this was verified experimentally. The post-data-taking models, whose results are presented here, were specifically constructed to save computation time by ignoring these internal effects.

The fidelity in three dimensions of the numerical modeling is somewhat more difficult to judge. In the naive perfect stack, which consisted of identical springs perfectly aligned, the purely vertical normal modes, which number only 8, are the sole contributors to T_{zz}. An analytic model might be sufficient to understand these. The other transfer functions involve the other 52 modes. In a stack with the symmetry broken with random spring strengths or crooked springs, in general all 60 contribute to each the transfer function components, but to lowest order, the non-T_{zz} components will be most sensitive to the modeling of motions involving all three dimensions.

The transfer function predicted by the naive identical-spring model of the mixed-rubber stack differs from the measured data in several ways: T_{xz} is predicted to be zero, as is discussed above. Two of the modeled perturbations, the random moduli, and the off-axis springs, were shown to predict non-zero T_{xz}, although we have not attempted to duplicate the data with some ad hoc combination of these effects. While T_{xx} falls at approximately the same rate at high frequencies as the prediction, it occurs at an overall larger transmission. The crooked spring perturbation can add to T_{xx} but again it is not possible to reconstruct the exact vector contribution in the measured stack without much more detailed measurements. Finally, T_{zx} is lower in the naive model than the measured data. The tilt model can be employed to make a plausible explanation of this discrepancy: the horizontal drive motor is known to produce rocking, introducing of order 0.1 of the horizontal motion as vertical motion at the lower table edge. If we multiply the $T_{x\theta}$ curve from Fig. 7 by 0.1, the result would add, with a difficult-to-predict phase, to any measurements of T_{xz}.

The stack showed no signs of unstability when the 20% limit on the strain was observed, in agreement with the finite element model. A brief experiment with greater ($\approx$ 30%) loads showed a tendancy for the stack to tilt dangerously to one side, probably due to a particularly 'soft' spring element. We believe that the stack as measured is safe and stable.

We have found finite element analysis to be a reasonably inexpensive and fast way to test ideas for mechanical isolation systems. A system which costs thousands of dollars for the steel and spring molding can be pre-tested using a few hours of supercomputer time.

VI. CLOSING REMARKS

This stack design with minor modifications will likely be used in the first LIGO interferometers, and more immediately in prototype interferometers in the LIGO development effort. This will make advances in prototype interferometer performance possible, and allow additional stack tests, for example sensitive measurements of possible non-linear upconversion of low-frequency large-amplitude motions to GW-band excitation of the stack top plate (e.g., 'creaking'). The measurements presented show this simple passive isolator can meet the diverse requirements for the seismic isolation system for the LIGO interferometer, and the agreement of the model with the measurements gives us confidence that variations on the design can be engineered easily and quickly.

The authors would like to thank Justin Greenhalgh of Rutherford Appleton Laboratory for discussions and exchanges of stack development results which helped lead us to this design. We would also like to thank the rest of the LIGO team, especially Rainer Weiss, for help in carrying out this work. This work was supported in part by NSF grant PHY-8803557.

---

[1] R. Weiss, Quarterly Progress Report of the MIT Research Laboratory of Electronics **105**, 54.

[2] A. Abramovici, W. Althouse, R. Drever, Y. Gürsel, S. Kawamura, F. Raab, D. Shoemaker, L. Sievers, R. Spero, K. Thorne, R. Vogt, R. Weiss, S. Whitcomb and M. Zucker, Science **256**, 325.

[3] A. Oliva, V. Sosa, R. de Coss, R. Sosa, N. López Salazar, and J. Peña, Rev. Sci. Instrum. **63**, 3326.

[4] R. DelFabbro, A. DiVergilio, A. Giazotto, H. Kautzky, V. Montelatici, D. Passuello, Phys. Lett. A **132** (**5**), 237.

[5] M. Stephens, P. Saulson, J. Kovalik, Rev. Sci. Instrum. **62** (**4**), 924.

[6] P. Saulson, Rev. Sci. Instrum. **55**, 1145 (1986)

[7] N. Mavalvala, L. Sievers, D. Shoemaker, internal LIGO report.

[8] D. Shoemaker, R. Schilling, L. Schnupp, W. Winkler, K. Maischberger, and A. Rüdiger, Phys. Rev. D **38**, 423.

[9] J. Greenhalgh, internal report of the Rutherford Appleton Laboratory, Chilton, Didcot, Oxon.

[10] T. Aldcroft, P. Michelson, R. Taber, and R. McLoughlin, Rev. Sci. Instrum. **63** (**8**), 3815.

[11] e.g., E. J. Douze, Bull. Seism. *Soc. Am.* **57** 55-81; CIT, JILA lab measurements (unpublished); German seismic measurements (unpublished).

[12] P. Saulson, Phys. Rev. D **42**, 2437.

[13] These springs were obtained from the Karman Rubber Company, of Akron, Ohio. They used an injection mold from their catalog part number K132, but with 70 durometer Fluorel instead the neoprene usually used.

[14] Finite element analysis program ABAQUS, version 4.9 (Hibbit, Karlsson and Sorenson, Inc., Providence, RI.)

BATCH
START

STACKS BOOK 3

STAPLE
OR
DIVIDER

1/17/93

Rebuilt stacks with 2 Layers of RTV and 2 Layers of Viton

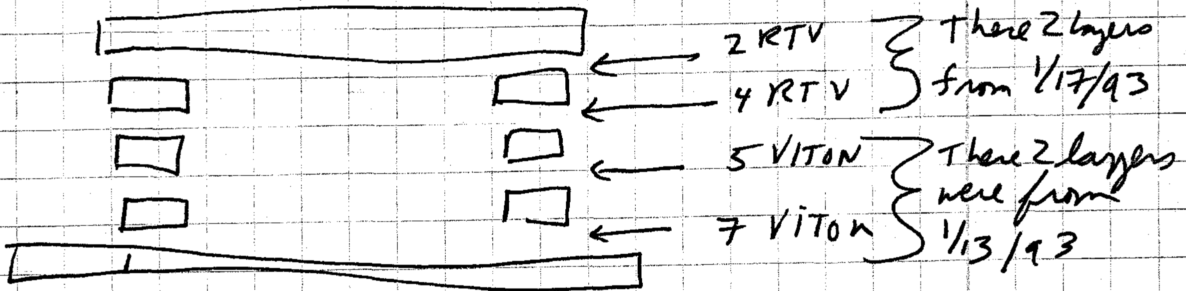

These 2 layers from 1/17/93

These 2 layers were from 1/13/93

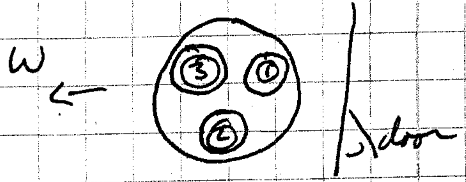

Stack Height (Vs) time

			Leg 1	Leg 2	Leg 3
th guide s in	1/18/93	3:30 PM	20 15/16"	20 15/16"	20 15/16"
h no e pins	1/18/93	4:30 PM	20 15/16"	20 15/16"	20 15/16"
guide pins	1/19/93	12:00 AM	20 15/16"	20 15/16"	20 15/16"

XF OF STACK TOP PLATE
SAME AS 1/15/93 17:28
EXCEPT SILICONE
SPRINGS IN UPPER 2 LAYE

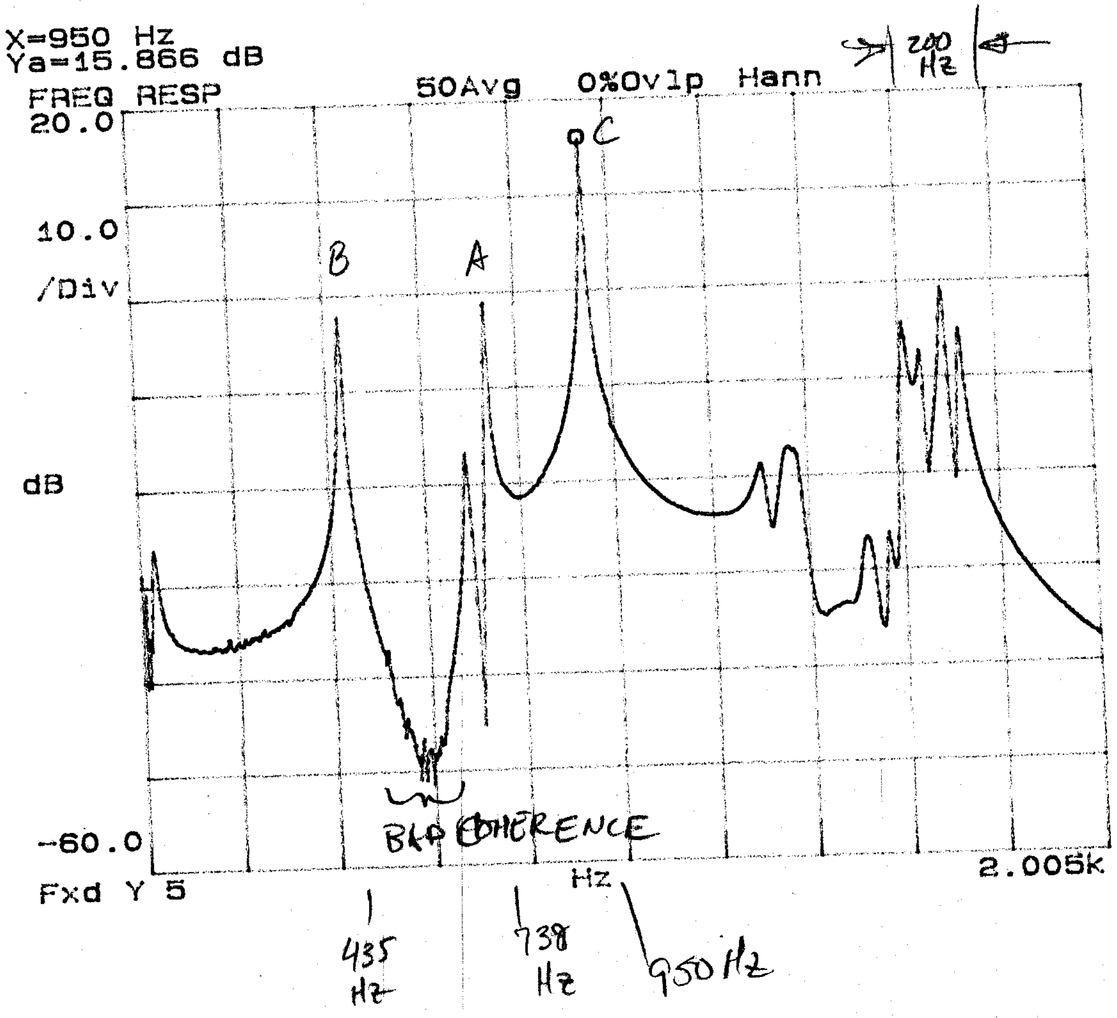

1/18/93 LS/MEZ 17:00

STACK TOP PLATE TRANSFER FUNCTION NEAR RESONANCE "B" TOP TWO LAYERS NOW USING SILICONE SPRINGS

(SAME SETUP AS 1/15/93 17:05)

Q IS MUCH HIGHER WITH SILICONE – SEE ZOOM-IN FOR Q ESTIMATE!

```
X=433 Hz      ΔX=3.75 Hz
Ya=14.8267    ΔYa=8.313 dB
 FREQ RESP             41Avg   0%Ovlp  Hann         Ov1
```

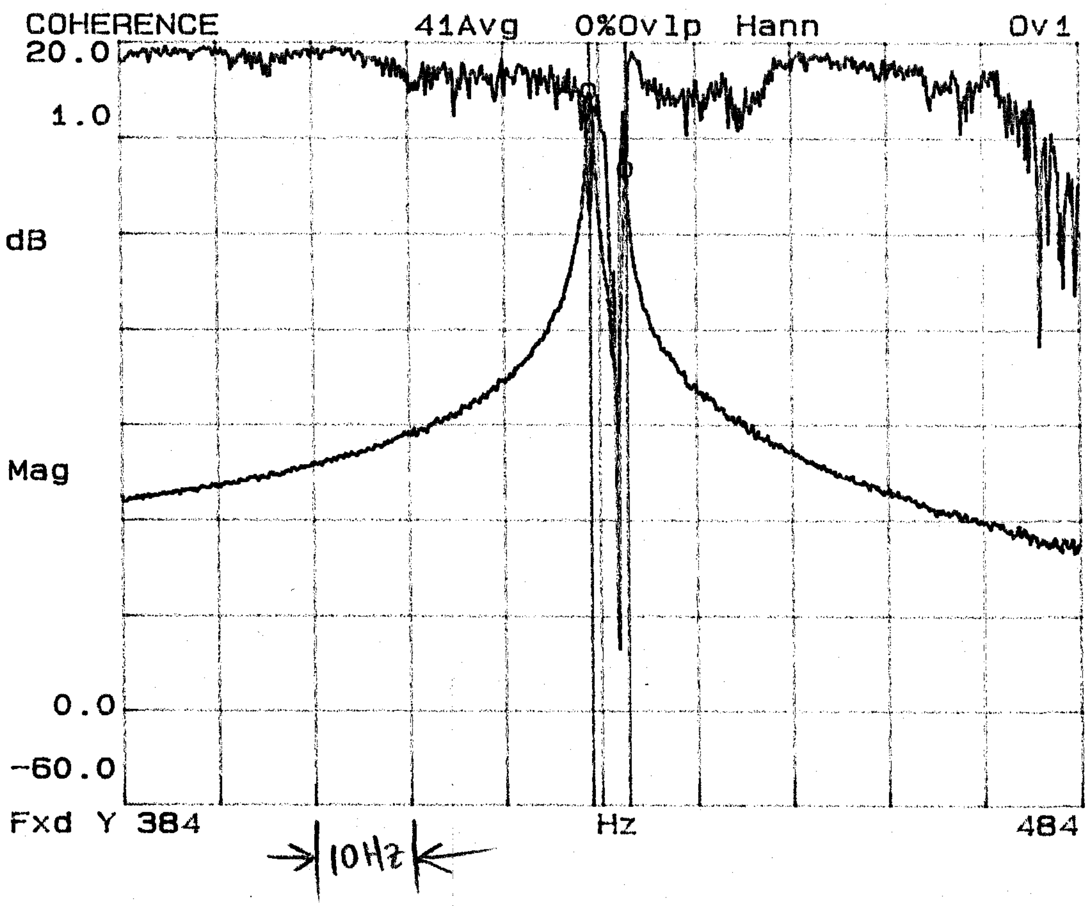

17:09

HIGH-RESOLUTION ZOOM OF 17:00 XF (2 Hz/DIV)

-3 dB WIDTH OF BOTH PKS IS ABOUT EQUAL

"MODE B"

$Q \simeq 10^3$!

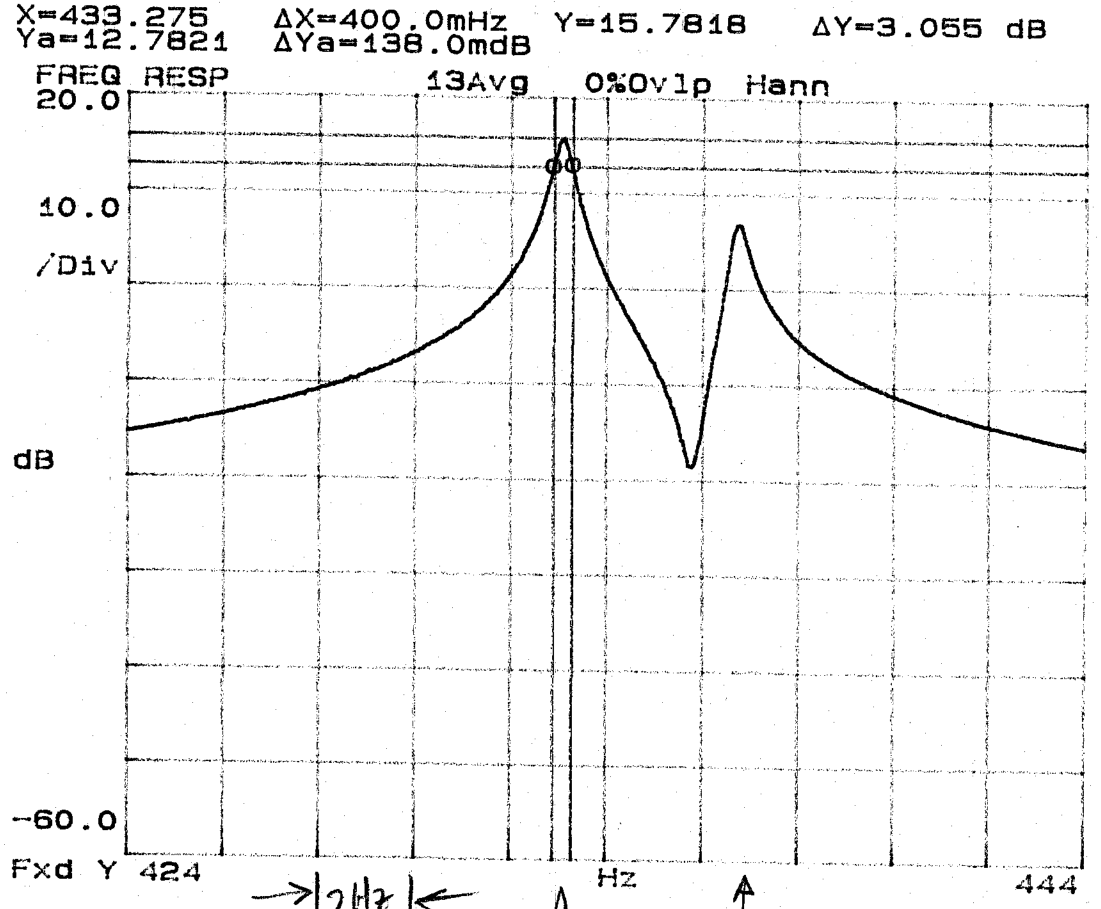

→|2Hz|←

433.10 Hz

436.8 Hz
(Q is about the same as 433.1 Hz)

1/18/93 es/mez 17:24

STACK TOP PLATE XF,
SILICONE SPRINGS,
SETUP AS 17:00
BUT 2 Hz/DIV

⇒ Q = 450

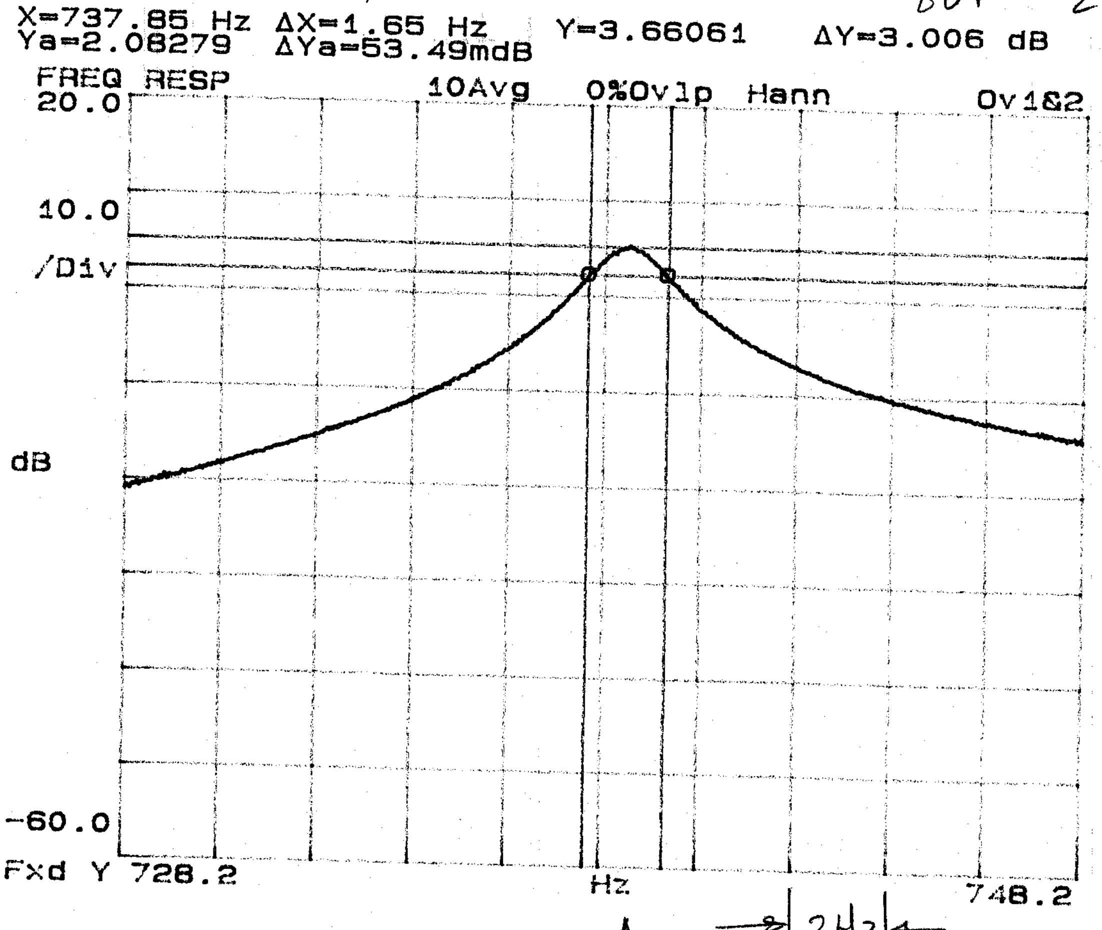

"MODE A"

f_0 = 738.7 Hz

1/18/93 cs/meg 1008

STACK TOP PLATE X-F
SILICONE SPRINGS,   17:30
SETUP AS 17:00

Q≈620

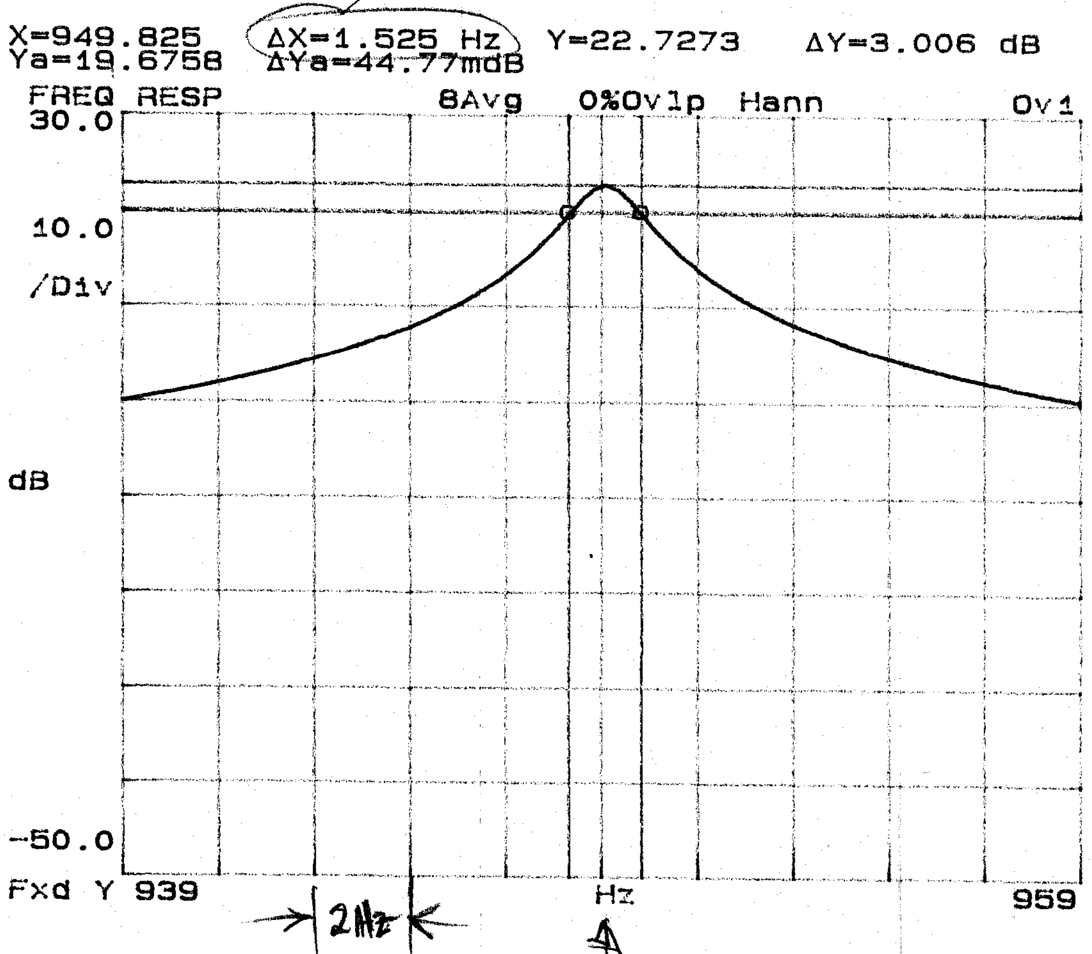

"MODE C"

f_o = 949.1 Hz

1/19/92 1:00 PM

Transfer Fctn from H to V (accel on center of top plate)

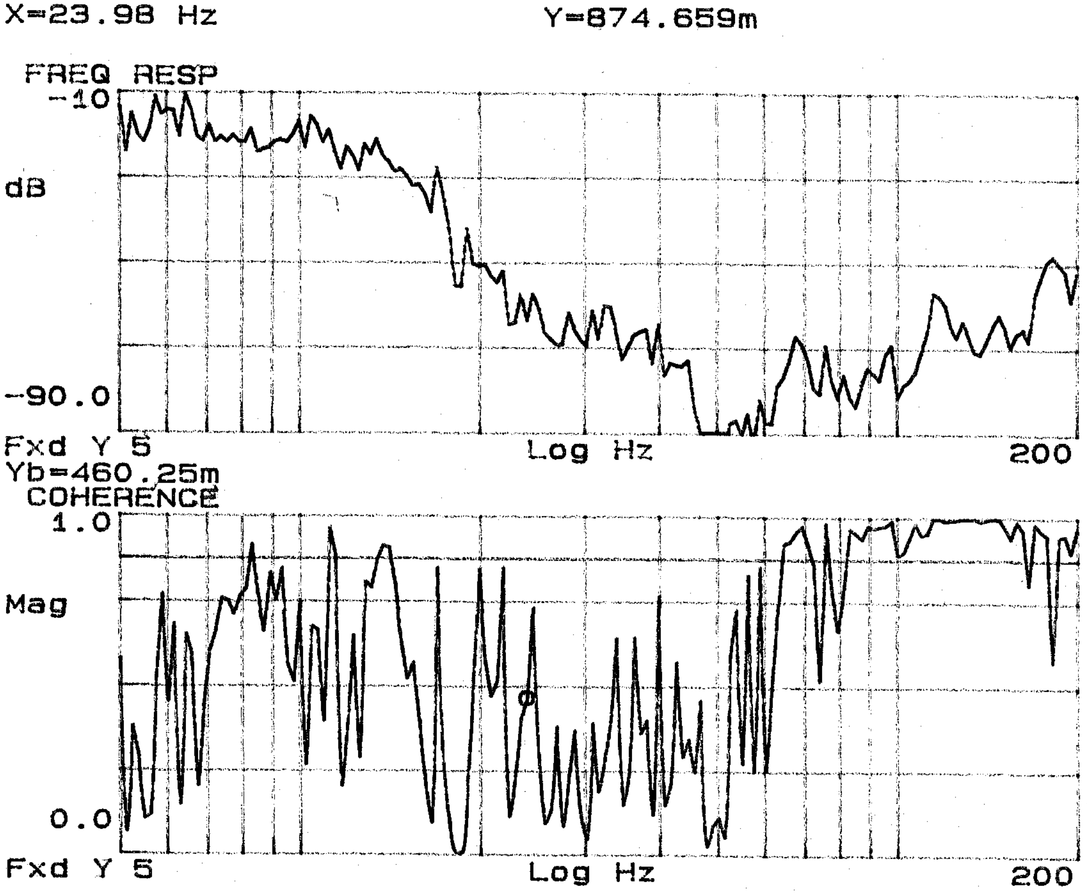

SOR4

SOR5

source level	freq
200mVrms	5-10
300 "	10-18
400 "	>18

AV = 5
Integ time = 1 sec
Resln = 100 pts/dec

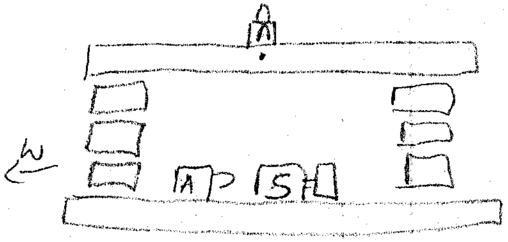

Stack with 2 layers of viton on bottom + 2 Layers of RTV on top

- Top accel on center of plate
- Bottom accel near north drift compensator
- Shaker in H position

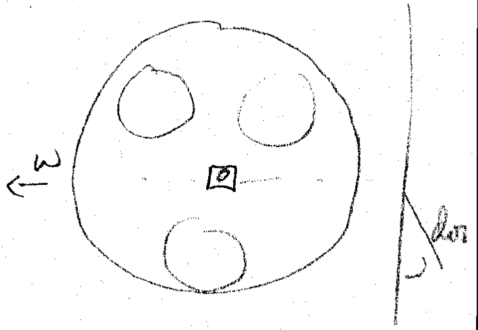

1/19/93 12:30 AM

Transfer Fcn from H to V (accel on edge of [illegible])

Source level	Freq
200 mVrms	5-10 Hz
300 mVrms	11-18 Hz
400 mVrms	>18

AV = 5
Integ time = 300 msec < 18 Hz
= 1 sec > 18 Hz

Res = 100 pt/dec

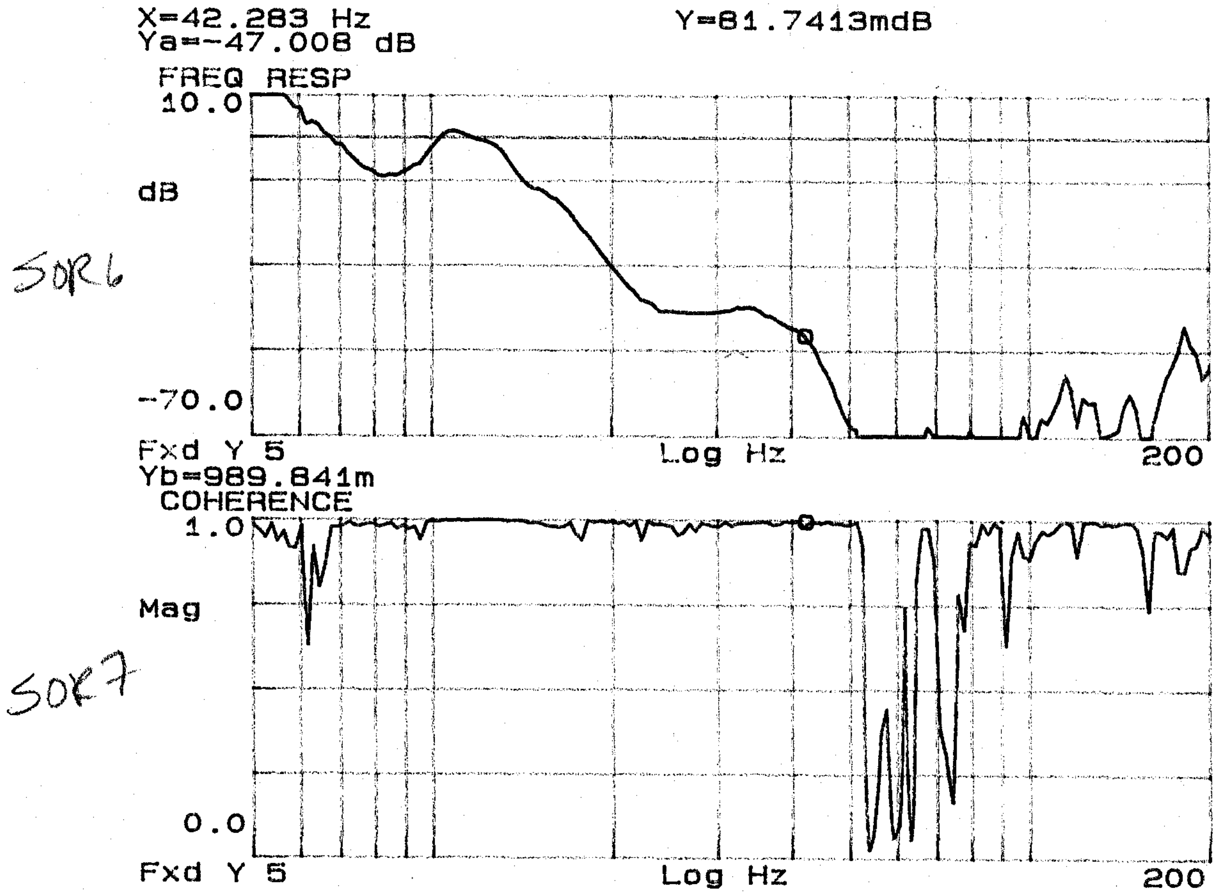

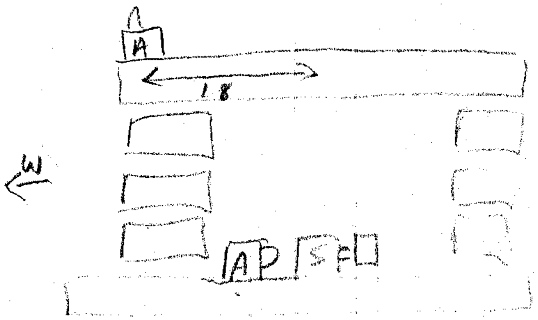

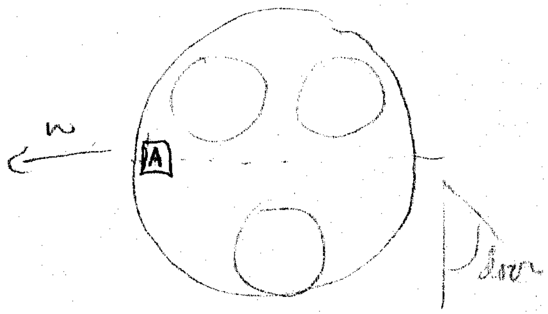

Stack with 2 Layers of RTV on top + 2 Layers of viton on bottom and got identical transfer fctn

SOR14 + SOR15

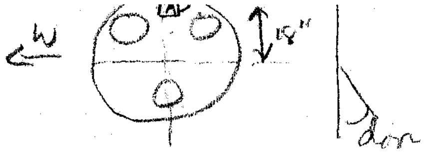

1:30 PM

Transfer Fctn From
H to H

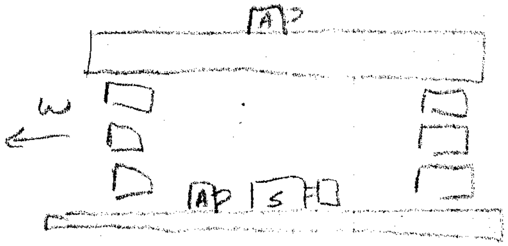

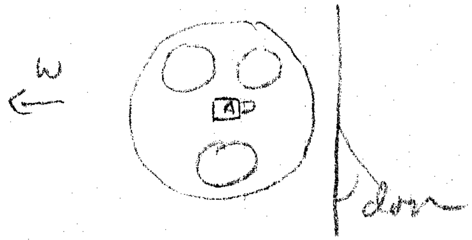

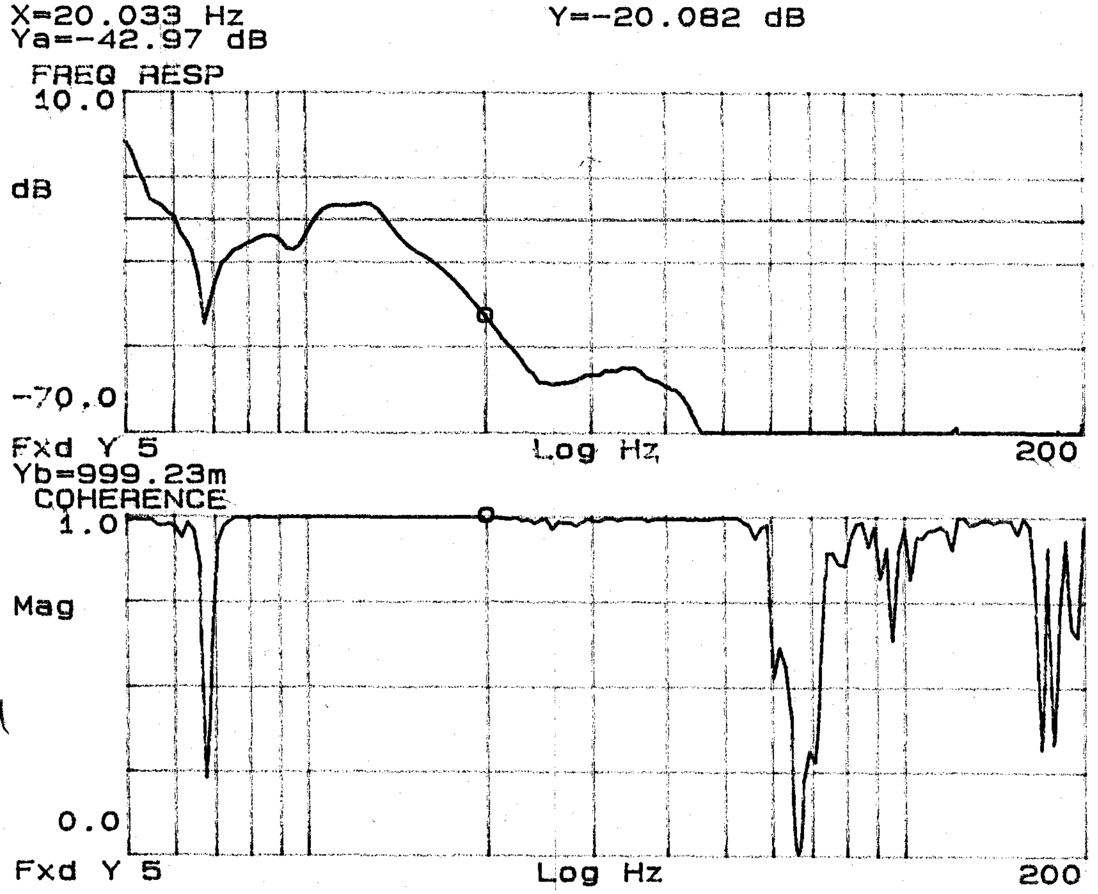

SOR 8

SOR9

integ time = 1sec < 60
300msec > 60

Source level = 200mV rms < 20
= 400mV rms > 70

Ave = 5
Resln = 100 pts/dec

- Top accel in center
- Bottom accel at N
drift compensator
- Shaker in H position

Stacks with 2 layers of viton on
bottom + 2 layers of RTV on top

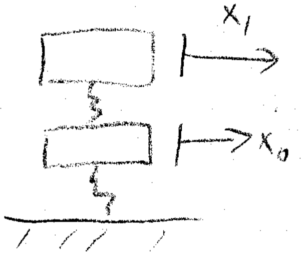

1/19/94 C 2:00 PM

Check to see if features between 20-40 Hz are acoustic pickup or real signal

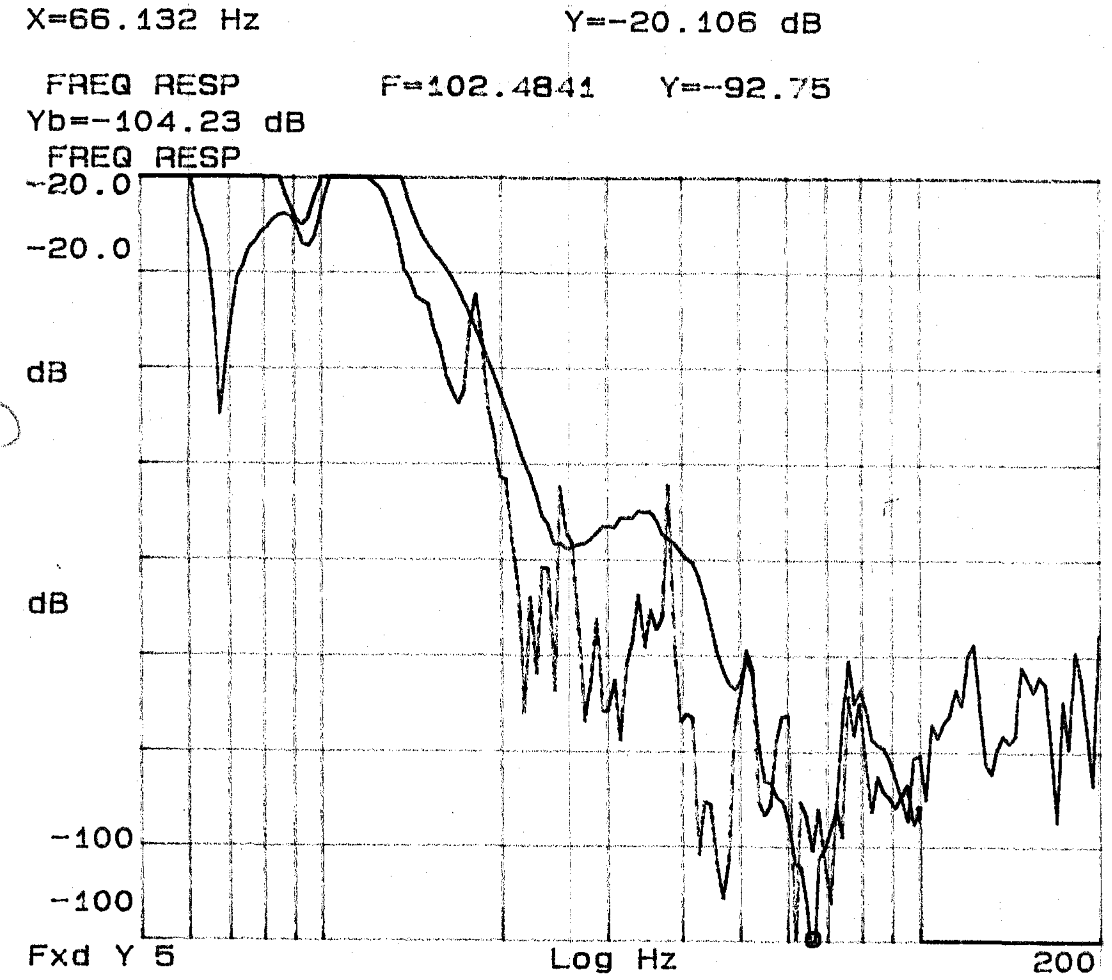

Blade SOR10 (SOR11)

Blue SOR8

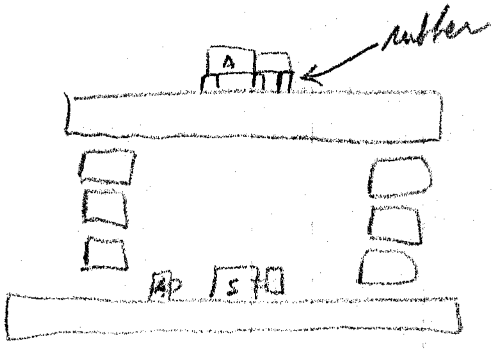

Transfer Fct is SOR10

This shows that it is real signal between 25 + 40 Hz

2:35 PM 1/19/92

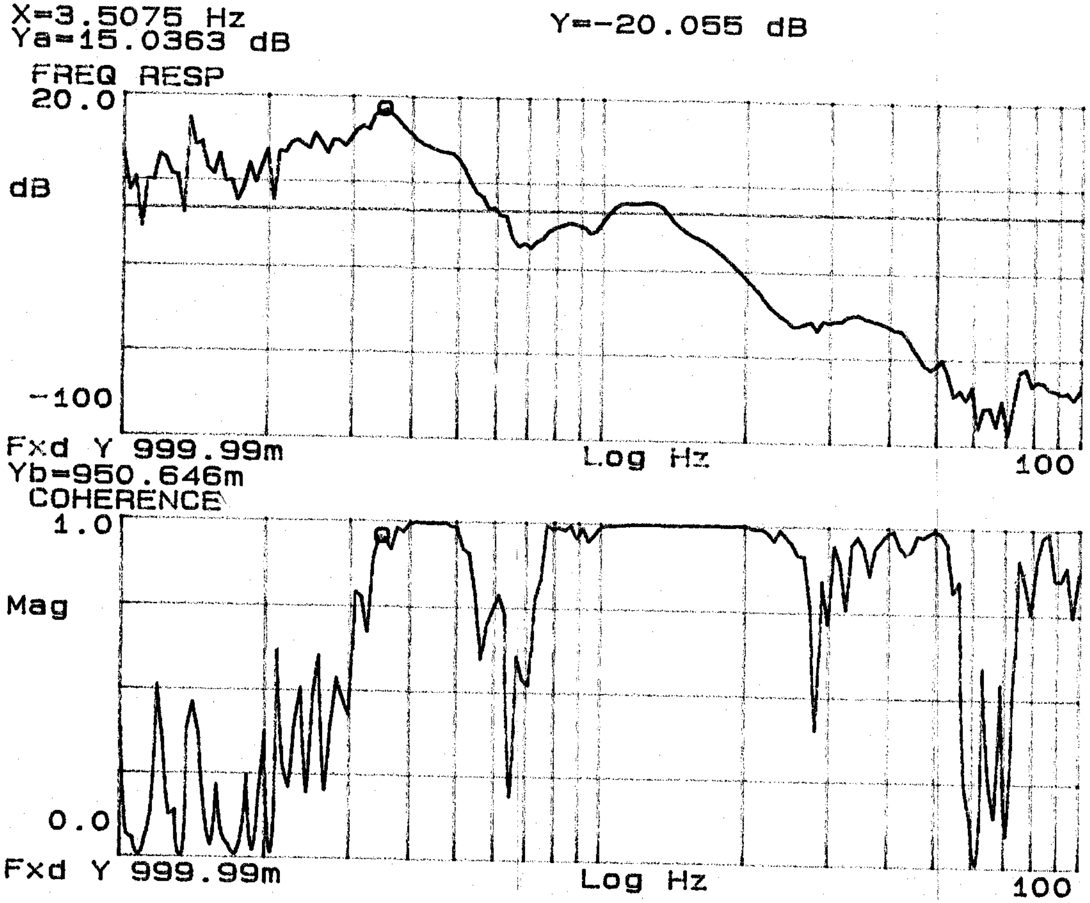

SOR12

SOR13

- Same as SOR8 But with frequency sweep down to 1Hz
- Only got coherence above 3Hz

1/19/92   3:30 PM

Random noise excited transfer fcn of H vs H

- Source = random noise
- 9 avg
- Source level = 100m Vrms

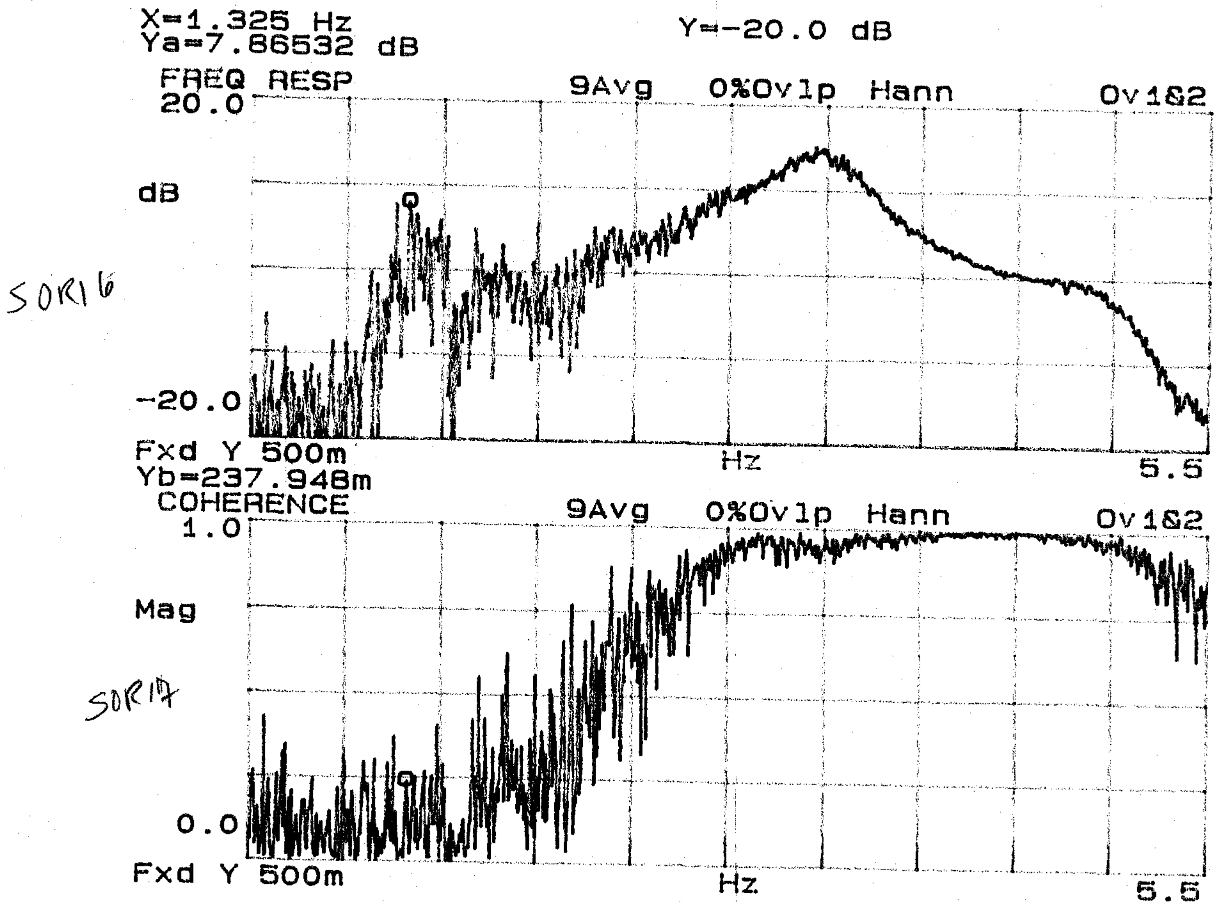

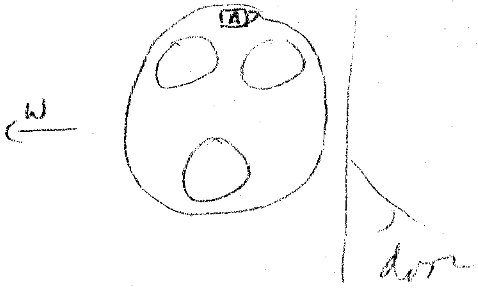

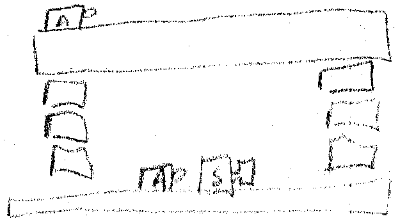

- Shows first 2 resonant frequencies of H(vs) H

$f_0 \cong 1.3 Hz$ $f_1 \sim 3.5 Hz$

4:15 PM 1/19/92

V to H transfer fn

Top accel on edge of plate

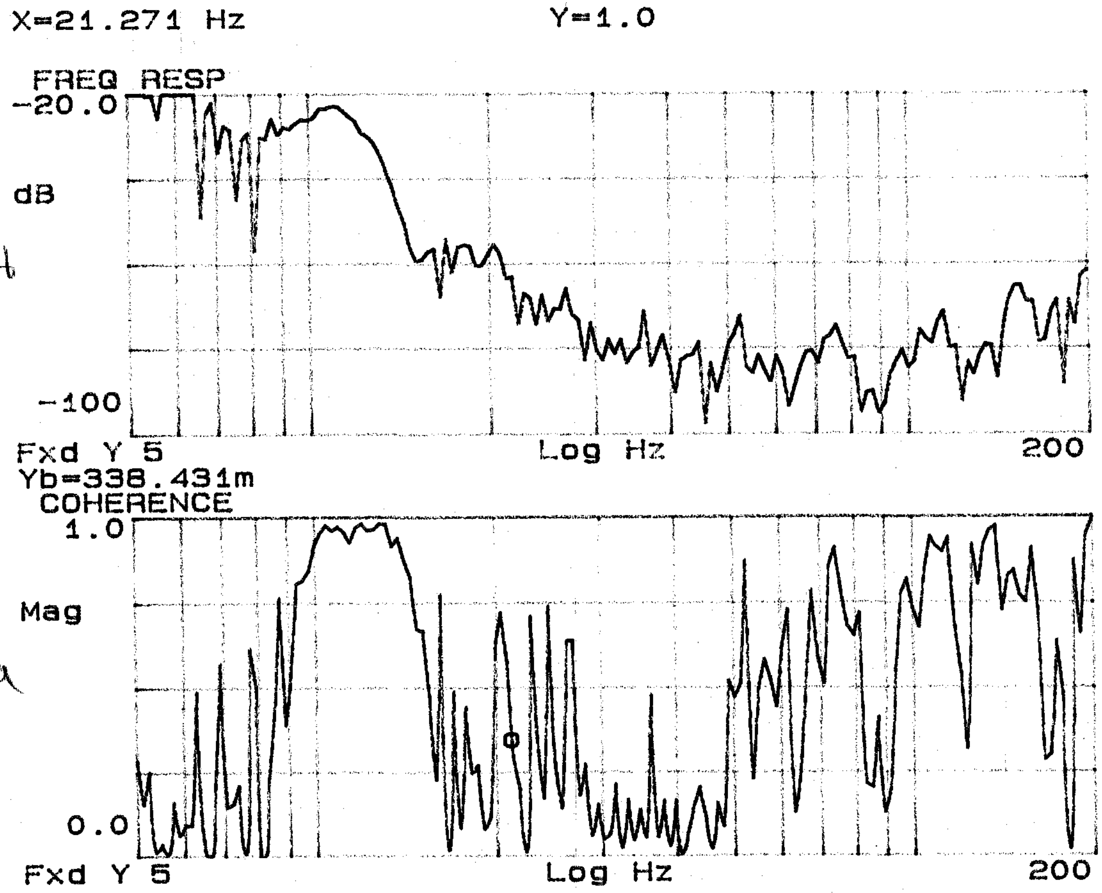

50R14

50R19

< 18 Hz
Ave = 5
Integ = 300msec
Resln = 100 pts/dec
Source = 150 mV$_{RMS}$

> 18 Hz
Source = 300 mV$_{rms}$

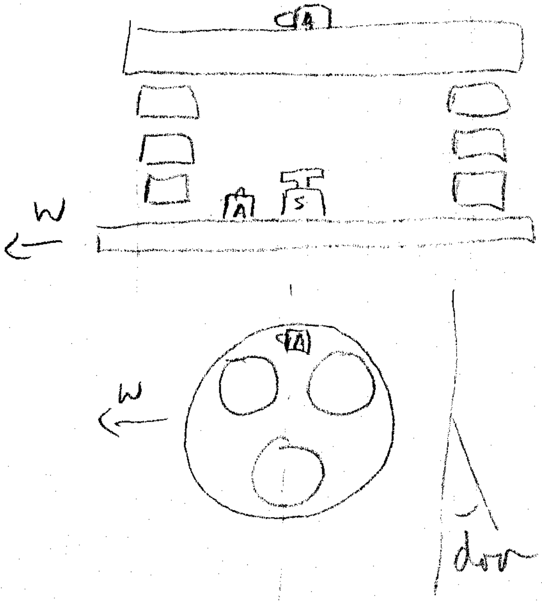

Stack:
- 2 Layers Viton on Bottom
- 2 Layers RTV on Top

- shaker in V position
- bottom accel at N drift compensator in V position
- top accel on center of plate in H position

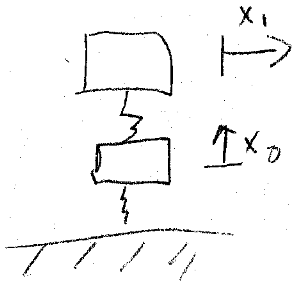

6:30 PM 1/19/02

V to H transfer Fctn
for top accel on center of pl

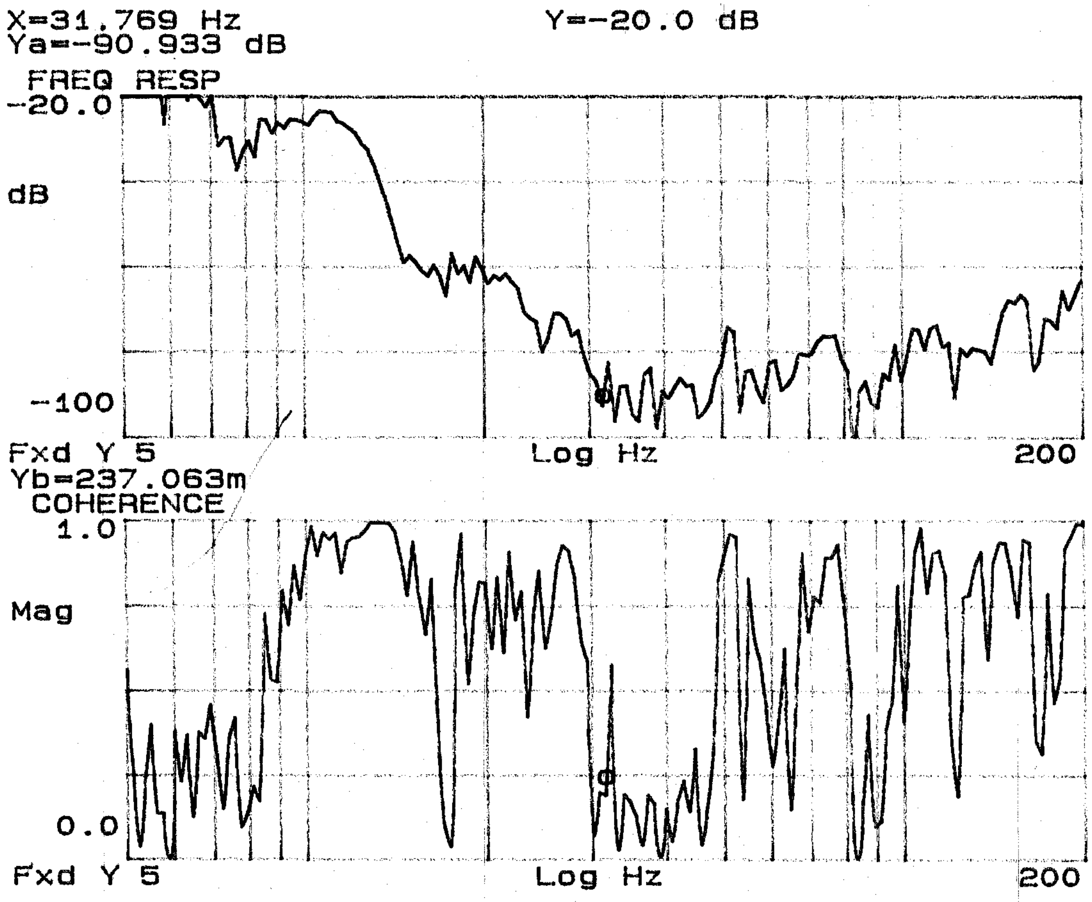

SOR20

SOR21

<18Hz

Ave=5
Integ = 1sec
Resln = 100 pts/dec
Source = 150mVrms

>18Hz

Source = 300 mVrms
Integ = 300 msec

Same config as
SOR18 but with
top accel at center of pl

11/19/92 4:30 PM

V to V transfer fctn
will accel on edge of plate

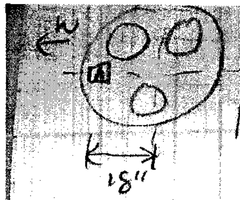

- Transfer function [illegible]
accel on edge is identical to
SOR22 + SOR23:
In files SOR24 + SOR25
Integ = 150 msec

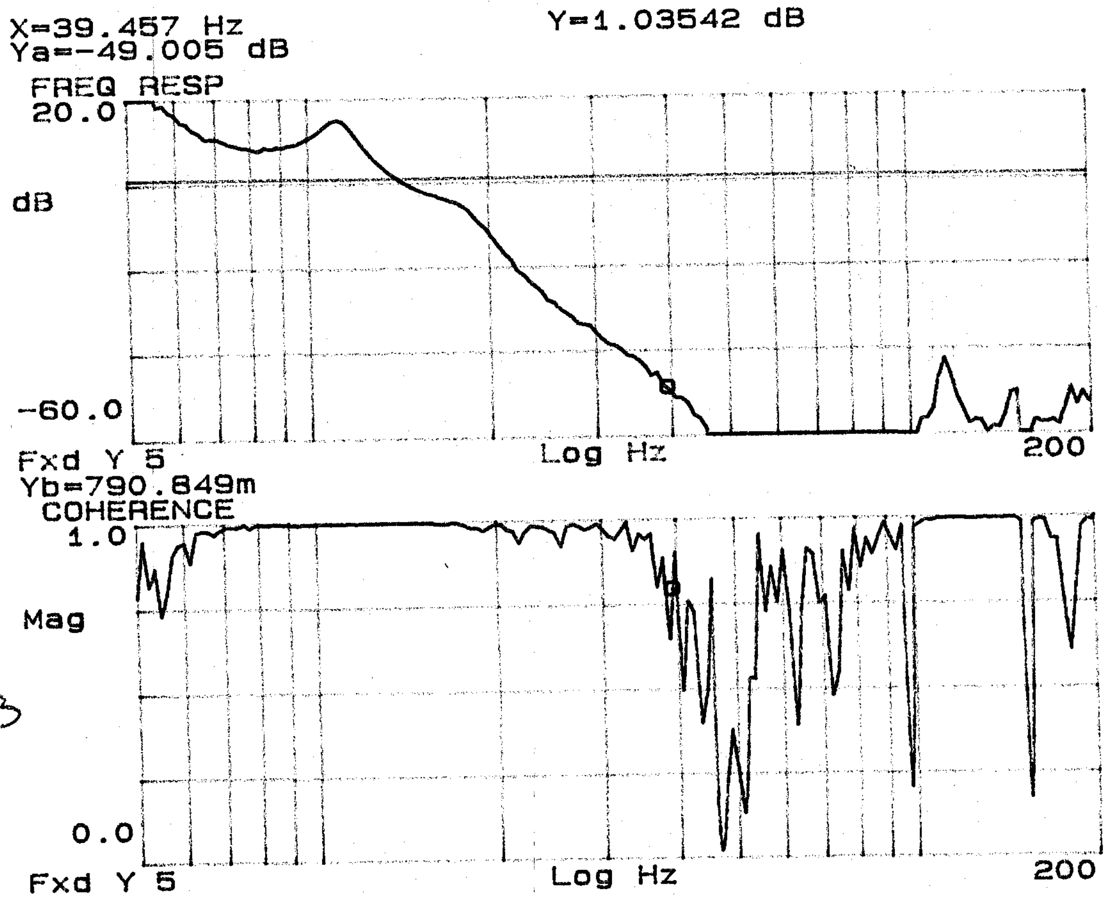

SOR 22

SOR23

integ time = 1 sec

Source voltage: 150mV RMS f<18Hz
=300mV RMS f>18Hz

Resln: 100 pts/dec
Ave = 5

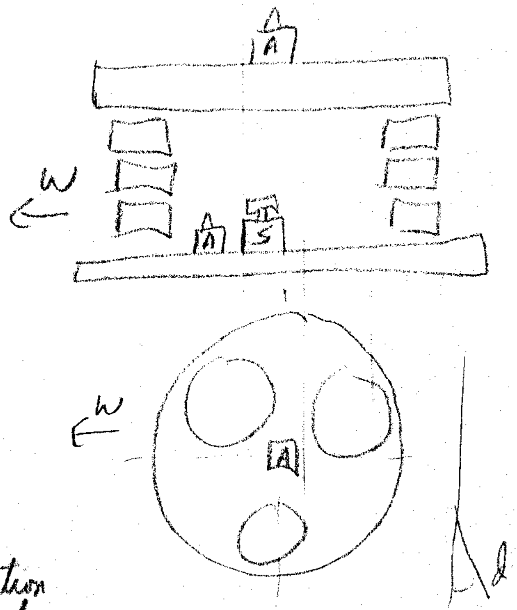

Stack has 2 layers of viton on bottom
+ 2 layers of RTV on top

- shaker in V position
- bottom accel next to
north drift comp. in V position
- Top accel in center of plate

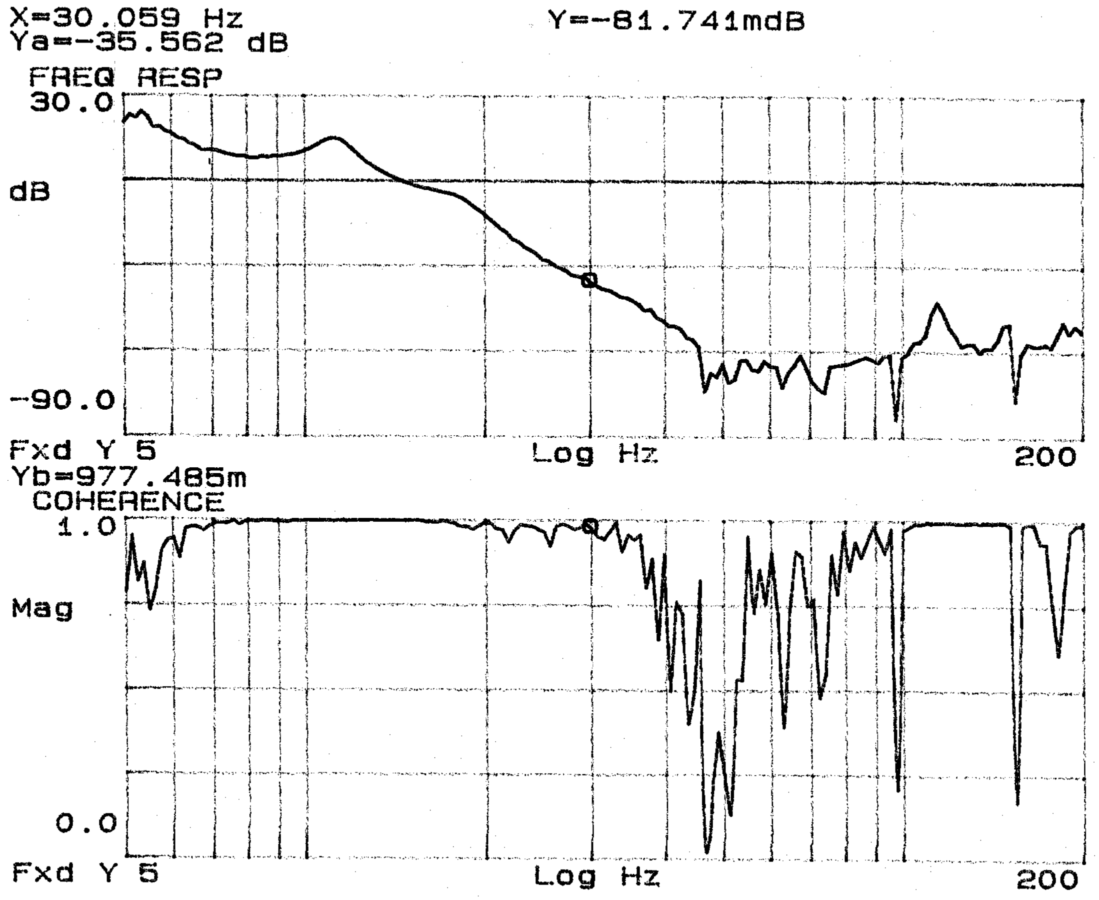

SOR22 (previous page) but on larger scale

1/20/93 4:30 PM

Reconfigured stack with all RTV springs. Springs were soaked in hot methelene chloride for 10 days and baked in air oven at 175°C for 3 days

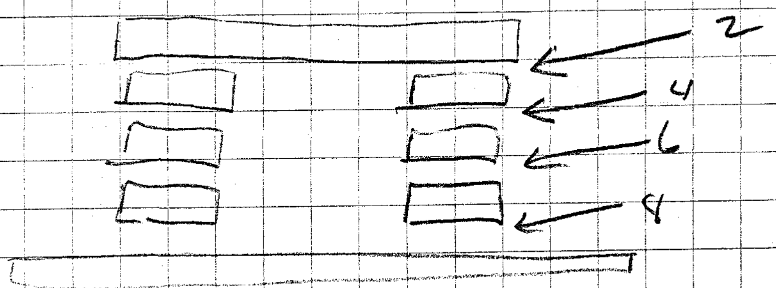

stack height (vs) time

		M1	M2	M3
1/21/93	10:30 AM	21"	21"	21 1/32"
1/23/93	3:35 PM	20 15/16"	21"	21"
1/25/93	9:30 AM	21"	21"	21"

Comparison of V to V transfer fctn of an all viton stack and a stack with 2 layers of RTV & 2 Layers of viton

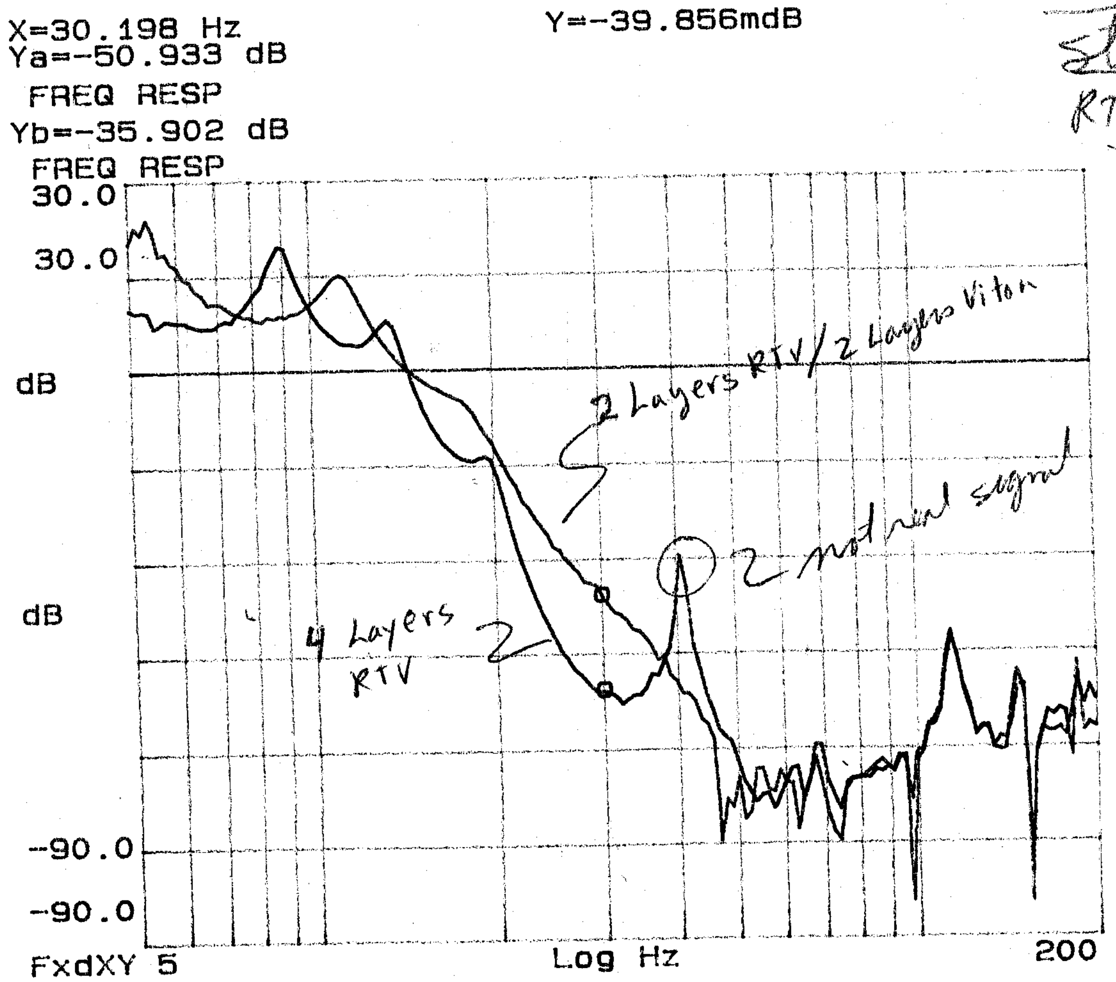

Black-SOR26
Blue-SOR22

Black-all RTV
Blue-Top 2 layers RTV
Bottom 2 layer viton

coherence is bad for 4 Layer RTV stack at 30Hz

⇒ get at least 15 dB at 30Hz; probably more

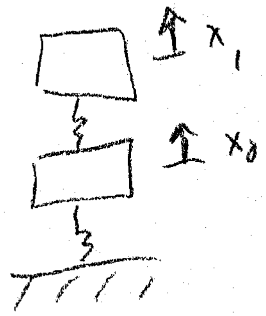

- Also hung accelerometer vertically
- Saw a small peak at 41 Hz but was not conclusive evidence that we were seeing acoustic coupling

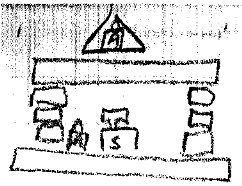

SOR30 - TF
SOR31 - coherence

>20Hz
integ time=1sec
AVE=8
Source=300

1/21/93 2:30 PM

Check to see if peak at 40 Hz is mechanical or acoustic

X=41.129 Hz
Ya=-36.175 dB
FREQ RESP
Yb=-31.406 dB
FREQ RESP

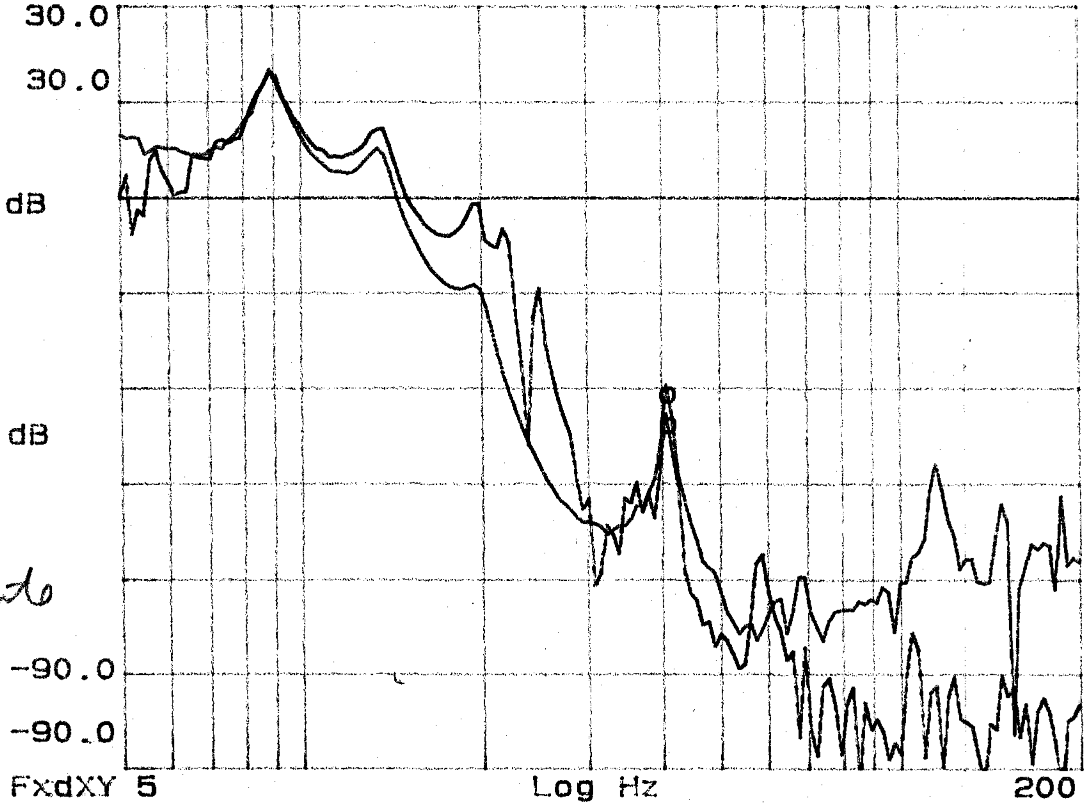

Y=-119.54mdB

Black - SOR 28 (SOR 28a) Top accel on rubber

Blue - SOR 26 Top accel on Al plate

SOR28

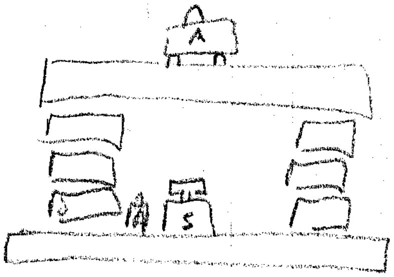

Put accel on springs to see if peak at 40 Hz is real

- same setting as SOR26 from 20<f<50

1/21/93 4:00 PM

Another check on 41 H

Resonance

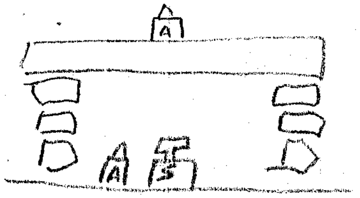

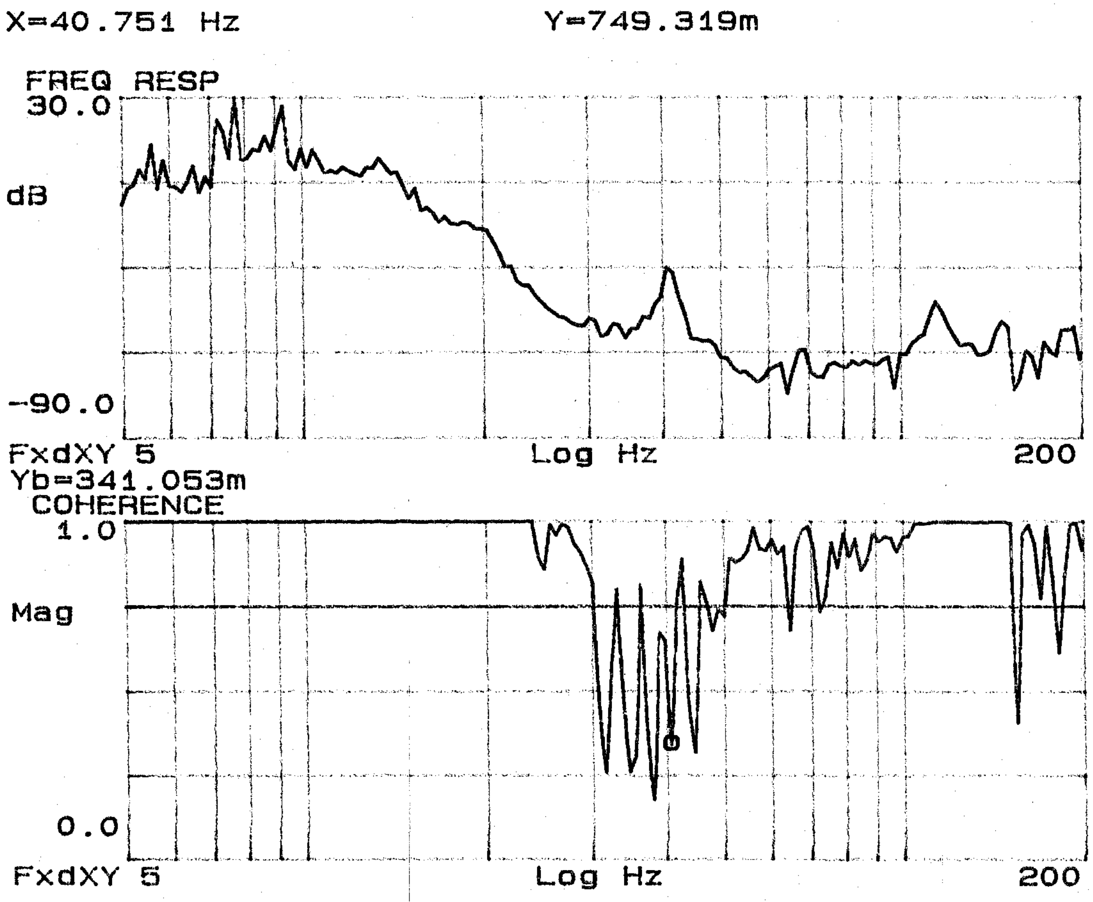

SOR32

SOR33

Wanted to look at power spectra in both acceler between 20 + 50 Hz

< 23 Hz
1 AV
integ time = 300 msec
Source = 150 mV rm

> 23 Hz
5 AV
Source = 300 mV RMS

Power Spectra on next page

1/21/93 4:30 PM

Power Spectra of upper + lower accel of SOR 32

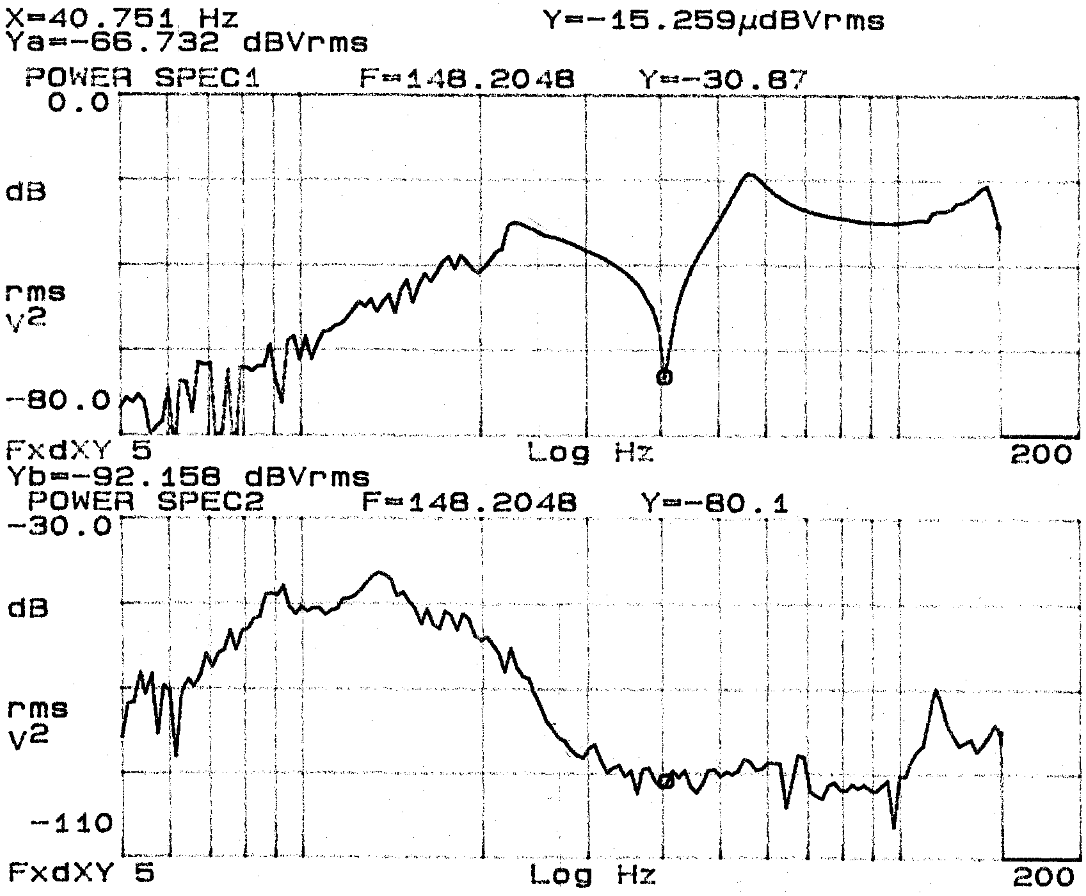

SOR34 (bottom accel)

SOR35 (top accel)

- There is a big resonance at 40.75 Hz in the Table

- Above 30 Hz it appears that either electronic or acoustic noise is dominant

When look at ratio of 2 power spectra can see that 41 Hz peak in transfer fctn is due to resonance in table and not to dynamics of stack

1/14/92 4:30PM

Transfer Fctn from V to V (Tapped in center of Al plate)

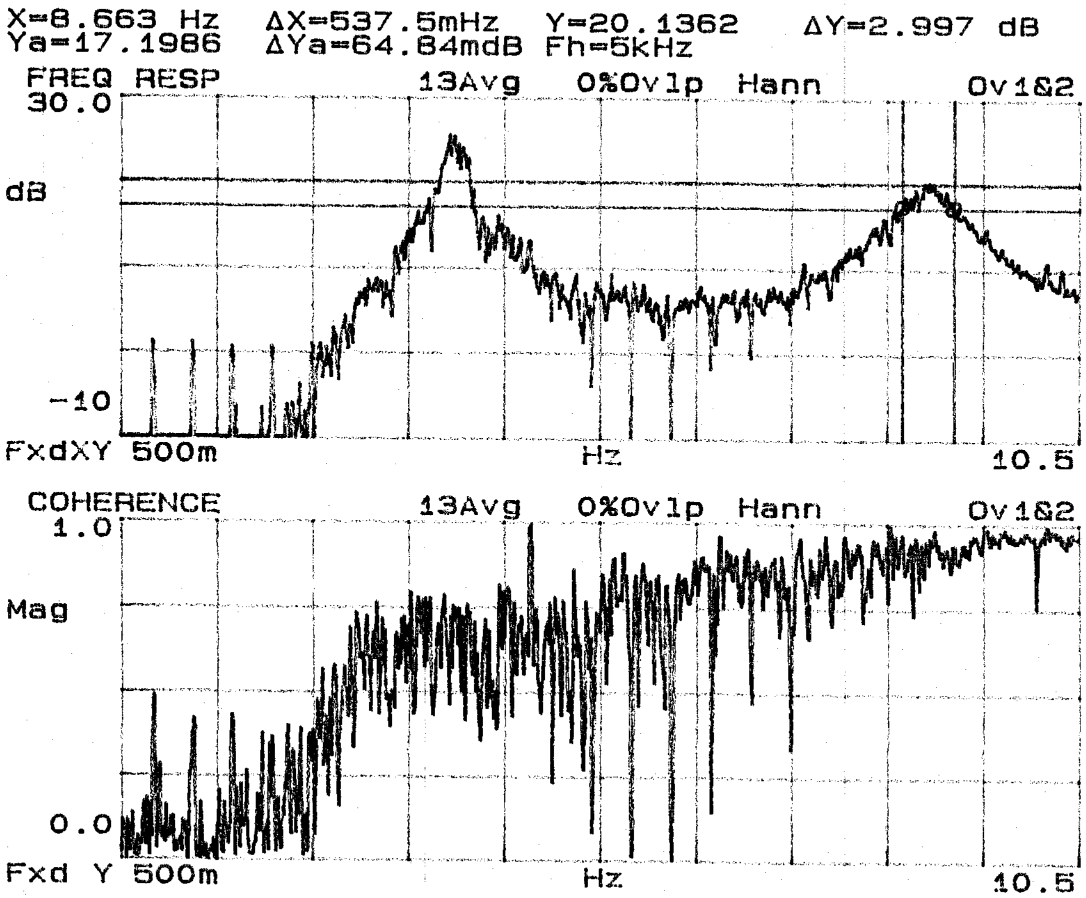

```
X=8.663 Hz   ΔX=537.5mHz  Y=20.1362    ΔY=2.997 dB
Ya=17.1986   ΔYa=64.84mdB Fh=5kHz
```

SOR36

SOR37

- Same accel, shaker configuration as SOR06

- Transfer fctn is done using random noise + 9AV
- Source level = 100mV rms

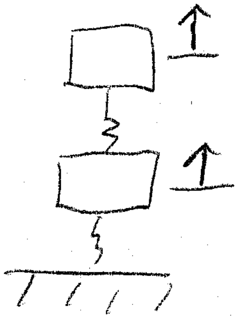

Can calculate Q of second stack mode

1/21/93 12:00 AM

Transfer Fcn from V to V
(accel on center of top plate)

A measurement was done with the top accel on the edge of the plate. The transfer fcn was identical

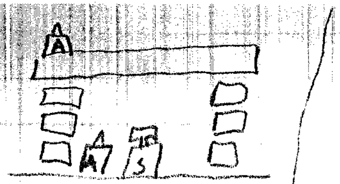

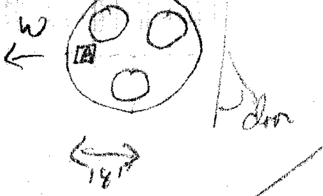

SOR26

SOR27

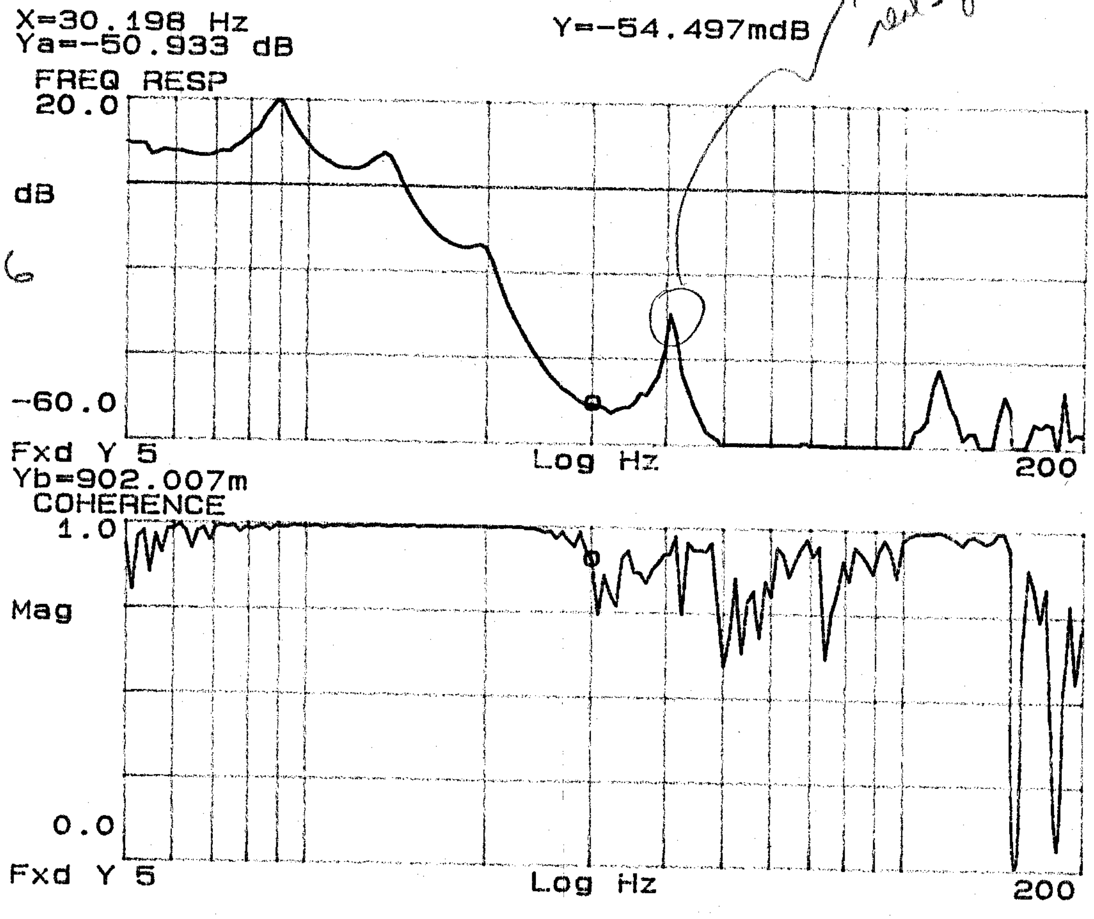

noise-not real signal

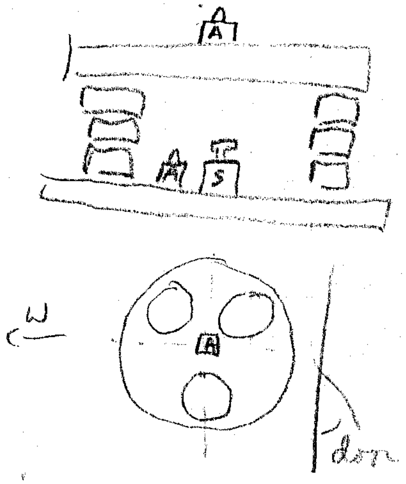

f < 20Hz

Source level: 150mV

integ time = 1.5-2 sec

Resln = 100 pts/dec

AVE = 8

20 < f < 40

Source level: 300mV

f > 40 Hz

integ time = 300 msec

- shaker in center of base plate
- base accel next to N drift compensator
- top accel in center of Al plate

Redid sine measurement with accel on side of Al plate. Got identical transfer fctn

R4 + R5

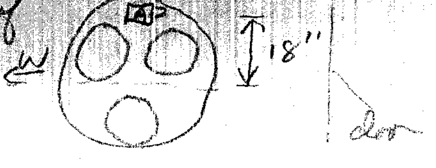

1/22/93 12:45 AM

Transfer Fctn from V to H with top accel on center of Al plate

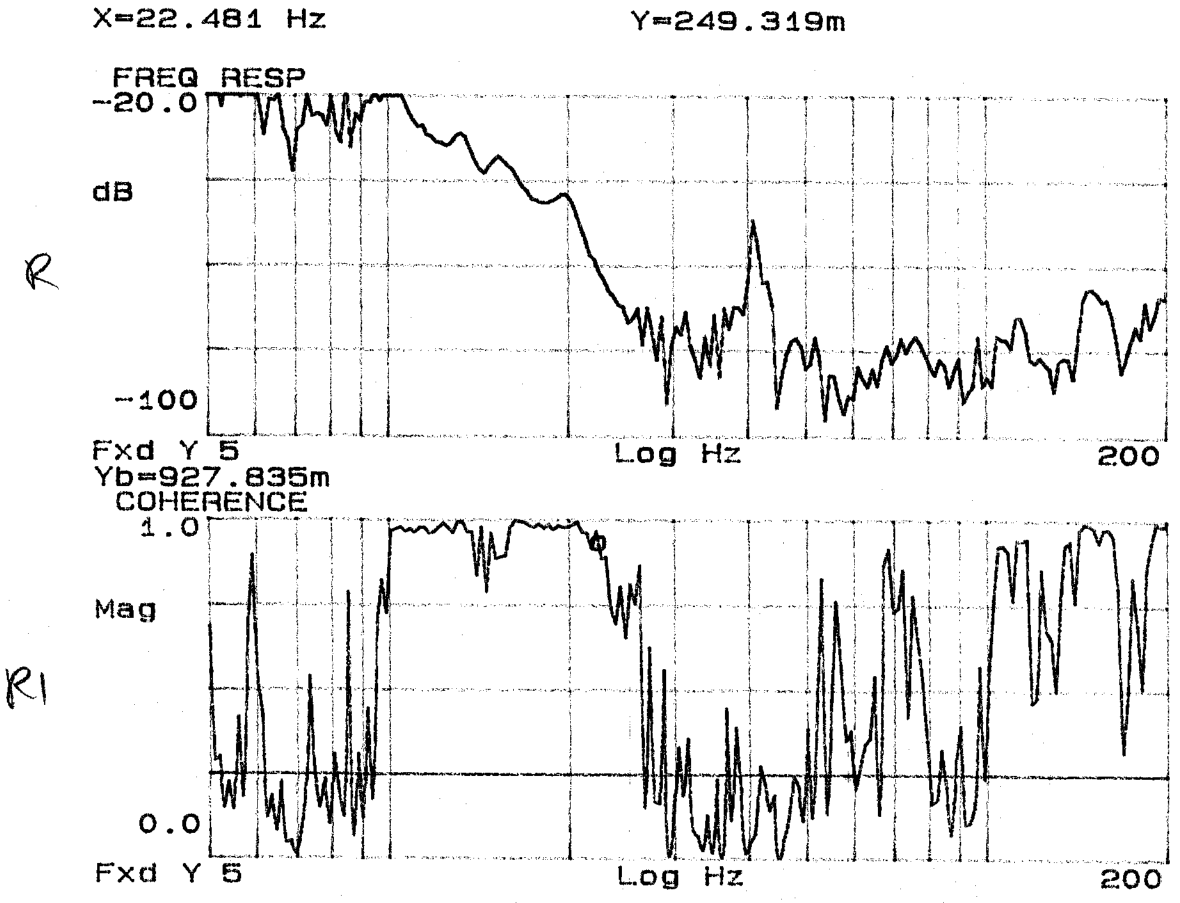

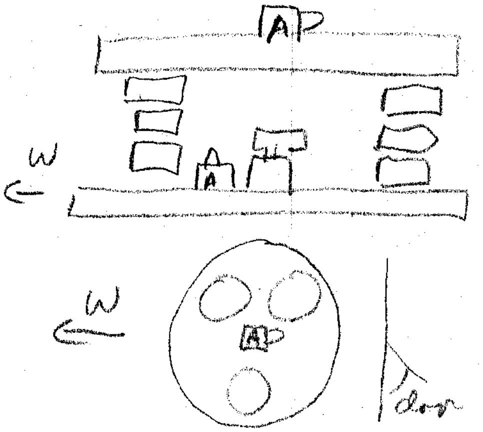

- Top accel on center of plate
- Shaker in center in V position
- Bottom accel next to N drift compensator

All RTV shields

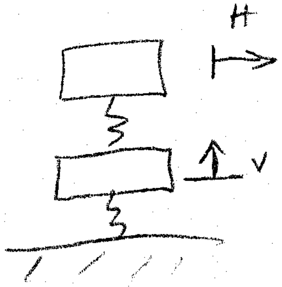

5-10 Hz source level = 150mV rms
integ time = 300msec
AV = 5
Resln = 100 pts/dec

10-50 Hz integ time = 1sec
>20 Hz source level = 300mV rms
>50 Hz integ time = 300 sec

1/22/93 12:45 PM

Power spectra of upper + lower accel of "R" transfer fctn

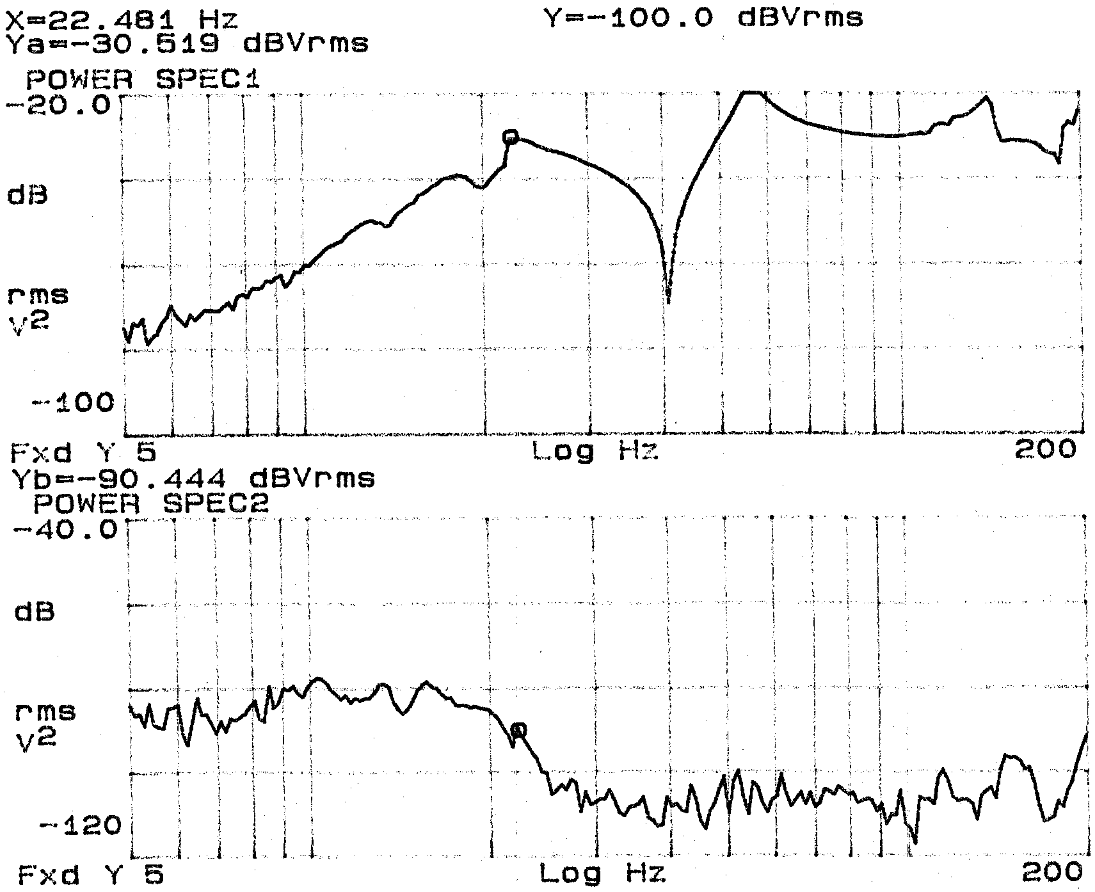

Accel on Al plate R2

Accel on Support plate R3

Repeated these measurements with top accel on edge of plate & got same transfer fcts R12 & R13

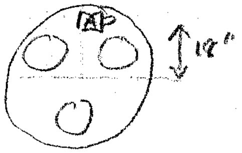

1/22/93 2:30 PM

Transfer Fctn from H to H (Top accel on center of Al plate)

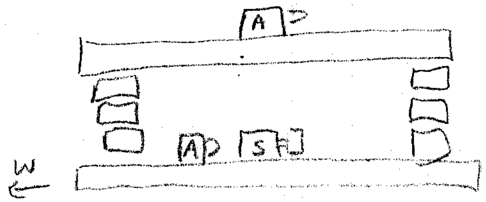

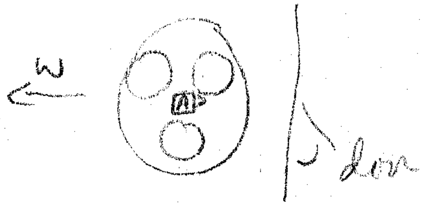

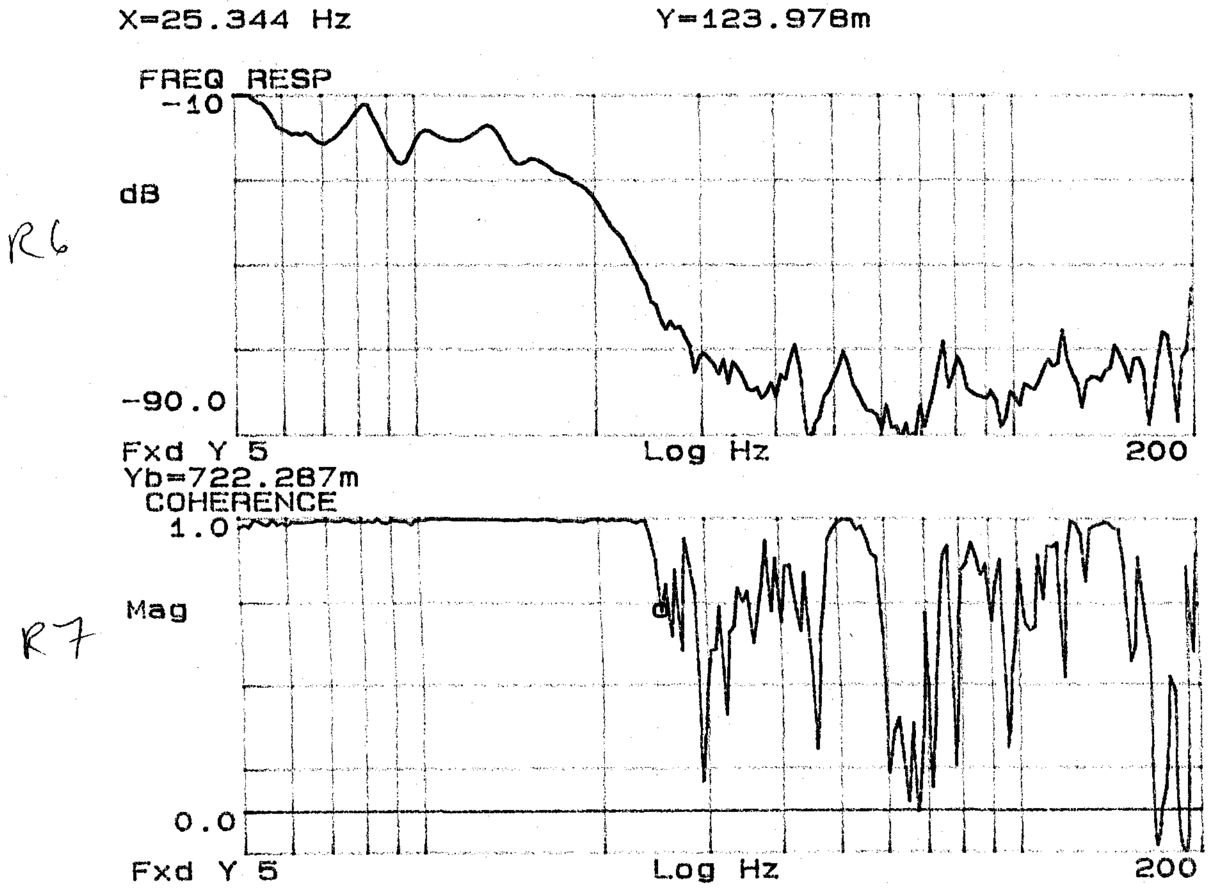

integ time = 300msec
AV=5
Resln = 100pts/dec
Source level = 150mVrms f<20
= 300mVrms f>20

- Top accel on center of Al plate
- Bottom accel near N drift compensator
- Shaker in H position

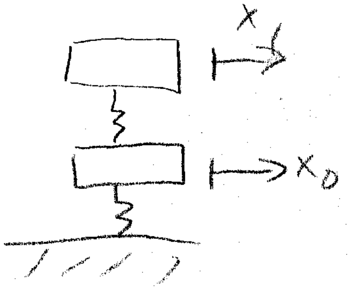

All RTV stacks

Comparison of H2/H1 transfer fctn for a stack with 2 Layers of viton/RTV + Stack with 4 layers RTV

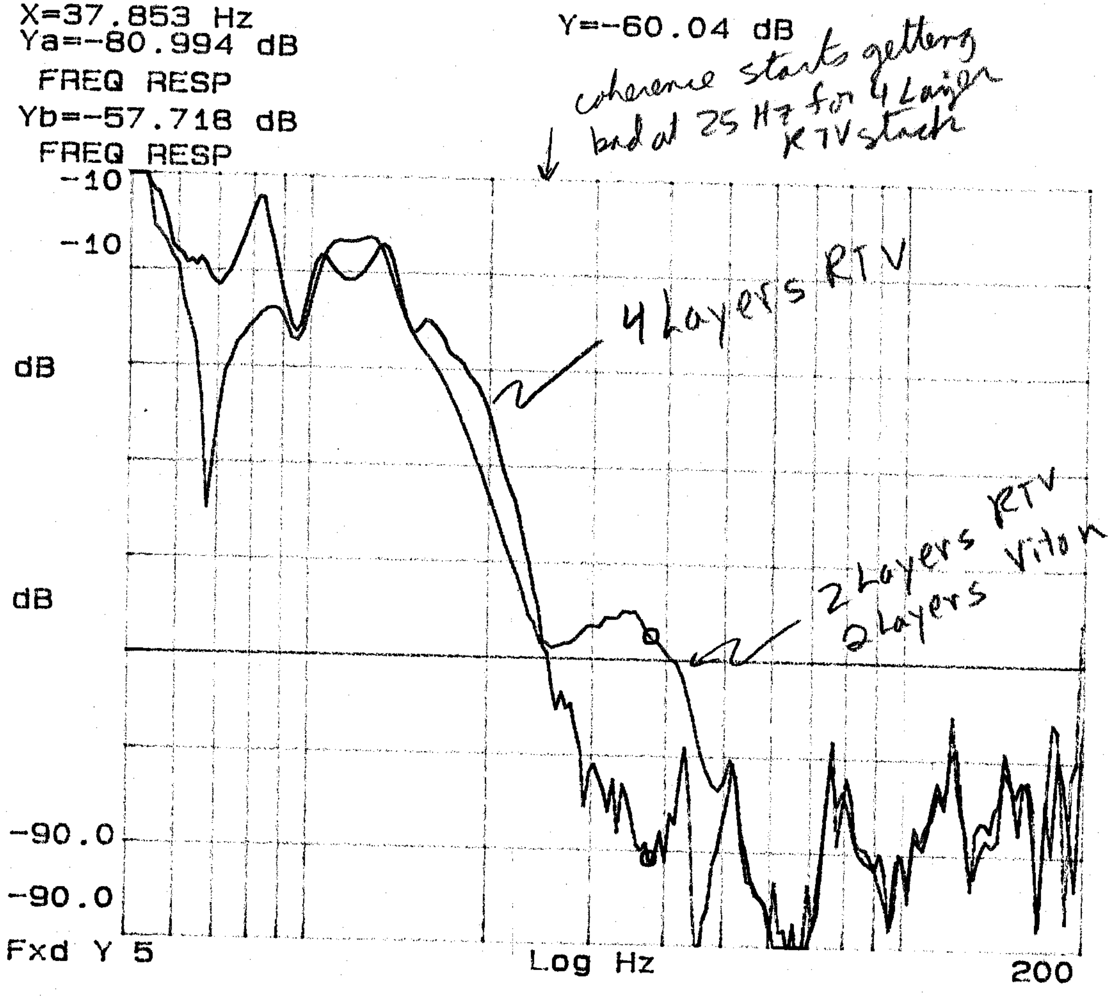

coherence starts getting bad at 25 Hz for 4 Layer RTV stack

Blue - SOR6
(Stack with 2 Layers of RTV + 2 Layers of Viton)

Black - R6
(Stack with 4 Layers of RTV)

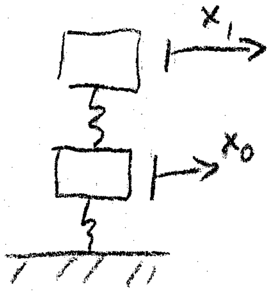

At 30 Hz - get at least 15 dB
At 40 Hz - get at least 20 dB

4/24/94 > 5:30PM

Transfer fctn from

H to H (Top accel on center)

- Same accel + shaker config as R6
- Transfer fctn taken using random noise
- Source level: 150 mVrms
- Window is uniform

R10

R11

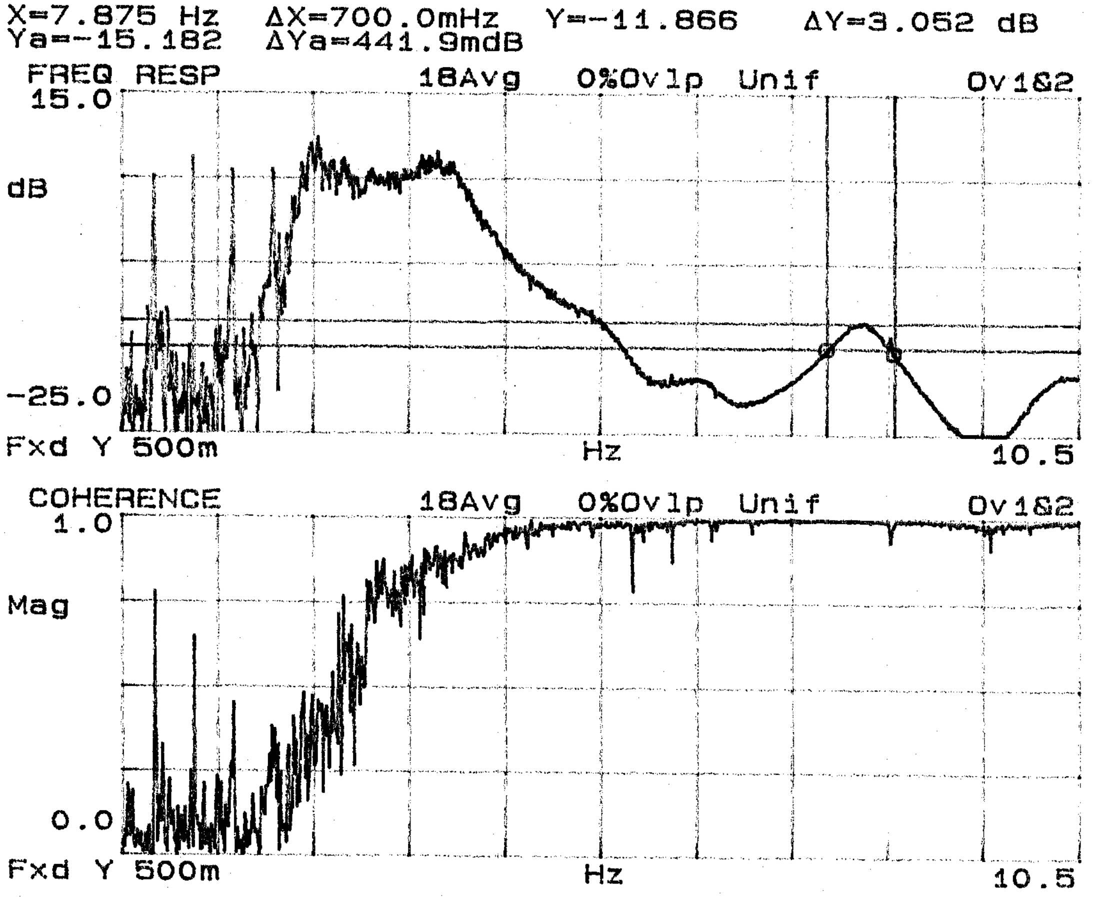

All RTV stack

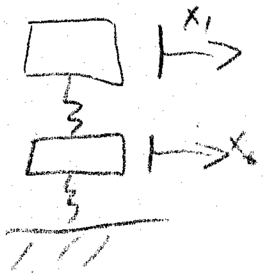

1/23/93 4:00 PM

Transfer fcts from H to V (accel on edge of Al plate)

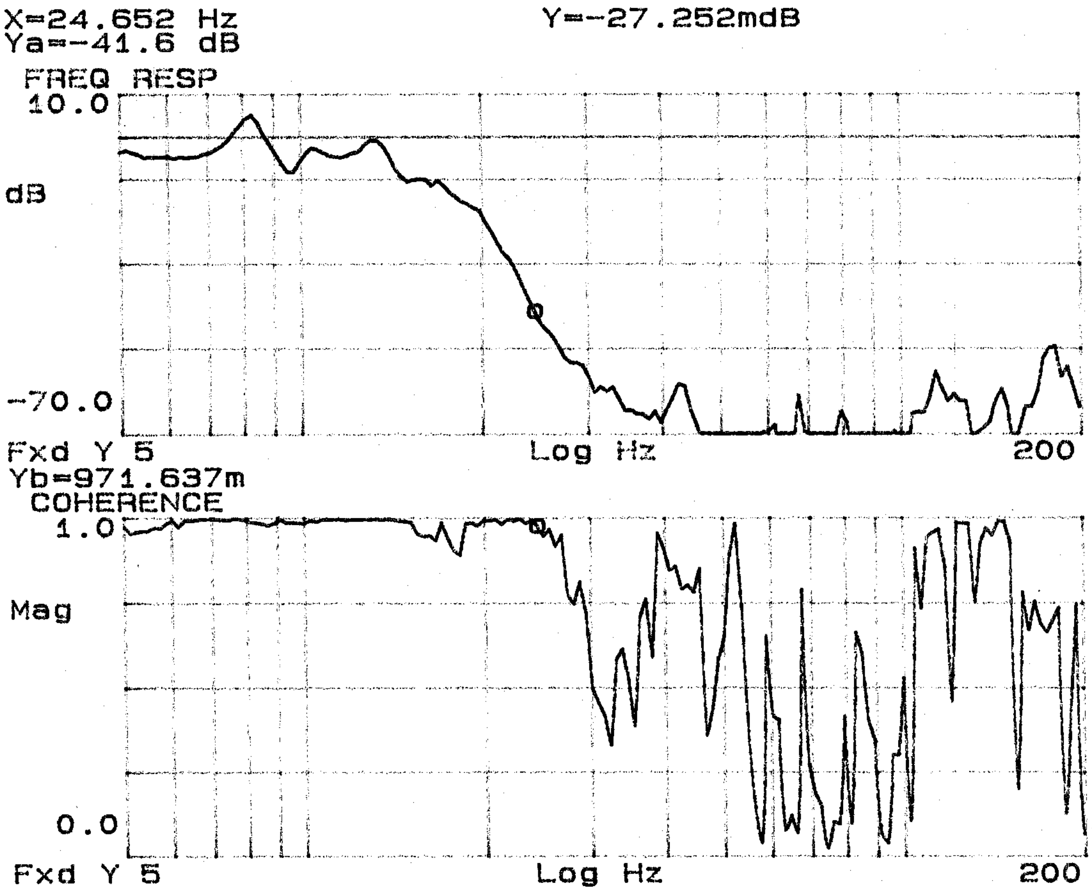

R14

R15

source level = 150 mVrms
5-20 Hz
= 400 mVrms
20-40 Hz
= 100 mVrms
> 40 Hz

integ time = 300 msec
5-20 Hz
> 40 Hz
= 1 sec
20-40 Hz

AV = 5
Resln = 100 pt/dec

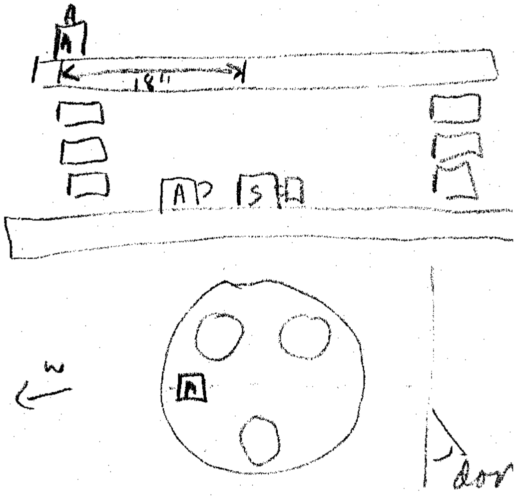

w ←

All RTV stack

Power Spectra of

R14 (see previous plot)

Power spectra of lower accel. R16

Power Spectra of Upper Accel. R17

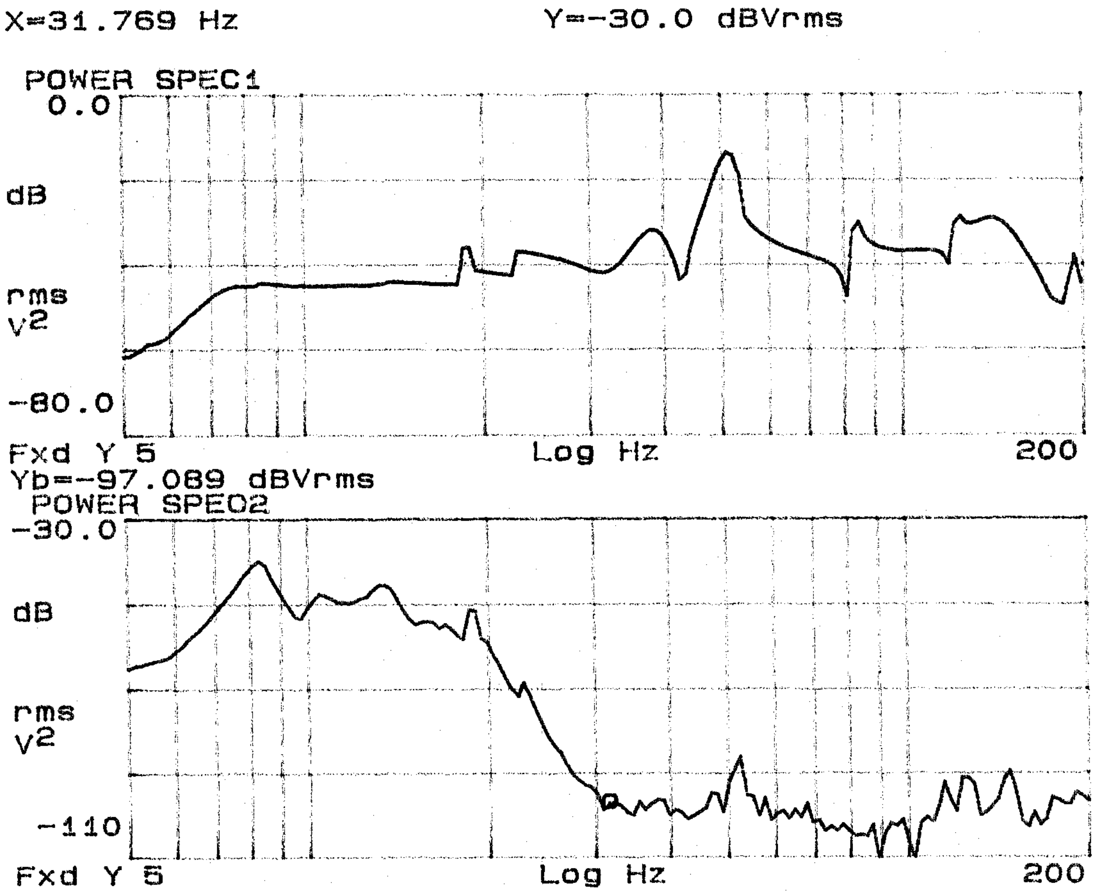

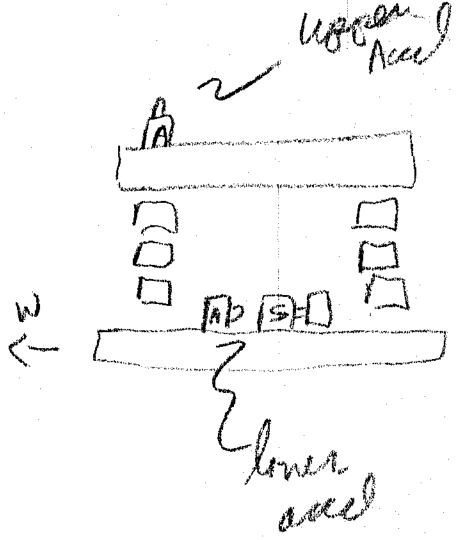

Comparison of H to V transfer function for 4 layer RTV Stack + 2 layer RTV/Viton stack

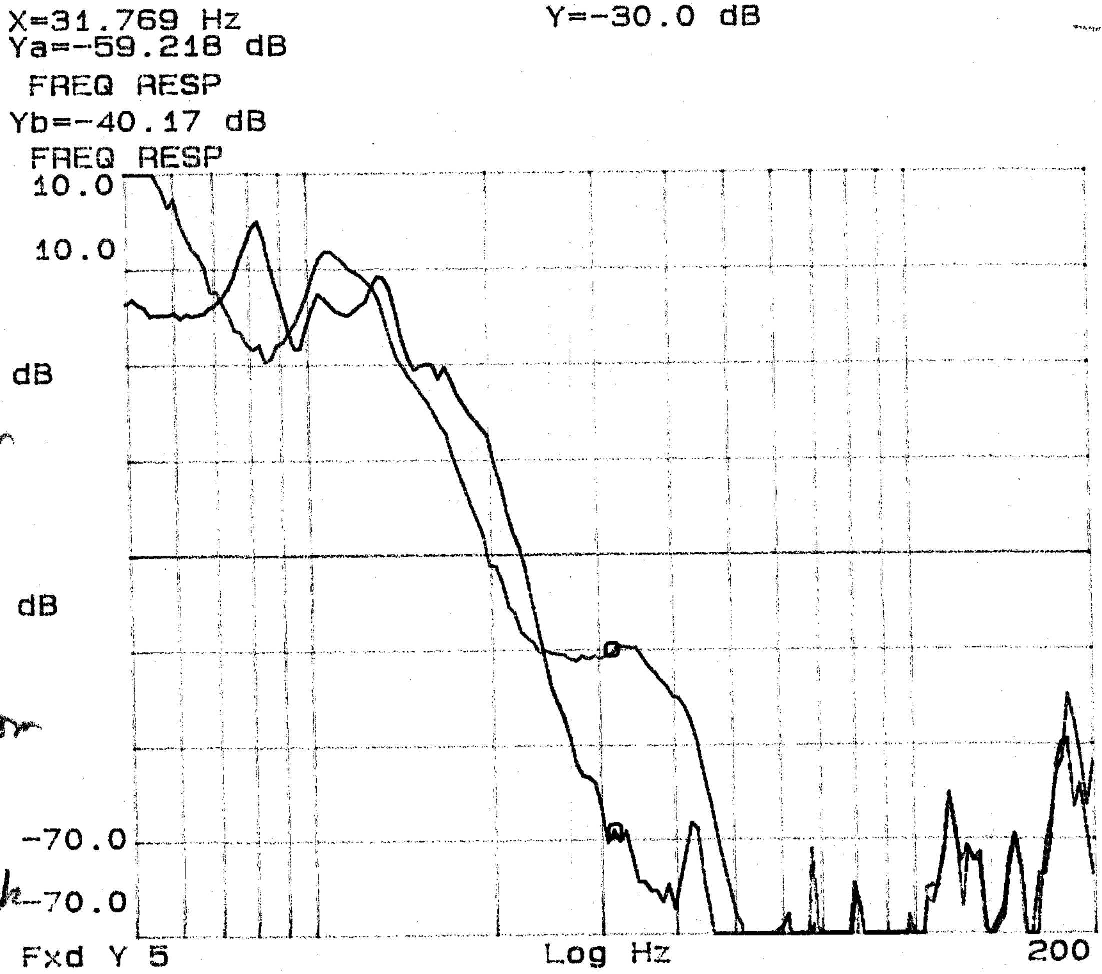

<u>Black-R14</u>
Transfer Fctn from H to V for 4 layer RTV stack

<u>Blue-SORG</u>
Transfer Fctn from H to V for 2 layer RTV + 2 bottom layers viton stack

1/23/93 4:30 Pm

Transfer Fctn Source
toV (accel on center of Al plate)

Source : 150 mV$_{rms}$ 5-20Hz

= 400 mV$_{rms}$ 20-40Hz

= 100 mV$_{rms}$ >40

integ time = 1 sec 5-36 Hz

= 300 sec >36 Hz

Ave = 5

Resln = 100 pts/dec

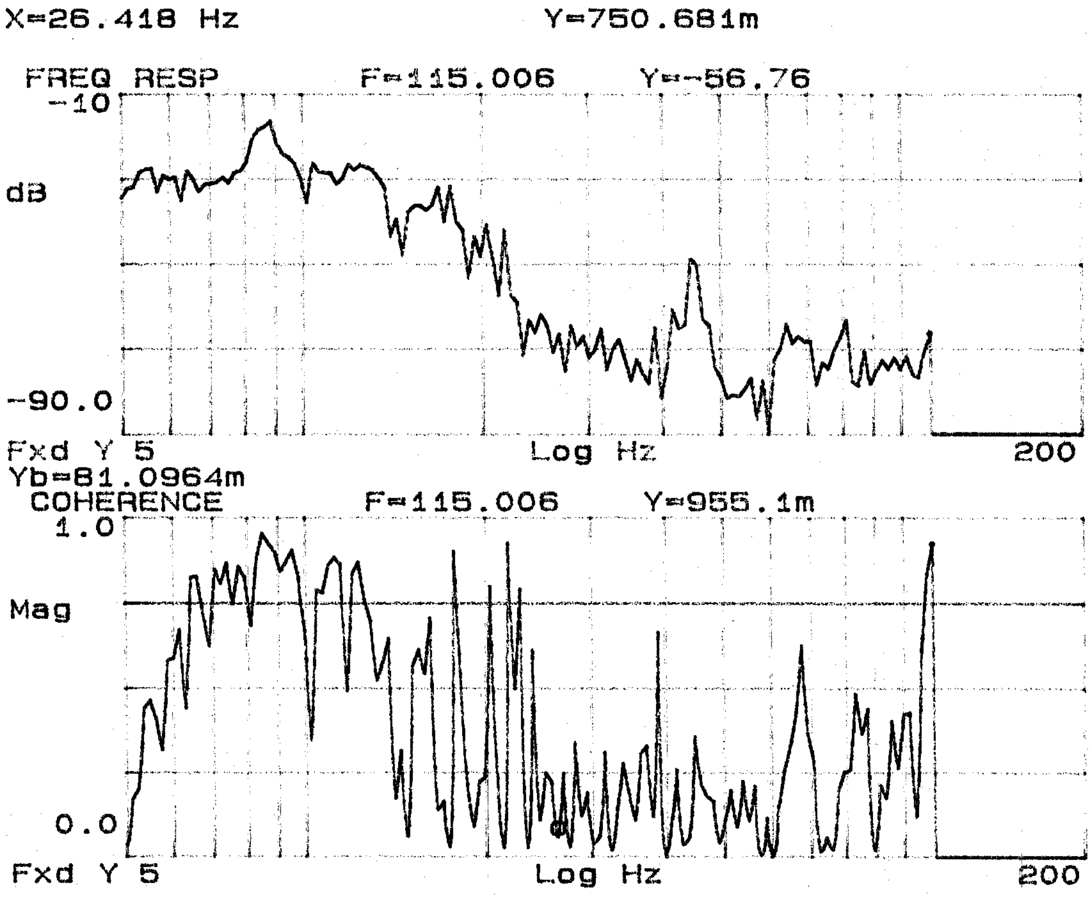

R18

R19

All RTV stack

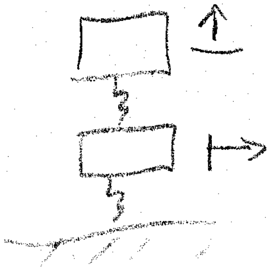

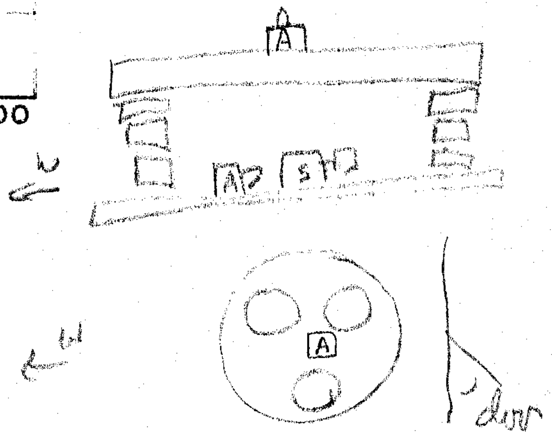

Comparison of H to V transfer fctn when top accel is switched from center to edge of Al plate

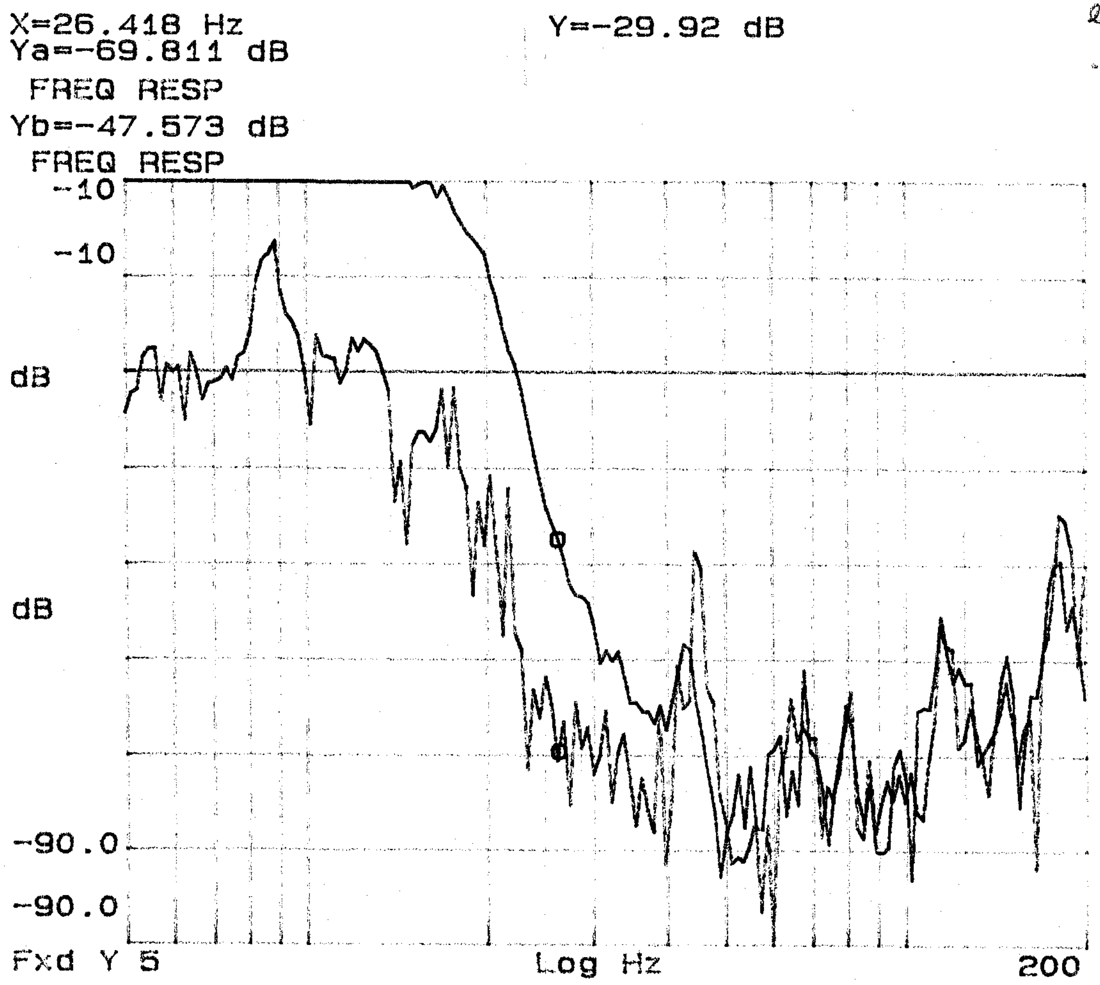

Black - R18

Accel on center of Al plate

Blue - R14

Accel on edge of Al plate

All RTV stock

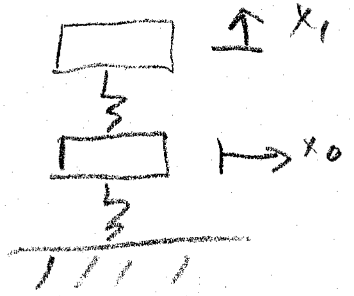

1/25/93 11:15 AM

Remade Stack With All Viton to Do Drift Measurements

- Used springs that we used previously for stack tests (Springs from MIT with voids in the middle)

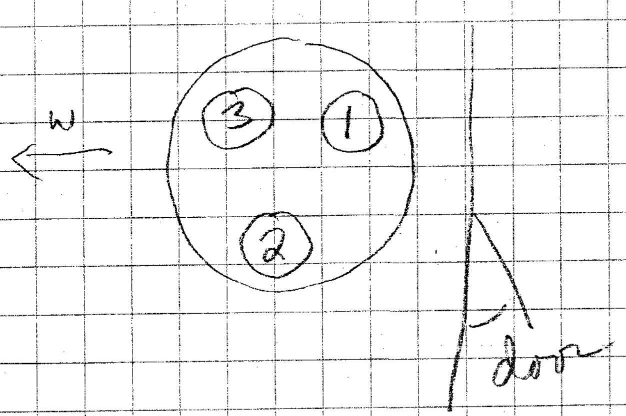

Stack height (3 layers were precompressed during stack tests - 2nd layer was un-compressed springs)

		Leg 1	Leg 2	Leg 3
Height	1/25/93 11:15AM	53.5 cm	53.5 cm	53.5 cm

DRIFT CHECK

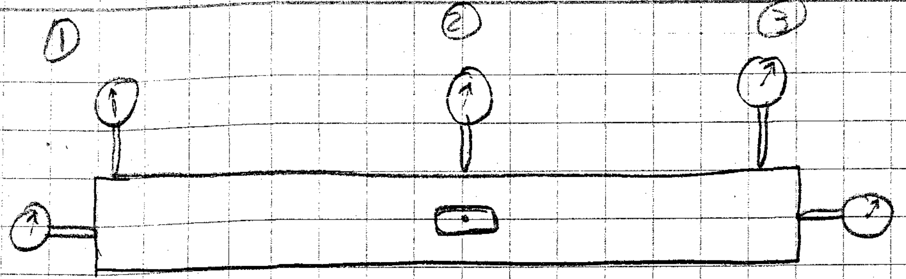

		①		②		③	
Day	Time	Top	Side	Top	Side	Top	Side
1-25	3:10	.0002	.0999	.0995	.0999	.0004	.000
	3:20	.000	.0999	.0982	.0998	.0995	.0999
	3:31	.0987	.0999	.0969	.0998	.0980	.0999
	4:20	.0923	.0999	.0900	.0998	.0918	.000
	5:35	.0842	.0999	.0817	.0998	.0839	.000
1-26	9:51	.0377	.0983	.0346	.0990	.0387	.0025
	1.08	.0337	.0982	.0302	.0987	.0341	.0025
	5:32	.0294	.0982	.0261 (maybe bad data)	.0984	.0296	.0026
1-27	9:44	.0162	.0978	.0250	.0984	.0161	.0028
	4:36	.0082	.0974	.0074	.0982	.0123	.0037
1-28	3:45	.0013	.0969	.0978	.0981	.0014	.0042

→ Disassembled indicators to put on Optical mounts

Time ①	Top	Side	Time	Top	Side	Time	Top	Side
3:10pm	.0002	.0999	3:10pm	.0995	.0999	3:10pm	+.0004	.000
3:20	.000	-.0999	3:18	.0982	.0998	3.20	.0995	.0999
3:31	.0987	.0999	3:31	.0969	.0998	3:31	.098	.0999
4:20	.0923	.0999	4:21	.0900	.0998	4:22	.0918	.000
5:35pm	.0842	.0999	5:36	.0817	.0998	5:36pm	.0839	.000
9:51am	.0377	.0983	9:50	.0346	.0990	9:47am	.0387	.0025
1:08pm	.0337	.0982	1:08	.0302	.0987	1.09	.0341	.0025
5:32pm	.0294	.0982	5:32	.0261	.0984	5:33	.0296	.0026
9:44am	.0162	.0978	9:44am	.0250 added .1335 shim	.0984	9:45	.0161	.0028
4:36	.0082	.0974	4:35pm	.0414	.0982	4:37	.0123	.0037
3:45	.0013	.0969	3:45	.0308	.0981	3:46	.0014	.0042

Looking Down

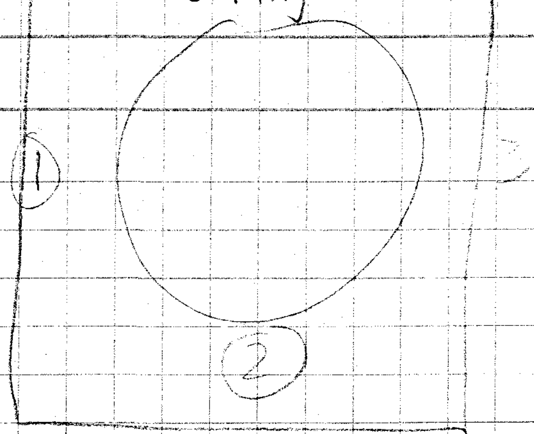

		①		②		③	
Day	Time	Top	Side	Top	Side	Top	Side
1-28	~4:25	.000	.000	.000	.000	.000	.000
1-28	4:58	.0910	.0020	.0948	.0090		.0986
	5:11	.0895	.0021	.0948	.0103	.0920	.0981
1-29	9:10	.0656	.0033	added .504" block .0331	.0272	.0767	.0963
	2:13	.0618	.0041	.0303	.0280	.0740	.0957
	4:12	.0607	.0046	.0286	.0287	.0732	.0945
2-1	10:04	.0382	.0055	.0981	.0345	.0547	.0937
	12.49	.0378	.0064	.0978	.0351	.0543	.0934
	2:32	.0377	.0068	.0977	.0354	.0543	.0932
	5:36	.0376	.0079	.0975	.0362	.0549	.0923
2-2	9:12	.0360	.0082	.0950	.0378	.0534	.0920
	12:57	.0331	.0750 ?? ~~.0075~~	.0940	.0381	.0529	.0919
	5:38	.0331	.0760	.0939	.0389	.0535	.0917

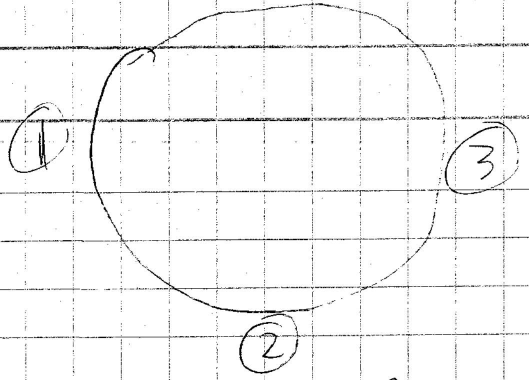

Day	Time	①		②		③	
		Top	Side	Top	Side	Top	Side
2-3	904	.0309	.0757	.0908	.0391	.0512	.0909
	11:42	.0301	.0756	.0900	.0392	.0505	.0911
	3:30	.0300	.0760	.0891	.0399	.0505	.0909
2-4	9:58	.0275	.0761	.0854	.0404	.0474	.0904
	2:05	.0270	.0762	.0849	.0404	.0470	.0903
	5:33	.0276	.0765	.0848	.0406	.0475	.0906
2-5	8:54	.0259	.0760	.0831	.0407	.0465	.0899
	2:00	.0250	.0760	.0817	.0416	.0456	.0904
	5:40	.0254	.0761	.0817	.0417	.0459	.0904
2-8	9:11	.0163	.0760	.0719	.0420	.0379	.0890
	12:47	.0159	.0767	.0714	.0421	.0375	.0890
	4:41	.0159	.0775	.0710	.0429	.0378	.0890
2-9	10:15	.0154	.0777	.0704	.0430	.0368	.0843
	2:39	.0149	.0787	.0698	.0430	.0362	.0891
2-10	1:42	.0120	.0791	.0661	.0433	.0336	.0879

How to calculate H_G to H_{TM} assuming excitation is due only to tilt coupling

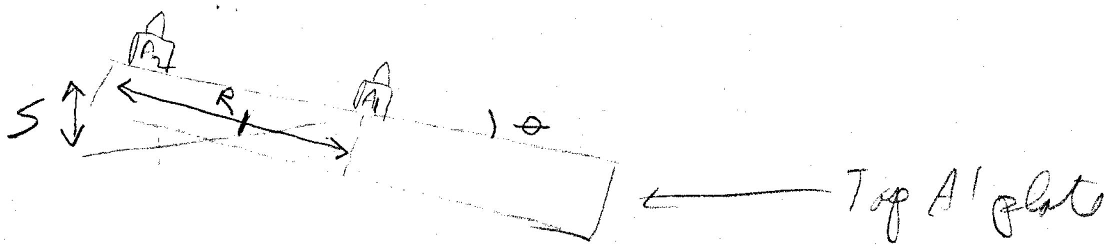

$$\frac{S}{H_{ground}} = \frac{\theta R_1}{H_{ground}} = \frac{V_{A2}-V_{A1}}{H_{ground}} \approx \frac{V_{A2}}{H_{ground}}$$

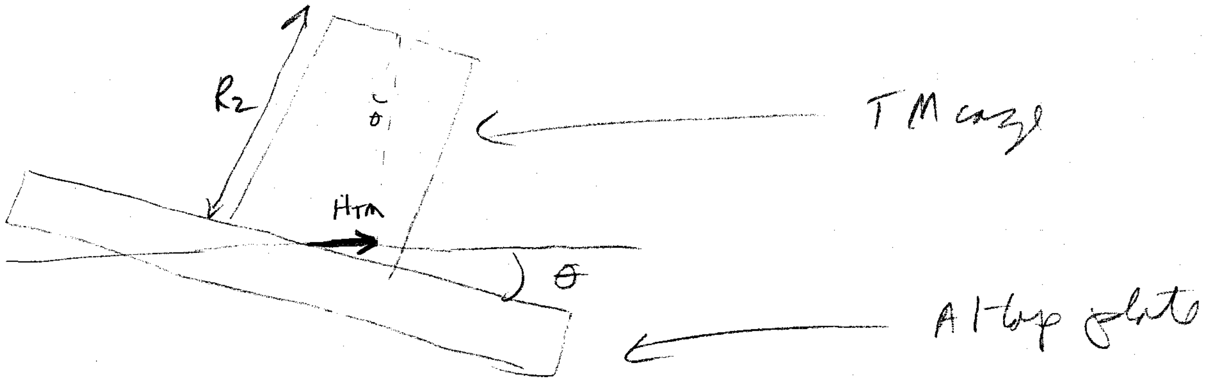

$$H_{TM} = R_2\theta$$

Want $$\frac{H_{TM}}{H_{ground}} = \frac{R_2\theta}{H_{ground}} = \frac{R_2 S}{H_g R_1} = \frac{R_2}{R_1}\boxed{\frac{V_{A2}}{H_{ground}}}$$

This transfer fcn is in JA

GET DATA FROM TRANSFER FUNCTION TESTS PLOTTED AGAINST MIT DATA

Joe Giaime and others at MIT
would also like to see the plots when they are done.

I would like to get all of these transfer functions plotted on the same scale so we could overlay them:

- a) All viton stack: HtoH, VtoV, HtoV and VtoH
  - MIT
  - Caltech (8-6-4-2)
- b) RTV/Viton stack: HtoH, VtoV, HtoV, and VtoH
  - MIT
  - Caltech (7-5-4-2)
- c) All RTV: HtoH, VtoV, HtoV, and VtoH
  - Caltech (8-6-4-2)

    (make sure when show this plot that people know in some sense we are comparing apples with oranges since the compression of the MIT stack is probably alot greater than the caltech stack---would like to get these numbers)

CALTECH DATA FILES FOR ALL VITON 2-4-6-8 STACK:
(appears to be no coupling from vertical shaking to rotation or tilt or from horizontal shaking to rotation)

HtoH(assuming only direct horizontal coupling) : VST2
HtoH(assuming only tilt coupling): JA*18in/(height of TM cage)
(see note for explanation)
HtoV: Jan6
VtoV: JA4
VtoH: JA8

CALTECH DATA FILES FOR RTV/VITON STACKS; 2-4 RTV AND 5-7 VITON STACK:
(appears to be no coupling from vertical shaking to rotation or tilt or from horizontal shaking to rotation. Another thing to note when comparing these plots with the all-viton plots is that the coherence becomes bad at lower frequencies)

HtoH(assuming only direct horizontal coupling) : SOR8
HtoH(assuming only tilt coupling): SOR6*18in/(height of TM cage)
(This approximation is an upper bound; possibly a bad approximation. See SOR4 and SOR6)
HtoV: SOR4
VtoV: SOR22
VtoH: SOR20

CALTECH DATA FILES FOR ALL RTV 2-4-6-8 STACK:
(appears to be no coupling from vertical shaking to rotation or tilt or from horizontal shaking to rotation. Another thing to note when comparing these plots with combination RTV/Viton stack plots is that the coherence becomes bad at lower frequencies)

HtoH(assuming only direct horizontal coupling) : R6
HtoH(assuming only tilt coupling): R14*18in/(height of TM cage)
HtoV: R18
VtoV (peak at 40 hertz is noise and not real data): SOR26
VtoH: R

2/4/93 3:30 PM

Test to see if Mark II springs crack under loading

Loaded 3 designated Mark II springs with 3-20Kg disks + 11-lead bricks

$$20 \times 3 + 11 \times 9 = 60 + 99 = 159$$

$$\Rightarrow 159\text{kg}/3\text{ springs} = \frac{53\text{kg}}{\text{springs}}$$

Still need to do tests to compare stiffness of viton we used for stack tests & stiffness of new Mark II springs

2/11/93

Q tests for Al Plate loaded with Beam Splitter Optics

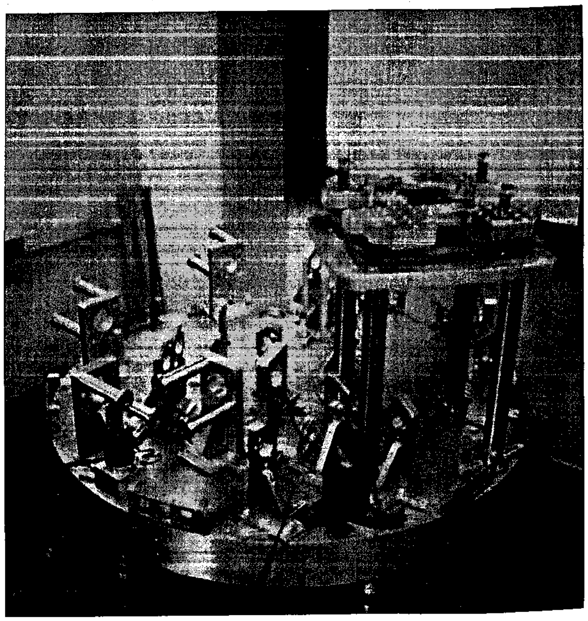

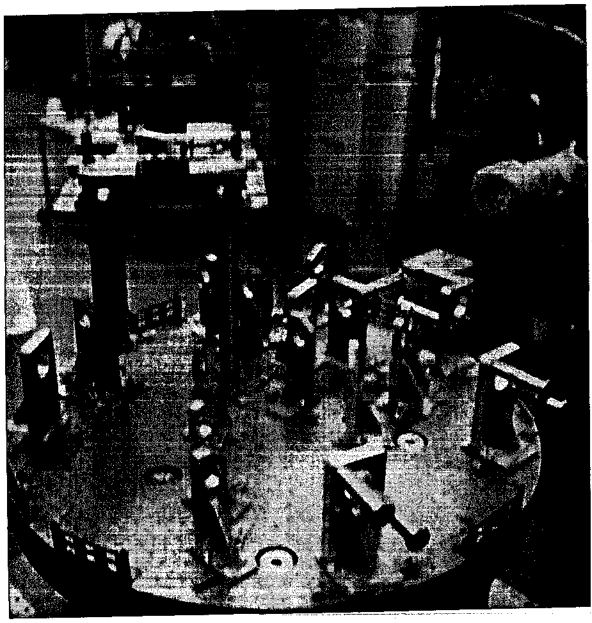

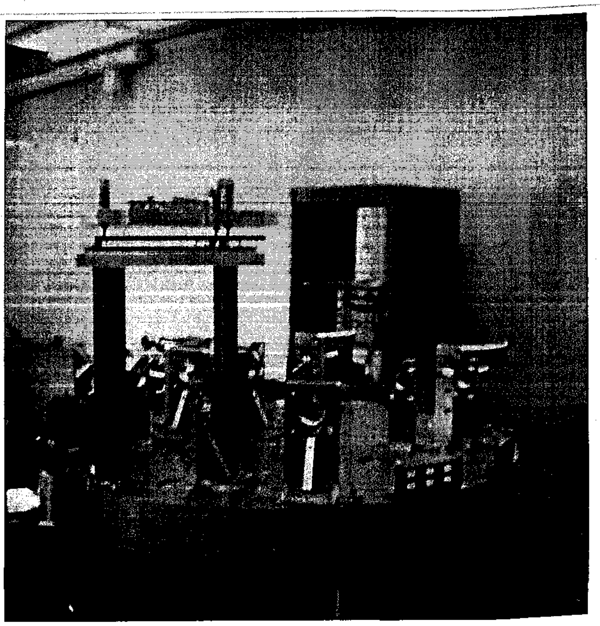

11:00AM 2/1/93

Transfer fcts from Shaker voltage to accelerometer

- 1 Volt RMS random noise excitation

Puk: Stack 4

Black - Q

(Al plate has mirror mounts + TM cage - no TM, mirrors, or motor mikes)

Blue - Q1

(Al plate has mirror mounts, TM cage + motor mikes - see picture)

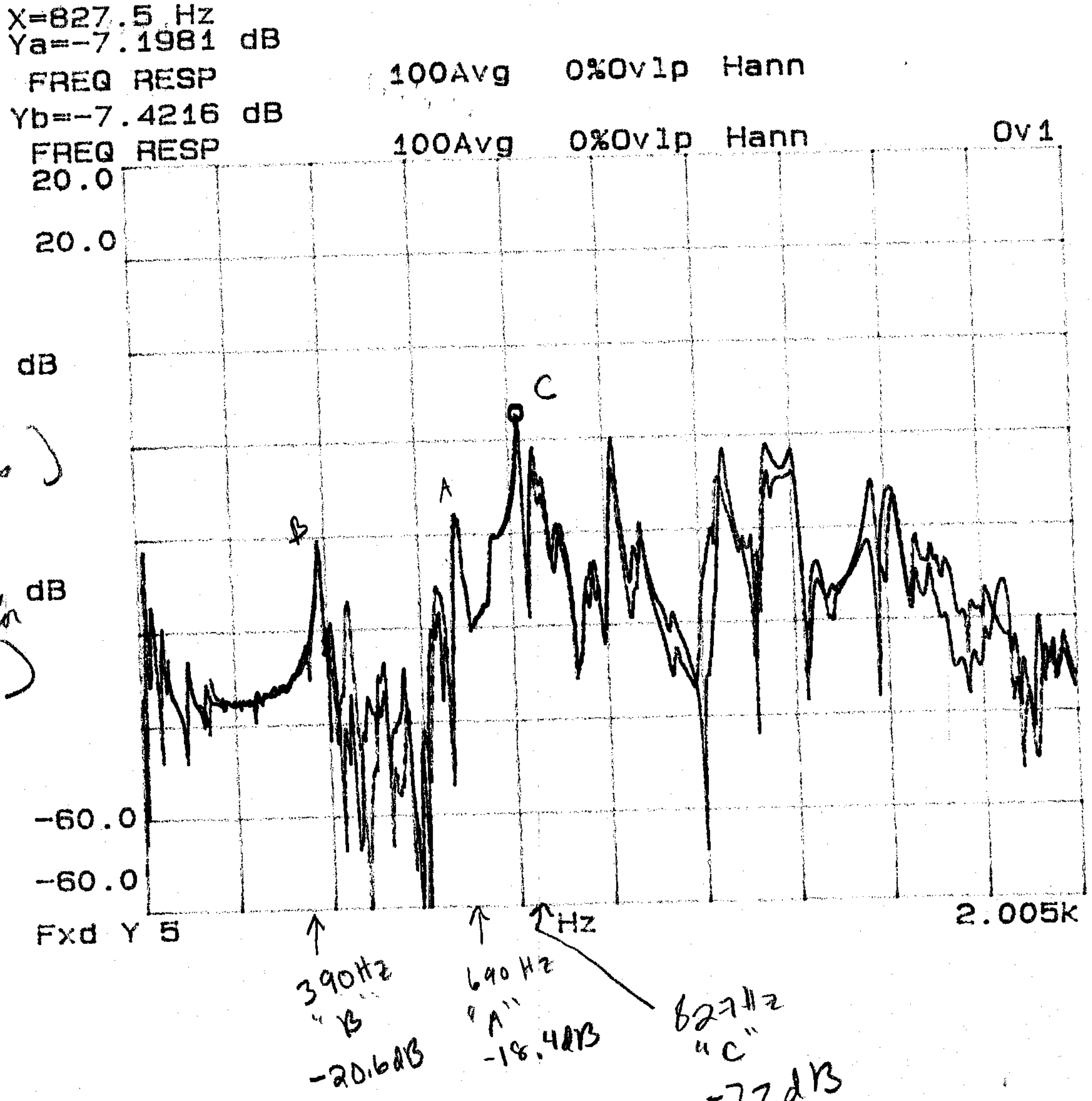

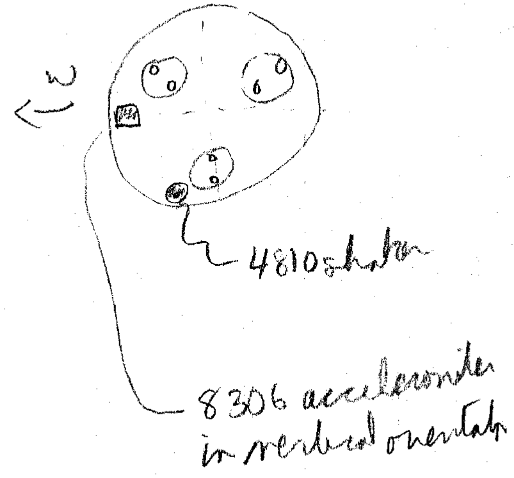

- Viton stack with 6 springs contacting Al plate in radial position

11:15 AM 2/11/93

Q = 34

Measurement to determine Q of peak at 385 Hz

X=385.87 Hz ΔX=11.37 Hz Y=-23.187 ΔY=3.081 dB
Ya=-23.113 ΔYa=612.4mdB

FREQ RESP 37Avg 0%Ovlp Hann Ov1&2

FREQ RESP 37Avg 0%Ovlp Hann Ov1&2

Same setup as Q1

Q2
Pick: Stack 4

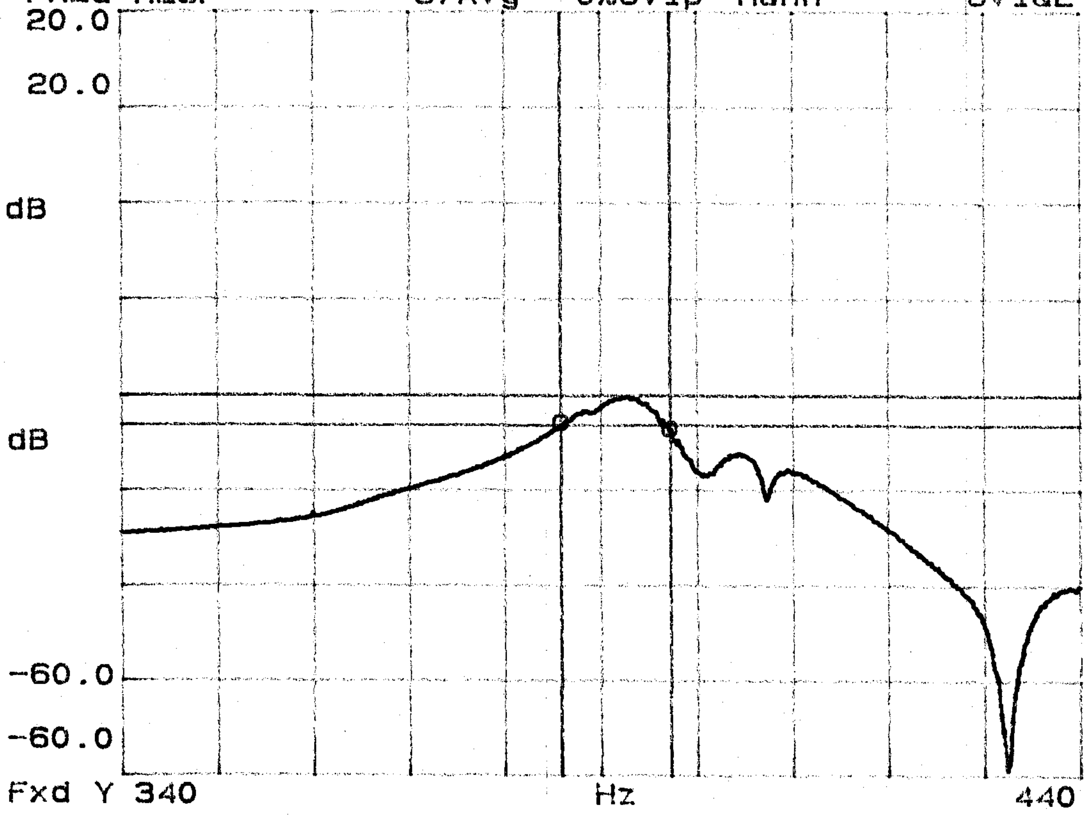

11:30AM 2/11/93

Measurement to determine
Q of peak at 682 Hz

$\Rightarrow Q = \frac{w}{\Delta w} = 48$

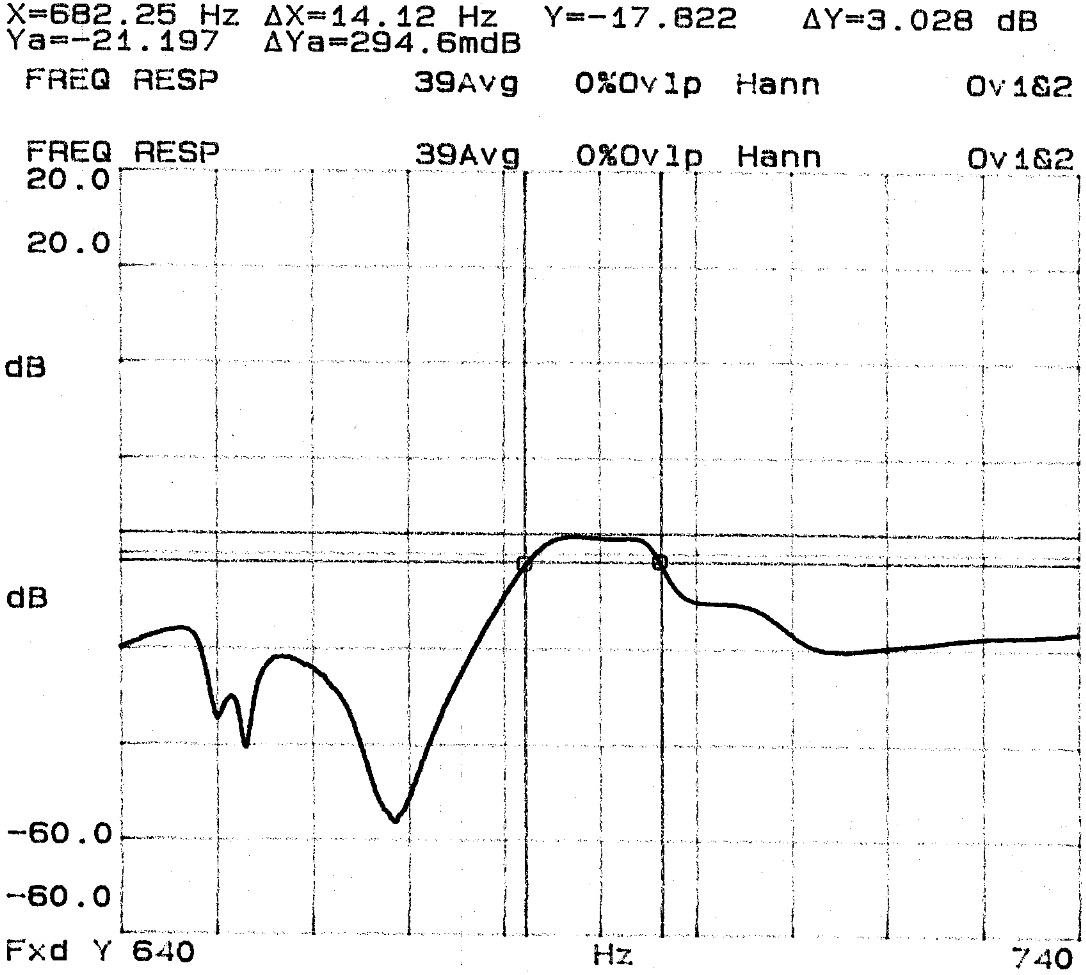

Same setup as Q1

Q3
Pick: Stack 4

11:45AM 3/11/93

Measurement to Solomons

Q of peak at 825.12 Hz

Q=153

```
X=825.12 Hz  ΔX=5.375 Hz   Y=-5.9761    ΔY=3.028 dB
Ya=-9.2355   ΔYa=158.3mdB
 FREQ RESP               31Avg   0%Ovlp  Hann        Ov1
```

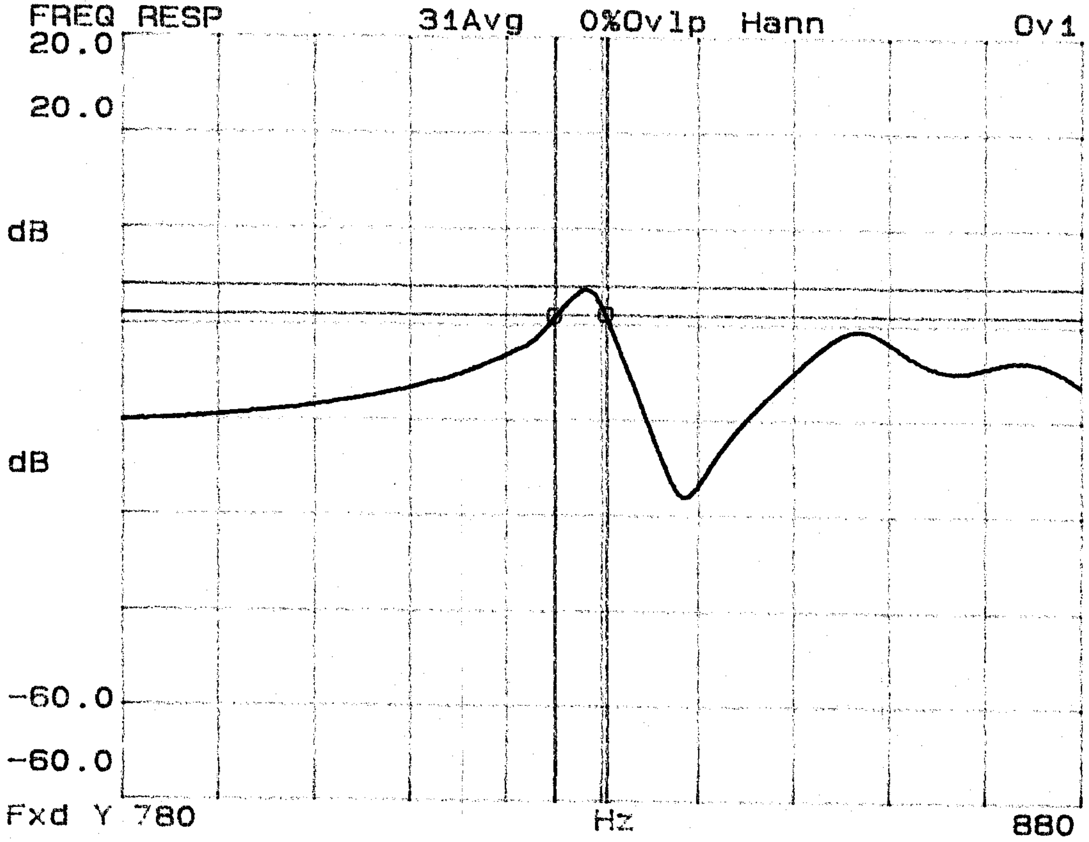

Same set up as Q1

Q4

Disk: Stack 4

12 MARCH 93
res

Test of vertical force vs. displacement, using Viton springs disassembled from test stack

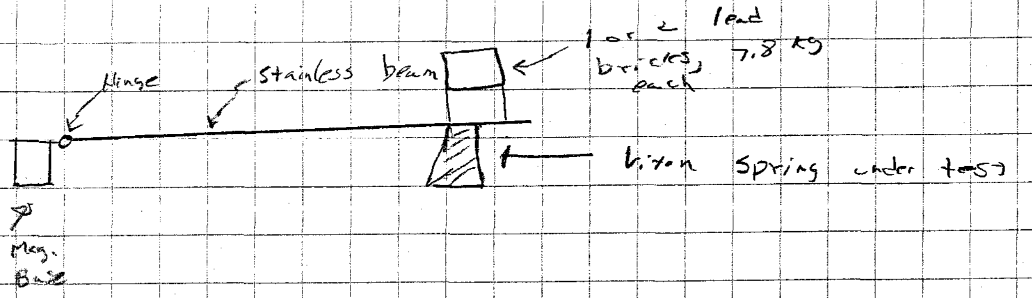

Height of beam measured with calipers, with 0, 1, or 2 bricks

P. 25 W: Raw data, from calipers + dial indicator
P. 25 Y: Plot showing ~2 minute time scale sag
P. 26 W: 123 worksheet calculation of displacement change for 1-brick load change, using various springs + for different observation times.

Conclude: because of exponentially decaying sag, precise timing (i.e. to ± 20 sec) + ~ 200 sec relaxation time delay is required to measure spring constant (vertical force/Displacement) to $\frac{\Delta k}{k} \lesssim 5\%$.

Untimed (quick) measurements provide accuracy of $\frac{\Delta k}{k} \approx 15\%$

Viton Spring Sag

Spring L412; 18 March 93

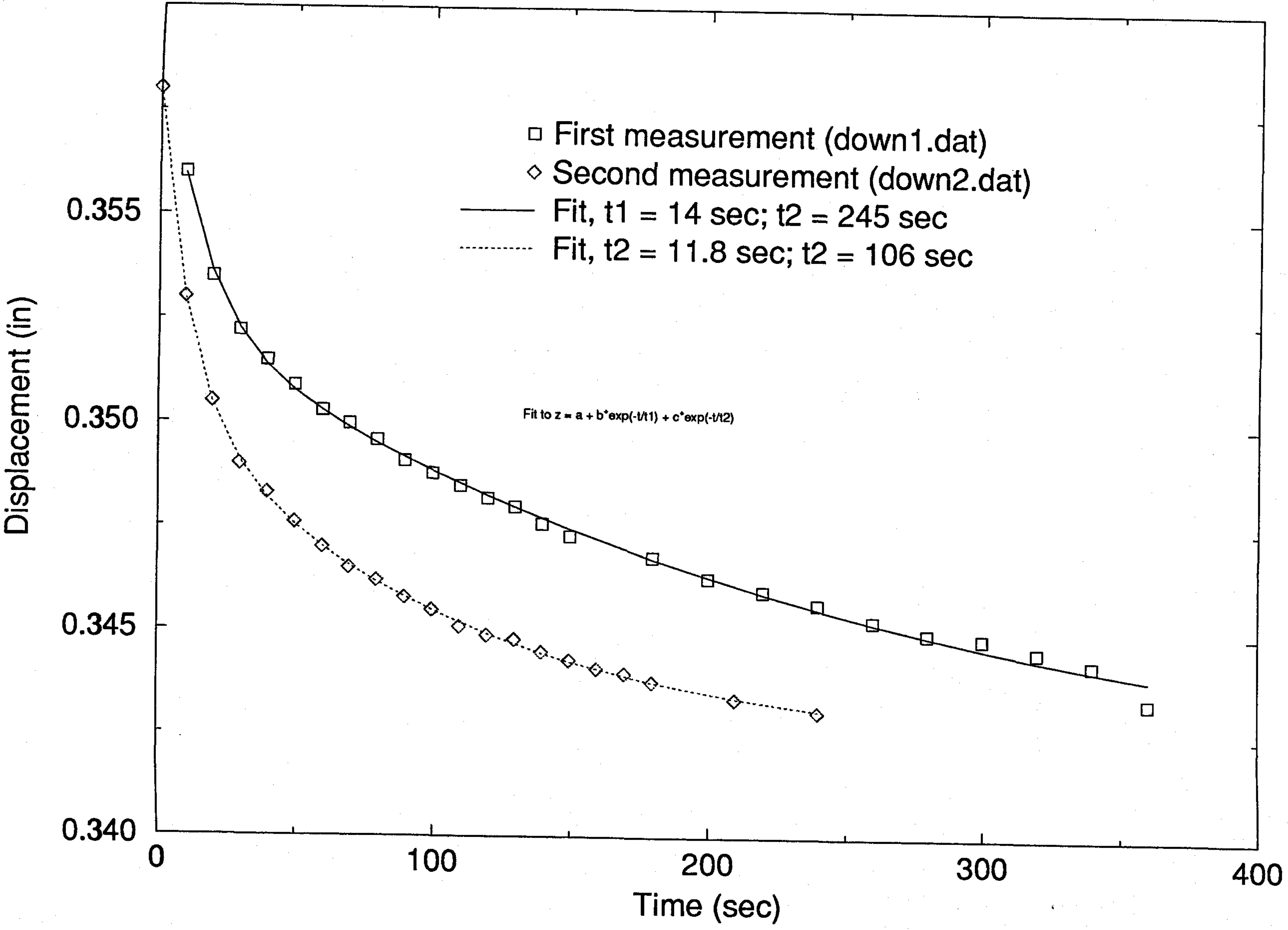

Tue Mar 23 20:36:53 1993

Data of 15 March 93
Displacement in cm of spring-measuring apparatus.
Mass: 7.75 kg

1-2 bricks, 15, 50 sec

2-1 bricks, 50, 100 sec

Spring	0B	1B	Delt 01	2B-15	Delt12-15	2B-50	Delt12-50	2B-100	Delt12-100	0B	Delt21	1B	Delt10	Avg	
L4-2	6.328	6.261	0.067	6.19	0.071	6.18	0.081	6.17	0.091	6.289	-0.053	6.223	-0.066	0.0715	
L4-3	6.362	6.301	0.061	6.228	0.073	6.219	0.082	6.207	0.094	6.328	-0.055	6.262	-0.066	0.071833	
L2-1	6.368	6.295	0.073	6.233	0.062	6.22	0.075	6.207	0.088	6.326	-0.057	6.264	-0.062	0.0695	
L2-2	6.375	6.298	0.077	6.239	0.059	6.23	0.068	6.218	0.08	6.336	-0.052	6.27	-0.066	0.067	
L2-3	6.356	6.286	0.07	6.222	0.064	6.212	0.074	6.2	0.086	6.317	-0.055	6.255	-0.062	0.0685	
L3-1	6.337	6.268	0.069	6.193	0.075	6.182	0.086	6.173	0.095	6.296	-0.058	6.231	-0.065	0.074667	
L3-2	6.322	6.254	0.068	6.185	0.069	6.177	0.077	6.17	0.084	6.286	-0.057	6.227	-0.059	0.069	
L3-3	6.35	6.286	0.064	6.221	0.065	6.211	0.075	6.2	0.086	6.316	-0.052	6.252	-0.064	0.067667	
Avg			0.068625		0.06725		0.07725		0.088		-0.05487		-0.06375	0.069958	0.069958

Average spring constant: $\left[(0.070\,\text{cm})/(g\cdot 7.75\,\text{kg})\right]^{-1} \times \mu$

$= 1.09\cdot 10^5\ \text{nt/m} \times \mu$

$\mu = \frac{x_2}{x_1+x_2} = .94$

$\boxed{k = 1.03\cdot 10^5\ \text{nt/m}}$

Comparison of **HtH** transfer fctn for a stack with 2 Layers of viton/RTV + Stack with 4 layers RTV

X=37.853 Hz
Ya=-80.994 dB
FREQ RESP
Yb=-57.718 dB
FREQ RESP

Y=-60.04 dB

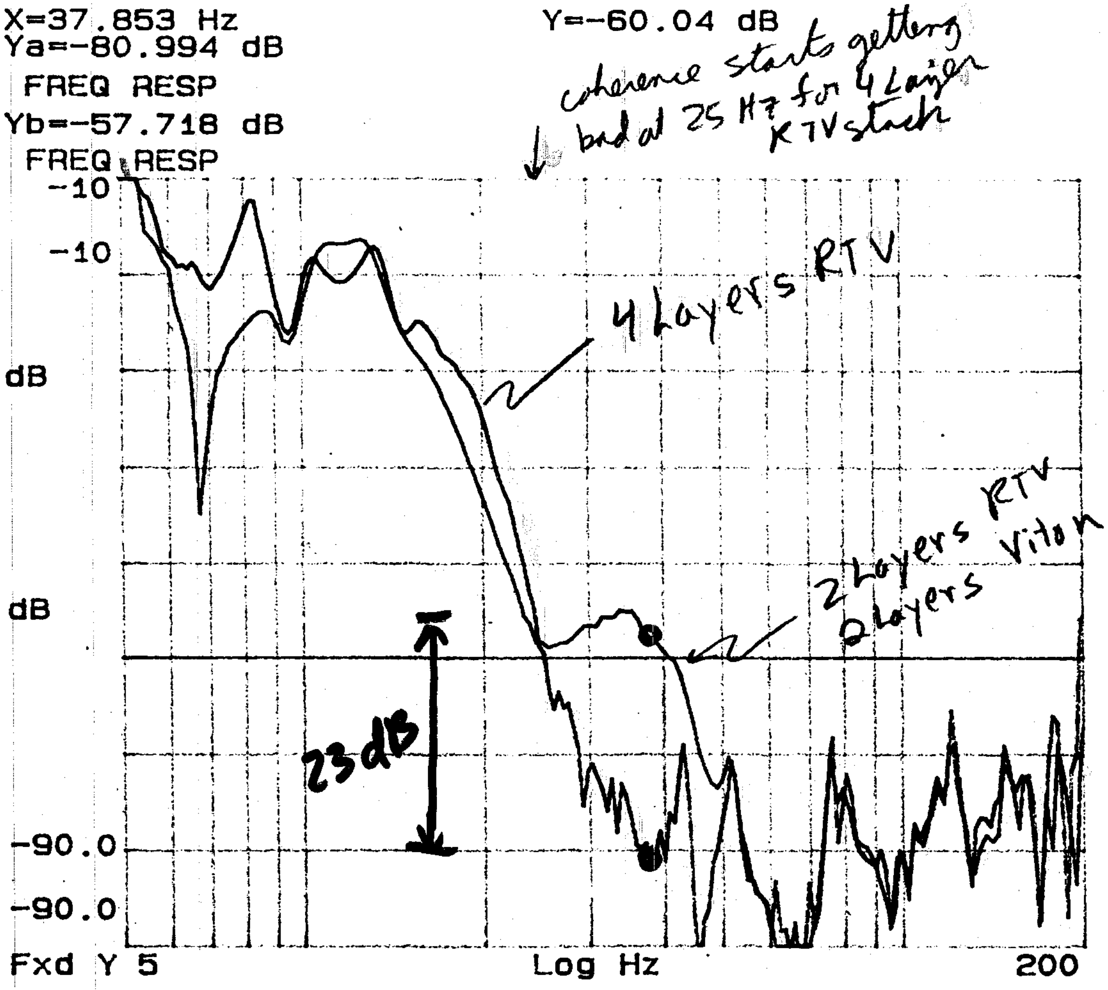

coherence starts getting bad at 25 Hz for 4 Layer RTV stack

Blue-SOR6 Stack with 2 Layers of RTV + 2 Layers of Viton)

Black-Rb (Stack with 4 Layers of RTV)

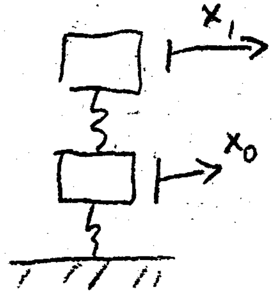

At 30 Hz - get at least 15dB
At 40 Hz - get at least 20dB

Comparison of **VtoV**
transfer fctn of an all
viton stack and a
Stack with 2 layers of
RTV & 2 Layers of viton

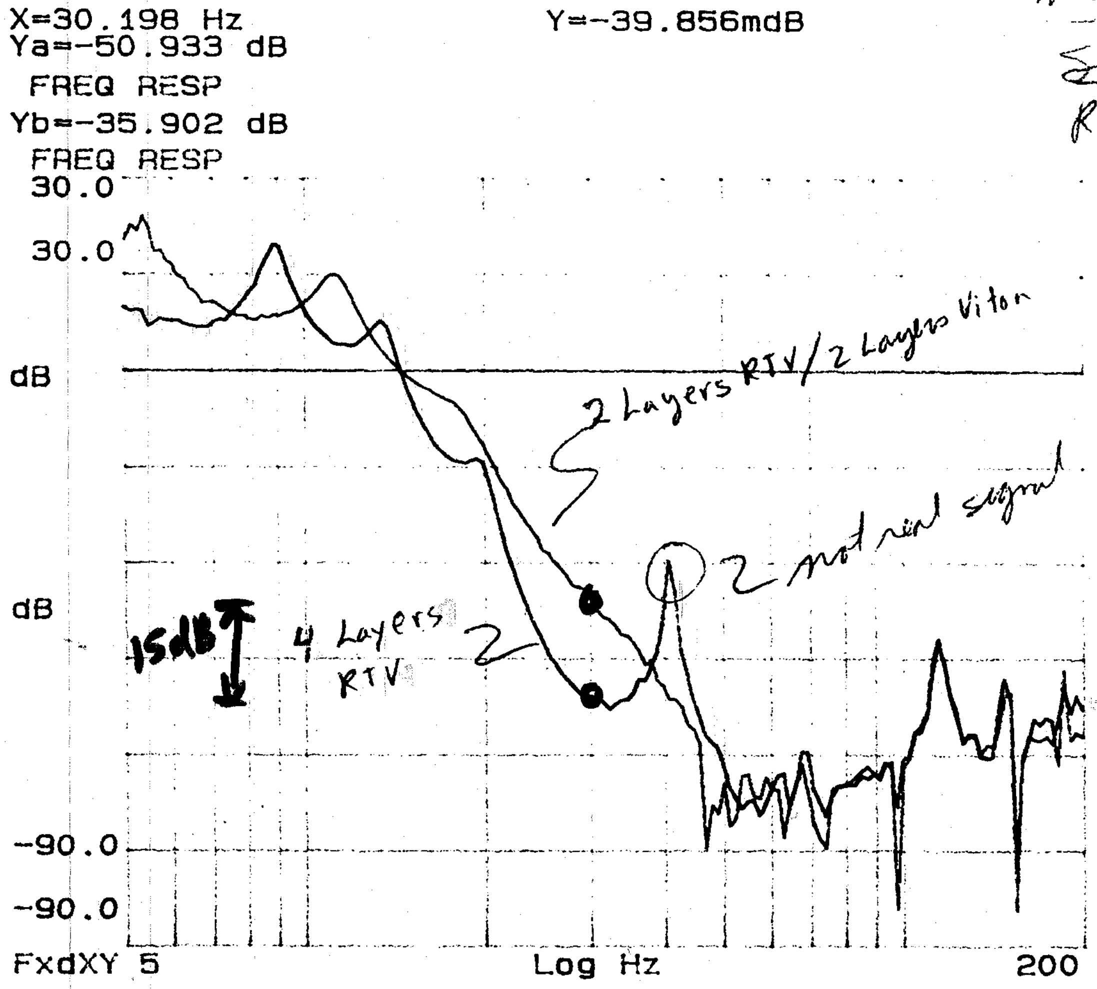

Black-SOR26
Blue-SOR22

Black-all RTV
Blue - Top 2 layers RTV
Bottom 2 layer viton

coherence is bad for
4 Layer RTV stack at 30Hz

⇒ get at least 15 dB at 30Hz;
probably more